Naval Surface Warfare Center
Carderock Division
West Bethesda, MD 20817-5700

NSWCCD-50-TR-2011/032 **April 2011**
Hydromechanics Department Report

Evaluation of the Exceedance Rate of a Stationary Stochastic Process by Statistical Extrapolation Using the Envelope Peaks over Threshold (EPOT) Method

by
Vadim Belenky
Bradley L. Campbell

REPORT DOCUMENTATION PAGE

Form Approved
OMB No. 0704-0188

1. REPORT DATE (DD-MM-YYYY)	2. REPORT TYPE	3. DATES COVERED (From-To)
30-04-2011	Final	Jan 2009 – Nov 2010

4. TITLE AND SUBTITLE
Evaluation of the Exceedance Rate of a Stationary Stochastic Process by Statistical Extrapolation Using the Envelope Peaks over Threshold (EPOT) Method

5a. CONTRACT NUMBER

5b. GRANT NUMBER

5c. PROGRAM ELEMENT NUMBER
0604300N

6. AUTHOR(S)
Vadim Belenky
Bradley L. Campbell

5d. PROJECT NUMBER

5e. TAKS NUMBER

5f. WORK UNIT NUMBER
10-1-5080-748

7. PERFORMING ORGANIZATION NAME(S) AND ADDRESS(ES)
NAVAL SURFACE WARFARE CENTER CARDEROCK DIVISION
9500 MACARTHUR BLVD
WEST BETHESDA, MD 20817-5700

8. PREFORMING ORGANIZATION REPORT NUMBER
NSWCCD-50-TR-2011/032

9. SPONSORING / MONITORING AGENCY NAME(S) AND ADDRESS(ES)
NAVAL SEA SYSTEM COMMAND PMS 500
WASHINGTON NAVY YARD
WASHINGTON, D.C. 20374

10. SPONSOR/MONITOR'S ACROYNM(S)
PMS500

11. SPONSOR/MONITOR'S REPORT NUMBER(S)

12. DISTRIBUTION / AVAILABILITY STATEMENT
Distribution unlimited.

13. SUPPLEMENTARY NOTES

14. ABSTRACT

The statistical analysis of dynamic stability failures of ships is made extremely difficutl due to the problem of rarity. Few or no events of interest may be observed in the amount of time that is feasible for model testing or even simulation. These events, however, may have a finite and non-trivial possibility. The Envelope Peaks Over the Threshold (EPOT) method is a statistical extrapolation technique that was developed to address this problem. It uses the principle of separation to decompose the problem into rare and non-rare sub-problems. The non-rare problem is solved trivially with direct statistics, while the rare problem is solved by fitting a distribution to the peaks or maxima over a threshold. The notion of statistical condfidence it carried through the whole process. The algorithm and principles behind the algorithm are defined and explored in detail.

15. SUBJECT TERMS
Dynamic stability, stability failure, partial stability failure, statistical extrapolation, extreme value theory, extreme value, EPOT, peaks over threshold, Poisson flow

16. SECURITY CLASSIFICATION OF:			17. LIMITATION OF ABSTRACT	18. NUMBER OF PAGES	19a. NAME OF RESPONSIBLE PERSON
a. REPORT	b. ABSTRACT	c. THIS PAGE			Bradley L. Campbell
UNCLASS	UNCLASS	UNCLASS	UNCLASS	215	19b. TELEPHONE NUMBER (include area code) 301 227-5936

Standard Form 298 (Rev. 8-98)
Prescribed by ANSI Std. Z39.18

This page is intentionally left blank.

Contents

Figures

Tables

This page is intentially left balnk

Abstract

The statistical analysis of dynamie stability failures of ships is made extremely diffieutl due to the problem of rarity. Few or no events of interest may be observed in the amount of time that is feasible for model testing or even simulation. The Envelope Peaks Over the Threshold (EPOT) method is a statistieal extrapolation technique that was developed to address this problem. It uses the principle of separation to decompose the problem into rare and non-rare sub-problems. The non-rare problem is solved trivially with direet statisties, while the rare problem is solved by fitting a distribution to the peaks or maxima over a threshold. The notion of statistical condfidence it carried through the whole process. The algorithm and principles behind the algorithm are defined and explored in detail.

Administrative Information

The work deseribed in this report was performed by the Seakeeping Division (Code 5500) of the Hydromeehanies Department at the Naval Surfaee Warfare Center, Carderock Division (NSWCCD). The work was funded by the DDG-1000 program offiee (PMS500) in FY 2009 and FY 2010 under work units 09-1-5080-635 and 10-1-5080-748.

Acknowlegements

The authors gladly recognize the important role George Hazen (DRS) played in this study with his idea on relating an extreme value distribution and time. This allowed the authors to relate extreme value theory and upcrossing theory, whieh is a cornerstone of this researeh.

The authors are grateful to William M. Richardson for his meticulous review of the report with detailed insight into the critical issues of the study. His suggestions were very useful for the final formulation of the algorithm.

The author appreeiate numerous and very fruitful diseussions with Prof. Pol Spanos (Riee University) and Dr. Arthur Reed. These diseussions helped the authors to develop better understanding of the nature of the problem involved.

The authors also appreciate help from Jesse Parkhurst and Calvin Krishen for proofreading and copyediting the report.

Finally the authors wish to thank Jude Brown, Todd Carrico and Anthony Constable for their great patienee while they managed the projeet that this report is a part of.

This is page intentially left balnk

Introduction

Ships of novel hull form shapes may be vulnerable to dynamic stability failures as currently existing stability standards, which are based on previous experience, do not include these unconventional shapes. Some of the failures related to dynamic stability are caused by irregular waves and gusty wind. The inherent randomness of these environmental factors makes the probability of stability failure a very useful measure for both design and operation. This work's particular focus is partial stability failure related to large roll angle events caused mostly by pure loss of stability on the wave crest.

Difficulties evaluating the probability of large roll angles are related to both the rarity of the event and the nonlinearity of the dynamical system describing the motion of a ship in moderate to severe seas. The nonlinearity of the dynamical system comes mostly from nonlinear stiffness that also could be a random quantity due to changing stability in waves; however other terms (including yaw moment and roll damping) also make their contribution. As these nonlinearities are essential to the problem, options for realistic assessment may be limited to numerical simulations using advanced potential codes and model tests.

The rarity of the large roll event defines another set of requirements for the solution of this problem. Conditions are possible when the large roll event is not observed during the available run-time of the simulation or model test. Other conditions may lead to very few observed large roll events so that use of direct statistical counting cannot be considered as a practical option. Therefore, the solution must be an extrapolation.

Probabilistic or statistical extrapolation is widely used in technology; prediction of extreme events utilizes extreme value theory. This type of methodology is based on the extreme value distribution being fit to statistical data; then the distribution can be used to predict an extreme value that can occur with a given probability or mean time that passes before such an extreme value is observed. Mathematical background of these methods comes from theorems of the extreme value theory stating that a maximum of a random variable has a limiting distribution that does not depend on type of distribution of this variable.

The problem, with straight-forward application of this method, is related with the significant nonlinearity of the dynamical system. A sample of roll motions resulted both from experiment or numerical simulation is statistically dominated by relatively small roll angles. As the stiffness of the dynamical system is significantly nonlinear, properties of the system change significantly with the roll angle. Therefore, extreme-value distribution fitted with all the data may not be representative of the properties of the system at large roll angles. This problem is generally known in the extreme value statistics; its standard solution is a "peak-over-threshold" (POT) method. The idea is to use data which exceeds a certain threshold.

Interpretation and adaptation of the POT method for probabilistic evaluation of dynamic stability is the main core of this work. The most principle aspects are as follows:

- Relation with time of exposure; probabilistic measure of dynamic stability should have explicit relation with time. The most natural way is to present it in a form of the rate of failures (average number of failures per unit of time; it equals to inverse value of a mean time before/between failures). This allows using Poisson flow to express

probability of failure during given time of exposure (assuming stability failures being independent random events).

- Statistical uncertainty; considered probabilistic measure of dynamic stability is calculated based on a finite-size dataset. That makes the measure a random value and it has to be treated accordingly. Confidence interval is a standard way to handle statistical uncertainty of a value derived from a finite-size sample. Statistical uncertainty is also a major factor choosing a numerical value for the threshold.
- Check of consistency and convergence; correct interpretation of the POT method needs to be checked by comparison with other methods, such as upcrossing theory. Convergence also can be tested by comparison with the results of direct counting using a sample of larger size.

Practical application of the method is meant for partial stability failures. This event occurs when a ship encounters large roll (or pitch) angle that may be dangerous for crew or equipment on board. That means that a roll angle may be dangerous on either side, port or starboard, so exceedance on both sides constitute stability failure. As roll (and pitch) motions have certain inertia, a large amplitude on one side is likely to be followed by a large amplitude on the other side. This make events statistically dependent and may create a problem with the application of Poisson distribution and therefore with an explicit relationship with time. To avoid this complication, an envelope may be considered instead of the original process. So the envelope peaks-over-the-threshold is actually used for extrapolation.

In summary, this work is focused on the application of the Envelope Peak-Over-Threshold (EPOT) method for the probabilistic evaluation of dynamic stability using a dataset originated from numerical simulation or model experiment. The method can be tuned to handle the nonlinearity of the dynamical system. The method provides an explicit relation with time of exposure and comes with a confidence interval as a measure of statistical uncertainty. Finally, the method is meant to be tested for consistency against other theoretical methods and for convergence against the result of direct counting on a larger-size sample.

The original idea to use peak-over threshold as a method to treat the problem of rarity in a nonlinear dynamical system belongs to author B. Campbell. He also proposed to use an envelope as a means to evaluate the rate of exceedances of both sides while keeping applicability of Poisson flow. Author V. Belenky provided theoretical justification and initial numerical testing of the method. Numerical implementation of the method is a result of joint efforts of the authors. Section 1 through 5 are written by V. Belenky; Section 6 is written by B. Campbell.

1. Theoretical Background

1.1. Relation with Time

Here we review the available formulations for relating the probability of the occurrence of a large roll event with a time of exposure.

1.1.1. Introduction of Time - Binomial Distribution

A fundamental building block of the probability of event occurrence is the connection between time duration and the number of events likely to be seen. Consider n instants of time of short duration Δt. Assume that an event (i.e. a large roll angle) may happen at an instant of time t_i with probability p_i. Also assume that if there is more than one large roll event, they can be considered as independent random events. This assumption can be justified by the expected rarity of large roll events and, therefore, the sufficient time is expected to pass between two subsequent events to eliminate any dependence.

Consider the probability that an event occurs exactly at i-th time step. This implies that the event does not happen in all other instants of time.

$$P(t = t_i) = q_0 q_1 .. q_{i-1} p_i q_{i+1} \cdots q_{n-1} q_n ; \qquad q_i = 1 - p_i \tag{1.1}$$

It is clear from the formula (1.1) that probability P depends on how many time instants are included, therefore this formula already expresses the relationship between probability and time.

If the conditions during the exposure time under assessment can be considered unchanged (that is, the process is stationary), then there is no difference between any two instants of time; therefore probability p_i must be the same for all instants of time. This allows re-writing formula (1.1):

$$P(t = t_i) = pq^{n-1} ; \qquad q = 1 - p \tag{1.2}$$

Note that the probability in the formula (1.2) does not depend at which instant of time the event has occurred, but it still must be a particular instant of time t_i.

Consider the probability that the event occurs once at any instant of time. This means that it can occur in the 1st instant or in the 2nd instant and further on. There are exactly n possible scenarios how the event can occur once during n time steps.

$$P(m = 1) = npq^{n-1} \tag{1.3}$$

Where m is the number of events that occur in the length of the record.

Consider the probability of two events happening exactly at the instants i and j. Following the logic of formula (1.2):

$$P(m = 2 \mid t = t_i, t = t_j) = p^2 q^{n-2} \tag{1.4}$$

To express the probability that two events occur at any two moments of time, it is

necessary to find all possible combinations of how two elements can be chosen from n. The formula for such a value is known from combinatorics:

$$C(n,2) = \frac{n!}{2(n-2)!} \tag{1.5}$$

The probability of the event occurring at any two instants of time can be expressed as:

$$P(m=2) = C(n,2)p^2 q^{n-2} \tag{1.6}$$

Generalizing formula (1.6) for the case when the event occurs k times at any instant:

$$P(k) = C(n,k)p^k q^{n-k} \tag{1.7}$$

Here $C(n, k)$ defines a number of combinations of how k values can be chosen out of n. The general formula is also available from combinatorics:

$$C(n,k) = \frac{n!}{k!(n-k)!} \tag{1.8}$$

Finally, the probability that exactly k events occur during the time of exposure represented by n time steps is:

$$P(k) = \frac{n!}{k!(n-k)!} p^k (1-p)^{n-k} \tag{1.9}$$

Formula (1.9) is known in probability theory as the binomial distribution.

1.1.2. Probability of Event - Upcrossing Theory

We now consider the transition from discrete time steps to continuous time and let Δt approach zero. We want to find the probability of an event occurring at time instant t. We can approach this by considering the underlying process, such as the rolling of a ship. A large roll event is defined as the exceedance of some level a by roll angle ϕ. Consider the process of roll angle as differentiable process with known joint distribution of roll angle and roll rate, $f(\phi, \dot{\phi})$.

Exceeding the level a at time instant t can be expressed in the form of the following system of inequalities:

$$\begin{cases} \phi(t) < a \\ \phi(t+dt) > a \end{cases} \tag{1.10}$$

As the process of roll angle is differentiable:

$$\begin{cases} \phi(t) < a \\ \phi(t) + \dot{\phi} \cdot dt > a \end{cases} \tag{1.11}$$

Obviously, the system of inequalities (1.11) can only be satisfied if the roll rate is

positive. Therefore adding the condition of positive roll rate does not change the system of inequalities (1.11):

$$\begin{cases} \phi(t) < a \\ \phi(t) > a + \dot{\phi} \cdot dt \\ \dot{\phi} > 0 \end{cases} \tag{1.12}$$

The probability of the event occurring at the instant t is expressed as the probability of satisfying the system of inequalities (1.12) and the probability can be written as the integral of the joint distribution of roll and roll rate:

$$p = \int_{a-\dot{\phi}dt}^{a} \int_{0}^{\infty} f(\phi, \dot{\phi}) d\dot{\phi} d\phi \tag{1.13}$$

The limits of the first integral are infinitely close to each other. The mean value theorem allows re-writing the equation (1.13) as follows:

$$p = dt \int_{0}^{\infty} f(a, \dot{\phi}) \dot{\phi} d\dot{\phi} \tag{1.14}$$

Formula (1.14) shows that the probability of the large roll event occurring at time instant t becomes infinitely small if the time is considered continuous;

$$\lim_{\Delta t \to 0} p = \lim_{n \to \infty} p = dp \tag{1.15}$$

Therefore, the nomenclature dp is more appropriate for the formulae (1.13) and (1.14) in this case:

$$dp = dt \int_{0}^{\infty} f(a, \dot{\phi}) \dot{\phi} d\dot{\phi} \tag{1.16}$$

Then integral in formula (1.16) has a meaning of derivative of the instantaneous probability of the event with respect to time:

$$\frac{dp}{dt} = \int_{0}^{\infty} f(a, \dot{\phi}) \dot{\phi} d\dot{\phi} = \lambda(t) \tag{1.17}$$

Here λ is the rate of events. In general, it is function of time.

$$\lim_{\Delta t \to 0} p = \lim_{n \to \infty} p = dp = \lambda(t) dt \tag{1.18}$$

If the process of roll is stationary, the rate of events becomes constant and formula (1.17) can be simplified, as the first derivative a of stationary process is independent of the process itself.

$$f(\phi,\dot{\phi}) = f(\phi)f(\dot{\phi}) \tag{1.19}$$

and formula (1.17) becomes:

$$\lambda = \frac{dp}{dt} = f(a)\int_0^{\infty} f(\dot{\phi})\dot{\phi}d\dot{\phi} \tag{1.20}$$

1.1.3. Continuous Time – The Poisson Distribution

Continuing the transition to continuous time, we set Δt infinitely small, which means $n=\infty$ and look for the probability that there would be exactly k events during time T:

$$P_T(k) = \lim_{n\to\infty}\left(P(k)\right) = \lim_{n\to\infty}\left(C(n,k)p^k(1-p)^{n-k}\right) \tag{1.21}$$

Taking into account formula (1.20), the probability of the event occurring at time t can also be expressed in terms of discretized time:

$$p = \lambda\Delta t = \frac{\lambda T}{n} \tag{1.22}$$

Substituting formula (1.8) into (1.21) and expanding some of factorials, we obtain:

$$P_T(k) = \lim_{n\to\infty}\left(\frac{1\cdot 2\cdot ...(n-k)\cdot(n-k+1)..(n-1)\cdot n}{k!\left(1\cdot 2\cdot ...(n-k)\right)}p^k(1-p)^{n-k}\right) \tag{1.23}$$

After dividing the numerator and denominator by $\left(1\cdot 2\cdot ...(n-k)\right)$:

$$P_T(k) = \lim_{n\to\infty}\left(\frac{(n-k+1)..(n-1)\cdot n}{k!}p^k(1-p)^{n-k}\right) \tag{1.24}$$

Substitution of formula (1.22) into (1.24) yields:

$$\begin{aligned} P_T(k) &= \lim_{n\to\infty}\left(\frac{(n-k+1)..(n-1)\cdot n}{k!}\left(\frac{\lambda T}{n}\right)^k\left(1-\frac{\lambda T}{n}\right)^{n-k}\right) = \\ &= \lim_{n\to\infty}\left(\frac{(n-k+1)..(n-1)\cdot n}{n^k}\cdot\left(1-\frac{\lambda T}{n}\right)^{-k}\cdot\left(\frac{(\lambda T)^k}{k!}\right)\cdot\left(1-\frac{\lambda T}{n}\right)^{n}\right) \end{aligned} \tag{1.25}$$

Now consider the limits of each factor:

$$\lim_{n\to\infty}\left(\frac{(n-k+1)..(n-1)\cdot k}{n^k}\right)=1 \tag{1.26}$$

$$\lim_{n\to\infty}\left(\left(1-\frac{\lambda T}{n}\right)^{-k}\right)=1 \tag{1.27}$$

$$\lim_{n\to\infty}\left(\frac{(\lambda T)^k}{k!}\right)=\frac{(\lambda T)^k}{k!} \tag{1.28}$$

$$\lim_{n\to\infty}\left(\left(1-\frac{\lambda T}{n}\right)^{n}\right)=\exp(-\lambda T) \tag{1.29}$$

Taking into aecount equations (1.26)-- (1.29), formula (1.25) can be presented as:

$$P_T(k)=\frac{(\lambda T)^k}{k!}\cdot\exp(-\lambda T) \tag{1.30}$$

Equation (1.30) is known as the Poisson distribution. It expresses probability of exactly k events occurring during the exposure time T for a eontinuous proeess.

1.1.4. Time Before/Between Events

Consider the cumulative distribution function (CDF) of time before the first event or between eonseeutive events. As an event may oeeur at any instant of time, the interval between them is a random variable. This interval also ean be defined as a time while no events oeeurs.

Consider CDF of the time while no event oeeurs. By the definition, this is the probability that a random variable is less than or equal to an argument.

$$F_T(x)=P(T\le x) \tag{1.31}$$

The CDF also can be expressed through the probability of a eomplimentary event:

$$F_T(x)=1-P(T>x) \tag{1.32}$$

If no event oeeurs then the time between them is obviously larger than the argument. Therefore, this is a probability that no event oeeurs during time T. It can be found from formula (1.30) by setting k to 0:

$$P(x>T)=P_T(k=0)=\exp(-\lambda T) \tag{1.33}$$

Formula (1.32) ean then be expressed as:

$$F_T(T)=1-\exp(-\lambda T)\quad;\quad T\ge 0 \tag{1.34}$$

This CDF is known in probability theory as the exponential distribution. The probability density funetion (PDF) of the exponential distribution can be found by

differentiating the CDF, equation (1.34) with respect to its argument:

$$f_T(T) = \frac{dF_T(T)}{dT} = -\lambda \exp(-\lambda T) \quad ; \quad T \geq 0 \tag{1.35}$$

The exponential distribution has a single parameter λ, the rate of events. The inverse of λ is the mean value and standard deviation of the time without an event.

$$m(T) = \int_0^\infty T f_T(T) dt = 1/\lambda \tag{1.36}$$

$$V(T) = \int_0^\infty (T - m(T))^2 f_T(T) dt = 1/\lambda^2 \quad ; \quad \sigma(T) = 1/\lambda \tag{1.37}$$

Here $m(T)$, $V(T)$ and $\sigma(T)$ are the mean value, variance, and standard deviation of time between / before the event, respectively.

It is possible to demonstrate that formula (1.34) also can be interpreted as the probability of at least one event (one event, two events or more) occurring in time duration T. Expressing this probability through the probability of complimentary event yields expression identical to (1.34)

$$P_T(k \neq 0) = 1 - P_T(k = 0) = 1 - \exp(-\lambda T) \tag{1.38}$$

1.2.Statistical Evaluation of Upcrossing Rate

We now shift our focus to the statistical estimation of the rate of upcrossing events (upcrossing rate), including an appropriate confidence interval. We also wish to relate the upcrossing rate to statistics of other related parameters, including the time between events and the time before the first event.

1.2.1. Statistical Estimate of the Parameter of the Distribution

Consider a sample of a stochastic process x, presented in the form of an ensemble of N_R records. Each record is represented by a time history of N_{PT} points with the time step Δt and $n = N_{PT}-1$ time steps. Then the event of upcrossing of the level a can be associated with a random variable U defined for each time step as follows:

$$U_{i,j} = \begin{cases} 1 & x_{i,j} \leq a \cap x_{i+1}, j > a \\ 0 & Otherwise \end{cases} \qquad i = 1,...,n \; ; \quad j = 1,...,N_R \tag{1.39}$$

The number of upcrossing events occurring at the i^{th} time step of each record is calculated as:

$$N_{Ui} = \sum_{j=1}^{N_R} U_{i,j} \tag{1.40}$$

The estimate of the probability that the upcrossing event occurs at time instant t_i is:

$$p_i^* = \frac{1}{N_R} \sum_{j=1}^{N_R} U_{i,j} \tag{1.41}$$

This value is a statistical estimate of infinitely small probability, dp, as introduced in formula (1.15):

$$dp(t = t_i) = \lim_{\substack{N_R \to \infty \\ \Delta t \to 0}} p_i^* \tag{1.42}$$

Then, following the formula (1.22) the estimate of λ_i^*, the parameter of the Poisson distribution estimated at the i^{th} time step, is expressed as:

$$\lambda_i^* = \frac{p_i^*}{\Delta t} \tag{1.43}$$

If process x is stationary, the parameter of the Poisson distribution, λ, does not depend on time and the value λ_i^* estimated for different time steps tends to the same limit with increasing number of records. If the process x can also be considered ergodic (that is, the statistical characteristics of x can be estimated from one record if it is long enough), then the estimates of p_i^* and λ_i^* can be evaluated using all the time steps:

$$\begin{aligned} p^* &= \frac{1}{n} \sum_{i=1}^{n} p_i^* = \frac{1}{nN_R} \sum_{i=1}^{n} \sum_{j=1}^{N_R} U_{i,j} \\ \lambda^* &= m(\lambda_i^*) = \frac{1}{nN_R \Delta t} \sum_{i=1}^{n} \sum_{j=1}^{N_R} U_{i,j} \end{aligned} \tag{1.44}$$

Regrouping formula (1.43), we see that it contains the number of events in each record:

$$N_{Uj} = \sum_{i=1}^{n} U_{i,j} \tag{1.45}$$

The value N_U is a random number represented by its sample. The volume of this sample the number of records N_R. The mean value of this random number is estimated as:

$$m_U^* = \frac{1}{N_R} \sum_{j=1}^{N_R} N_{Uj} \tag{1.46}$$

Substitution of formulae (1.45) and (1.46) into equation (1.44) yields:

$$\lambda^* = m(\lambda_i^*) = \frac{m_U^*}{n\Delta t} = \frac{m_U^*}{T_R} \tag{1.47}$$

Where: T_R is time duration of a record.

Formula (1.46) also allows an interpretation of the meaning of the λ parameter of the exponential distribution; that is the average number of crossings per unit of time also known as the "rate of events".

1.2.2. Confidence Interval for Rate of Events

Formula (1.47) also reveals the statistical meaning of the rate of events. It is a value proportional to the average estimate of the number of events in each record. Therefore, in order to calculate the confidence interval for the rate of events, it is enough to find the confidence interval for m_U^*.

The value m_U^* is an estimate of the mean of the random variable N_U. This variable has the binomial distribution, as it represents the number of upcrossings occurring within a finite number of time steps. As the number of events is countable, this random variable is discrete and it is defined by the following probability mass function (discrete counterpart of PDF)

$$f(k) = \frac{n!}{k!(n-k)!} p^k (1-p)^{n-k} \tag{1.48}$$

Where k is a number of crossings observed during the time duration of a record. In this case, N_{Uj} represents a realized sample of k. The theoretical mean value m_U and variance V_U of the binomial distribution (1.48) are known:

$$m_U = np\,; \qquad V_U = np(1-p) \tag{1.49}$$

The estimate of the mean value (1.46) is a random number as it is a sum of N_R random variables, each of which has the binominal distribution with the same parameter. The distribution of the mean value estimate is important to the method of evaluating the confidence interval.

Independent of is distribution, the variance of m_U^* can be found as a variance of a sum of independent variables:

$$\begin{aligned} V(m_U^*) &= V\left(\frac{1}{N_R}\sum_{j=1}^{N_R} N_{Uj}\right) = \frac{1}{N_R^2} V\left(\sum_{j=1}^{N_R} N_{Uj}\right) = \\ &= \frac{1}{N_R^2}\left(\sum_{j=1}^{N_R} V(N_{Uj})\right) = \frac{N_R V_U}{N_R^2} = \frac{V_U}{N_R} \end{aligned} \tag{1.50}$$

As the exact value of the variance V_U is not known, we substitute an estimate for it:

$$V\left(m_U^*\right) = \frac{V_U^*}{N_R} = \frac{np^*}{N_R}\left(1 - p^*\right) \tag{1.51}$$

As equation (1.46) represents the sum of identically distributed random variables, the distribution of the value m_U^* tends to normal, as sample size N_R increases (Central Limit Theorem). Belenky, *et al* (2007) used this approach to evaluate the confidence interval and found that the distribustion of the estimate is expressed as:

$$f(m) = \frac{1}{\sqrt{2\pi V\left(m_U^*\right)}} \exp\left(- \frac{\left(m - m(m_U^*)\right)^2}{2V\left(m_U^*\right)} \right) \tag{1.52}$$

It is known that the mean value estimate is unbiased; therefore, the mean value of the estimate is equal to itself:

$$m\left(m_U^*\right) = m_U^* \tag{1.53}$$

The upper and lower boundaries of the confidence interval *UB* and *LB* must satisfy the following equation:

$$\beta = \int_{LB}^{UB} f(m)dm = F(UB) - F(LB) \quad ; \quad F(m) = \int_{-\infty}^{m} f(z)dz \tag{1.54}$$

where β is the accepted confidence level (typically 90% or 95%) and $F(m)$ is the CDF. To find the boundaries, the inverse function of the CDF, $Q(P)$, (also known as the Quantile function) is introduced:

$$m = Q(P) = Inv\{F(m)\}; \quad P = F(m) \tag{1.55}$$

Where P is a probability. The inverse function returns the value corresponding to that probability. Then:

$$LB = Q\left(\frac{1-\beta}{2}\right) \quad ; \quad UB = Q\left(1 - \frac{1-\beta}{2}\right) = Q\left(\frac{1+\beta}{2}\right) \tag{1.56}$$

Recognizing that the normal distribution is symmetric around its mean value, the half-breadth of the confidence interval can be expressed as:

$$LB(m_U^*) = m_U^* - \varepsilon; \quad UB(m_U^*) = m_U^* + \varepsilon; \quad \varepsilon = Q\left(\frac{1+\beta}{2}\right) \tag{1.57}$$

Here ε is the half-breadth of the confidence interval. Typical values are:

$$\varepsilon = K_\beta \cdot \sigma$$

$$\beta = 0.95; \qquad K_\beta = 1.959964$$

$$\beta = 0.9973; \qquad K_\beta = 3.0$$

Here σ is the standard deviation of the variable; the latter pair of values is also commonly referred as the "six-sigma rule".

Following (Belenky, *et al*, 2007), boundaries of the confidence interval for the rate of events λ^* are defined as:

$$\lambda^*_{low} = \frac{LB(m^*_U)}{T_R} \quad ; \quad \lambda^*_{up} = \frac{UB(m^*_U)}{T_R} \tag{1.58}$$

Use of the normal distribution (1.52) is only justified if N_R is large as it is based on the Central Limit Theorem. The question of how large N_R should be to employ the normal distribution may require additional study.

At the same time, the sum of independent variables with a binomial distribution, all with the same parameter p, also have a binomial distribution with the same parameter p, but with a sum of the number of cases. If the number of cases are the same then the new number of cases becomes $2n$. In the case of N_R records, the total number of cases becomes:

$$N = N_R \cdot n \tag{1.59}$$

Then, the probability that N_R records, each with n time steps, will contain k upcrossings can be expressed as:

$$P(k) = \frac{N!}{k!(N-k)!} p^k (1-p)^{N-k} \tag{1.60}$$

The formula (1.60) also can be interpreted as the probability mass distribution for the number of upcrossings for all the records:

$$f(k) = \frac{N!}{k!(N-k)!} p^k (1-p)^{N-k} \tag{1.61}$$

The mean value for this distribution is:

$$m_{NU} = Np \tag{1.62}$$

Taking into account (1.44), the estimate for this mean value is equal to the number of crossings that were actually observed:

$$m^*_{NU} = Np^* = N_R n p^* = \sum_{i=1}^{n} \sum_{j=1}^{N_R} U_{i,j} \tag{1.63}$$

The variance of the number of crossings according to distribution (1.60) can be expressed as follows:

$$V_{NU} = Np(1-p) \tag{1.64}$$

The estimate of this variance is related to the V^*_U estimate of the variance of the number of crossings during one record, as defined in (1.49) and $V(m^*_U)$, the estimate of the variance of the mean number of crossings per record from equation (1.51):

$$V_{NU} = Np^*(1-p^*) = N_R np^*(1-p^*) = N_R V_U^* = N_R^2 V\left(m_U^*\right) \tag{1.65}$$

The boundaries of confidenee interval for the observed number of crossings for all the records are still define by formula (1.56), interpreting Q as the inverse funetion of binomial CDF of the number of erossing for all the reeords. As the binomial distribution has non-zero skewness, symmetrical presentation (1.57) is not applieable:

$$LB(NU^*) = Q\left(\frac{1-\beta}{2}\right) \quad ; \quad UB(NU^*) = Q\left(\frac{1+\beta}{2}\right) \tag{1.66}$$

The boundaries of the eonfidenee interval for the rate of events λ^*, without the assumption of normality, are defined as:

$$\lambda_{low}^* = \frac{LB(NU^*)}{N_R n\Delta t} = \frac{LB(NU^*)}{N_R T_R} \quad ; \quad \lambda_{up}^* = \frac{UB(NU^*)}{N_R n\Delta t} = \frac{UB(NU^*)}{N_R T_R} \tag{1.67}$$

Here λ_{low}^* and λ_{up}^* are the lower and upper boundaries of the confidence interval, respectfully.

1.2.3. Numerical Example

Consider the process of simulated wave elevations (from a linear model) characterized by a Bretshneider speetrum ealculated for significant wave height H_S=11.5 m and modal period of T_m =16.4 s. Then the mean period is:

$$T_1 = 0.773T_m \tag{1.68}$$

The following formulation of spectral density was used (see also Figure 1.1):

$$s(\omega) = A\omega^{-5}\exp\left(-B\omega^{-4}\right); \quad A = 173H_S^2T_1^{-4} \; ; \quad B = 691T_1^{-4} \tag{1.69}$$

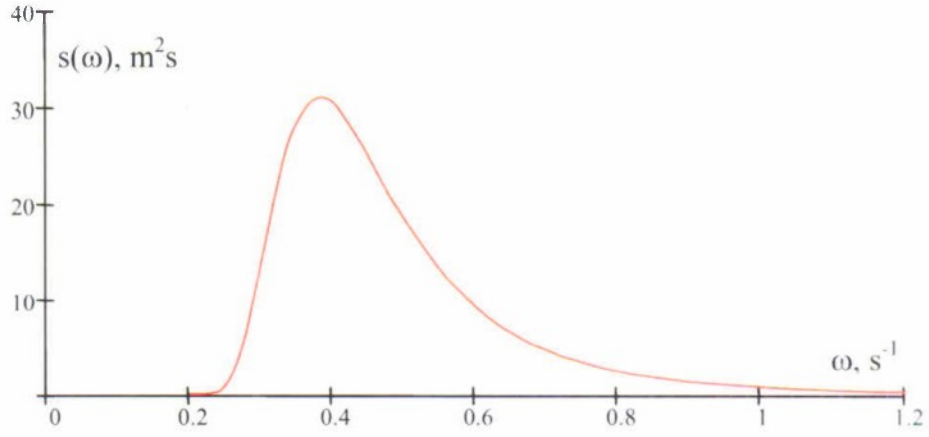

Figure 1.1 Bretschneider Spectral Density Significant Wave Height H_S=11.5 m and Modal Period T_m =16.4 s

The wave-elevation time history for a fixed point of space was computed using an inverse Fourier transform as follows:

$$\zeta_W(t) = \sum_{i=1}^{N_\omega} r_{Wi} \cos(\omega_i t + \varphi_i) \tag{1.70}$$

Here ω_i is a set of frequencies used for discretization of the spectral density (1.68), r_{Wi} is amplitude of the i^{th} component and φ_i is a phase shift for the i^{th} component.

The frequency set for this sample consists of uniformly spaced frequencies. The number of frequencies has been chosen to avoid the self-repeating effect described in (Belenky, *et al.,* 2007). The total number of frequencies was 180, with 42 components before the peak of the spectral density curve and 138 after the peak. The width of frequency band was expressed through the frequency of the peak of the spectral density curve.

$$Bnd(\omega) = 1.15\omega_{w\max} = 0.44\, s^{-1}; \quad \omega_{w\max} = \frac{2\pi}{T_m} \tag{1.71}$$

Then the frequency step is calculated as follows:

$$\Delta\omega = \frac{Bnd(\omega)}{N_\omega} = 0.0032 \tag{1.72}$$

The lower and upper limits frequencies are $\omega_1 = 0.25\, s^{-1}$ and $\omega_{N_\omega} = 0.824\, s^{-1}$, respectively. As the frequency spacing is uniform, the duration of a single record should not exceed:

$$T_{S\max} = \frac{2\pi}{\Delta\omega} = 1968\ s = 32.8\ \text{min} \tag{1.73}$$

Taking into account (1.73), the time duration for a single record was set to T_S=30 min. To ensure that this spectral discretization does not lead to the self-repeating effect, the autocorrelation function needs to be checked:

$$R(\tau) = \int_0^\infty s(\omega)\cos\omega\tau\, d\omega; \quad R_j = \sum_{i=1}^{N_\omega} S_i \cos\left(\omega_i \Delta t \cdot (i-1)\right) \quad j = 1,2..N_t \tag{1.74}$$

Here the time step Δt = 0.5 s; S_i is the value of the power spectrum at frequency ω_i and N_t is the number of time steps.

$$S_i = \int_{\omega_i - 0.5\Delta\omega_{i-1}}^{\omega_i + 0.5\Delta\omega_{i-1}} s(\omega)d\omega = 0.5\Delta\omega\left(s(\omega_i - 0.5\Delta\omega) + s(\omega_i + 0.5\Delta\omega)\right) \tag{1.75}$$

The autocorrelation function is shown in Figure 1.2. It can be seen from this figure there is no self-repeating effect.

The variance of wave elevations calculated from the discretized spectrum should also be checked. As the frequency band is limited, some energy at high frequencies was not included in the discretized model.

$$V_{\zeta d} = \sum_{i=1}^{N_\omega} S_i = 7.8\ m^2\ ; \quad \sigma_{\zeta d} = \sqrt{V_{\zeta d}} = 2.79\ m; \quad H_{Sd} = 4\sigma_d = 11.17\ m \tag{1.76}$$

Here $V_{\zeta d}$ is the variance of wave elevations as discretized, $\sigma_{\zeta d}$ is the standard deviation and H_{Sd} is the significant wave height as discretized. Because of the frequency truncation limits, the significant wave height as discretized is slightly less than the input value of 11.5 m. The difference, however, is less than 3% and can be considered acceptable.

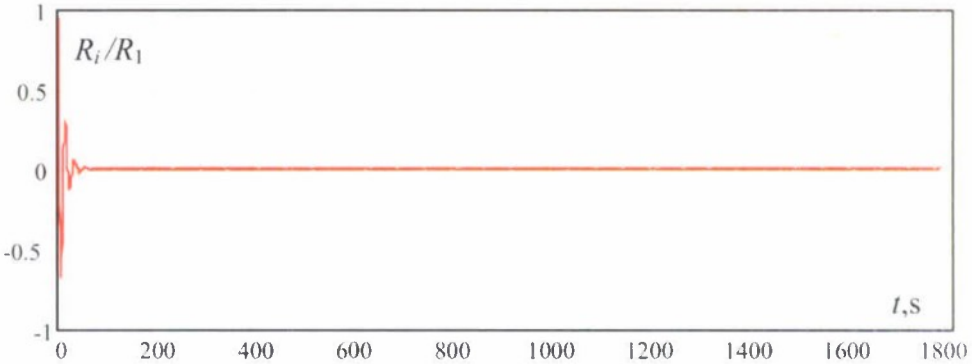

Figure 1.2 Autocorrelation Function of Wave Elevations Calculated from Discretized Spectrum

The amplitudes of the wave components in (1.70) are calculated from discretized power spectrum as:

$$r_{Wi} = \sqrt{2S_i} \tag{1.77}$$

Finally the phase shift φ_i is assumed to be a random variable uniformly distributed from 0 to 2π. Each set of N_ω=180 phase angles corresponds to one record of 30 minutes. The dataset used in this example includes 200 such records.

As shown in Figure 1.3 for the level of a=7.5 m, three crossings were found in the first record

$$N_{U1} = \sum_{i=1}^{n} U_{i,1} = 3 \tag{1.78}$$

A total of 721 up-crossing events were observed for all the records:

$$N_{UT} = \sum_{i=1}^{n} \sum_{j=1}^{N_R} U_{i,j} = 721 \tag{1.79}$$

The total number of cases of the auxiliary variable U is:

$$N = N_R \cdot n = 200 \cdot 3599 = 719800 \tag{1.80}$$

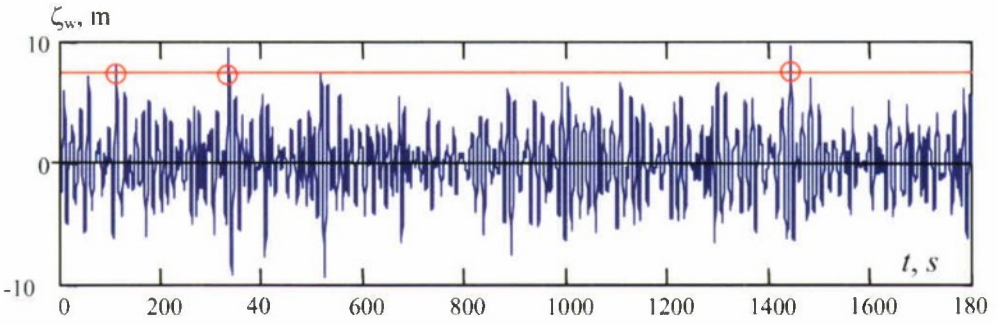

Figure 1.3. Record 1 of the Process of Wave Elevations; With Three Upcrossings Through a Level of 7.5 m

Using formula (1.45) the parameter of the Binomial Distribution, p, and the upcrossing rate, λ, are estimated as:

$$p^* = \frac{1}{n}\sum_{i=1}^{n} p_i^* = \frac{1}{nN_R}\sum_{i=1}^{n}\sum_{j=1}^{N_R} U_{i,j} = 0.001002 \tag{1.81}$$

$$\lambda^* = m(\lambda_i^*) = \frac{1}{nN_R\Delta t}\sum_{i=1}^{n}\sum_{j=1}^{N_R} U_{i,j} = 0.002003\, s^{-1} \tag{1.82}$$

The theoretical value for the rate of events can be found by substitution of the Normal Distribution (Equation 1.55) into Formula (1.19)

$$\lambda = f(a)\int_0^{\infty} f(\dot{\phi})\dot{\phi}d\dot{\phi} = \sqrt{\frac{V_{\dot{\zeta}d}}{V_{\zeta d}}}\exp\left(-\frac{a^2}{2V_{\zeta d}}\right) = 0.002055\, s^{-1} \tag{1.83}$$

Formula (1.83) includes the variance of the temporal derivative of wave elevations as discretized:

$$V_{\dot{\zeta}d} = \sum_{i=1}^{N_m} S_i\omega_i^2 = 1.77\ \ m^2s^2 \tag{1.84}$$

The theoretical value and estimate for upcrossing rate seem to be quite close, but it cannot really be judged. The estimate of upcrossing rate λ^* is a random number. Therefore a confidence interval needs to be calculated in order to judge the closeness of the estimate and theoretical value.

Two methods of calculation of the confidence interval for the upcrossing rate were considered in the section above. The first one considers the estimate of the average number of crossings per record (see formula 1.45):

$$m_U^* = \frac{1}{N_R}\sum_{j=1}^{N_R} N_{Uj} = 3.605 \tag{1.85}$$

This figure is assumed to follow normal distribution with the mean value equal to itself:

$$m(m_U^*) = m_U^* = 3.605 \tag{1.86}$$

The varianee of this estimate is:

$$V(m_U^*) = \frac{V_U^*}{N_R} = \frac{np^*}{N_R}(1-p^*) = 0.018007 \tag{1.87}$$

For a eonfidenee level of β=0.95, the half width of the eonfidenee interval for m_U^* is:

$$\varepsilon = 1.959964 \cdot \sqrt{V(m_U^*)} = 0.263007 \tag{1.88}$$

This yields the following values for lower and upper boundary for the rate of uperossings (see equation 1.57):

$$\lambda_{low}^* = \frac{m_U^* - \varepsilon}{T_R} = 0.001857 \;\; ; \;\; \lambda_{up}^* = \frac{m_U^* + \varepsilon}{T_R} = 0.002149 \tag{1.89}$$

The seeond method is to ealeulate the confidenee interval for λ direetly from the random variable *NU*, using its binomial distribution with parameter p^* estimated with formula (1.79) with the boundaries defined by formulae (1.65)

$$NU^* = 721$$

$$LB(NU^*) = Q\left(\frac{1-\beta}{2}\right) = 669 \;\; ; \;\; UB(NU^*) = Q\left(\frac{1+\beta}{2}\right) = 774 \tag{1.90}$$

The boundaries of the confidenee interval for λ are given by formula (1.66):

$$\lambda_{low}^* = \frac{LB(NU^*)}{N_R T_R} = 0.001858 \;\; ; \;\; \lambda_{up}^* = \frac{UB(NU^*)}{N_R T_R} = 0.00215 \tag{1.91}$$

Both methods gave almost identieal results for the confidenee interval. The theoretical value of the uperossing rate is contained within the confidence interval, as shown in Figure 1.4.

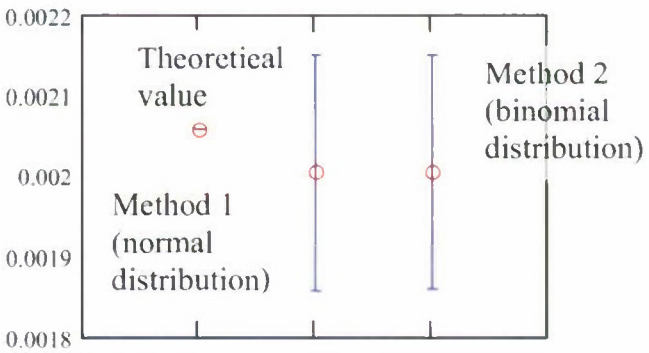

Figure 1.4 Confidence Intervals for the Upcrossing Rate Calculated with Normal or Binomial Distribution for a Level of 7.5 m

The reason the results of two different methods are so close is the relatively large number of crossings. With a large sample, the binomial distribution of the total number of crossings can be very well approximated with the normal distribution with the following mean value and variance:

$$m^*_{NU} = NU^* = 721\,; \quad V^*_{NU} = Np^*(1-p^*) = 720.28 \tag{1.92}$$

The binomial distribution of total number of crossings with parameter p^* and normal distribution with mean value and variance (1.90) are shown in Figure 1.5.

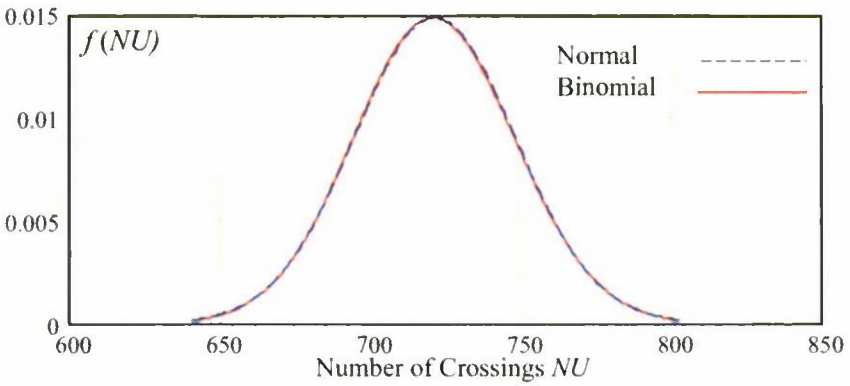

Figure 1.5 Normal and Binomial Distribution of Number of Crossing for the Level 7.5 m

The difference between the two distributions can be slightly more if the level for crossing is raised and number of crossings is less, but even in the case of level 11 m with only 10 crossings, the difference in confidence intervals calculated with the two different methods is not significant, see Figure 1.5 and Figure 1.6.

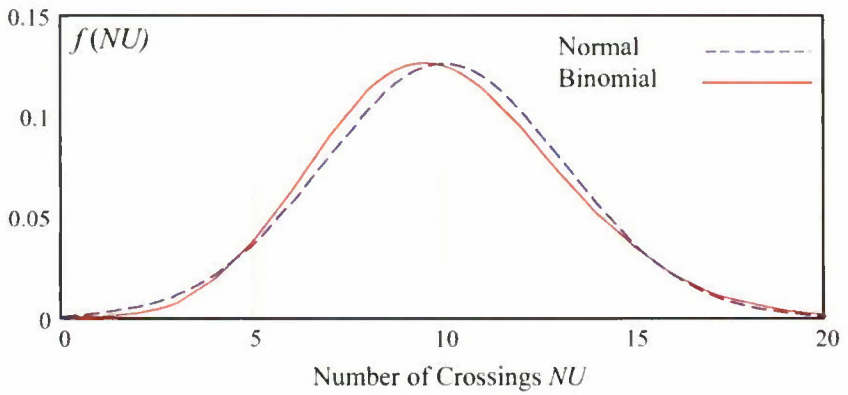

Figure 1.6. Normal and Binomial Distribution of Number of Crossings for the Level 11 m

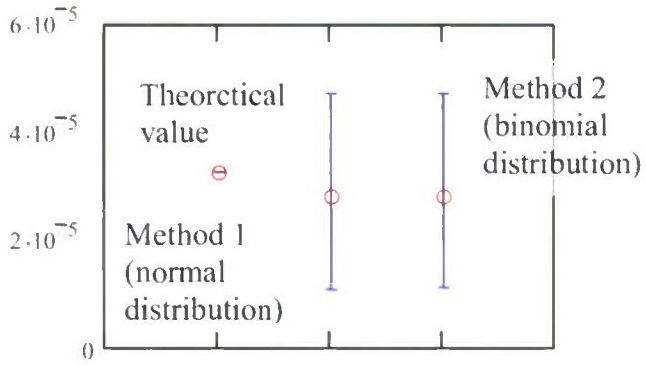

Figure 1.7. Confidence Intervals for the Upcrossing Rate Calculated with Normal and Binomial Distributions for a Level of 11.0 m

1.2.4. Mean Time Before and Between Events

An estimate for the rate of events can also be evaluated from statistics of time before or between events using formula (1.35). This provides an important link to reliability engineering, where time to failure is one of the principal metrics.

In general, stability failure can be considered in terms of conventional reliability theory (Sevastianov, 1963, 1994). Most of engineering practice in reliability works with statistics of time-to-failure, where the Exponential Distribution is only one of many models used (see, for example Meekar and Escobar 1998). One of the authors applied this approach for stability failures using statistical data resulting from numerical simulation (Ayyub, *et al* 2006). These data included time before failure, so a classic reliability approach was used. The main advantage of such an approach is that it does not require a-priori knowledge of the distribution of time before or between the failures. While an exponential distribution was used, it is not required and any other appropriate model could be applied.

The assumption that time before or between failures follows an exponential distribution allows significant simplification of the problem as only one parameter needs to be estimated. As shown above, the exponential distribution is derived formally from upcrossing theory assuming the independence of upcrossings (this assumption is considered in details in the next section). The exponential distribution connects the mean number of upcrossings and parameters of the distribution of time before or between the failures.

The assumption of an exponential distribution does not contradict to experimental results obtained by Ananiev and Savchuck (1982). A description of these experiments (in English) is available from Belenky and Sevastianov (2007).

Once the exponential distribution is accepted a-priori, it can be demonstrated that counting events provides a more efficient way to estimate the distribution parameters. To carry out such a demonstration, the wave dataset described above was used. In addition to counting upcrossings, a sample of time between crossings (including the interval between the start and the first crossing) and a sample of intervals before the first crossing have been populated:

$$Tcr_k = t_{i+1,j} - t_{i,j} \qquad k = 1,2...N_{cr} \tag{1.93}$$

Here Tcr is the set of time intervals between upcrossings, index i relates to i^{th} crossing occurring at j^{th} record, k is a counter for upcrossing for the entire dataset and N_{cr} is total number of upcrossings in the dataset:

$$Tf_j = t_{1,j} \tag{1.94}$$

Here Tf is time before the first upcrossing and the index j refers to j^{th} record.

The estimate of the mean value for the time between and before the crossings is:

$$m^*_{Tcr} = \frac{1}{N_{cr}} \sum_{k=1}^{N_{cr}} Tcr_k \tag{1.95}$$

The estimate m^*_{Tcr} is a random number, as it is a finite sum of random variables with an exponential distribution. The distribution of a sum tends to normal per the Central Limit Theorem (Strictly speaking, it is a truncated normal distribution as the estimate of mean time cannot be negative).

As the mean value is an unbiased estimate, the mean value of its distribution equals to the estimate itself (1.93), while the variance is expressed as:

$$V(m^*_{Tcr}) = \frac{V^*_{Tcr}}{N_{cr}} \tag{1.96}$$

The variance of time between upcrossings V^*_{Tcr} can be estimated as:

$$V^*_{Tcr} = \frac{1}{N_{cr} - 1} \sum_{k=1}^{N_{cr}} \left(Tcr_k - m^*_{Tcr}\right)^2 \tag{1.97}$$

Then, the estimate of the mean time between crossings is expressed as:

$$m^*_{TcrU} = m^*_{Tcr} + K_\beta \sqrt{V(m^*_{Tcr})} \qquad m^*_{TcrL} = m^*_{Tcr} - K_\beta \sqrt{V(m^*_{Tcr})} \tag{1.98}$$

Here m^*_{TcrU} and m^*_{TcrL} are upper and lower confidence interval boundaries of the estimate. The estimate of the upcrossing rate can then be expressed as:

$$\lambda^*_T = \left(m^*_{Tcr}\right)^{-1}; \quad \lambda^*_{TU} = \left(m^*_{TcrL}\right)^{-1}; \quad \lambda^*_{TL} = \left(m^*_{TcrU}\right)^{-1} \tag{1.99}$$

Where λ^*_T is the upcrossing rate estimate based on time between upcrossings while λ^*_{TU} and λ^*_{TL} are the upper and lower boundaries of the confidence interval, respectively.

Another estimate can be evaluated using only time interval before the first upcrossing:

$$m^*_{Fcr} = \frac{1}{N_{Fcr}} \sum_{k=1}^{N_{Fcr}} Tf_k \qquad (1.100)$$

Here N_{Fcr} is number of records with at least one upcrossing. The boundaries of the confidenee interval are calculated in a manner similar to formulae (1.94-1.97)

$$V^*_{Fcr} = \frac{1}{N_{Fcr} - 1} \sum_{k=1}^{N_{Fcr}} \left(Tf_k - m^*_{Fcr}\right)^2 \quad ; \quad V(m^*_{Fcr}) = \frac{V^*_{Fcr}}{N_{Fcr}} \qquad (1.101)$$

$$m^*_{FcrU} = m^*_{Fcr} + K_\beta \sqrt{V(m^*_{Fcr})} \qquad m^*_{FcrL} = m^*_{Fcr} - K_\beta \sqrt{V(m^*_{Fcr})} \qquad (1.102)$$

$$\lambda^*_{FT} = \left(m^*_{Fcr}\right)^{-1} ; \quad \lambda^*_{FU} = \left(m^*_{FcrL}\right)^{-1} ; \quad \lambda^*_{FL} = \left(m^*_{FcrU}\right)^{-1} \qquad (1.103)$$

Here V^*_{Fcr} is the estimate of the variance of the time before the first uperossing. $V(m^*_{Fcr})$ is the estimate of the variance of the mean of time before the first upcrossing, m^*_{FcrU} and m^*_{FcrL} are the upper and lower boundaries of the confidence interval for the mean time before the first crossing. λ^*_{FT}, λ^*_{FU} , and λ^*_{FL} are the estimates of the upcrossing rate based on the time before the first erossing and its upper and lower boundaries, respectively.

Figure 1.8 compares the theoretical rate of upcrossing for a level of 5 m with estimates carried out with several methods. The data set consists of 5407 events based on the previously described numerical example. As is ean be seen from this figure, all the estimates contain the theoretical value in their eonfidence intervals, therefore all the methods were able to yield correct result in this case. It is also clear from the Figure 1.8 that the methods based on counting of events and time between events provide better estimates then the method based on the time to the first upcrossing, as the latter one utilizes a smaller sample.

Figure 1.9 eompares theoretieal rate of uperossing for a level of 9 m with estimates carried out with several methods. The data set consists of 153 upcrossings totally and 111 first uperossings. The estimates obtained with time between or before the crossing(s) do not inelude the theoretieal value in their eonfidence intervals, while the method based on counting events still yields a correct estimate.

The reason why time-based estimates are biased is that the sample is limited in time. It eannot include any data beyond the length of a record. Therefore the mean time before the erossing is biased towards smaller values and rate of events overestimates the true value. The standard way of correcting such a bias is a procedure of eensoring (see, for example Meekar and Escobar, 1998).

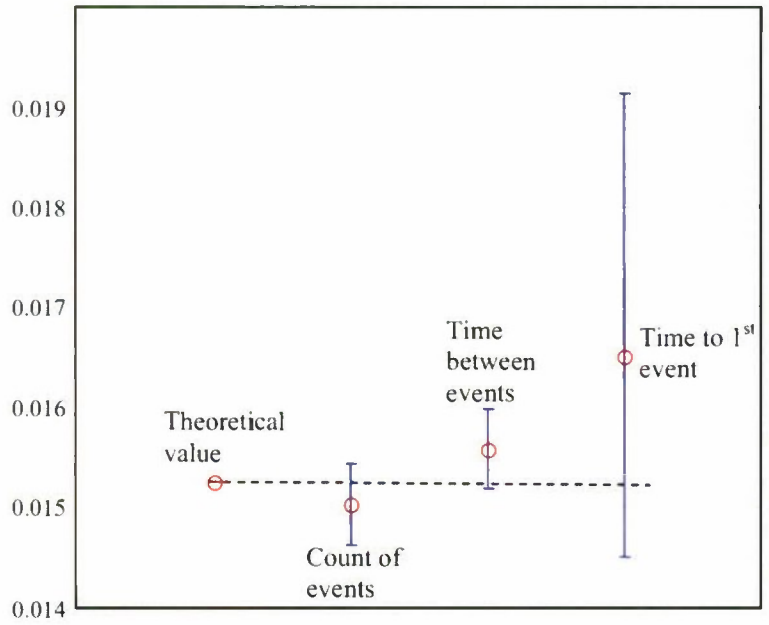

Figure 1.8. Comparison of Different Methods to Estimate Upcrossing Rate for the Numerical Example for a Level of 5 m (Total Number of Upcrossings 5407).

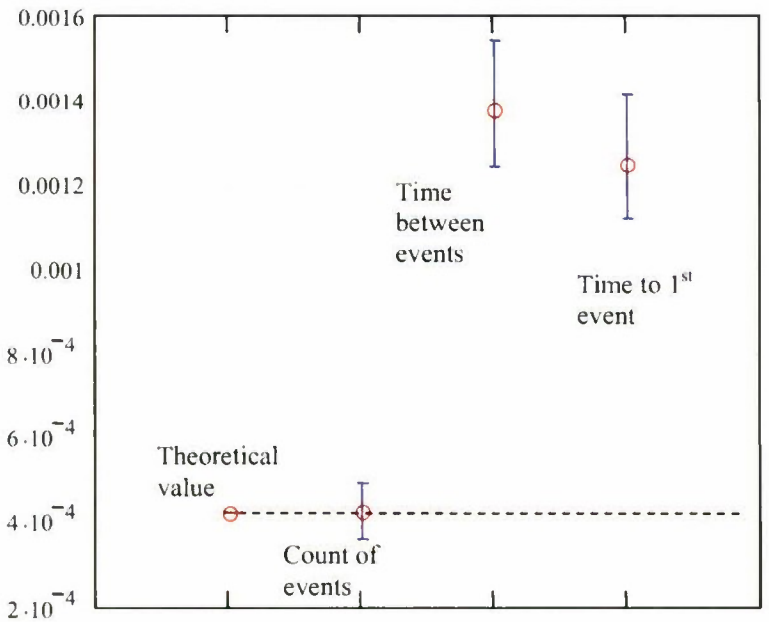

Figure 1.9. Comparison of Different Methods to Estimate Upcrossing Rate for the Numerical Example for a Level 9 m (Total Number of Upcrossings 153).

Subsequently a censoring procedure (Ayyub, *et al*, 2006) was applied to estimate the rate of events from time intervals before the first upcrossing. The sample is made up in the following way:

$$Tfc_j = \begin{cases} Tf_j & if \quad N_{Uj} > 0 \\ T_S & if \quad N_{Uj} = 0 \end{cases} \tag{1.104}$$

The censored mean time before the first crossing is expressed as

$$m^*_{FC} = \frac{1}{N_{Fcr}} \sum_{k=1}^{N_R} Tfc_k \tag{1.105}$$

Here N_R is a number of records while N_{Fcr} is the number of records with at least one upcrossing.

Direct evaluation of the confidence interval of the censored mean may present certain difficulties. If the number of observed crossings is small, the variance estimate of the censored data also tends to be small as most of the data points equals to the duration of simulation. Small variance estimate leads to a narrow confidence interval; this creates a paradox as decreasing of the sample size is expected to increase statistical uncertainty. This paradox is caused by the fact that censored data are expected to estimate bounds, not the actual value; see, for example, (Meekar and Escobar 1998). Generally censoring the data does not increase or decrease the statistical uncertainty. Therefore, the width of confidence interval for the uncensored mean estimate can be used with censored mean estimate;

$$\lambda^*_{FC} = \left(m^*_{FC}\right)^{-1}; \quad \lambda^*_{FCU} = \lambda^*_{FU} - \lambda^*_{FT} + \lambda^*_{FC}; \quad \lambda^*_{FCL} = \lambda^*_{FL} - \lambda^*_{FT} + \lambda^*_{FC} \tag{1.106}$$

Here $\lambda^*_{FC}, \lambda^*_{FCU}, \lambda^*_{FCL}$ are the estimated event rates based on the censored time before the first crossing and its upper and lower boundaries, respectively.

Figure 1.10 compares theoretical rate of events with statistical values estimated with two different methods; the level of upcrossings was equal to 9 m and the sample size was 111. The rate of events estimated with time between events is not considered here, as it is not clear how to censor this type of data.

As it can be seen from Figure 1.10, the censoring removed the bias observed in Figure 1.9; so both methods have shown a correct estimate for the example considered. The confidence interval for the second method (based on censored time to the first event) is slightly wider, as a sample size for the time before the first upcrossing is less than the sample size for counting crossings (111 vs. 153; 34 records had more than one upcrossing).

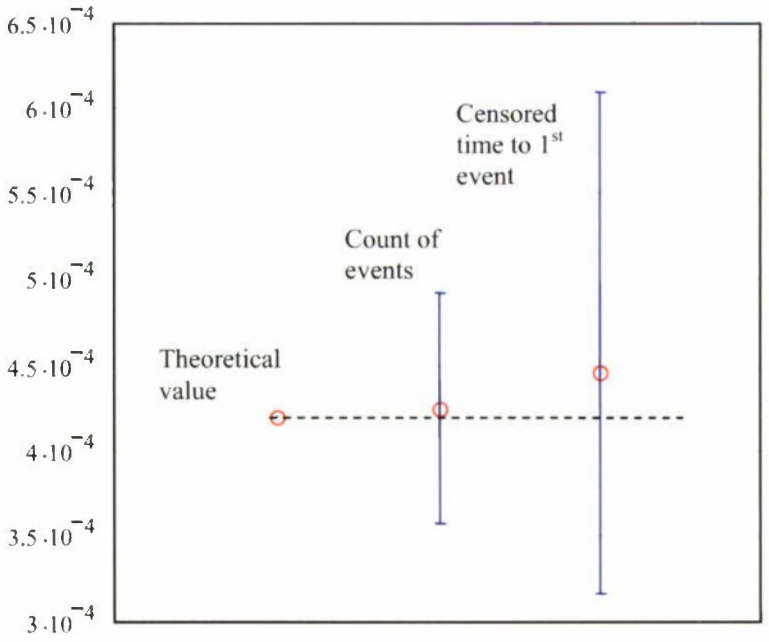

Figure 1.10. Comparison of Different Methods to Estimate Upcrossing Rate for the Numerical Example for a Level of 9 m (Total Number of Upcrossings 153, Number of First Upcrossings 111).

1.3. Distributions Related with Upcrossing Events

1.3.1. Limitations of Poisson Distribution

As it was shown in the previous section, the derivation of the Poisson distribution leads to a very important practical result: the distribution of time before or between crossings is exponential. To characterize the exponential distribution, only one parameter has to be estimated. This parameter is the average number of upcrossings per unit of time (mean upcrossing rate). It is equivalent to the inverse of the average time before/between crossings. Once this parameter is known, the probability of at least one crossing can be trivially evaluated for any given time of exposure.

The derivation of the Poisson and exponential distributions were, however, not free of assumptions. Application of the binomial distribution assumes repeating independent Bernoulli trials on each time step. A Bernoulli trial is a random event that can produce only two outcomes, usually called "success" or "failure". These outcomes are related here to either the occurrence or non-occurrence of an upcrossing at this instant of time.

The independence of Bernoulli trials, however, is not always guaranteed for the upcrossing of a general stochastic process (i.e. it is not a white noise and its autocorrelation function is generally not a delta-function). Stochastic processes, such as wave elevation, wave slope, or roll angle, posseses a certain amount of inertia. The instantaneous value of the process cannot change abruptly. Therefore the values in neighboring time steps are dependent, provided the time step is reasonably small. This dependence has a finite duration and the time it takes the autocorrelation function to drop

below a given level is often used as a measure of this dependence. As it can be seen from Figure 1.11 (a zoomed in version of Figure 1.2), it takes 40-45 seconds for this autocorrelation to die out to a level below 0.05. While this criterion remains somewhat arbitrary, it can still be used in the first expansion. For a Guassian (normal) process, the autocorrelation function captures all of the information about dependence. For non-Guassian processes, the absence of correlation does not guarantee independence.

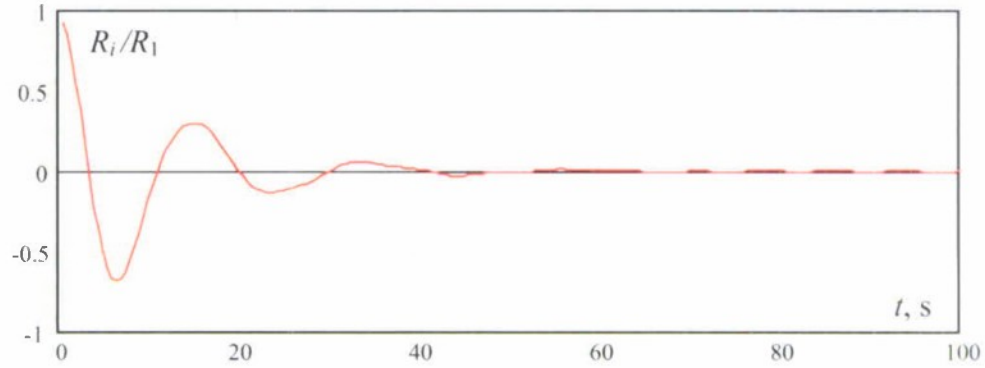

Figure 1.11. Sample Autocorrelation Function (Zoomed in From Figure 1.2)

Therefore, if time between neighboring upcrossing events exceeds the time for autocorrelation function to die out, one can assume these events are independent. The time between the events, however, is a random number; therefore, the judgment on independence only can be made in probabilistic sense.

Since the exponential distribution of the time before and between the events is the most important consequence of the Poisson distribution, it makes sense to evaluate if such hypothesis contradicts observed data. Standard statistical procedures used for these purposes can be employed as part of the procedure to test if impendence of upcrossing can be assumed and Poisson distribution is applicable.

1.3.2. Distribution of Time before Event

Following the previous works of Ayyub, *et al* (2006) and Belenky, *et al* (2007), a sample of time before the first upcrossing is analyzed. This analysis is carried out for several crossing levels to examine the influence of the dependence between crossings and sample size on the statistical estimates of the upcrossing rate.

For the given example with a Gaussian distribution, the theoretical mean time before of between events may be calculated by simply inverting formula (1.20) or (1.83):

$$m_{Tcr} = \left(f(a) \int_0^{\infty} f(\dot{\phi}) \dot{\phi} d\dot{\phi} \right)^{-1} = \sqrt{\frac{V_{\zeta d}}{V_{\zeta d}}} \exp\left(\frac{a^2}{2V_{\zeta d}} \right) \qquad (1.107)$$

Formula (1.107) is an exponential funetion. The dependenee is depicted in Figure 1.12 for the wave example considered in this section. It can be seen from this figure that the time for the autocorrelation function to die out corresponds to a level of 4.2-4.4 m.

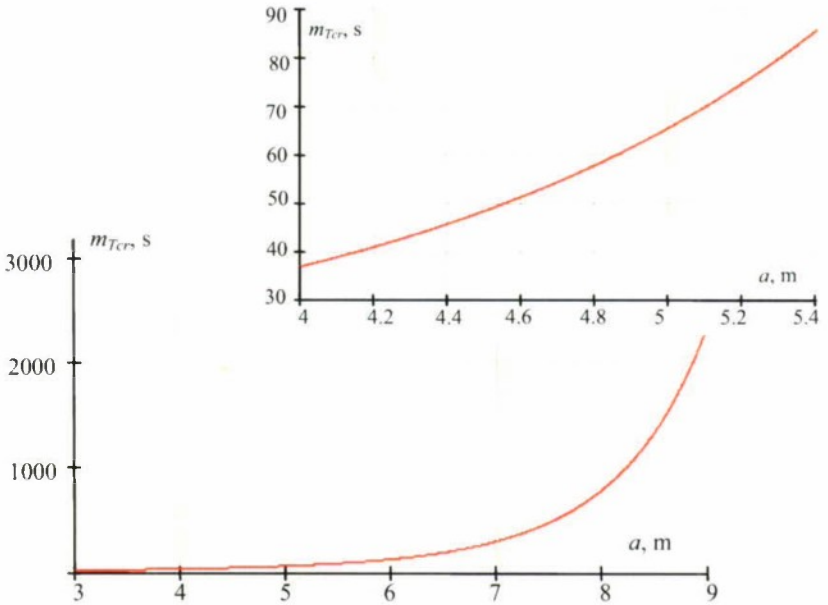

Figure 1.12. Theoretical mean time before ore between upcrossing events shown as a function of level of upcrossing *a*

It is well known the mean value and standard deviation of the exponential distribution are identical. This condition was analyzed by Belenky *et al* (2007) as a possible indicator of the applicability of the Poisson distribution and it was shown to not be the best way. At the same time, a lower boundary of their confidence interval compared with the autocorrelation decay time may produce relevant information.

The estimate of the mean value and variance of the time before the first event is given by formula (1.98) and (1.99), while the confidence interval for mean value estimate can be calculated with formulae (1.100). In order to calculate confidence interval for the variance estimate, the value of the fourth central moment M_4 is necessary:

$$V\{V^*\} = \frac{1}{N} M_4 - \frac{N-3}{N(N-1)} (V^*)^2 \tag{1.108}$$

Here N is number of points and V^* is estimate of variance. Estimating the fourth central moment directly form a statistical sample is known to be difficult, due to sensitivity of the numerical values to outliers. Therefore expressing a fourth moment through the variance using a certain assumption of the character of distribution has been a standard technique. As the distribution of the time before the first event is expected to be exponential, Belenky, *et al* (2007) used the relation derived from the exponential distribution:

$$M_4 = 9 \cdot V^2 \tag{1.109}$$

This leads to the following expression for the variance of the variance estimate:

$$V\{V^*\} = \frac{8N-6}{N(N-1)}(V^*)^2 \tag{1.110}$$

Once the mean value and variance of the variance estimate are found, a normal distribution is used to find boundaries of the confidence interval. This approach is quite common, however, caution should be exercised, as the normal distribution is defined from -∞ to +∞, while variance by the definition is a non-negative value. Therefore, an additional check is needed or the distribution must be truncated at zero.

$$V^*_{FcrU} = V^*_{Fcr} + K_\beta\sqrt{V(V^*_{Fcr})} \qquad V^*_{FcrL} = V^*_{Fcr} - K_\beta\sqrt{V(V^*_{Fcr})} \tag{1.111}$$

The standard deviation is calculated:

$$\sigma^*_{Fcr} = \sqrt{V^*_{Fcr}} \quad ; \quad \sigma^*_{FcrU} = \sqrt{V^*_{FcrU}} \quad ; \quad \sigma^*_{FcrL} = \sqrt{V^*_{FcrL}} \tag{1.112}$$

The results are shown in Figure 1.13 for the level of crossing of 5 m. As it can be seen, the estimates of the mean value and standard deviation are statistically identical. Also the lower boundary of the mean value is above 50 seconds, i.e., more than the interval of time for the autocorrelation function to die out. Both of these observations are symptoms of the exponential distribution.

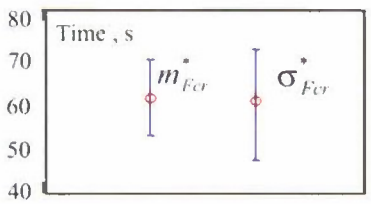

Figure 1.13. Estimates of mean value and standard deviation for time before the first event. Level of crossing 5m, 200 crossings total.

Figure 1.14 shows a histogram, the theoretical distribution, and three distributions based on different statistical parameters. For the level at 5m, all 200 records had at least one upcrossing, so the size of the sample equals 200. The bin width for the histogram was calculated as (Scott, 1979):

$$W = \frac{3.5\sigma^*_{Fcr}}{\sqrt[3]{N}} \tag{1.113}$$

The histogram in Figure 1.14 is presented in terms of PDF:

$$h_j = \frac{H_j}{W \cdot N} \tag{1.114}$$

Here H_j is the number of cases that fits in the j^{th} bin and N is total number of cases.

A Pearson chi-square goodness-of-fit test was performed for each of the distributions. The value of χ^2, number of degrees of freedom d, and $P(\chi^2,d)$ – probability that the difference between the fit and the histogram is caused by random reasons are also placed into Figure 1.14. The test shows that the fit is good for all four curves, as the probability is well above the accepted significance value of 0.05.

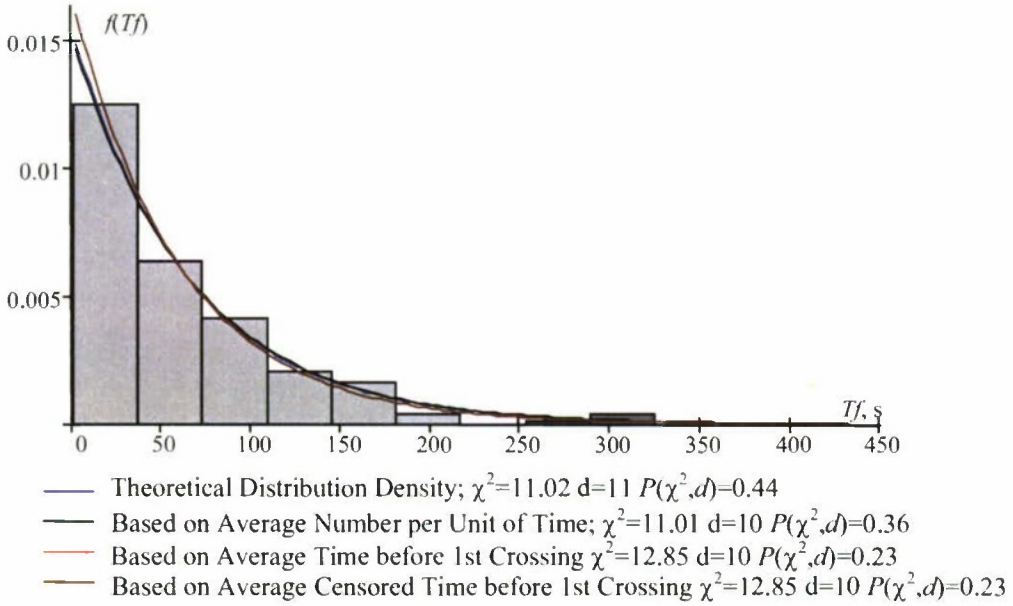

Figure 1.14. Distribution of time intervals before the first crossing. Level of crossing 5m, 200 crossings total.

Another example considered above was for 9 m level of crossing. The importance of this example is that it contains 89 records without any upcrossings, so the effect of the censoring technique can be demonstrated. Figure 1.15 shows a histogram (in terms of PDF) along with distribution curves using different parameters as well as results of Pearson chi-square goodness-of-fit test. The insert shows estimates for mean value and standard deviation with the appropriate confidence interval.

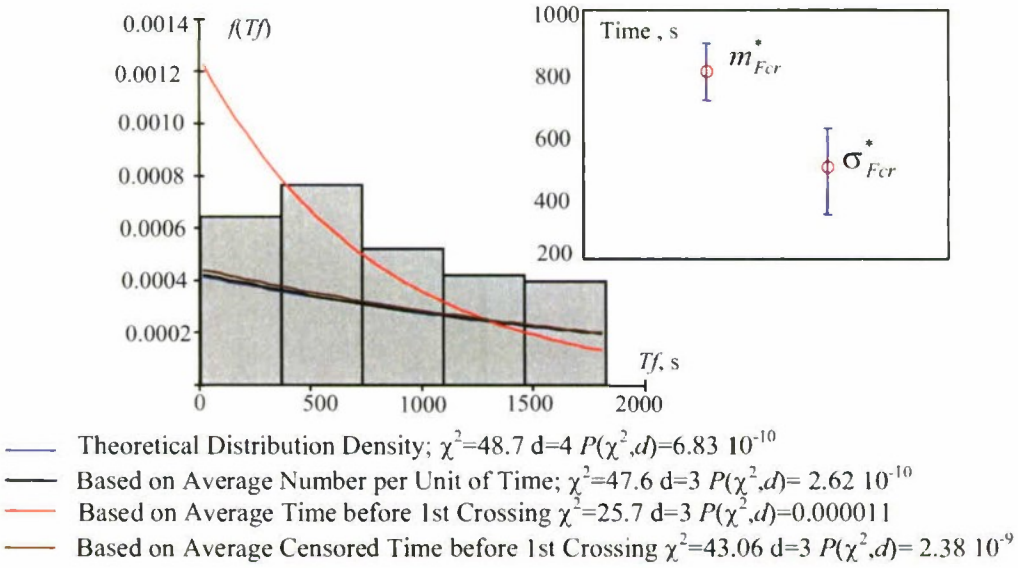

Figure 1.15. Histogram of Time Before the First Crossing for a Level of 9m (111 Crossings Total)

The estimates of the mean value and standard deviation are statistically different; their confidence intervals do not have any overlap. None of the curves fit the histogram. Obviously, the hypothesis of an exponential distribution is not supported by the observed data. At the same time, it is known from the upcrossing theory (and was shown in the derivations above) that time intervals before the first crossing must follow an exponential distribution if the number of upcrossings follows a Poisson distribution.

The most important condition to satisfy is the independence of upcrossings. For the considered example with a Gaussian process, independence of upcrossings is achieved when the time between the neighboring upcrossings exceeds the time for the autocorrelation function to die out. Increasing the level of crossing increases the mean value of the time before upcrossing from about 60 seconds for a level of 5 m to about 800 seconds for a level of 9 m. At the same time, the hypothesis of an exponential distribution was not rejected for a level of 5 m, but was rejected for a level of 9 m. The reason for this rejection is likely to be unrelated to the applicability of the Poisson distribution to the number of crossings.

In a sense, a similar situation was observed in Figure 1.9, where the results for upcrossing rates calculated by counting events or averaging the time before the first event were found to be drastically different. The reason for the difference was the limited simulation duration, which can bias the average time, but not the number of events. This discrepancy was resolved by censoring the data of time intervals before the first upcrossing, where it was assumed that more upcrossings could be encountered if the duration of records would be longer.

The same assumption can be made for a histogram, as well, by adjusting the total number of cases:

$$h_{Sj} = \frac{H_j}{W \cdot N_R} \tag{1.115}$$

Here N_R =200 is the total number of records. Obviously, the normalization condition for this expression is no longer met, as the rest of the data is assumed to be beyond the length of a record.

The "censored" histogram is shown in Figure 1.16 along with the same set of distribution curves. The Pearson chi-square goodness-of-fit test has shown that only the curve based on uncensored average time before the first upcrossing does not fit the data. All other curves show robust agreement with the data.

To complete the examination of the time before the first upcrossing, we now examine cases where the conditions for a Poissonian process are violated. The crossing level has been set to 3 m where 15201 upcrossings were observed. As it can be seen from Figure 1.17, most of upcrossings are clustered and there are many cases when neighboring periods have upcrossings. At the same time, some peaks remain below the level and some of the time between crossings may be longer than just a period.

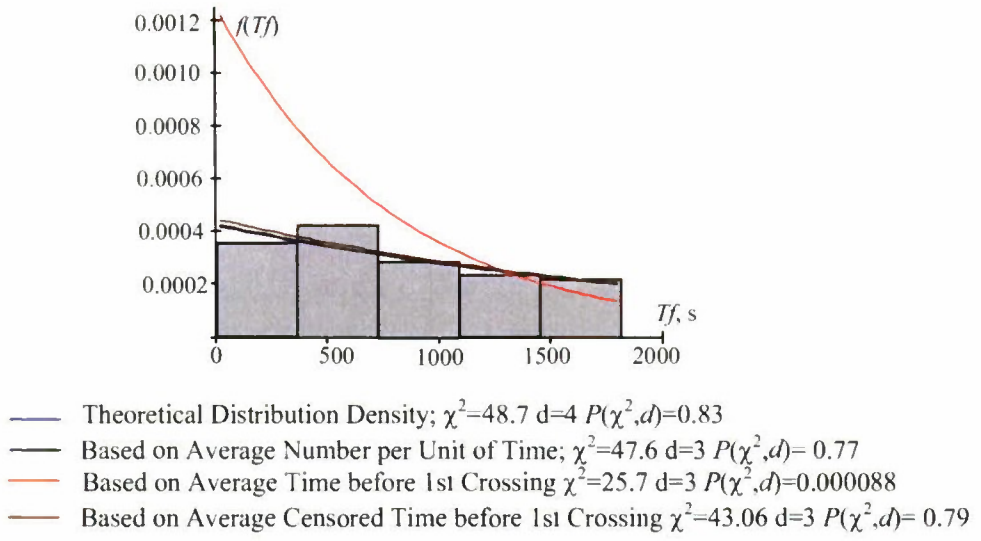

Figure 1.16. Censored Histogram of Time Before the First Crossing For a Level of 9 m (111 Crossings Total)

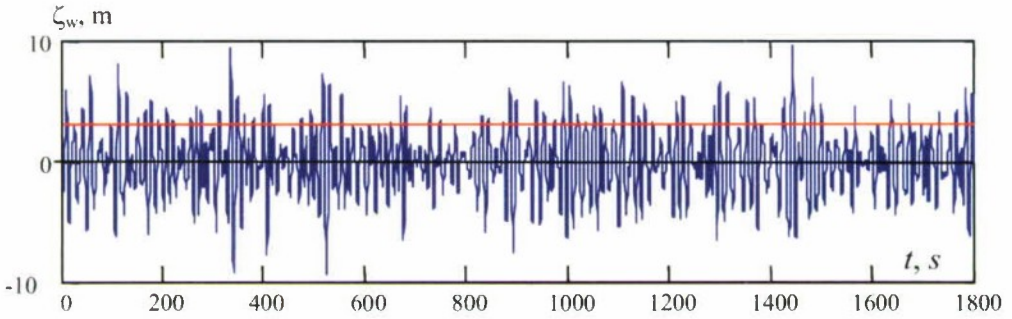

Figure 1.17. Record 1 of the Process of Wave Elevations; Upcrossing Level 3 m

Figure 1.18 shows a histogram of the time before the first upcrossing. The estimates for the mean value and variance (with confindence interval) are shown in the inset of the figure. Despite the fact that these estimates are statistically equal, the entire confidence interval of the mean value estimate is well below 40 seconds– the time duration needed for the autocorrelation function to die out.

A Pearson chi-square goodness-of-fit test rejects the exponential distribution based on the theoretical upcrossing rate as well as based on the upcrossing rate estimated from counting of events. At the same time, the test does not reject the exponential distribution based on estimate of mean time before the first upcrossing (there is no difference between censored and uncensored mean values, as every record has at least one upcrossing). These results may seem confusing, but certain conclusions can still be drawn.

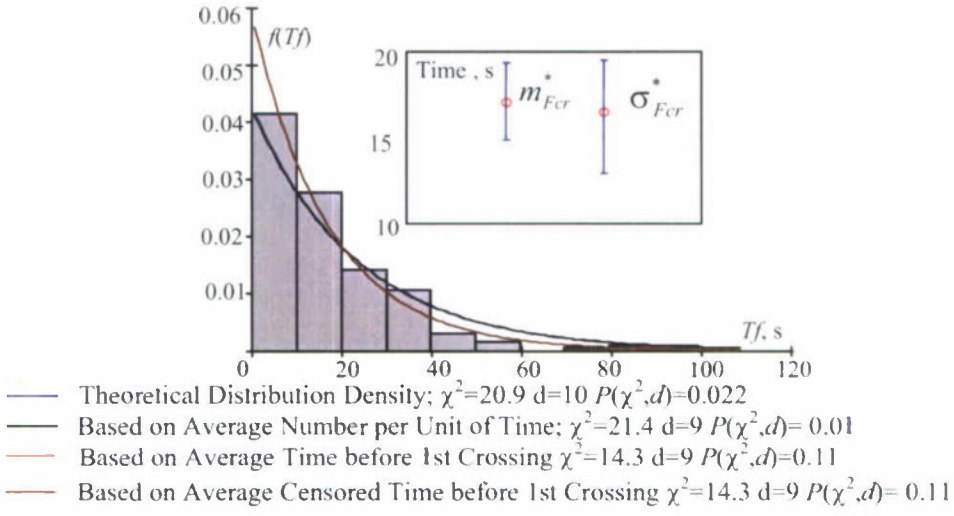

Figure 1.18. Distribution of time intervals before the first crossing. Level of crossing 3 m, 200 crossings total.

The equality of mean value and standard deviation is a necessary, but not a sufficient condition for the exponential distribution. If the mean value and standard deviation (including confidence interval extents) are smaller than the time required for the autocorrelation function to die out, the Poisson distribution is likely inapplicable due to data dependence. The entire confidence interval laying in the domain, where autocorrelation still is not insignificant (see Figure 1.11), suggests possible dependence of neighbor upcrossing and therefore the inapplicability of Poisson distribution.

There is a difference between the upcrossing rate calculated from the mean value of time before the upcrossing and by the counting of events, exhibited in the different outcomes of the goodness-of-fit test. Based on the previous paragraph, the difference between the two could be explained by insufficient duration of a record or dependence of neighboring upcrossing resulting in violation of the Poisson distribution. Since every record has at least one upcrossing, there is no difference between censored and uncensored data. Therefore, the reason for the discrepancy is the violation of Poisson distribution.

The derivation of the theoretical formula for upcrossing rate (equations 1.10-1.19) relied only on the assumptions of continuity and stationarity, but not on the assumption of the Poisson distribution. The formula (1.20) is correct for any level of crossing and the theoretical curve in Figure 1.19 can be considered as a true answer. This confirms the conclusion made above on the non-Poissonian character of the distribution of the number of upcrossings for the level of 3m.

Further lowering the crossing level down to 1 m in order to observe what changes, if any, there are, we see an upcrossing on almost every period, see Figure 1.19.

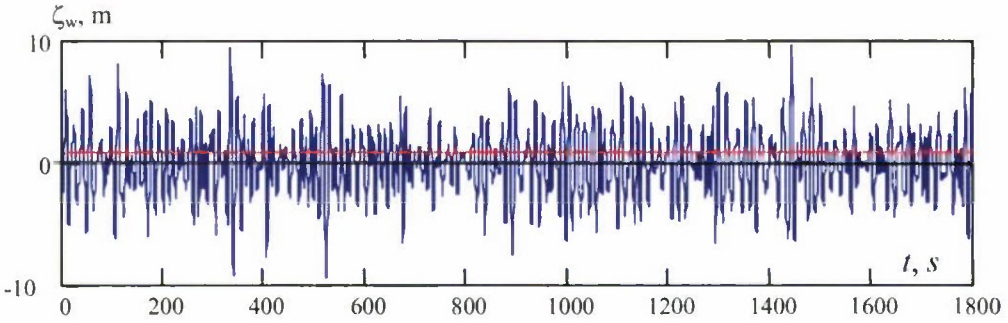

Figure 1.19. Record 1 of the Process of Wave Elevations; Upcrossing Level 1 m

Figure 1.20 shows a histogram of time before the first crossing (in terms of PDF) for the level of crossing of 1m along with estimates of mean value and standard deviations. In contrast with the previous example, with 3 m level of crossing, there is no indication of the applicability of the exponential distribution for the time before the first crossing or the Poisson distribution for the number of upcrossings.

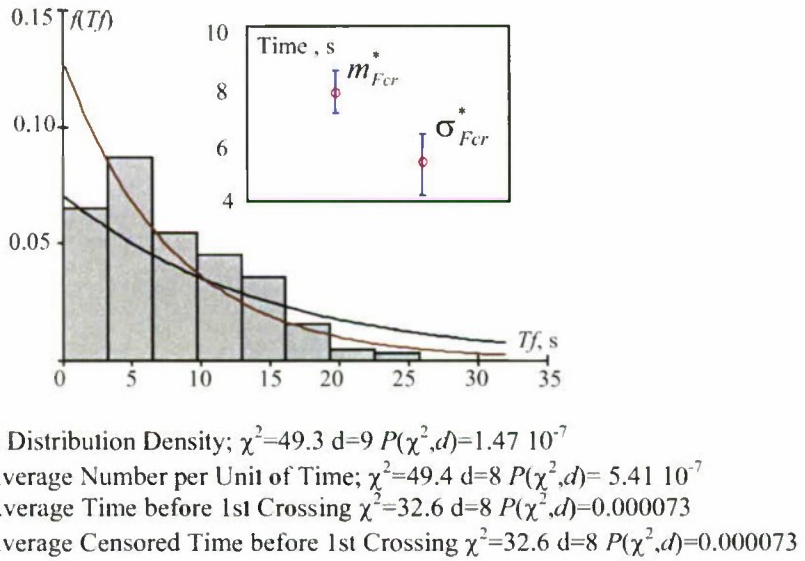

Figure 1.20. Distribution of Time Before the First Crossing for a Level 1 m (200 Crossings Total)

The histogram shows a peak around 5 seconds. This is a little short than a half of the mean zero-crossing period of 11.6 seconds and, probably represents the most probable time from the start until the first upcrossing is encountered.

Note that if a record starts above the given level, the first upcrossing will only be detected when the process comes back below the level and crosses it again. This may have an influence on the shape of the histogram.

1.3.3. Distribution of the Time Between Events

The derivation of the formulae for the time between and before events (1.30-1.37) is based on the Poisson distribution for the number of upcrossings and targets a time without upcrossings. This random number can be interpreted as the time before the first upcrossing or as the time between upcrossings. Therefore, the exponential distribution must be equally applicable to both these random variables. Consideration of the distribution of time before the first event, as in the section above, has shown that the duration of a record is another major factor. In order to demonstrate the exponential distribution statistically the records have to be long enough, so all (or a statistically significant number) of records must have at least one upcrossing in addition to satisfying Poisson distribution conditions.

The objective of this section is to demonstrate, with numerical examples, how the upcrossing level affects the statistical distribution of time between events. Setting the lower level gives a statistically significant number of upcrossings (or records with upcrossings), but may lead to a violation of the Poisson distribution condition, if upcrossings occur too frequently to be independent random events. On the other hand, if the level is too high, the duration of a record may be insufficient.

Figure 1.21 shows a histogram (in terms of PDF) of time intervals between upcrossings along with estimates of mean value and standard deviation. Results of Pearson chi-square goodness-of-fit tests are also shown for the five curves as specified in the figure. The confidence intervals of the mean value and standard deviation have significant overlap. Also, the lower boundary of the confidence interval for the mean value estimate is about 340 seconds, enough time for the autocorrelation function to die out, so applicability of the exponential distribution is not excluded. The shape of the histogram also suggests exponential distribution.

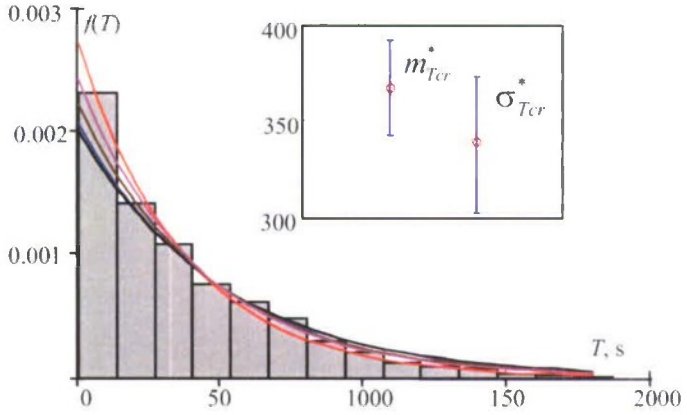

Figure 1.21. Distribution of Time Between Upcrossings for a Level of 7.5 m (721 Crossings Total, 196 Records with at Least One Crossing)

As indicated above, five different curve fits were tried. All of these curves were exponential distributions but the parameter was calculated differently.. The Pearson chi-square goodness-of-fit test shows that three of the methods for selecting the distribution parameter yield a fitted distribution that is not rejected (the probability is greater and 0.05, the generally accepted significance level), that is the curves match the data. At the same time two curves show a probability less than 0.05, so the hypothesis is rejected; meaning that these particular curves do not match the data.

The distribution parameter calculated through averaging of the intervals between upcrossings (1.95) passes the test. This confirms the above observation on exponential character of the distribution, in general.

However, theoretical distribution does not match the data. The distribution parameter was calculated by formula (1.83) using variance of wave elevations and their derivatives "as discretized". This discrepancy is caused by an insufficient length of record for this particular level of crossing (Belenky, *et al*, 2007). The reason is that the sample is limited by the length of a record and intervals between upcrossing longer than duration of a record are absent from the sample. These intervals are statistically significant for the level of 7.5 m.

The rate of events calculated as an average number of upcrossings per unit of time (1.82) was found to be quite close to the theoretical value, see Figure 1.22. Therefore, the exponential distribution based on this value is very close to theoretical one. Then for the same reason, as the theoretical one, it is rejected by the observed data; as the intervals between upcrossings that are longer than the duration of a record still have statistical significance for the considered level.

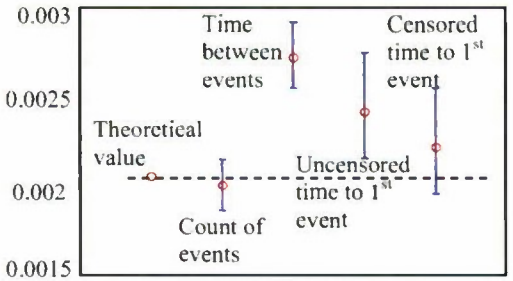

Figure 1.22. Comparison of Different Methods to Estimate the Parameter of the Exponential Distribution (Upcrossing Rate) for a Level of 7.5 m (721 Crossings Total, 196 Records With at Least One Crossing)

The distribution based on the uncensored average time before the first upcrossing, is not rejected by the observed data. This method gives similar results to the one based on average time between the upcrossing, see also Figure 1.22. It is suggested by both Figures Figure 1.21 and Figure 1.22 that the average time before the 1st upcrossing has a bias leading to overestimation the rate of events, as was discussed in the previous section. This is notable, that the bias exists for the level of 7.5 m, with only 4 records without upcrossing, however it was enough to move the estimate away from the theoretical solution and provide a significant probability that the fit to biased data is good.

The censoring procedure moves the estimate back to the theoretical solution;

however, the relatively wide confidence interval still allows the goodness-of-fit test not to reject the distribution based on censored average time before the first crossing.

Figure 1.23 shows a histogram (in terms of PDF) of time intervals between upcrossing along with estimates of the mean value and standard deviation calculated for a level of 9 m. The results of the Pearson chi-square goodness-of-fit test are also shown for five curves as specified in the figure. None of them fit. Confidence intervals for estimates of the mean value and standard deviation do not have any overlap. Similar observations were made for distribution of time intervals before the first crossing, see Figure 1.15. However, the "censored" histogram in Figure 1.16 has confirmed that this was the case when there is a significant deficiency in the duration of the records, as the censored data confirms that the distribution is, in fact, exponential.

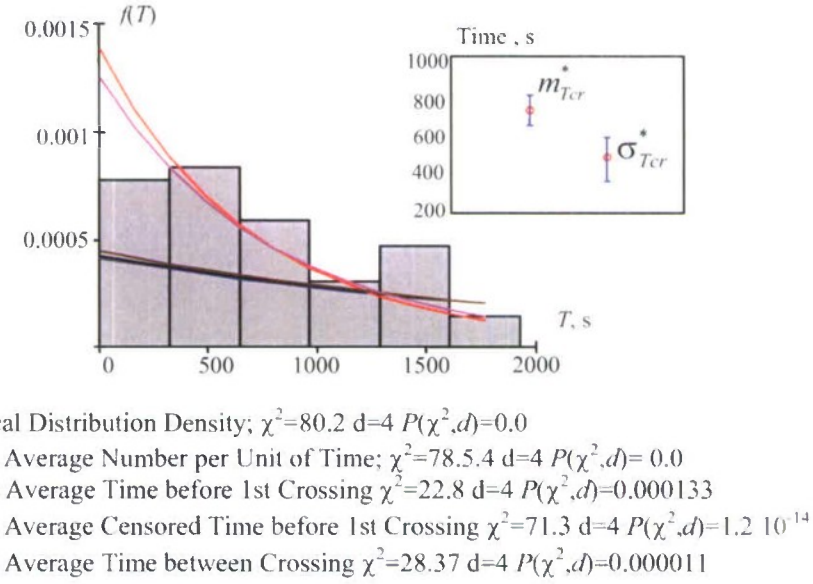

Figure 1.23. Distribution of Time Between Upcrossings For a Level of 9 m (153 Crossings Total, 111 Records with at Least One Crossing)

It is not clear how censoring can be applied for time intervals between the events; therefore, the case in Figure 1.23 cannot be resolved with this kind of statistics. In reality, the distribution, of course, must be exponential, as increasing the level cannot lead to violation of the Poisson distribution.

Comparing Figure 1.22 and Figure 1.23 is useful as it shows a tendency in the behavior of the curves when the level is increased. The theoretical distribution practically coincides with the curves based on average number of upcrossings per unit of time and on censored average time before the first upcrossing. The curves based on uncensored average time before the first upcrossing and average time between upcrossing move away from theoretical distribution, but remain close to each other. This tendency can also be seen in Figure 1.8 and Figure 1.9.

The opposite tendency can be observed when the crossing level is lowered, see

Figure 1.24. All five curves are visually closer to each other in comparison with Figure 1.21. Appearance of the histogram also suggests the exponential character of distribution. The confidence intervals for the estimates of the mean value and standard deviation have significant overlap. This also suggests that the exponential distribution is possibly applicable.

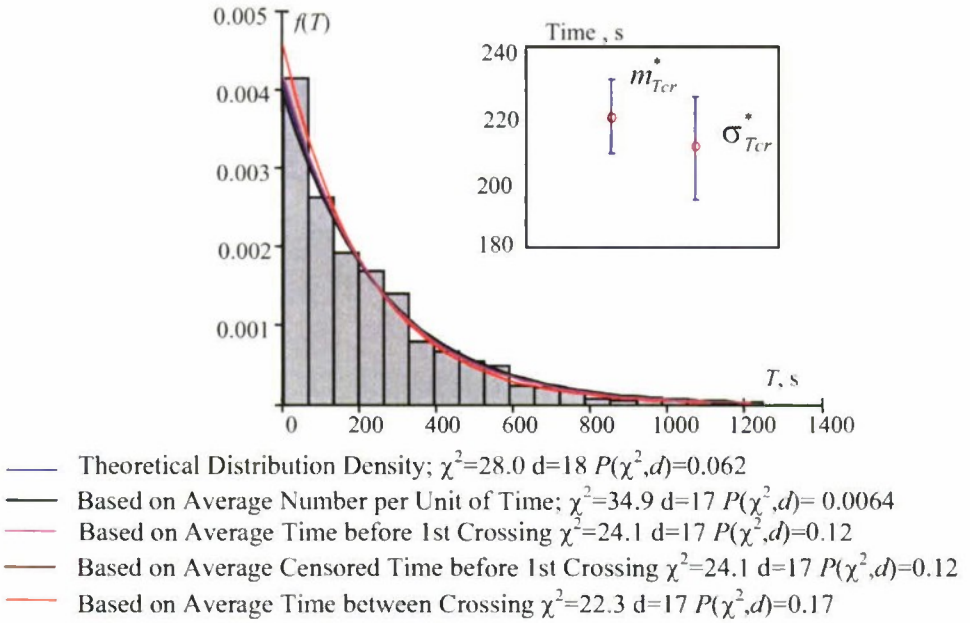

Figure 1.24. Distribution of Time Between Upcrossings For a Level of 6.75 m (1421 Crossings Total, All 200 records With at least One Crossing)

Only the distribution based on average number of crossings per unit of time is rejected by the goodness-of-fit test, while all other fits are supported by the data. The reason can be seen in Figure 1.25, where all the parameters are compared. First, the rate calculated as an average of time between the upcrossing still is different from the theoretical value. Apparently, duration of the record is still insufficient. The rate of upcrossing in Figure 1.25 calculated by counting includes the theoretical solution in its confidence interval, but the middle of the confidence interval happens to be a bit lower than the theoretical solution. This small difference was enough to reject the distribution based on counting of events.

Further lowering the crossing level (5.75 m) leads to an unexpected result: none of the curves fit the data, however all the curves are very close to each other, see Figure 1.26. At the same time, estimates of mean value and standard deviation have substantial overlap. In addition, the lower boundary of the 95% confidence interval lies around 100 seconds. This is still enough time for the autocorrelation function to die out. Detailed analysis shows that the absence of agreement is due to the value at the first bin; it is noticeably higher than expected. Additionally, the value at the second bin seems to be a bit lower. This may suggest some sensitivity to width of the bin that was calculated with formula (1.113) so far. A relatively small change of the bin width, from 23.9 s (Figure

1.26 upper) to 30 s (Figure 1.26 lower), eliminates this effect. All of the curves are supported by the data in the lower histogram shown in Figure 1.26.

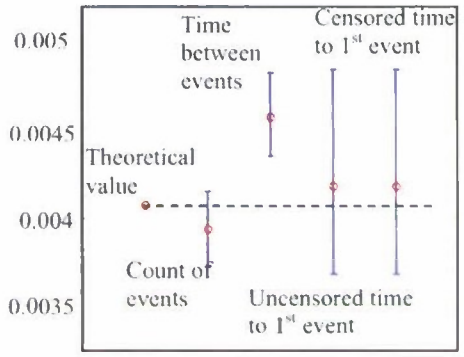

Figure 1.25. Comparison of Different Methods to estimate parameter of the exponential distribution (upcrossing rate). Level of crossing 6.75 m, 1421 crossings total, all 200 records with at least one crossing

Figure 1.27 shows histograms for the crossing level of 5 m. The top histogram in the figure shows the histogram with bin width according to formula (1.113); similar to the previous case, all the curves are very close to each other, but none of them fit the data. Now the value in the first bin is very small, while the second bin gives a very large number. It is still possible to make curves fit by a manual change of the bin width. However, the required change is much larger, increasing the bin width from 12 s (upper histogram in Figure 1.27) to 36 s (lower histogram in Figure 1.27). Setting the maximum time to 400 s was also needed in order to acheve satisfactory goodness-of-fit.

At the same time, other symptoms of exponential distribution are still present; the estimates of the mean value and the standard deviation show substantial overlap in their confidence intervals. The lower boundary of the confidence interval for the mean value estimate is about 62 seconds, still enough time for the autocorrelation function to die out.

The first bin of the upper histogram in Figure 1.26 and the second bin of the upper histogram in Figure 1.27 correspond to the value of 10-15 seconds. This range includes the mean period of the stochastic process. This may indicate that the reason the histogram deviates from the exponential distribution is the presence of wave groups. The level is low enough so that successive waves in a group all cross it. As these wave groups are still rare, they cannot yet break the Poisson distribution completely. Some integral characteristics are still present. At the same time, they are frequent enough to cause a local distortion of the exponential distribution, which is detected by the chi-square goodness-of-fit test.

Wb=23.9 s

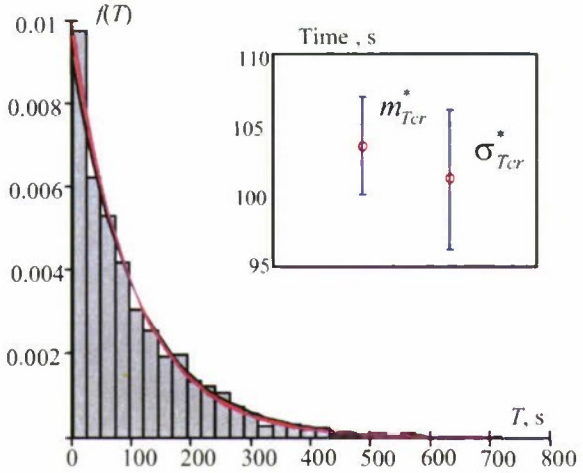

Theoretical Distribution Density; χ^2=64.4 d=29 $P(\chi^2,d)$=0.00017
Based on Average Number per Unit of Time; χ^2=64.8 d=28 $P(\chi^2,d)$= 0.000096
Based on Average Time before 1st Crossing χ^2=61.6 d=28$P(\chi^2,d)$=0.00025
Based on Average Censored Time before 1st Crossing χ^2=61.6 d=28 $P(\chi^2,d)$=0.00025
Based on Average Time between Crossing χ^2=56.2 d=28 $P(\chi^2,d)$=0.0012

Wb=30 s

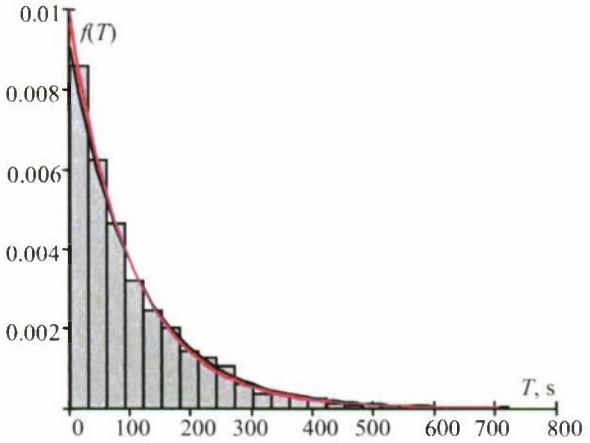

Theoretical Distribution Density; χ^2=32.9 d=23 $P(\chi^2,d)$=0.084
Based on Average Number per Unit of Time; χ^2=33.2 d=22 $P(\chi^2,d)$= 0.059
Based on Average Time before 1st Crossing χ^2=31.1 d=22 $P(\chi^2,d)$=0.094
Based on Average Censored Time before 1st Crossing χ^2=31.1 d=22 $P(\chi^2,d)$=0.094
Based on Average Time between Crossing χ^2=25.7 d=22 $P(\chi^2,d)$=0.27

Figure 1.26. Distribution of Time Between Upcrossings For a Level of 5.75 m (3269 Crossings Total, All 200 Records With at Least One Crossing)

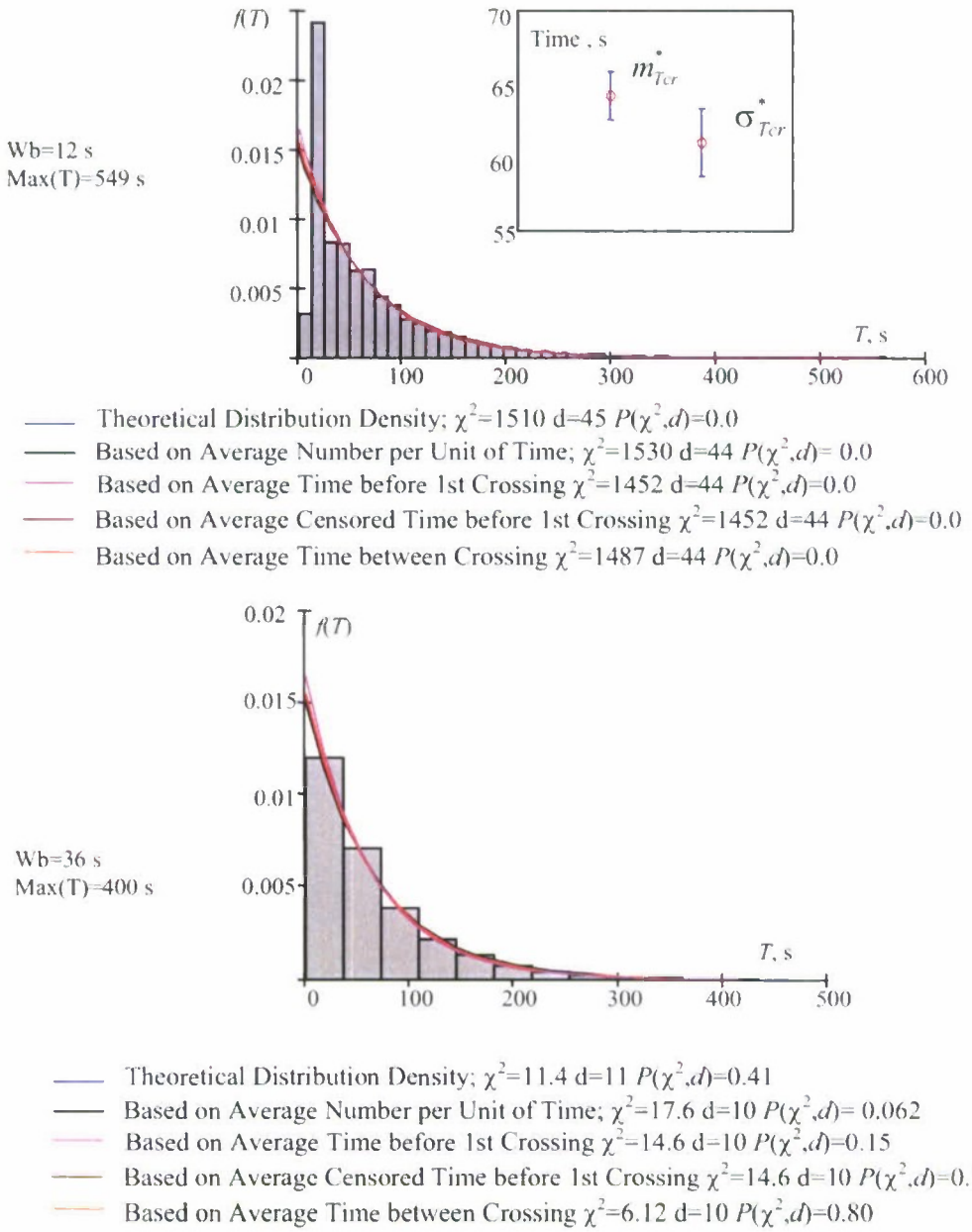

Figure 1.27. Distribution of Time Between Upcrossings For a Level of 5 m (5407 Crossings Total, All 200 Records With at Least One Crossing)

To complete the study of influence of the crossing level, two more distributions are considered here. At the level of 3 m, shown in Figure 1.28, the estimates of the mean value and standard deviation do not have any overlap of confidence intervals. Both confidence intervals are very small, as would be expected from a sample containing 15,201 data points. The mean value range is below 25 seconds, where the autocorrelation function has not entirely decayed. The curves are separated in two groups, as the mean value of time before the first upcrossing is apparently no longer equal to mean time before the events nor is it equal to the inverse of the event rate.

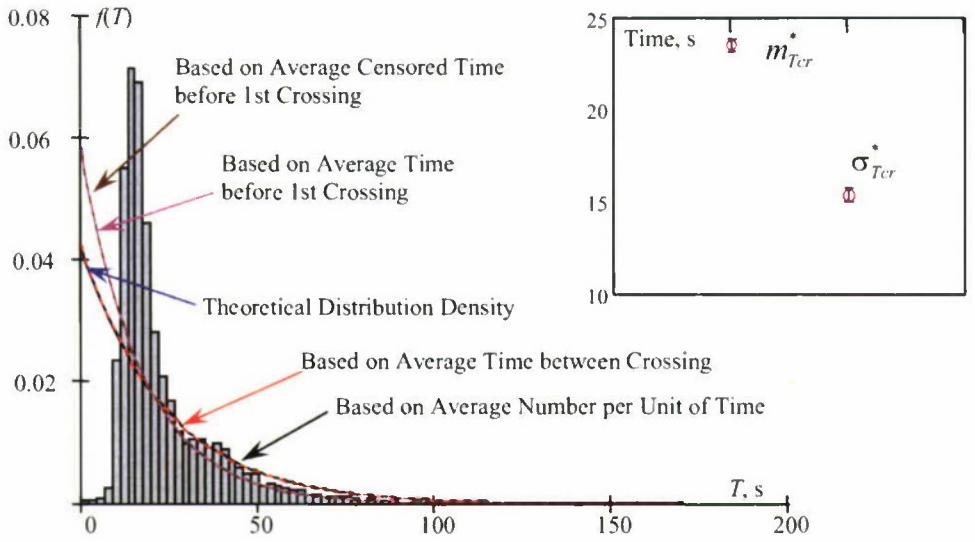

Figure 1.28. Distribution of Time Between Upcrossings For a Level of 3 m (15201 Crossings Total, All 200 Records With at Least One Crossing)

The histogram in Figure 1.28 demonstrates a pronounced peak around 10-15 seconds; its character is obviously not exponential. A similar picture can be seen when the level is set to 1 m, see Figure 1.29. The separation of the two groups of curves is even larger, while the shape of histogram may bear some resemblance to the normal distribution.

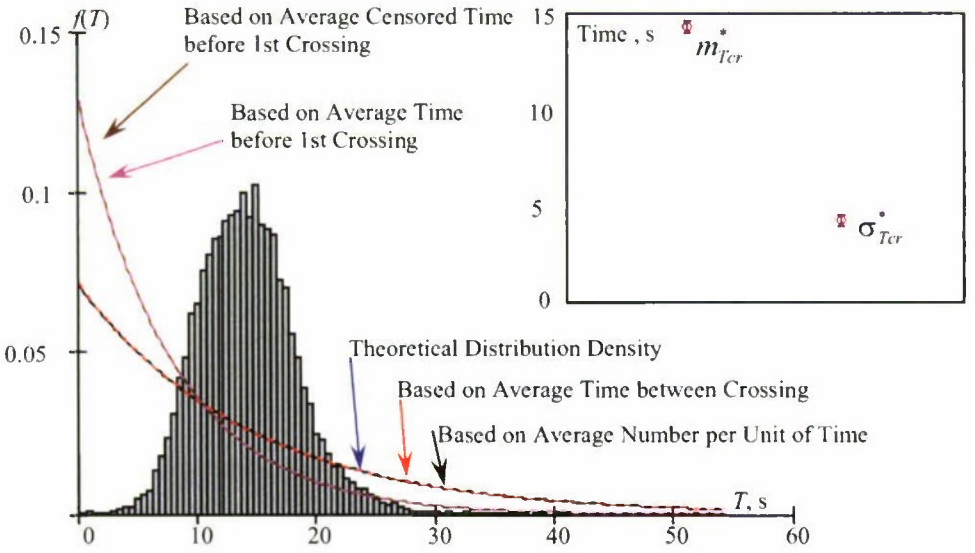

Figure 1.29. Distribution of Time Between Upcrossings For a Level of 1 m (25543 Crossings Total, All 200 Records With at Least One Crossing)

1.3.4. Cumulative Distribution of Time between Events

The derivations (1.30-1.37) prove that time interval between upcrossings must follow an exponential distribution if the number of upcrossings during a fixed time is governed by the Poisson distribution. However an attempt to use statistics for the time interval between upcrossings encounters certain difficulties. Computing the upcrossing rate calculated as the inverse of the average time between upcrossings may be prone to a bias, which is caused by insufficient record duration.

Therefore, it is desirable to have another method to check if the assumption of a Poisson distribution is still valid, that would be free of drawbacks described above. One such method was described by Belenky, *et al.*, (2007). This method was based on estimating the probability of at least one upcrossing during a given time span.

Consider a time interval from a time instance t_b until t_e with the duration $\Delta T = t_e - t_b$. The probability that at least one upcrossing occurs during this time interval is estimated as:

$$P_T^*(k \neq 0) = 1 - \frac{N_{k=0}}{N_R} \tag{1.116}$$

Here k is number of upcrossings, $N_{k=0}$ is a number of records without a single upcrossing within the given interval and N_R is total number of records available. This calculation is illustrated in Figure 1.30, where upcrossings are shown as black dots. For the example shown in this figure, the probability of at least one upcrossing from the instant t_b to the instant t_e is 0.75. Only one record out of four did not have any upcrossings during the interval T.

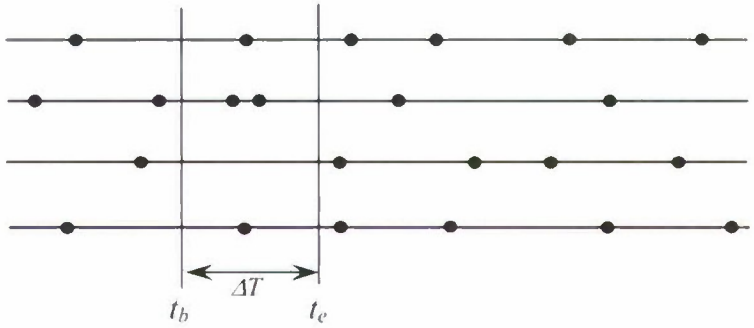

Figure 1.30. On Estimation of the Probability of at Least One Event During Given Interval T

This estimate tends to theoretical probability as the number of records goes to infinity:

$$P_T(k \neq 0) = \lim_{N_R \to \infty} \left(P_T^*(k \neq 0) \right) = \lim_{N_R \to \infty} \left(1 - \frac{N_{k=0}}{N_R} \right) \tag{1.117}$$

Assuming a Poisson distribution and for the number of upcrossings leads to the following expression:

$$\lim_{N_R\to\infty}\left(1-\frac{N_{k=0}}{N_R}\right)=P_T(k\neq 0)=1-\exp(-\lambda\Delta T) \tag{1.118}$$

Here λ is the theoretical upcrossing rate. For a finite number of records, equation (1.116) can be expressed in terms of the estimate of the rate λ^*:

$$1-\frac{N_{k=0}}{N_R}=1-\exp(-\lambda^*\Delta T) \tag{1.119}$$

Where the estimate of rate λ^* can be evaluated as:

$$\lambda^*=-\frac{1}{\Delta T}\ln\left(\frac{N_{k=0}}{N_R}\right) \tag{1.120}$$

As it was shown above (see formula 1.33), expression (1.117) can be interpreted as an estimate of the CDF of the time between crossings calculated for argument ΔT:

$$F^*(\Delta T)=1-\exp(-\lambda^*\Delta T)=1-\frac{N_{k=0}}{N_R} \tag{1.121}$$

Since the stochastic process is considered stationary, the theoretical probability $P_T(k\neq 0)$ is not time dependent. Therefore, the uncertainty of the estimate $F^*(\Delta T)$ can be reduced by averaging its value multiple intervals of size ΔT:

$$F^{**}(\Delta T)=\frac{1}{N_{\Delta T}}\sum_{i=0}^{N_{\Delta T}-1}\left(1-\frac{N_{k=0}(t_b=i\Delta T,t_e=(i+1)\Delta T)}{N_R}\right) \tag{1.122}$$

Here $N_{k=0}(t_b,t_e)$ is the number of records that did not have any upcrossings from t_b till t_e; $N_{\Delta T}$ is a number of whole intervals ΔT contained a record length T_S:

$$N_{\Delta T}=\frac{T_S}{\Delta T} \tag{1.123}$$

Formula (1.120) is an estimate for the cumulative distribution function for one value of ΔT. To calculate the rest of the estimated functions, all the calculations have to be repeated for an array of points T_j

$$\{T_j\}=\Delta T, 2\Delta T, 3\Delta T,..., \ j\Delta T,..., \ T_S \tag{1.124}$$

Finally, the estimate of the CDF at points T_j can be expressed as:

$$F_j^{**}=\frac{j\Delta T}{T_S}\sum_{i=0}^{\frac{T_S}{j\Delta T}-1}\left(1-\frac{N_{k=0}(t_b=ij\Delta T,t_e=(i+1)j\Delta T)}{N_R}\right) \quad j=1,..,N_{\Delta T} \tag{1.125}$$

To check the goodness-of-fit of the exponential CDF, Belenky *et al.*, 2007 used the Kolmogorov-Smirnov test (also known as the K-S test) for goodness-of-fit.. The description of the K-S test approach, taken from Belenky *et al.*, 2007, is provided below for convenience. The metric for the goodness-of-fit is derived from the absolute value of

the maximum difference between the suggested and statistical CDF.

$$D = \max\left|F_i^{**} - F(t_i)\right| \tag{1.126}$$

The criterion itself is expressed though the maximum difference D:

$$\nu = D \cdot \sqrt{n} \tag{1.127}$$

Here, n is the number of data points. It is proven that if the statistical estimate of cumulative distribution function is evaluated for independent data, for any distribution $F(x)$, with increasing number of points:

$$\lim_{n\to\infty}(\nu \geq \lambda) = 1 - \sum_{k=-\infty}^{\infty}(-1)^k \exp\left(-2k^2\nu^2\right) \tag{1.128}$$

In practice, an upper bound of 10^4 (instead of infinity) for the summation yields satisfactory results. Formula (1.126) yields the probability that the difference between the observed and suggested distributions is caused by random reasons, if n is large enough.

$$P_{RND} = 1 - \sum_{k=-\infty}^{\infty}(-1)^k \exp\left(-2k^2\nu^2\right) \tag{1.129}$$

It should be noted, however, that the K-S test does not account for the number of statistical "degrees of freedom", and it is only sensitive to a sample size. This implies that the theoretical distribution must be suggested on the theoretical background only and that it should not contain any parameters derived from the statistical sample.

Belenky *et al.*, 2007 used the K-S test to check if upcrossings follows Poisson flow. However that source does not contain any information on how to set step ΔT. Here it is associated with the bin width for time intervals between the upcrossings:

$$\Delta T = \frac{3.5\sigma_T}{\sqrt[3]{N_T}} \tag{1.130}$$

Here σ_T is the standard deviation of the intervals between the upcrossing and N_T is their quantity.

Figure 1.31 shows the statistical CDF calculated with formula (1.123) along with the theoretical curve. The CDF for two levels of crossing are shown here, 7.5 m and 6.75 m. Other statistics and data for these levels are shown in Figure 1.3-Figure 1.5, Figure 1.21, Figure 1.22 and Figure 1.24 and Figure 1.25 respectively. The K-S test did not reject the hypothesis of an exponential distribution. The statistical CDF did not reach unity for the level 7.5 m, as there were four records without upcrossings at all. However, for the level of 6.75 m, all the records had at least one upcrossing, so the statistical CDF did reach unity.

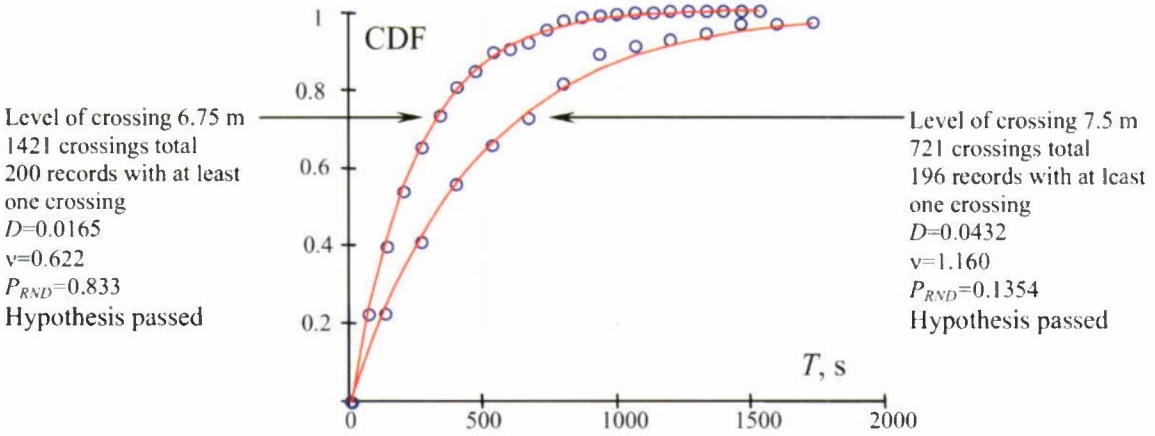

Figure 1.31. Cumulative Distributions of Time Between Upcrossings for Levels of 7.5 m and 6.75 m

The outcome of the test for both levels 7.5 m and 6.75 m is not surprising. All analysis carried out before have indicated that the exponential distribution was, in fact, applicable. As it can be seen from the insert in Figure 1.21, the lower boundary of the mean value is around 340 s, which is enough time for the autocorrelation function to die out (see Figure 1.11). The overlap between confidence intervals of the mean value estimate and standard deviation is significant (See insert in Figure 1.21).

The hypothesis that time intervals between the upcrossings have exponential distribution was not rejected with the Pearson chi-square test (probability 0.77, see Figure 1.21). This hypothesis was also not rejected by the K-S test, see Figure 1.31. The difference between these tests is that the Pearson chi-square test was applied to the sample of time intervals between the upcrossing. The Pearson chi-square test has shown that the exponential distribution with theoretical parameter does not fit that data (probability is only 0.0024, see Figure 1.21). The K-S test in Figure 1.21 has shown that the theoretical distribution fits the observed data (probability is 0.13).

The reason for this difference was actually already explained in the previous section. It is a statistical bias of the sample of time intervals between upcrossing. This bias is introduced by absence of longer-than-record intervals. This bias decreases the mean value of the time between the upcrossing and drives the statistical estimate of the distribution parameter (rate of events) up, see Figure 1.22. As can be seen from this figure, the bias is absent in the parameter calculated through averaging of the number of upcrossing per unit of time. The bias also can be corrected by censoring the estimate of the mean time before the first upcrossing. Therefore, rejection of the theoretical distribution in Figure 1.21 does not constitute rejection of the hypothesis of exponential distribution and Poisson flow as it is the result of the statistical bias.

This bias is absent in the distribution (1.122) as it is essentially based on counting upcrossings rather than on calculating the time interval between them. The absence of the bias gives the CDF (1.122) an advantage over a histogram of time intervals between the events. Use of the CDF, however, requires using the K-S test, which has known limitations. Strictly speaking, the K-S test is fully applicable only if parameters of the

fitted curve are known a priori and do not come from statistical estimates. As mentioned above the K-S test does not have any mechanism to penalize the result for using statistically estimated parameters. If these parameters have been used, the K-S test may overestimate the probability that the difference between observed data and the fitted curve caused by a random reason. Using the K-S test in this example is justified, as the true value of the parameter is known. Using the K-S test for the real numerical simulation or experimental results where all the parameters are statistical estimates, therefore, is not desirable but may be unavoidable.

The results for the second dataset (the left curve in Figure 1.31), corresponding to the level of 6.75 m, are completely analogous. The analysis of the time intervals between the crossing shown in Figure 1.24 as well as the insert in Figure 1.24 points out that Poisson flow is applicable. The only difference is that all the records have at least one upcrossing, so the statistical CDF reaches unity in Figure 1.31 and uncensored and censored estimates coincide in Figure 1.25.

Figure 1.32 shows results for crossing levels of 9 m and 11 m. Only 153 upcrossings occurred for the level of 9 m and only 111 records (out of 200) had at least one upcrossing. The bias of time interval between the crossings was so large that none of the curves fit the data in Figure 1.23. Also, probably for the same reason, there was no overlap between the confidence intervals of the estimates of mean value and standard deviation in the insert on Figure 1.23. As it was noted before, this outcome can only be explained by the influence of bias, as there is no reason why the exponential distribution should not be applicable when the level is raised and upcrossings become less frequent. This statement is supported by comparison of Figure 1.15 and Figure 1.16, where time before the first crossing is analyzed. None of the curves fit the data in Figure 1.15. Figure 1.16 shows agreement with the censored data for curves based on theoretical parameters as well as based on two statistical estimates. The left curve in Figure 1.32 shows agreement with the data and no censoring is needed. This confirms the bias explanation for Figure 1.15.

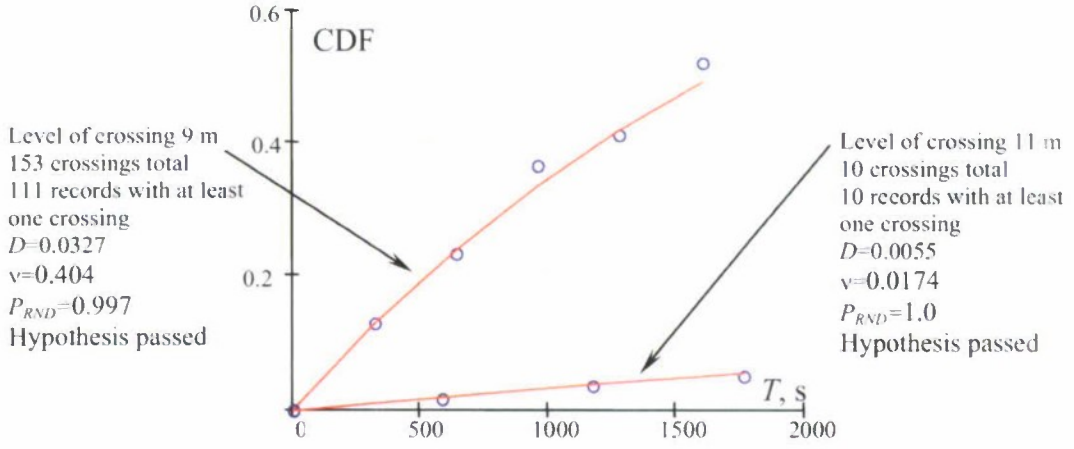

Figure 1.32. Cumulative Distributions of Time Between Upcrossings for Levels of 11 m and 9 m

For the level of 11m, only 10 upcrossings were observed. This is not enough data for a meaningful histogram of time intervals before the first upcrossing nor for time between the upcrossings. However, the methods based on counting number of upcrossings still work. Figure 1.7 shows the estimate of upcrossing rate based on average number of upcrossing per unit of time, while the right curve in Figure 1.32 shows CDF for time between/before the upcrossing. It has very few points, but this was enough for the K-S test to be used. The hypothesis of an exponential distribution was not rejected by the K-S test.

Figure 1.33 shows the statistical CDF for the levels 5.75 m and 5.0 m. The hypothesis of an exponential distribution is not rejected by the K-S test in either case. Analysis of the distribution of the time intervals between the upcrossings delivered mixed results. Figure 1.26 shows how results of the Pearson chi-square test become sensitive to a small change of the bin width for the level of 5.75 m. To reach a similar result for the 5 m level the "adjustments" need to be much larger, see Figure 1.27. At the same time all other symptoms of exponential distributions are present: substantial overlap of confidence intervals of the mean value and standard deviations estimates in the insert of both Figure 1.26 and Figure 1.27. Additionally, the distribution of time before the first crossing remains exponential for a level of 5 m, see Figure 1.13 and Figure 1.14.

The conclusion made in the previous section was that the exponential distribution was rejected (upper parts of Figure 1.26 and Figure 1.27) because of the values in the first bin. This is a reflection of increased cases of upcrossings occurring on successive periods; essentially, it is an influence of the group structure of the stochastic process. As it was expected in the previous subsection, the local distortion of the histogram did not lead to rejection of the exponential distribution based on analysis of the statistical CDF. However, it is clear that both levels 5.75 m and 5.0 m are not very far from the boundary of applicability of the exponential distribution and Poisson flow.

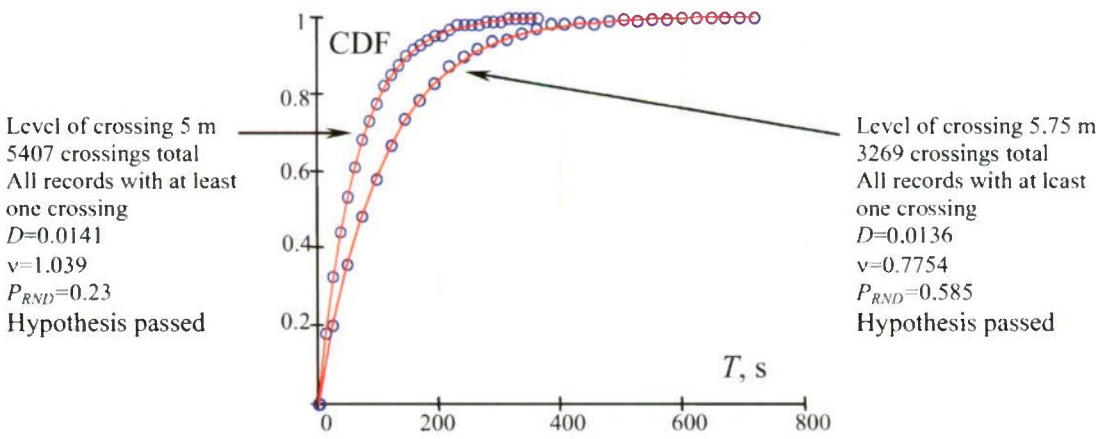

Figure 1.33. Cumulative Distributions of Time Between Upcrossings for Levels of 5.75 m and 5 m

To examine when and how the breaking of Poisson flow can be detected by the K-S test, upcrossings through levels of 4.75 m and 3 m were analyzed (see Figure 1.34). For the 3 m level, Poisson flow is clearly inapplicable, as it can be seen from the Figure 1.28; the histogram of the intervals between the upcrossing no longer has the appearance of an exponential distribution and the confidence intervals in the insert do not overlap.

The results of the K-S test shown in Figure 1.34 clearly reject the hypothesis of an exponential distribution. The shape of the statistical CDF is different from that of an exponential curve. This seems to be a natural outcome of the non-exponential character of PDF in Figure 1.28. This also demonstrates the robustness of the considered technique; combination of CDF (1.122) and K-S test has spotted inapplicability of Poisson flow as well as all other methods with exception of analysis of the time before the first crossing (Figure 1.18).

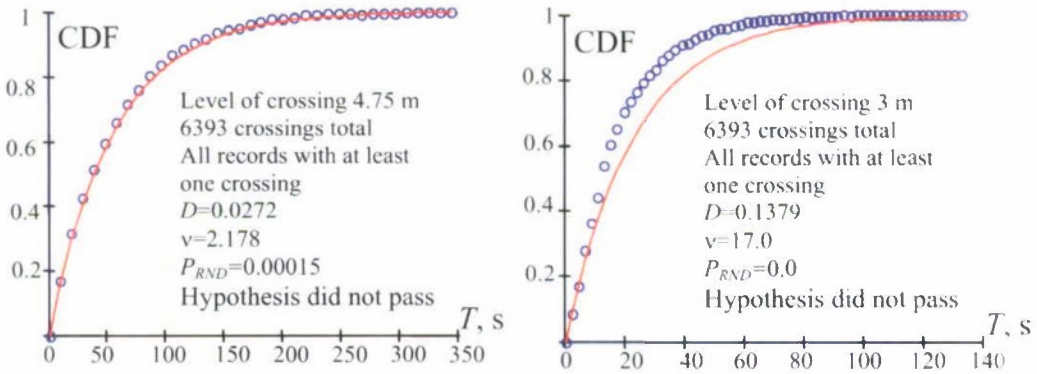

Figure 1.34. Cumulative Distributions of Time Between Upcrossings for Levels of 4.75 m and 3 m

Another important result shown in Figure 1.34 is a rejection of the exponential distribution for the level of 4.75 m. The rejection means that, according to K-S test, the boundary of applicability of the exponential distribution is somewhere between the levels of 5 m and 4.75 m. This is in agreement with the previous conclusion that the levels 5.0 to 5.75 m are not very far from that boundary; so the sensitivity of Pearson chi-square test to the bin width may be giving a hint that the boundary of applicability is somewhere near.

1.3.5. Direct Test of Applicability of Poisson Flow

The CDF formula (1.122) in combination with a K-S test seems to be a robust technique for checking the applicability of the exponential distribution and Poisson flow. However, if the parameter of the distribution is a statistical estimate, the K-S test may overestimate the probability that the difference between the observed data and fitted curve is caused by random reasons. The Pearson chi-square test allows a penalty to be introduced for the statistical estimate by reducing the degrees of freedom by one, and is therefore preferable.

The applieability of Poisson flow ean be judged direetly by ealeulating a histogram of the random number of upcrossings observed during a given time and then cheeking if the Poisson distribution fits the observed data. The goodness-of-fit then ean be judged with the Pearson chi-square test.

Formula (1.30) gives the expression for the Poisson distribution in the form of the probability mass funetion (PMF), as the number of upcrossing is an integer figure:

$$P_T(k) = \frac{(\lambda T_k)^k}{k!} \cdot \exp(-\lambda T_k) \tag{1.131}$$

Here λ is the rate of events that is estimated statistieally, but is also known theoretieally for the eonsidered example, k is the number of uperossings observed during time T_k.

To formulate the procedure, time T_k needs to be chosen. The record length seems to be the natural choice; however, this limits the size of the sample to the number of reeords. This sample size may be not suffieient even for the considered numerieal example with 200 reeords. If this teehnique is to be applied for a model test, then a smaller window has to be introdueed, as there may be few reeords.

Consider a size of sample N_k that is the total number of time windows.

$$N_k = \frac{nN_R\Delta t}{T_k} \tag{1.132}$$

Here N_R is s number of reeords. n is a number of points in each reeord. Δt is the time step. The duration of time window ean be eonveniently presented as a fraetion of the duration of the record, or as the number of windows per record.

$$N_W = \frac{n\Delta t}{T_k} \tag{1.133}$$

One of the properties of Poisson distribution is the mean value numerieally equals the variance:

$$m_k = V_k = \lambda T_k \tag{1.134}$$

Table 1 and Table 2 eontain the ratio of estimates of mean value and varianee. The mean value and varianee of the Poisson distribution ean be statistically estimated.

$$m_k^* = \frac{1}{N_k}\sum_{i=1}^{N_k} k_i \quad ; \quad V_k^* = \frac{1}{N_k - 1}\sum_{i=1}^{N_k}(k_i - m_k^*)^2 \tag{1.135}$$

Here k_i is a number of upcrossings that was observed in the window i. It ean be shown that:

$$m_k^* = \lambda^* T_k \tag{1.136}$$

Where λ^* is an estimate of rate of events based on "counting" – the average number of uperossings per unit of time (1.46). For the proof, consider an auxiliary random variable U defined at each time step that equals one if there is an uperossing and zero if there is not (1.38). Without a loss of generality, the definition of this auxiliary variable ean be altered by the introduction of counting of time windows:

$$U_{i,j,l} = \begin{cases} 1 & x_{i,j,l} \le a \cap x_{i,j,l+1} > a \\ 0 & Otherwize \end{cases} \quad i = 1,..,N_R ; \quad j = 1,...,N_W \quad l = 1,...,N_P \tag{1.137}$$

Where N_P is a number of points in a window:

$$N_P = \frac{N}{N_W} \tag{1.138}$$

Based on this definition, the number of uperossings in a window can be expressed as:

$$k_{i,J+N_P,l} = \sum_{l=1}^{N_P} U_{i,j,l} \tag{1.139}$$

Then, the estimate of the mean value of the number of upcrossings during the time windows yields:

$$m_k^* = \frac{1}{N_k}\sum_{i=1}^{N_k} k_i = \frac{1}{N_W N_R}\sum_{i=1}^{N_R}\sum_{j=1}^{N_W} k_i = \frac{1}{N_W N_R}\sum_{i=1}^{N_R}\sum_{j=1}^{N_W}\sum_{l=1}^{N_P} U_{i,j,l} \tag{1.140}$$

Taking into aecount that the two internal sums represent the number of uperossings observed during one record:

$$N_{Ui} = \sum_{j=1}^{N_W}\sum_{l=1}^{N_P} U_{i,j,l} \tag{1.141}$$

Substitution of (1.139) into (1.138) and then using formula (1.45)

$$m_k^* = \frac{1}{N_W N_R}\sum_{i=1}^{N_R} N_{Ui} = \frac{m_U^*}{N_W} \tag{1.142}$$

Here m_U^* is a mean value estimate of the auxiliary random variable U. It is related to the estimate of the rate of events with formula (1.46). Substitution of (1.46) into (1.139) yields:

$$m_k^* = \frac{m_U^*}{N_W} = \frac{\lambda^* T_R}{N_W} \tag{1.143}$$

Here T_R is the duration of a record;

$$T_R = n\Delta t \tag{1.144}$$

Substituting (1.142) into (1.141) and taking into aecount (1.129) leads to the expression (1.130) and this completes the proof.

While numerieal proximity of estimates of the mean value and variance may be used as a qualitative indicator of possible applicability of Poisson flow, a chi-square goodness-of-fit test provides a more rigorous technique. As an example, Figure 1.35 shows details of these results for the level 6.75 m.

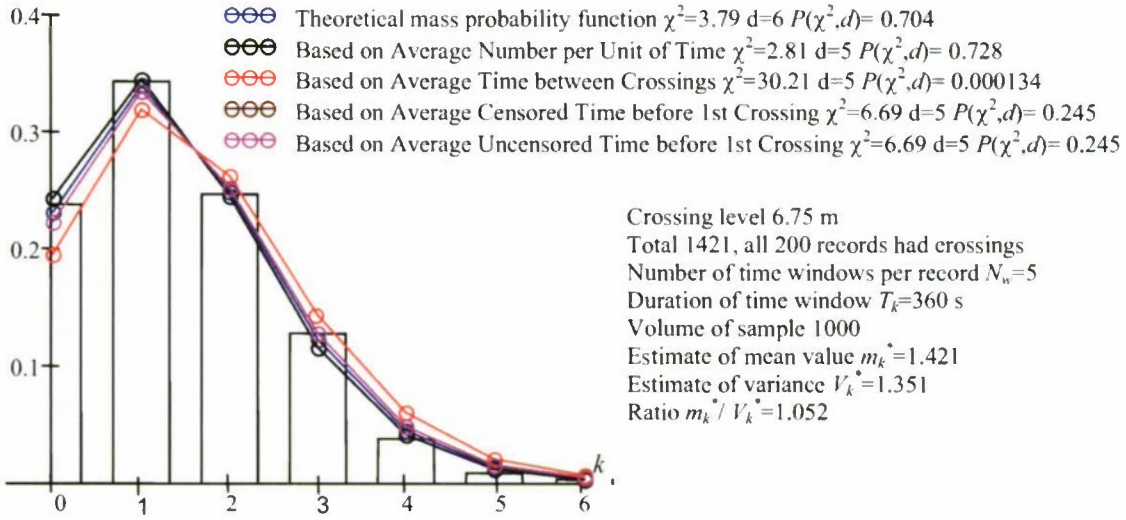

Figure 1.35. Probability Mass Function of the Number of Upcrossings During a Time Window

As in the previous analysis, five different methods were used to evaluate the single parameter of Poisson distribution. The results of a Pearson chi-square goodness-of-fit test for all five methods are presented in Figure 1.35. This test did not reject the hypothesis for the theoretical distribution, demonstrating correct interpretation of the theory and a reasonable choice of parameters. This is consistent with the result in shown Figure 1.31.

The distribution defined using the parameter estimated as the average number of upcrossings per unit of time was not rejecting either, confirming the robustness and reliability of the "counting" method. This is consistent with the results shown in Figure 1.25, where the "counting" method produced the number closest to the correct answer known from theory.

The chi-squared goodness-of-fit test rejected the distribution based on average time between crossings, most likely because of insufficient record length. This effect can be seen in both Figure 1.24 and Figure 1.25.

As all the records had at least one crossing, the methods based on uncensored and censored mean time before the first upcrossing produced identical results and were not rejected. These results are generally consistent with the previous analysis, see Figure 1.25.

To complete the formulation of the procedure, the size of the time window T_k has to be chosen. As the number of upcrossings is an integer, the width of the histogram bin is one and the number of bins, N_{max}, is defined by a maximum number of upcrossings observed during a time window.

Obviously, N_{max} is expected to be larger for larger values of T_k. Therefore, taking into account (1.129), N_{max} is expected to be larger for smaller sample size N_k. Naturally, the constant duration of the time window for different levels of crossings makes a very obscure histogram as the decrease of sample size leads to a large number of bins.

Therefore, it makes sense to keep N_{max} relatively constant by adjusting the

duration of time window. This leads to an increase of hits in each bin, once the sample size grows, which seems more natural. The number of windows per record can be chosen to satisfy a condition for a constant number of bins, say:

$$N_{max} = 7 \qquad (1.145)$$

If condition (1.143) could not be met, especially for a small number of crossings, the number of windows yielding N_{max} closest to 7 is chosen. If there are several window sizes that satisfy (1.143), the largest one is chosen. Deviations from this rule should be especially noted and commented.

It is known that results of Pearson chi-square goodness-of-fit-test may be sensitive to the number of bins. For analysis of time intervals before and between the upcrossings, the formula for the width of a bin (1.110) was used. The condition (1.143) used to size the histogram is somewhat arbitrary; therefore a sensitivity study was carried out. The level is 6.75 m. This crossing level was chosen because there are enough upcrossings (1421) and the tests carried out previously did not reject the hypothesis of Poisson flow. The windows size was changed systematically and the results are summarized in Table 1.

Table 1. Sensitivity to Time Window Size for the Crossing level of 6.75 m

N_w	T_k, s	N_{max}	Sample size N_k	m_k^* / v_k^*	Results Pearson chi-square goodness-of-fit test for distribution based on:							
					Theory		Counting		Time between crossings		Time before the 1st crossing	
					χ^2	$P(\chi^2,d)$	χ^2	$P(\chi^2,d)$	χ^2	$P(\chi^2,d)$	χ^2	$P(\chi^2,d)$
1	1800	14	200	1.76	23.98	0.0313	24.14	0.0195	42.44	2.81E-5	25.53	0.0125
2	900	10	400	1.26	16.81	0.0518	16.33	0.0378	39.15	4.61E-6	19.05	0.0146
3	600	8	600	1.11	6.88	0.441	6.83	0.336	29.84	4.21E-5	9.00	0.1737
4	450	7	800	1.05	1.81	0.936	1.06	0.957	27.34	4.9E-5	4.51	0.478
5	360	7	1000	1.05	3.8	0.704	2.82	0.728	30.21	1.34E-5	6.69	0.245
6	300	6	1200	1.03	3.48	0.627	2.68	0.613	29.46	6.31E-6	6.26	0.181
7	257	6	1400	1.03	1.32	0.933	0.20	0.995	28.4	1.04E-5	4.36	0.360
8	225	6	1600	1.01	5.46	0.363	4.44	0.349	32.79	1.32E-6	8.47	0.0759
9	200	6	1800	1.02	2.02	0.847	0.71	0.950	29.91	5.11E-6	5.22	0.266
10	180	5	2000	0.99	3.26	0.515	2.3	0.513	30.59	1.04E-6	6.25	0.100
11	163.5	6	2200	1.00	2.74	0.741	1.44	0.838	30.92	3.18E-6	5.96	0.202
12	150	5	2400	0.97	6.74	0.150	6.04	0.110	33.81	2.17E-7	9.59	0.0224
13	138.5	5	2600	1.00	6.09	0.192	5.00	0.172	33.74	2.25E-7	9.18	0.027
14	128.5	5	2800	0.97	6.84	0.145	5.63	0.131	35.47	9.68E-8	10.07	0.018
15	120	5	3000	0.99	5.81	0.214	4.76	0.190	33.58	2.43E-7	8.89	0.0308
20	90	5	4000	0.97	6.12	0.191	4.81	0.186	34.91	1.27E-7	9.41	0.0243
25	72	5	5000	0.95	9.93	0.0416	8.78	0.0324	38.76	1.95E-8	13.17	4.29E-3
30	60	4	6000	0.97	5.18	0.159	4.07	0.131	33.27	5.97E-8	8.32	0.0156
40	45	4	8000	0.98	8.92	0.0304	7.87	0.0196	36.73	1.06E-8	12.01	2.47E-3

50	36	4	10000	0.98	4.28	0.233	2.92	0.232	32.99	6.85E-8	7.60	0.0223

The results of testing four distributions are placed into Table 1. All the records did have at least one uperossing, so there is no difference between censored and uncensored data for the mean time before the first upcrossing.

The hypothesis of a Poisson distribution was not rejected for the theoretical parameter for a continuous range from 2 to 15 widows per record. There were only three window sizes for which the probability of a good fit was less than the significance level of 5% (1, 25 and 40 windows per record). However, even for these cases, the probability did not go below 3%. The theoretieal eriterion for any goodness-of-fit test is just a finitcness of the probability that the difference between the observed data and hypothesis is eaused by random reasons. Therefore, variation of these probabilities from 93% to 3% does not nccessarily constitute sensitivity. It does not change the outcome that the hypothesis is not rejected. Therefore, the sensitivity to windows size is very small when using a theoretical parameter.

A similar eonclusion ean be made on the distributions based on eounting and time between upcrossings. The outcome of goodness-of-fit analysis does not change signifieantly with ehanging window size.

The situation is less stable for the distribution based on time before the first upcrossing. The instability can be explained by the fact that this estimate uses less statistical information then the others, which is reflected in wider confidence intervals, see Figure 1.25.

Once insensitivity to window size has been demonstrated, the next objective is to see how this method behaves when the assumption of Poisson flow is no longer applieable.

Table 2 contains results of systematic calculations for different crossing thresholds. The table includes results of a chi-square test eomputed five different ways: theoretieal (1.81), statistieal, based on counting uperossings (1.46), statistical, based on mean time between upcrossings (1.96), statistical, based uncensored mean time before the first uperossing (1.100) and statistical, based on censored mean time before the first upcrossing (1.103).

Results for both the theoretical distribution and the distribution based on eounting indicate the applieability of Poisson flow above the level of 6 m. Levels 5.75 m and 5.5 m show some sensitivity to windows size (see Table 3 for the level 5.75 m). The area of sensitivity to window size generally corresponds to the area of sensitivity to bin size, see Figure 1.26 and Figure 1.27. It seems plausible that sueh "grey" areas are indicators that the independence of upcrossings is about to be violated and Poisson flow will beeome inapplicable soon (or is inapplieable already). The inapplicability of Poisson flow is indicated consistently for all the levels below 5.5 m. The boundary between applicability and inapplieability determined by this method is a little higher than one evaluated using the K-S test (between 5 m and 4.75 m).

The distribution based on time between upcrossings was rejected for all the levels. The sample of time intervals between the crossings did not produce representative

statistical estimates for the accepted calculation parameters (number and length of record, time step, etc.). As it can be seen form Figure 1.9, Figure 1.22, and Figure 1.25, the length of the record was too small to estimate the rate of events correctly for the levels of 9 m, 7.5 m and 6.75 m, respectively. As a result, a Poisson distribution based on this estimate was rejected. The length of records seems to be barely enough for the level of 5 m, see Figure 1.8, but this level was too low to assure independence of upcrossing, and as a result Poisson flow was not applicable and the distribution was rejected again.

Table 2. Evaluation of applicability of Poisson flow

Level, m	Number of crossings	Mean time estimate			CDF & K-S Test			Direct test of applicability of Poisson flow							
											Pearson chi-square test χ^2/ P_{RND}				
		Between crossings	Before 1st crossing	Censored before 1st crossing	St. dev. time between σ_T	Step for CDF ΔT	P_{RND}	N_w	m_k/V_k	N_{max}	theory	count	Time between	Time before	censored time before
11	10	849	849	35000	362	589	1	1	1.05	2	0.097 0.76	-	-	-	-
10	58	894	925	5918	482	435	0.98	1	1.13	3	5.46 0.065	0.8 0.37	587 0	535 0	0.7 0.4
9	152	726	801	2244	389	320	0.996	1	1.08	5	2.34 0.67	2.26 0.52	409 0	299 0	2.31 0.51
8	425	502	582	750	414	193	0.54	1	1.37	7	7.23 0.3	7.23 0.2	124 0	55 9e-11	10 0.07
7.5	721	367	414	451	340	133	0.735	2	1.08	8	2.56 0.92	2.24 0.89	70 3e-13	25.6 .0002	8.78 0.18
7	1140	263	292	292	254	85	0.78	4	1.05	7	1.65 0.95	0.72 0.98	35 1.2e-6	6.78 0.23	6.78 0.23
6.75	1421	219	239	239	210	65	0.83	5	1.05	7	3.8 0.7	2.82 0.73	30.2 1.3e-5	6.69 0.25	6.69 0.25
6.5	1780	179	186	186	173	50	0.19	9	1.02	7	4.0 0.67	3.44 0.63	28.3 3.2e-5	15.3 .009	15.3 .009
6.25	2195	149	154	154	145	39	0.27	11	.997	7	4.84 0.56	4.56 0.47	22.6 4.0e-4	12.6 .027	12.6 .027
6	2684	124	121	121	121	31	0.48	13	1.04	7	3.57 0.73	3.42 0.63	17.3 .0043	28.2 3. e-4	28.2 3.e-4
5.75	3269	103	100	100	101	24	0.58	13*	1.08	7	9.84 0.13	9.88 0.08	19.8 .001	33.8 2.7e-6	33.8 2.7e-6
5.5	2840	89	86	86	97	19.5	0.64	15*	1.07	7	10.25 0.11	9.47 0.09	17.3 .0036	34.6 1.8e-6	34.6 1.8e-6
5.25	4597	75	71	71	73	15.3	0.82	19	1.11	7	32.5 1.0e-5	33 3.e-5	36.5 7.5e-6	60.8 8.e-12	60.8 8.e-12
5	5407	64	60	60	61	12.2	0.23	21	1.17	7	72 1.3e-8	73 2e-14	73 2e-14	101 0	101 0
4.75	6393	54.7	53	53	50	9.5	.00015	22	1.22	7	88 0	88 0	88 0	99 0	99 0
3	15201	23.5	17.1	17.1	15.4	2.17	0	32	2.27	7	1437 0	1446 0	1435 0	2340 0	2340 0
1	22543	14.0	7.75	7.75	4.22	0.5	0	39	6.71	7	6996 0	6998 0	6991 0	21693 0	21693 0

* N_w was manually chosen to see if the hypothesis can pass. Possible sensitivity to number of windows

The distribution based on uncensored time before the first upcrossing was not rejected for the level of 7 m and 6.75 m. It was rejected for the levels of 6.5 m and 6 m, probably because of insufficient accuracy of the estimate. For the level of 5.75 m and below, Poisson flow may be already inapplicable. For the levels above of 7 m the

hypothesis was rejected, because of bias in the estimate caused by insufficient length of record, see Figure 1.9 and Figure 1.22.

The distribution based on censored mean time before the first upcrossing, however, is not rejected up to the level of 10 m. This is not surprising as the censoring procedure takes care of bias in the parameter estimate, see Figure 1.8 and Figure 1.22. The rejection of the level below 6 m is caused by the same reasons as the rejection of the distribution based on the uncensored estimate.

Table 3. Sensitivity to Time Window Size for the Crossing level 5.75 m

N_w	T_k, s	N_{max}	Sample size N_k	m_k^* / V_k^*	Results Pearson chi-square goodness-of-fit test for distribution based on							
					Theory		Counting		Time between crossings		Time before the 1st crossing	
					χ^2	$P(\chi^2,d)$	χ^2	$P(\chi^2,d)$	χ^2	$P(\chi^2,d)$	χ^2	$P(\chi^2,d)$
1	1800	27	200	2.29	55.07	7.44E-04	55.08	4.81E-04	64.55	2.40E-05	77.61	2.69E-07
2	900	16	400	1.43	22.45	9.65E-02	22.48	6.93E-02	31.01	5.50E-03	43.29	7.70E-05
3	600	14	600	1.34	25.1	2.24E-02	25.14	1.42E-02	33.25	8.86E-04	45.51	8.43E-06
4	450	11	800	1.13	9.74	4.63E-01	9.8	3.67E-01	17.99	4.00E-02	30.9	3.08E-04
5	360	11	1000	1.14	16.82	7.86E-02	16.84	5.13E-02	26.74	1.54E-03	40.39	6.45E-06
6	300	10	1200	1.15	21.05	1.24E-02	21.08	6.93E-03	30.41	1.79E-04	43.75	6.33E-07
7	257	11	1400	1.07	12.54	2.50E-01	12.6	1.81E-01	21.56	1.00E-02	35.45	4.96E-05
8	225	9	1600	1.06	5.1	7.47E-01	5.11	6.46E-01	16.16	2.00E-02	30.79	6.78E-05
9	200	9	1800	1.11	11.61	1.70E-01	11.64	1.13E-01	21.31	3.34E-03	35.07	1.09E-05
10	180	8	2000	1.07	6.65	4.66E-01	6.68	3.52E-01	0.3519	8.31E-03	31.66	1.90E-05
11	163.5	7	2200	1.05	5.05	5.38E-01	5.09	4.05E-01	14.67	1.00E-02	28.62	2.75E-05
12	150	8	2400	1.06	11.05	1.36E-01	11.09	8.57E-02	20.98	1.85E-03	35.08	4.16E-06
13	138.5	7	2600	1.08	9.85	1.31E-01	9.88	7.87E-02	19.8	1.36E-03	33.76	2.65E-06
14	128.5	8	2800	1.06	11.18	1.31E-01	11.23	8.16E-02	20.84	1.96E-03	34.84	4.64E-06
15	120	6	3000	1.05	5.78	3.29E-01	5.82	2.13E-01	15.53	3.72E-03	29.53	6.09E-06
16	112.5	7	3200	1.03	5.32	5.03E-01	5.34	3.76E-01	16.76	4.98E-03	31.74	6.69E-06
17	106	7	3400	1.06	13.81	3.18E-02	13.83	1.67E-02	24.57	1.69E-04	39.08	2.29E-07
18	100	6	3600	1.03	17.93	3.04E-03	17.97	1.25E-03	27.86	1.33E-05	42.17	1.54E-08
19	94.5	7	3800	1.05	19.52	3.36E-03	19.58	1.50E-03	28.63	2.74E-05	42.44	4.79E-08
20	90	6	4000	1.01	7.45	1.89E-01	7.47	1.13E-01	18.65	9.21E-04	33.65	8.78E-07
21	85.5	6	4200	1.06	24.55	1.70E-04	24.62	6.01E-05	32.96	1.22E-06	46.31	2.13E-09
22	82	6	4400	1.03	21.9	5.46E-04	21.93	2.07E-04	32.84	1.29E-06	47.69	1.09E-09
23	78.5	6	4600	1.03	6.92	2.27E-01	6.92	1.40E-01	18.98	7.94E-04	34.32	6.40E-07
24	75	6	4800	1.05	12.58	2.77E-02	12.61	1.33E-02	22.73	1.43E-04	36.96	1.83E-07
25	72	6	5000	1.02	13.59	1.85E-02	13.61	8.63E-03	24.31	6.91E-05	39.05	6.79E-08
30	60	5	6000	1.03	8.71	6.87E-02	8.75	3.28E-02	18.69	3.17E-04	32.9	3.37E-07
40	45	4	8000	1.04	3.79	2.85E-01	3.85	1.46E-01	12.47	1.96E-03	25.9	2.38E-06
50	36	4	10000	1.04	17.53	5.51E-04	17.6	1.51E-04	25.51	2.89E-06	38.66	4.03E-09

1.4. Summary

The probability of a large roll event (partial stability failure) is related to exposure time. This probability grows with time. The time before a large roll event is a random number.

If sequential large roll events can be considered independent, the number of such events during a given time follows a Poisson distribution and the time before a large roll event (or between them) has an exponential distribution.

Both Poisson and exponential distributions share a single parameter that completely defines both distributions. This parameter is the rate of events (average number of events per unit of time) and is equal to the inverse the mean time before or between the events.

If the distributions of instantaneous roll angle and roll rate, are known, the rate of events can be found using upcrossing theory.

Large-amplitude roll motion is the response of a dynamical system with significant nonlinearity. Even if the excitation of such a system has a normal distribution, the response can be significantly non-Gaussian. As reliable modeling of the distribution of roll angle may be difficult, statistical evaluation of the rate of events is of practical interest.

Three methods of statistical evaluation of the rate of events were considered. The first method is based on counting the upcrossing events and estimating an average number of events per unit of time. The second method was based on average time before the first event occurs, while the third method involved time estimation of average time between events. Evaluation of the confidence interval was included with all three methods.

A numerical example was formulated to examine how these methods work. Simulated wave elevations were chosen to serve as the data set for this example. Their distribution is known to be normal. Therefore, the theoretical value for the rate of events or upcrossing rate is available. These methods can therefore be judged based on how close the results come to the theoretical answer.

A different degree of rarity of the upcrossing events was modeled by varying the crossing level; high crossing level leads to fewer upcrossings, so the events become rarer and the methods can be tested for different conditions.

It was found that the methods based on time before and between the events may be biased due to insufficient record length. The method based on counting does not have this problem. This bias for the method based on average time before the first upcrossing can be corrected by censoring.

The counting method was found to be preferable as it not biased and has less statistical uncertainty in comparison with the method based on censored mean value of time before the first event.

Several methods were considered for checking if upcrossing events follow

Poisson flow and, therefore, if the exponential distribution can be used to compute probability of at least one event during given exposure time. All of these methods used a goodness-of-fit test to check if the distribution of the observed data follows either an exponential or Poisson distributions. These methods were:

1. Check if statistical PDF of time before the first event is exponential using Pearson chi-square goodness-of-fit test;
2. Check if statistical PDF of time between the events is exponential using Pearson chi-square goodness-of-fit test;
3. Check if statistical CDF of time between the events is exponential using Kolmogorov-Smirnov goodness-of-fit test;
4. Check if statistical probability mass function (PMF) of number of events during given time follows Poisson distribution.

The numerical example was also used to test all these methods. The theoretical distribution available for the numerical example was used to check if the calculation parameters (number and length of record, time step, etc.) were selected correctly so the results can be decisive.

The methods 2, 3 and 4 were found to be able correctly detect violation of Poisson flow caused by dependence of the upcrossing events. However, method 2 uses a biased distribution and method 3 may overestimate the goodness-of-fit if the statistical estimates were used for parameters of the distribution. Method 4 is therefore preferable.

In conclusion, two techniques are chosen for the procedure:

- The rate of events is to be estimated as an average number of upcrossings per unit of time – the "counting" method
- The applicability of Poisson flow is to be checked using a Pearson chi-square goodness-of-fit test applied to the statistical PMF of the number of upcrossings during a given time.

2. Extreme Value Theory

2.1. Background

Gumbel (1958) formulated Extreme Value Theory (EVT) in its modern form. One of the immediate applications of EVT was the prediction of extreme flooding based on multi-year observations. There is a series of measurements of the water level in a river observed during a year. Taking the largest measurement for each year a series of extreme values is created. The basic question posed was then, "What would be the level for a one-hundred-year flood?"

Extreme value theory looks at another aspect of the problem of rare events. While the Poisson distribution (considered in detail in the previous section) answers how many rare events could occur in a given time period, EVT looks into the distribution of the magnitude of the rare events.

The concept of order statistics is another mathematical tool that is related to extreme value theory. Order statistics are reviewd briefly in the next subsection.

2.1.1. Distribution of Order Statistics

As order statistics can be applied to both roll angle and time before or between large roll events, the following text uses the generic nomenclature X for observations of a continuous random variable x. The following represents a generic derivation that could be found in a number of statistical textbooks. Similar to derivations in the previous section, it has been placed here for the sake of completeness.

Consider a series of n independent observations of a continuous random variable $X_1, X_2,..., X_n$. The largest (or the smallest) observation out of n is also the random variable with a distribution that is different from the distribution of x.

The set of values $X_1, X_2,..., X_n$ is sorted (ordered) from smallest to largest, so that $X_{(1)}$ is the smallest observed value while $X_{(n)}$ is the largest. The value $X_{(k)}$, which is k-th from the smallest, is defined as the k^{th}-order statistic. The objective is to find the PDF of k-order statistic $f_{(k)}(x)$.

The PDF is, by definition, the derivative of the CDF:

$$f_{(k)}(x) = \frac{dF_{(k)}(x)}{dx} \tag{2.1}$$

The cumulative distribution function (CDF) of the k^{th}-order statistic is defined as the probability that the encountered value of the k^{th}-order statistic is less than an argument of this function.

$$F_{(k)}(x) = P\left(X_{(k)} \le x\right) \tag{2.2}$$

However, if

$$\{X_{(k+1)} \le x\} \Rightarrow \{X_{(k)} \le x\} \tag{2.3}$$

Because values $X_{(i)}$ are sorted in aseending order (due to definition of order statistic), so

$$X_{(k)} < X_{(k+1)} \tag{2.4}$$

The eonverse is not true: if $X_{(k)} \le x$ it not neeessarily mean that it is also larger than $X_{(k+1)}$. The following expression is bieonditional, but it is for $k = n - 1$ only

$$\{X_{(n)} \le x\} \cup \{X_{(k)} \le x < X_{(n)}\} \Leftrightarrow \{X_{(k)} \le x\} \quad ; \quad k = n-1 \tag{2.5}$$

Formula (2.5) ean be generalized for any value of k

$$\{X_{(n)} \le x\} \cup \left(\bigcup_{i=k}^{n-1} \{X_{(i)} \le x < X_{(i+1)}\} \right) \Leftrightarrow \{X_{(k)} \le x\} \tag{2.6}$$

Formula (2.6) expresses all possible ways how the condition $X_{(k)} \le x$ can be fulfilled.

The CDF of k-order statisties ean be expressed by substitution of (2.6) into (2.2)

$$F_{(k)}(x) = P(X_{(k)} \le x) = P\left(\{X_{(n)} \le x\} \cup \left(\bigcup_{i=k}^{n-1} \{X_{(i)} \le x < X_{(i+1)}\} \right) \right) \tag{2.7}$$

Equation (2.7) is a probability of a union of random events where the corresponding conditions are true. As it can be clearly seen from the equation (2.7) all the conditions are incompatible and the probability of simultaneously oeeurring random events is zero. As it is known, the probability of the union of incompatible evcnts equals just a sum of probabilities:

$$F_{(k)}(x) = P(X_{(n)} \le x) + \sum_{i=k}^{n-1} P(X_{(i)} \le x < X_{(i+1)}) \tag{2.8}$$

Consider the first eomponent $P(X_{(n)} \le x)$. It is a probability that the argument is greater than the n-order statistie, whieh is the largest observed value. As there were n observations total, the eondition $P(X \le x)$ has to be satisfied n times:

$$P(X_{(n)} \le x) = (P(X \le x))^n = (F(x))^n \tag{2.9}$$

The component under the symbol of summation in expression (2.8) represents a probability that x will exceed a value that has been seen in i observations, but is less than any of the values encountered in n-i observations:

$$P\left(X_{(i)} \le x < X_{(i+1)}\right) = C(n,i)\left(P(X \le x)\right)^{i}\left(P(X > x)\right)^{n-i} \tag{2.10}$$

Here $C(n, i)$ stands for a number of distinct variants where x could exceed values that have been seen in i observations, but not exceed the rest n-i observations. It is a number of combinations of how i values can be chosen out of n.

$$C(n,i) = \frac{n!}{i!(n-i)!} \tag{2.11}$$

It is not difficult to recognize that expression (2.10) is, in fact the binomial distribution:

$$\begin{aligned} &P\left(\left(X_{(i)} \le x < X_{(i+1)}\right)\right) = C(n,i)\,p^{i}q^{n-i} \\ &p = P(X \le x) \quad ; \quad q = P(X > x) = 1 - P(X \le x) = 1 - p \end{aligned} \tag{2.12}$$

By definition, it is the CDF of random variable x,

$$p = P\left(X \le x\right) = F(x) \tag{2.13}$$

Substitution of formulae (2.9), (2.12) and (2.13) into the expression (2.8) yields:

$$F_{(k)}(x) = \left(F(x)\right)^{n} + \sum_{i=k}^{n-1} C(n,i)\left(F(x)\right)^{i}\left(1 - F(x)\right)^{n-i} \tag{2.14}$$

The first term in the expression (2.14) can be presented in the following form:

$$\left(F(x)\right)^{n} = C(n,n)\left(F(x)\right)^{n}\left(1 - F(x)\right)^{0} = C(n,i)\left(F(x)\right)^{i}\left(1 - F(x)\right)^{n-i}\Big|_{i=n} \tag{2.15}$$

Then, it can be incorporated into the sum. This leads to the following expression for CDF of k-order statistic:

$$F_{(k)}(x) = \sum_{i=k}^{n} C(n,i)\left(F(x)\right)^{i}\left(1 - F(x)\right)^{n-i} \tag{2.16}$$

Substitution of (2.16) into (2.1) leads to the PDF of k-order. Derivative of the sum,

$$\begin{aligned} f_{(k)}(x) &= \frac{d}{dx}\sum_{i=k}^{n} C(n,i)\left(F(x)\right)^{i}\left(1 - F(x)\right)^{n-i} \\ &= \sum_{i=k}^{n} \frac{d}{dx} C(n,i)\left(F(x)\right)^{i}\left(1 - F(x)\right)^{n-i} \end{aligned} \tag{2.17}$$

Appling the product rule of differentiation:

$$f_{(k)}(x)=\sum_{i=k}^{n}C(n,i)\left((1-F(x))^{n-i}\frac{d}{dx}\left((F(x))^{i}\right)+(F(x))^{i}\frac{d}{dx}\left((1-F(x))^{n-i}\right)\right) \tag{2.18}$$

Considering each of the derivatives, using the chain rule of differentiation:

$$\begin{aligned}&\frac{d}{dx}\left((F(x))^{i}\right)=i\cdot(F(x))^{i-1}\cdot f(x)\\&\frac{d}{dx}\left((1-F(x))^{n-i}\right)=(n-i)\cdot(1-F(x))^{n-i-1}\cdot(-f(x))\end{aligned} \tag{2.19}$$

Substitution of (2.19) into (2.18) yields:

$$f_{(k)}(x)=f(x)\sum_{i=k}^{n}C(n,i)\left(i(F(x))^{i-1}(1-F(x))^{n-i}-(n-i)(F(x))^{i}(1-F(x))^{n-i-1}\right) \tag{2.20}$$

Expand the formula (2.11) for a number of combinations $C(n, i)$ and consider each component of (2.20) separately:

$$\begin{aligned}&C(n,i)i(F(x))^{i-1}(1-F(x))^{n-i}=\frac{n!}{i!(n-i)!}i(F(x))^{i-1}(1-F(x))^{n-i}=\\&=\frac{n!}{(i-1)!(n-i)!}(F(x))^{i-1}(1-F(x))^{n-i}=\\&=\frac{(n-1)!n}{(i-1)!((n-1)-(i-1))!}(F(x))^{i-1}(1-F(x))^{n-i}=\\&=C(n-1,i-1)n(F(x))^{i-1}(1-F(x))^{n-i}\end{aligned} \tag{2.21}$$

$$\begin{aligned}&C(n,i)(n-i)(F(x))^{i}(1-F(x))^{n-i-1}=\frac{n!}{i!(n-i)!}(n-i)(F(x))^{i}(1-F(x))^{n-i-1}\\&=\frac{n!}{i!(n-i-1)!}(F(x))^{i}(1-F(x))^{n-i-1}=\\&=\frac{(n-1)!n}{i!((n-1)-i)!}(F(x))^{i}(1-F(x))^{n-i-1}=\\&=C(n-1,i)n(F(x))^{i}(1-F(x))^{n-i-1}\end{aligned} \tag{2.22}$$

Substitution of (2.21) and (2.22) back into (2.20) yields:

$$f_{(k)}(x) = nf(x)\left(\sum_{i=k}^{n} C(n-1,i-1)\left(F(x)\right)^{i-1}(1-F(x))^{n-i} - \right.$$
$$\left. - \sum_{i=k}^{n} C(n-1,i)\left(F(x)\right)^{i}(1-F(x))^{n-i-1} \right) \tag{2.23}$$

Consider the first sum in the expression (2.23); its expansion looks like:

$$\begin{aligned} &\sum_{i=k}^{n} C(n-1,i-1)\left(F(x)\right)^{i-1}(1-F(x))^{n-i} = \\ &\quad = C(n-1,k-1)\left(F(x)\right)^{k-1}(1-F(x))^{n-k} + \\ &\quad + C(n-1,k)\left(F(x)\right)^{k}(1-F(x))^{n-k-1} + \\ &\quad + C(n-1,k+1)\left(F(x)\right)^{k+1}(1-F(x))^{n-k-2} + \\ &\quad + \ldots + \\ &\quad + C(n-1,n-1)\left(F(x)\right)^{n-1}(1-F(x))^{0} \end{aligned} \tag{2.24}$$

Consider the first sum in the expression (2.24); its expansion looks like:

$$\begin{aligned} &\sum_{i=k}^{n} C(n-1,i)\left(F(x)\right)^{i}(1-F(x))^{n-i-1} = \\ &\quad + C(n-1,k)\left(F(x)\right)^{k}(1-F(x))^{n-k-1} + \\ &\quad + C(n-1,k+1)\left(F(x)\right)^{k+1}(1-F(x))^{n-k-2} + \\ &\quad + C(n-1,k+2)\left(F(x)\right)^{k+2}(1-F(x))^{n-k-3} + \\ &\quad + \ldots + \\ &\quad + C(n-1,n)\left(F(x)\right)^{n}(1-F(x))^{-1} \end{aligned} \tag{2.25}$$

Note that the second term in the expanded sum (2.24) is identical to the first term in the expanded sum (2.25), while the third term of (2.24) is equal to the second term of (2.25) and so forth. As the expression (2.23) is a difference between sum (2.24) and (2.25), only the first term of (2.24) and the last term of (2.25) survive.

$$f_{(k)}(x) = nf(x)\left(C(n-1,k-1)\left(F(x)\right)^{k-1}(1-F(x))^{n-k} - \right.$$
$$\left. - C(n-1,n)\left(F(x)\right)^{n}(1-F(x))^{-1} \right) \tag{2.26}$$

Consider the second term in the equation (2.26), the coefficient there expresses the number

$$C(n-1,n)=0 \tag{2.27}$$

As a result the second term in (2.26) equals zero. Finally the PDF of the k-order statistic is:

$$f_{(k)}(x)=f(x)\frac{n!}{(k-1)!(n-k)!}(F(x))^{k-1}(1-F(x))^{n-k} \tag{2.28}$$

2.1.2. Extreme Value Distributions

In general, the distribution of extreme values is a particular case of distribution of order statistics (Gumbel, 1958).

Consider a set of independent identically distributed random values $\{x_1,\ldots,x_n\}$ the limiting cumulative distribution has been shown to be of the form: (Davison, 2003):

$$P\left(x>x_{(n)}\right)=F_{GEV}(x)=\exp\left(-\left(1+\gamma\frac{x-\theta}{\alpha}\right)^{-\frac{1}{\gamma}}\right) \tag{2.29}$$

Here θ is a location parameter, α is a scale parameter and γ is a shape parameter.

This is the Generalized Extreme Value (GEV) distribution and holds for the maxima of observed values of x, regardless of how x is distributed itself. The parameter γ is often referred to as the *extreme value index* and controls the behavior of the upper tail of the distribution. A trio of extreme value distributions arises as special cases of the GEV distribution depending on the value of γ. These distributions are the Gumbel, Freschet, and Weibull distributions.

A Gumbel or Type I distribution arises when γ equals or approaches zero:

$$F_{gbl}(x)=\exp\left(-\exp\left(-\frac{x-\theta}{\alpha}\right)\right) \tag{2.30}$$

For the positive values of the shape parameter γ, a Freschet or Type II distribution arises:

$$F_{frt}(x)=\begin{cases}0 & x\le\theta\\ \exp\left(-\left(\frac{x-\theta}{\alpha}\right)^{-k}\right) & x>\theta\end{cases} \tag{2.31}$$

Here k is a positive shape parameter.

$$F_{wbl}(x) = \begin{cases} 0 & x < \theta \\ 1 - \exp\left(-\left(\frac{x-\theta}{\alpha} \right)^{k} \right) & x \geq \theta \end{cases} \tag{2.32}$$

Here k is a positive shape parameter.

2.1.3. Application Extreme Value Distributions: State-of-the-Art Review

Extreme Value Theory can be found in many applications in Naval Architecture. A typical application is estimating the maximum lifetime wave loads on a ship hull using Weibull distribution. McTaggart pioneered the application of extreme value distributions for the problem of assessing the dynamic stability of ships.

McTaggart (2000, 2000a, 2000b), McTaggart & de Kat (2000) focused on fitting extreme value distributions to roll maxima for predicting the hourly capsize risk of a naval combatant in a stationary seaway. He investigated the use of the several distributions for fitting the roll maxima generated from simulations using the time domain, ship motions code FREDYN. The following extreme distributions were investigated:

- Generalized Extreme Value
- Frechet, referred to as a Type II Maximum Distribution
- Gumbel
- Gumbel Limited Range (GLR)
- Transformed Gumbel

McTaggart found that is was often difficult to obtain a satisfactory distribution fit to the roll maxima. Since the prediction of capsize risk was the goal, the Gumbel Limited Range (GLR) fitting technique was developed. The distribution fit used a least squares method to the empirical CDF which he computed as:

$$F(\phi_{\max}, i) = \frac{i}{N_s + 1} \tag{2.33}$$

In applying the least squares method, only the error in the upper portion of the sample of roll maxima is considered. Through this method, the hope was that this partial distribution fit was useful for extrapolating to the roll angle that was considered for capsize.

The problem of poor distribution fit that McTaggart was attempting to solve with the Limited Range approach caused the extreme non-linearity of the motion of a ship around the peak of the ship's righting arm (stiffness) curve. The ship starts responding differently once the roll angle approaches or exceeds this value (to complicate matters, this point actually fluctuates in a seaway). This change in system dynamics calls into question one of the fundamental assumptions of Extreme Value Theory, that the data is *Independent and Identically Distributed* (IID). If a sample of roll maxima has values larger and smaller than the roll angle where the righting arm peaks, the data may not be *identically distributed.* By considering the upper portion of the data for the least squares

fitting, the Limited Range approaeh attempts to deal with this issue; however, the empiriеal CDF being fit still eontains all of the data.

In the applieation of the above approaeh, generally 30-minute simulation runs were exeeuted. The desired output from the proeess was hourly eapsize risk. The following equation is used to adjust the exposure period of the results:

$$Q_{X,D}(x) = 1 - \left[1 - Q_{X,D_S}(x)\right]^{D/D_S} \tag{2.34}$$

where $Q_{X,D}$ is the exeeedanee probability (referred to as the Quantile funetion or inverse CDF) of X in duration D. D_S is the duration of the simulation.

2.1.4. Method of Maximum Likelihood

The extreme value distributions eonsidered above have two or three parameters. Fitting the distribution to the eollected data requires finding these parameters. The idea of maximum likelihood method is to find such values of parameters that are "more likely" to fit the data.

What is "more likely"? The data points that have been observed are the facts. At the same time they are instanees of a random variable. Just beeause they were observed, these partieular values are more likely than others. That means that the probability of observing these partieular values reaehes maximum when the correct parameters are used for distribution.

To illustrate applieation of this principle, consider a set of n identieally distributed independent random variables. x_i, i=1,2,.., n. Assume the normal distribution for the first example:

$$f(x) = \frac{1}{\sqrt{2\pi}\sigma}\exp\left(-\frac{(x-\mu)^2}{2\sigma^2}\right) \tag{2.35}$$

Where μ stands for the mean value and σ is standard deviation. As all the random variables from the set x_i, i=1,2,.., n are independent of their joint distribution and is a produet of marginal distributions (2.35):

$$f(x_1,..,x_n) = \prod_{i=1}^{n}\frac{1}{\sqrt{2\pi}\sigma}\exp\left(-\frac{(x_i-\mu)^2}{2\sigma^2}\right) \tag{2.36}$$

It is not difficult to see that:

$$f(x_1,..,x_n) = \left(\frac{1}{2\pi\sigma^2}\right)^{n/2}\exp\left(-\frac{1}{2\sigma^2}\sum_{i=1}^{n}(x_i-\mu)^2\right) \tag{2.37}$$

The joint distribution (2.37) depends on two parameters: the mean value μ and the standard deviation σ. The objective is to find such estimates for μ and σ that

maximizes the joint distribution $f(x_1,..x_n)$. As $x_1,..,x_n$ are random numbers the result of maximization also is a random number. Therefore the estimate is aetually a result of averaging:

$$(\mu^*,\sigma^*)=E(\mu,\sigma)=E\left(\arg\max_{\mu,\sigma}(f(x_1,...,x_n))\right) \tag{2.38}$$

Here $E(..)$ is an averaging operator.

The instances of random variable $x_1,..,x_n$ are particular numbers, while the parameters μ and σ are unknowns. It is logieal to consider (2.37)as a funetion of the parameters:

$$f(\mu,\sigma)=\left(\frac{1}{2\pi\sigma^2}\right)^{n/2}\exp\left(-\frac{1}{2\sigma^2}\left(\sum_{i=1}^{n}(x_i-\mu)^2\right)\right) \tag{2.39}$$

The maximum of funetion (2.39) is to be searched; this function is usually referred to as the maximum likelihood estimator:

$$(\mu,\sigma)=\arg\max_{\mu,\sigma}(f(\mu,\sigma))=\arg\max_{\mu,\sigma}(L(\mu,\sigma)) \tag{2.40}$$

Here symbol L is used for the maximum likelihood estimator.

As positions of maxima eannot be affected by monotonic transformations, the same values will be obtained from the logarithm of the maximum likelihood estimator:

$$(\mu,\sigma)=\arg\max_{\mu,\sigma}(\log(L(\mu,\sigma)))=\arg\max_{\mu,\sigma}(L^*(\mu,\sigma)) \tag{2.41}$$

The basis of the logarithm to ehose depends on the particular form of the expression. The natural logarithm seems to be the most reasonable ehoice for the formula (2.42):

$$\begin{aligned}L^*(\mu,\sigma)&=\ln\left(\left(\frac{1}{2\pi\sigma^2}\right)^{n/2}\exp\left(-\frac{1}{2\sigma^2}\left(\sum_{i=1}^{n}(x_i-\mu)^2\right)\right)\right)=\\&=\frac{n}{2}\ln\left(\frac{1}{2\pi\sigma^2}\right)-\frac{1}{2\sigma^2}\left(\sum_{i=1}^{n}(x_i-\mu)^2\right)\end{aligned} \tag{2.42}$$

Most likely estimates for the mean value and standard deviation now can be found as:

$$\begin{cases} \dfrac{\partial L^*(\mu,\sigma)}{\partial \mu} = 0 \\ \dfrac{\partial L^*(\mu,\sigma)}{\partial \sigma} = 0 \end{cases} \tag{2.43}$$

The first equation in the system (2.43) yields:

$$\begin{aligned} &\frac{\partial L^*(\mu,\sigma)}{\partial \mu} = \frac{\partial}{\partial \mu}\left(\frac{n}{2}\ln\left(\frac{1}{2\pi\sigma^2}\right) - \frac{1}{2\sigma^2}\left(\sum_{i=1}^{n}(x_i-\mu)^2\right)\right) = \\ &= 0 - \frac{n}{2\sigma^2}\frac{\partial}{\partial \mu}\sum_{i=1}^{n}(x_i-\mu)^2 = -\frac{n}{\sigma^2}\left(\sum_{i=1}^{n}x_i - n\mu\right) = 0 \end{aligned} \tag{2.44}$$

The equation (2.44) is linear and has a unique solution:

$$\mu = \frac{1}{n}\sum_{i=1}^{n}x_i \tag{2.45}$$

Taking the average from both sides yields the searched estimate:

$$\mu^* = E(\mu) = E\left(\frac{1}{n}\sum_{i=1}^{n}x_i\right) = \frac{1}{n}\sum_{i=1}^{n}\mu = \mu \tag{2.46}$$

Therefore the observed average represents the most likely estimate for the mean value.

Consider the second equation of (2.43):

$$\begin{aligned} &\frac{\partial L^*(\mu,\sigma)}{\partial \sigma} = \frac{\partial}{\partial \sigma}\left(\frac{n}{2}\ln\left(\frac{1}{2\pi\sigma^2}\right) - \frac{1}{2\sigma^2}\left(\sum_{i=1}^{n}(x_i-\mu)^2\right)\right) = \\ &= -\frac{n}{\sigma} + \frac{1}{\sigma^3}\left(\sum_{i=1}^{n}(x_i-\mu)^2\right) = 0 \end{aligned} \tag{2.47}$$

Further consideration of (2.47) yields:

$$\frac{1}{\sigma^3}\left(\sum_{i=1}^{n}(x_i-\mu)^2\right) = \frac{n}{\sigma} \quad \Leftrightarrow \quad \sigma^2 = \frac{1}{n}\sum_{i=1}^{n}(x_i-\mu)^2 \tag{2.48}$$

To complete the solution of the second equation of (2.43), the solution of the first equation (2.45) has to be substituted into (2.48):

$$\sigma^2 = \frac{1}{n}\sum_{i=1}^{n}(x_i - \mu)^2 = \frac{1}{n}\sum_{i=1}^{n}x_i^2 - \frac{2\mu}{n}\sum_{i=1}^{n}x_i + \mu^2 = \frac{1}{n}\sum_{i=1}^{n}x_i^2 - 2\mu^2 + \mu^2 =$$
$$= \frac{1}{n}\sum_{i=1}^{n}x_i^2 - \mu^2 = \frac{1}{n}\sum_{i=1}^{n}x_i^2 - \left(\frac{1}{n}\sum_{i=1}^{n}x_i\right)^2 \qquad (2.49)$$

Standard deviation does not depend on a mean value. Therefore equation (2.49) remains valid after the following substitution:

$$y = x - \mu$$
$$\sigma^2 = \frac{1}{n}\sum_{i=1}^{n}x_i^2 - \left(\frac{1}{n}\sum_{i=1}^{n}x_i\right)^2 = \frac{1}{n}\sum_{i=1}^{n}y_i^2 - \left(\frac{1}{n}\sum_{i=1}^{n}y_i\right)^2 \qquad (2.50)$$

Expanding the square of a sum in the equation (2.50):

$$\left(\frac{1}{n}\sum_{i=1}^{n}y_i\right)^2 = \frac{1}{n^2}\sum_{i=1}^{n}y_i^2 + 2\frac{1}{n^2}\sum_{i=1}^{n}\sum_{j=1}^{n}y_i y_j\Big|_{i\neq j} \qquad (2.51)$$

This leads to the following expression:

$$\sigma^2 = \frac{1}{n}\sum_{i=1}^{n}y_i^2 - \frac{1}{n^2}\sum_{i=1}^{n}y_i^2 - 2\frac{1}{n^2}\sum_{i=1}^{n}\sum_{j=1}^{n}y_i y_j\Big|_{i\neq j} =$$
$$= \frac{n-1}{n^2}\sum_{i=1}^{n}y_i^2 - 2\frac{1}{n^2}\sum_{i=1}^{n}\sum_{j=1}^{n}y_i y_j\Big|_{i\neq j} \qquad (2.52)$$

Appling averaging to the formula (2.52):

$$\sigma^{*2} = E\left(\frac{n-1}{n^2}\sum_{i=1}^{n}y_i^2\right) - E\left(2\frac{1}{n^2}\sum_{i=1}^{n}\sum_{j=1}^{n}y_i y_j\Big|_{i\neq j}\right) \qquad (2.53)$$

As $x_1,..x_n$ and corresponding $y_1,..y_n$ are independent random variables, the second component in (2.53) represents, in fact, a correlation moment:

$$E\left(2\frac{1}{n^2}\sum_{i=1}^{n}\sum_{j=1}^{n}y_i y_j\Big|_{i\neq j}\right) = 0 \qquad (2.54)$$

Continuing consideration of (2.53) leads to:

$$(\sigma^*)^2 = E\left(\frac{n-1}{n^2}\sum_{i=1}^{n} y_i^2\right) = \frac{n-1}{n^2}\sum_{i=1}^{n} E(y_i^2) = \frac{n-1}{n^2} n\sigma^2 = \frac{n-1}{n}\sigma^2 \qquad (2.55)$$

Formula (2.55) confirms the well-known fact that the mean value of the variance is biased. The estimate with corrected bias is:

$$(\sigma^*)^2 = \frac{1}{n-1}\sum_{i=1}^{n}\left(x_i - \mu^*\right)^2 \qquad (2.56)$$

Finally, the maximum likelihood method leads to the conclusion that, for the normal distribution the most likely fit is achieved with well-known formulae for estimates of mean value and standard deviation.

2.2. Using Extreme Value Distribution for Evaluation of Upcrossing Rate

2.2.1. General Approach

According to the information of the authors, the idea to use extreme value distribution for calculation of upcrossing rate belongs to G. Hazen, who formulated this idea and demonstrated the method in early 2009. At the moment of writing this report, the authors are not aware of any publications of this method by G. Hazen or anybody else.

Consider an extreme value distribution in a form of the cumulative distribution function (CDF) fitted over record maxima, provided all the records are of the same duration T_S. By the definition of CDF:

$$F_{EV}(a) = P(x \le a) \qquad (2.57)$$

The probability of the complement event is:

$$P(x > a) = 1 - P(x \le a) = 1 - F_{EV}(a) \qquad (2.58)$$

This probability can be interpreted as a probability of at least one upcrossing of the level a by a process $x(t)$ during time of record T_S. Assuming that the level a is high enough to ensure applicability of Poisson flow, this probability can be expressed as:

$$P(x > a) = 1 - \exp(-\lambda T_S) \qquad (2.59)$$

The formulae (2.58) and (2.59) allow expressing the rate of upcrossing as:

$$\lambda = -\frac{\ln\left(F_{EV}(a)\right)}{T_S} \tag{2.60}$$

2.2.2. *Fitting Extreme Value Distribution*

Following the work of G. Hazen mentioned above, a three-parameter Weibull distribution (2.32) was used with a numerical example described in the previous section. This example included 200 records of wave elevations; each record was 30 minutes. More details can be found in the subsection 1.2.3.

The dataset for analysis is formed from the maximum value observed over a record or a window of a smaller size.

$$T_W = \frac{T_S}{N_W} \tag{2.61}$$

The windowing procedure was implemented to provide the ability to control the time of exposure.

$$x_i = \max\left(\zeta_{i,j}\right) \quad j = 1, ..., \frac{T_W}{\Delta t}; \quad i = 1, ..., N_W \tag{2.62}$$

The shift parameter is found as an observed minimum of the dataset:

$$\theta = \min\left(x_i\right); \quad i = 1, ..., N_W \tag{2.63}$$

Values for scale and shape parameters can be found using the known relations between the theoretical mean value m_x, theoretical variance V_x, and these parameters.

$$\begin{cases} m_x = \alpha\Gamma\left(1+\frac{1}{k}\right) - \theta \\ V_x = \alpha^2\Gamma\left(1+\frac{1}{k}\right) - m_x^2 \end{cases} \tag{2.64}$$

Theoretical values of the mean and variance are unknown, therefore their estimates are used instead:

$$m_x \approx m_x^* = \sum_{i=1}^{N_W} x_i; \qquad V_x \approx V_x^* = \frac{1}{1-N_W}\sum_{i=1}^{N_W}\left(x_i - m_x^*\right)^2 \tag{2.65}$$

Then, the scale parameter α and shape parameter k can be found numerically from the system of equations (2.64).

Alternatively these parameters can be evaluated using the method of maximum likelihood as described in detail in the previous subsection. The probability density function of the Weibull distribution is expressed as:

$$f_{wbl}(x)=\begin{cases}\dfrac{k}{\alpha}\left(\dfrac{x-\theta}{\alpha}\right)^{k-1}\exp\left(-\left(\dfrac{x-\theta}{\alpha}\right)^{k}\right) & x\geq\theta\\ 0 & x<\theta\end{cases} \tag{2.66}$$

Without limitation of generality, the maximum likelihood method can be applied for shifted random variable y:

$$y=x-0 \tag{2.67}$$

The PDF of the shifted variable can be expressed as:

$$f_{wbl}(y)=\begin{cases}\dfrac{k}{\alpha}\left(\dfrac{y}{\alpha}\right)^{k-1}\exp\left(-\left(\dfrac{y}{\alpha}\right)^{k}\right) & y\geq 0\\ 0 & y<0\end{cases} \tag{2.68}$$

The maximum likelihood estimator $L(\alpha, k)$ can be expressed as (Cohen, 1965):

$$L(\alpha,k)=\prod_{i=1}^{n}f(y_i)=\prod_{i=1}^{n}\frac{k}{\alpha}\left(\frac{y_i}{\alpha}\right)^{k-1}\exp\left(-\left(\frac{y_i}{\alpha}\right)^{k}\right) \tag{2.69}$$

For simplification of further derivations, it is convenient to use the substitution:

$$\vartheta=\alpha^{k} \tag{2.70}$$

Substitution of (2.70) into (2.69) yields:

$$L(\vartheta,k)=\prod_{i=1}^{n}\frac{k}{\vartheta}y_i^{k-1}\exp\left(-\frac{y_i^{k}}{\vartheta}\right) \tag{2.71}$$

The logarithmic estimator is expressed as:

$$\begin{aligned}L^{*}(\vartheta,k)&=\ln\left(\prod_{i=1}^{n}\frac{k}{\vartheta}y_i^{k-1}\exp\left(-\frac{y_i^{k}}{\vartheta}\right)\right)=\\&=n\ln(k)-n\ln(\vartheta)+(k-1)\sum_{i=1}^{n}\ln(y_i)-\frac{1}{\vartheta}\sum_{i=1}^{n}y_i^{k}\end{aligned} \tag{2.72}$$

Maximization of the estimator (2.72) requires:

$$\begin{cases} \dfrac{\partial L^*(\vartheta,k)}{\partial \vartheta} = 0 \\ \dfrac{\partial L^*(\vartheta,k)}{\partial k} = 0 \end{cases} \tag{2.73}$$

Differentiation in (2.71) leads to the following system of algebraic equations:

$$\begin{cases} \dfrac{n}{\vartheta} - \dfrac{1}{\vartheta^2}\sum_{i=1}^{n} y_i^k = 0 \\ \dfrac{n}{k} + \sum_{i=1}^{n} \ln(y_i) - \dfrac{1}{\vartheta}\sum_{i=1}^{n} y_i^k \ln(y_i) = 0 \end{cases} \tag{2.74}$$

The unknown ϑ can be expressed through the unknown k using the first equation of the system (2.74).

$$\vartheta = \frac{1}{n}\sum_{i=1}^{n} y_i^k \tag{2.75}$$

Substitution of (2.75) into the second equation of (2.74) excludes ϑ and leads to a nonlinear algebraic equation with only one unknown, k:

$$\frac{1}{k} + \frac{1}{n}\sum_{i=1}^{n} \ln(y_i) - \frac{\sum_{i=1}^{n} y_i^k \ln(y_i)}{\sum_{i=1}^{n} y_i^k} = 0 \tag{2.76}$$

Equation (2.76) then can be solved with any appropriate numerical method.

Figure 2.1 shows an example of fitting a Weibull distribution using both the moment method ((2.64)-(2.65)) and the method of maximum likelihood ((2.75)-(2.76)). These data represent 200 maximum wave elevations observed during each record, so it was only one window per record. This figure also shows the results of the Pearson chi-square goodness-of-fit test for both methods. As it can be seen, both methods have passed.

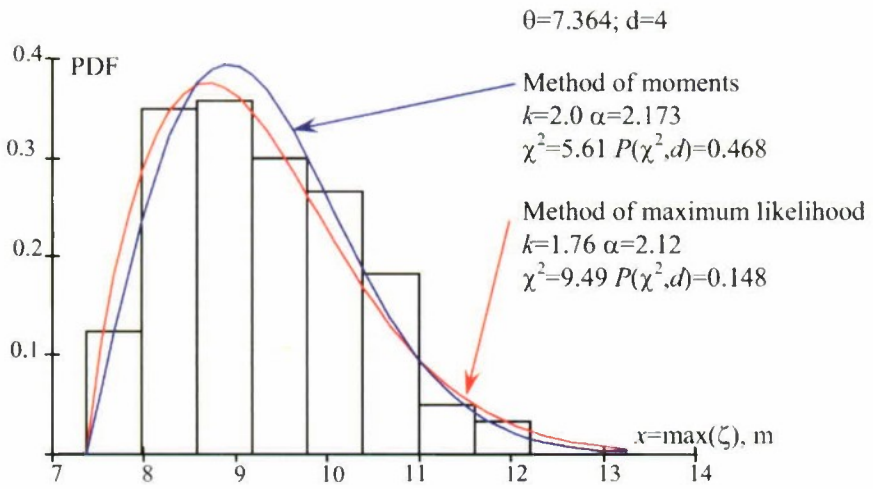

Figure 2.1. Histogram of Extreme Wave Elevation with Weibull distribution fitted

Table 4 shows the results of the goodness-of-fit test for a series of windows length. As ean be seen from that table, once a window beeomes too short the Weibull distribution does not fit the data anymore

Table 4. Results of Pearson chi-square goodness-of-fit test

N_w	T_w	n	σ_{max}	d	θ	Method of moments				Methods of maximum likelihood			
						k	α	χ2	P	k	α	χ2	P
1	1800	200	1.01	9	7.364	2.000	2.173	5.61	0.468	1.76	2.12	9.49	0.148
2	900	400	1.11	9	6.248	2.277	2.704	9.1318	0.425	2.13	2.671	11.3	0.259
3	600	600	1.17	12	5.579	2.407	2.979	18.20	0.110	2.304	2.958	18.4	0.105
4	450	800	1.21	14	5.123	2.481	3.160	38.72	4.03e-4	2.381	3.141	38.2	4.03e-4
5	360	1000	1.24	16	4.452	2.835	3.637	60.5	4.32e-7	2.703	3.622	54.3	4.68e-6

2.2.3. Evaluation of Confidence Intervals for Weibull Distribution

All three parameters of the Weibull distribution are determined from statistical data and, therefore, they are random numbers. This means that the uperossing rate evaluated with en extreme value distribution (2.60) is, indeed, a random number. As with any other estimate, the crossing rate (2.58) needs a eonfidenee interval to evaluate the statistieal uncertainty involved.

The expression (2.64) relates the estimates of the mean value and varianee with parameters of Weibull distribution. The eonfidenee interval for these estimates can be assessed trivially using conventional assumptions of the normal distribution of the estimates of the mean value and varianee. Caution has to be exereised, however, when applying the normal distribution for the varianee estimate, as the variance is a positive value, while the normal distribution is supported for negative values as well.

To determine the distribution for the mean value estimate, two parameters are needed – the mean value of the mean value estimate and the varianee of the mean value

estimate. As the mean value is an unbiased estimate, its mean value is equal to the estimate itself:

$$m(m_x^*) = m_x^* = \sum_{i=1}^{N_W} x_i \; ; \qquad V(m_x^*) = \frac{V_x^*}{N_W} = \frac{1}{(1-N_W)N_W} \sum_{i=1}^{N_W} \left(x_i - m_x^*\right)^2 \tag{2.77}$$

Then the half-breadth of confidenee interval for the mean estimate is:

$$\varepsilon(m_x^*) = K_\beta \cdot \sqrt{V(m_x^*)} \tag{2.78}$$

The eoeffieient K_β depends on eonfidenee probability β:

$$\begin{aligned} &\beta = 0.95 \; ; \qquad K_\beta = 1.959964 \\ &\beta = 0.9973 \; ; \quad K_\beta = 3.0 \end{aligned} \tag{2.79}$$

More details on the confidenee interval ean be found in the previous subsection (formulae (2.54)-(2.58)).

Finally, the eomplete estimate for the mean looks like:

$$m_x^* = m(m_x^*) \pm \varepsilon(m_x^*) \tag{2.80}$$

Construction of the eonfidence interval for the varianee estimate involves more assumptions. If a random variable would have a normal distribution, then the distribution of its varianee estimate would follow the ehi-square distribution. One of the most important qualities of the ehi-square distribution is it only supports positive values. This corresponds to one of the most basie properties of the variance – it is not negative. The PDF of the ehi-square distribution is defined by the following formula.

$$f_{\chi^2}(x) = \frac{1}{2^{\frac{d}{2}} \cdot \Gamma\left(\frac{d}{2}\right)} \left(\frac{x}{2}\right)^{\frac{d}{2}-1} \exp\left(-\frac{x}{2}\right) \quad ; \quad x \geq 0 \tag{2.81}$$

The ehi-square distribution depends on a single parameter d, whieh is commonly referred to as the "degrees of freedom". If the chi-square distribution is used for construction of the eonfidenee interval, the meaning of d is the number of points – instances of the random variable.

With an inereased number of random values, the chi-square distributions tends to a normal distribution; near 30 values, it is almost indistinguishable, see Figure 2.2. The reason for the convergenee of the two distributions is the Central Limit Theorem, which states that the sum of independent, identieally distributed random variables, tends to a normal distribution with the increase of number of eomponents in the sum. That is why

the normal distribution is also used for construction of the confidenec interval for the variance wherc the number of points is largc.

At the same time, the normal distribution is supported for negative valucs as well, which, in principle, allows a certain probability for negative variances. However, the mean value of a random variable following chi-square distribution equals the number of degrecs of freedom. Thus with the increase in the number of points,the entire curve moves to the right, as it can be clearly seen in Figure 2.2. In a limit, when a numbcr of points reaches infinity, the mean value is equal to positive infinity, leaving thc probability of negative variances essentially zero. Nevertheless, caution has to be exercised while using the normal distribution for the confidence interval of variances, especially when the number of points is not that large and the dcsired confidence level is relatively high.

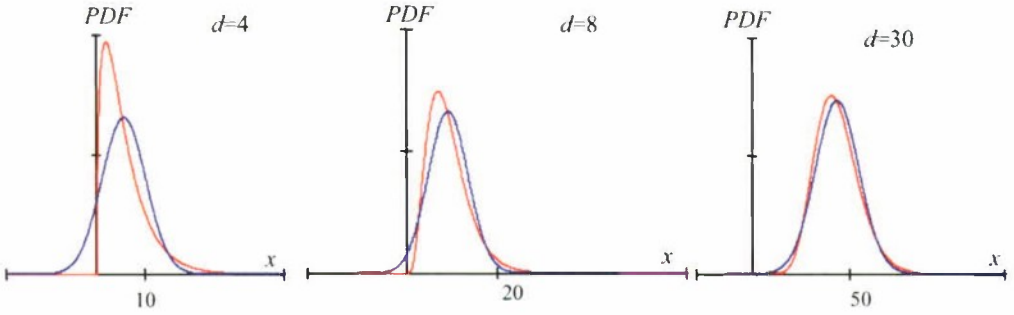

Figure 2.2 Chi-square (red) and normal distribution (blue)

The main advantage of the normal distribution is that it is universal for a large number of points, while the ehi-squarc distribution only can be applied when the variable has a normal distribution. When the variablc does not have normal distribution, like in cases with extrcme valucs, thc distribution of a sum of its squares may not be actually known. However, it is known that this sum will tend to thc normal distribution with the increase of the number of points due to thc Central Limit Theorem.

To define the normal distribution for the variance estimate, two parameters arc needed: the mean value of the variancc estimatc and the varianec of the variance estimate. As it is known (and shown in the previous subsection) that the variancc estimate is biased: its mean value is shifted from the mean sum of squares:

$$V_x^* = \frac{1}{n}\sum_{i=1}^{n}(x_i - m_x)^2$$
$$m(V_x^*) = \frac{n}{n-1}V_x^* \qquad (2.82)$$

The variance of the varianee is expressed with the well known formula:

$$V(V_x^*) = \frac{\mu_4}{n} - \frac{n-3}{n(n-1)} V_x \tag{2.83}$$

Here μ_4 is the fourth central moment of the distribution; as the Weibull distribution has been already fitted, the PDF is known so:

$$\mu_4 = \int_0^x f(x)(x - m_x)^4 dx \tag{2.84}$$

The fourth central moment of the Weibull distribution can also be directly calculated. The excess kurtosis of the Weibull distribution is given by:

$$\gamma_2 = \frac{-6 \cdot \Gamma_1^4 + 12 \cdot \Gamma_1^2 \cdot \Gamma_2 - 3 \cdot \Gamma_2^2 - 4 \cdot \Gamma_1 \cdot \Gamma_3 + \Gamma_4}{\left(\Gamma_2 - \Gamma_1^2\right)^2} \tag{2.85}$$

Where: $\Gamma_i = \Gamma(1+i/k)$

The fourth central moment is then:

$$\mu_4 = (3 + \gamma_2) \cdot \sigma^4 \tag{2.86}$$

The half-breadth of the confidence interval for the mean estimate is then:

$$\varepsilon(V_x^*) = K_\beta \cdot \sqrt{V(V_x^*)} \tag{2.87}$$

Finally the complete estimate for the variance is:

$$V_x^* = m(V_x^*) \pm \varepsilon(V_x^*) \tag{2.88}$$

The third parameter is the shift. It is defined as a smallest among observed extreme values. Therefore it is the first order statistic (see previous subsection) and has the following distribution:

$$f(\theta) = f_{(1)}(x) = N_R f(x)(1 - F(x))^{N_R - 1} \tag{2.89}$$

Where $f(x)$ and $F(x)$ are the PDF and CDF, respectively, of the Weibull distribution and are defined with formulae (2.34) and (2.68).

There is a problem with using the distribution (2.89) for the construction of the confidence interval directly. It does not support values less than the observed shift $x<\theta$. Therefore, all possible values of the shift are larger than the observed one. At the same time there is no reason to believe that the observed shift is the smallest possible. Therefore it is assumed that the observed shift is some sort of mean value, which can be calculated as:

$$m_{(1)} = \int_{\theta}^{\infty} f_{(1)}(x)x dx \tag{2.90}$$

Then the distribution (2.89) shifted by the value $m_{(1)}$;

$$f(\theta) = N_R f(\theta - m_{(1)})(1 - F(\theta - m_{(1)}))^{N_R - 1} \tag{2.91}$$

Both the original and shifted distribution are shown in Figure 2.3. Justification of such an approach could be offered as follows. For the uni-modal, slightly asymmetrical distribution, the mean value can be considered as an approximation for the mode. Following the principle of maximum likelihood, the observed value of the shift should have maximum probability, i.e. should correspond to the mode.

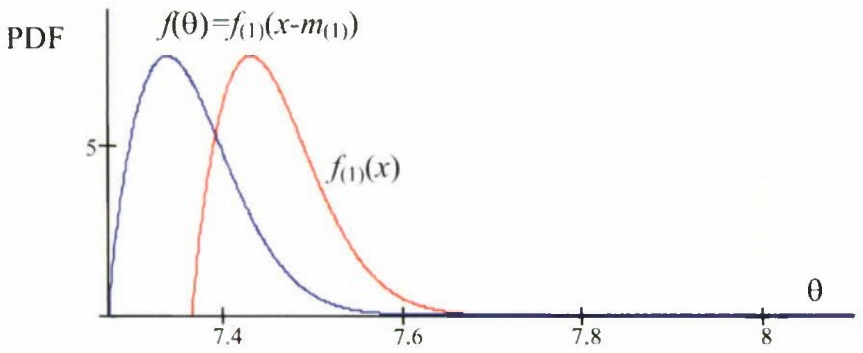

Figure 2.3 Distribution of the first order statistic and distribution of shift

Once the distribution of the shift parameter has been accepted, further calculations of the confidence interval are trivial (see details in the previous section, formulae(2.54)-(2.57)). The cumulative distribution function of the shift parameter and its derivative are expressed as:

$$F(\theta) = \int_{\theta^* - m_{(1)}}^{\theta} f(\theta)d\theta\,; \quad Q(P) = inv(F(\theta)) \tag{2.92}$$

Here the observed value of the shift is identified with an asterisk to avoid confusion with the shift parameter as a variable. The boundaries for the shift parameter are expressed as:

$$\theta_{low} = Q\left(\frac{1-\beta}{2}\right) \quad ; \quad \theta_{up} = Q\left(\frac{1+\beta}{2}\right) \tag{2.93}$$

Here β is the accepted confidence probability.

To complete the evaluation of the lower and upper boundaries of the Weibull distribution, the variable can be scaled to correspond to the upper and lower boundaries of the estimate of the variance and shifted to accommodate variability in the mean value estimate and the shift parameter.

The scaling is applied directly to the shifted data points (see formula (2.67)):

$$y_{low} = y\sqrt{\frac{m(V_x^*) - \varepsilon(V_x^*)}{m(V_x^*)}}; \quad y_{up} = y\sqrt{\frac{m(V_x^*) + \varepsilon(V_x^*)}{m(V_x^*)}} \tag{2.94}$$

Scaling of the variable does not affect the shape parameter. It can be verified by the solution of the equation (2.76) using data points scaled to the lower or upper boundary.

$$\frac{1}{k_{low}} + \frac{1}{n}\sum_{i=1}^{n}\ln\left(y_{low_i}^{k_{low}}\right) - \frac{\sum_{i=1}^{n} y_{low_i}^{k_{low}} \ln\left(y_{low_i}\right)}{\sum_{i=1}^{n} y_{low_i}^{k_{low}}} = 0 \tag{2.95}$$

$$\frac{1}{k_{up}} + \frac{1}{n}\sum_{i=1}^{n}\ln\left(y_{up_i}^{k_{up}}\right) - \frac{\sum_{i=1}^{n} y_{low_i}^{k_{up}} \ln\left(y_{up_i}\right)}{\sum_{i=1}^{n} y_{up_i}^{k_{up}}} = 0 \tag{2.96}$$

It was found that within the margin of numerical tolerance:

$$k = k_{low} = k_{up} \tag{2.97}$$

Therefore, as expected, scaling does not affect the shape parameter. The boundary for scaling parameters can be found using formulae (2.75) and (2.70)

$$\alpha_{low} = \left(\frac{1}{n}\sum_{i=1}^{n} y_{low_i}^{k}\right)^{-k} \qquad \alpha_{up} = \left(\frac{1}{n}\sum_{i=1}^{n} y_{up_i}^{k}\right)^{-k} \tag{2.98}$$

The lower and upper boundaries of the Weibull distribution itself can be found by applying a respective shift to accommodate variability of the mean value and shift parameter.

$$f_{wbl}^{low}(x)=\begin{cases}\dfrac{k}{\alpha_{low}}\left(\dfrac{x+\varepsilon(m_x^*)-0_{low}}{\alpha_{low}}\right)^{k-1}\exp\left(-\left(\dfrac{x+\varepsilon(m_x^*)-\theta_{low}}{\alpha_{low}}\right)^{k}\right) & x+\varepsilon(m_x^*)\geq\theta_{low}\\ 0 & x+\varepsilon(m_x^*)<\theta_{low}\end{cases}$$

$$f_{wbl}^{up}(x)=\begin{cases}\dfrac{k}{\alpha_{up}}\left(\dfrac{x-\varepsilon(m_x^*)-\theta_{up}}{\alpha_{up}}\right)^{k-1}\exp\left(-\left(\dfrac{x-\varepsilon(m_x^*)-\theta_{up}}{\alpha_{up}}\right)^{k}\right) & x-\varepsilon(m_x^*)\geq\theta_{up}\\ \theta & x-\varepsilon(m_x^*)<\theta_{up}\end{cases} \qquad (2.99)$$

Figure 2.4 shows Weibull distribution with upper and lower boundary calculated for. N_w=1.

Formulae similar to (2.99) can be written for CDFs as well:

$$F_{wbl}^{low}(x)=\begin{cases}1-\exp\left(-\left(\dfrac{x+\varepsilon(m_x^*)-\theta_{low}}{\alpha_{low}}\right)^{k}\right) & x+\varepsilon(m_x^*)\geq\theta_{low}\\ 0 & x+\varepsilon(m_x^*)<\theta_{low}\end{cases}$$

$$F_{wbl}^{up}(x)=\begin{cases}1-\exp\left(-\left(\dfrac{x-\varepsilon(m_x^*)-\theta_{up}}{\alpha_{up}}\right)^{k}\right) & x-\varepsilon(m_x^*)\geq\theta_{up}\\ 0 & x-\varepsilon(m_x^*)<\theta_{up}\end{cases} \qquad (2.100)$$

Figure 2.5 Shows CDF for Weibull distribution with the confidence interval

The procedure described above has not formally been proven. Rather, it has to be considered as an approximate method allowing the evaluation of statistical uncertainty of upcrossing rate calculated on the basis of extreme value theory. This analysis can be found in the next subsection.

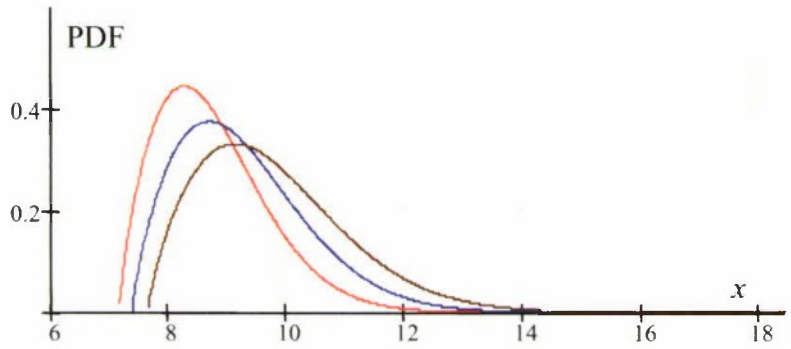

Figure 2.4 PDF for Weibull distribution for extreme values (blue), its upper (brown) and lower (red) boundaries

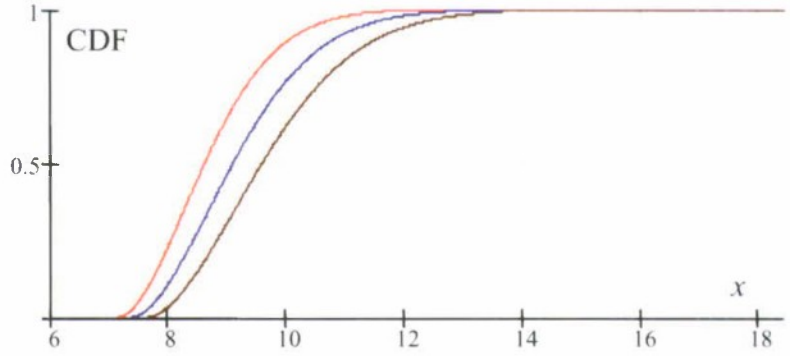

Figure 2.5 CDF for Weibull distribution for extreme values (blue), its upper (brown) and lower (red) boundaries

2.2.4. Evaluation of Confidence Intervals for Upcrossing Rates

Formula (2.60) relates the CDF of an extreme value distribution to the upcrossing rate. The procedure described in the above section derived the approximate CDF based on the Weibull distribution corresponding to lower and upper boundaries of confidence interval. This confidence interval reflects the uncertainty introduced by statistical estimates of the parameters. These boundaries are to be used to estimate the confidence interval for the rate of upcrossings:

$$\lambda_{low} = -\frac{\ln\left(F_{wbl}^{low}(a)\right)}{T_S}; \quad \lambda_{up} = -\frac{\ln\left(F_{wbl}^{up}(a)\right)}{T_S} \tag{2.101}$$

This confidence interval is shown in Figure 2.6 along with theoretical value and estimates obtained with other methods (described in the previous section). The level of crossing was 9 m. The method based on the extreme value distribution provided the correct estimate; the theoretical solution is inside the confidence interval. The width of the confidence interval is slightly wider than the result based on the censored time before the first crossing.

When the crossing level is raised up to 10 m (see Figure 2.7), the confidence interval of upcrossing rate based on extreme values becomes narrower than the confidence interval based on censored time before the first upcrossing. Once the crossing level becomes higher, the number of crossings decrease dramatically and the statistical uncertainty of mean time before the 1st upcrossing also increases. Meanwhile, the volume of samples for extreme values does not depend on how high the crossing level is or if there any crossings at all. The dependence of the width of the confidence interval on the crossing level will be examined later.

Further increase of the crossing level, up to 11 m, with only 10 crossings leads to dramatic widening of the confidence interval for the upcrossing rate based on time before the first upcrossing, see Figure 2.8. The rate estimated with extreme value distribution retains the meaningful width of the confidence interval that still contains the theoretical value.

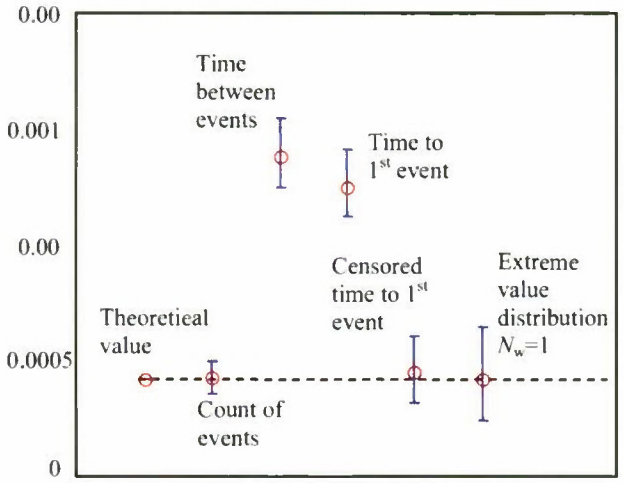

Figure 2.6 Comparison of different methods to estimate upcrocssing rate for the numerical example for level 9 m (Total number of upcrossings 153).

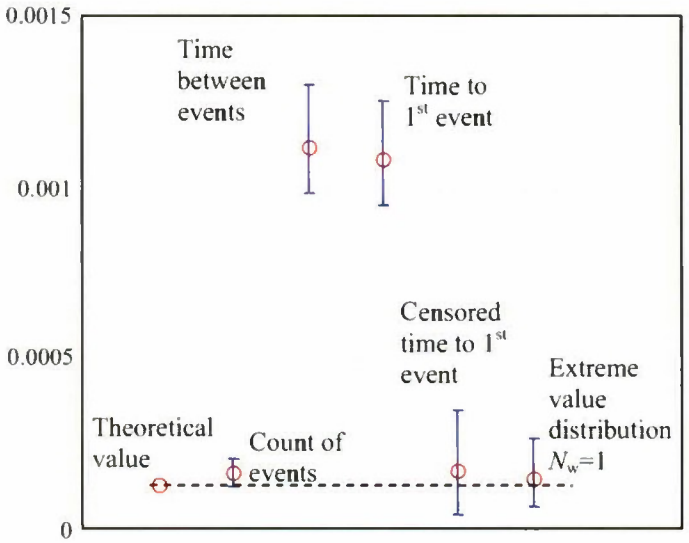

Figure 2.7 Comparison of different methods to estimate upcrocssing rate for the numerical example for level 10 m (Total number of upcrossings 58).

Lowering the level of crossing to 7.75 m leads to significant widening of the confidence interval of the crossing rate based on the extreme value distribution (see Figure 2.9). Attempts to lower the level further leads to the impossibility to calculate the confidence interval as the crossing level becomes larger than the lower boundary of the shift parameter. To alleviate this limitation the length of the windows needs to be shortened. It is also leads to a narrower confidence interval, see Figure 2.9.

The "big picture" is shown in Figure 2.10 and Figure 2.11. The estimate of the upcrossing rate along its confidence interval evaluated from the distribution of extreme values is shown as a function of the crossing level. The theoretical solution is also shown in these figures. Inserts show the same curve for higher crossing levels. Figure 2.10 shows the curves for N_w=1, so the window length equals to the length of the record, while Figure 2.11 contains the same picture for N_w=2, there are two windows per record.

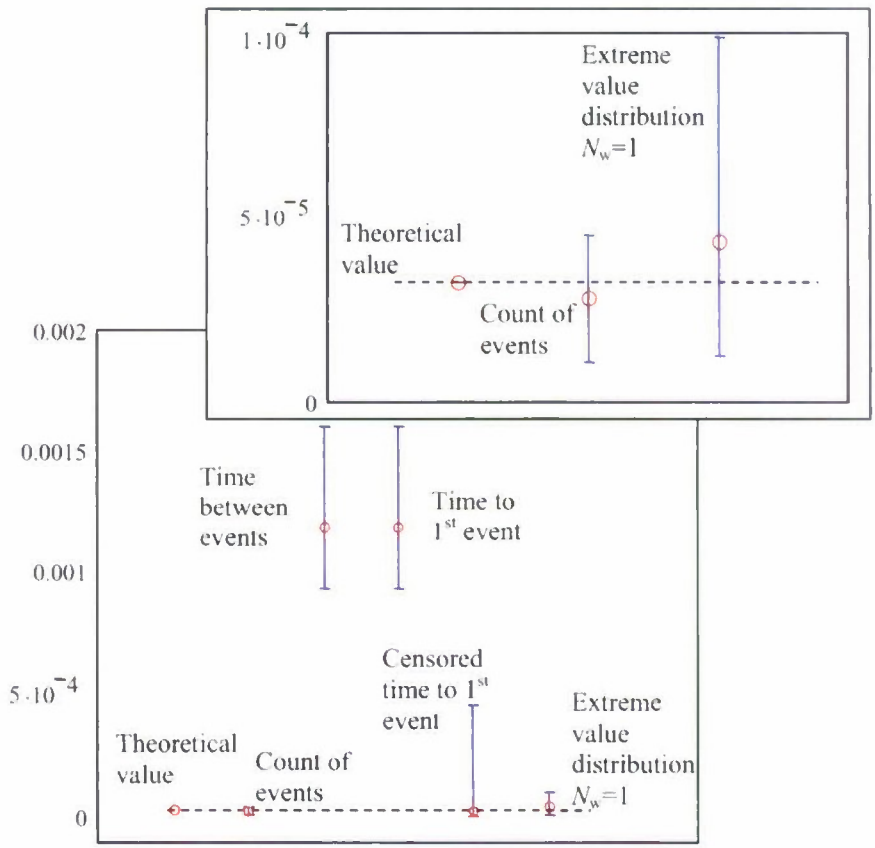

Figure 2.8 Comparison of different methods to estimate upcrocssing rate for the numerical example for level 11 m (Total number of upcrossings 10).

The curves on the both Figure 2.10 and Figure 2.11 follow the same pattern. The theoretical solution is contained within the confidence interval until it reaches a certain crossing level value. This value is about 7.4 m for N_w=1 and 6.2 m for N_w=2. This is caused by the limitation of Weibull distribution as it starts from the shift parameter which is the smallest among observed extreme values. Naturally, the probability of exceeding cannot be evaluated below this level. Using a shorter window makes the shift parameter smaller and, therefore allows working with lower crossing levels.

Looking at Figure 2.10 and Figure 2.11makes it clear why the confidence interval increased so much in Figure 2.9 for N_w=1. The crossing value 7.75 is not very far from the limit; the curves in Figure 2.10 turn upward and become almost vertical.

While the methods based on the extreme method do not work very well for smaller crossing levels, it seems to give excellent results for the higher level where no

statistics of crossing is available. In the example considered, there is only one crossing on the level 12 m. The maximum value observed is about 12.07 m, so there is not an upcrossing for the level of 13 m and higher. As it can be seen from the inserts in Figure 2.10, the method continues to produce correct results well beyond that level. Therefore it has a potential for statistical extrapolation.

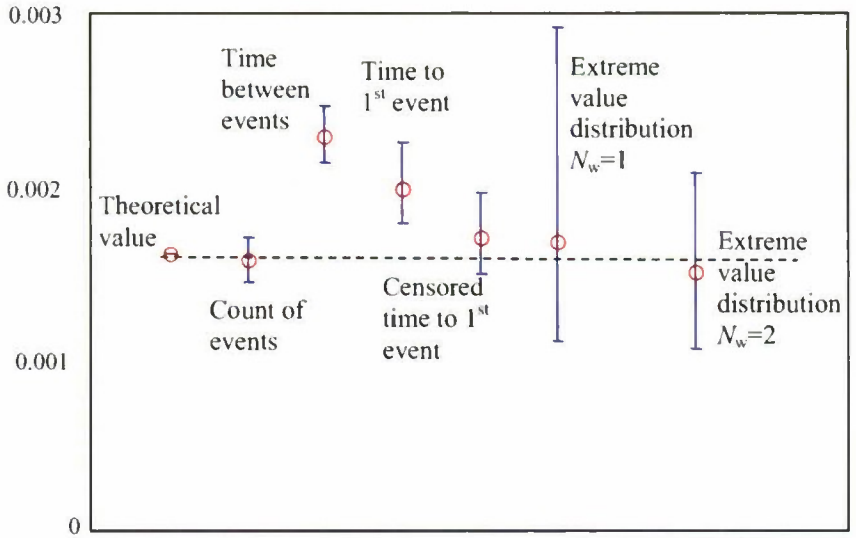

Figure 2.9 Comparison of different methods to estimate upcrossing rate for the numerical example for level 7.75 m (Total number of upcrossings 425)

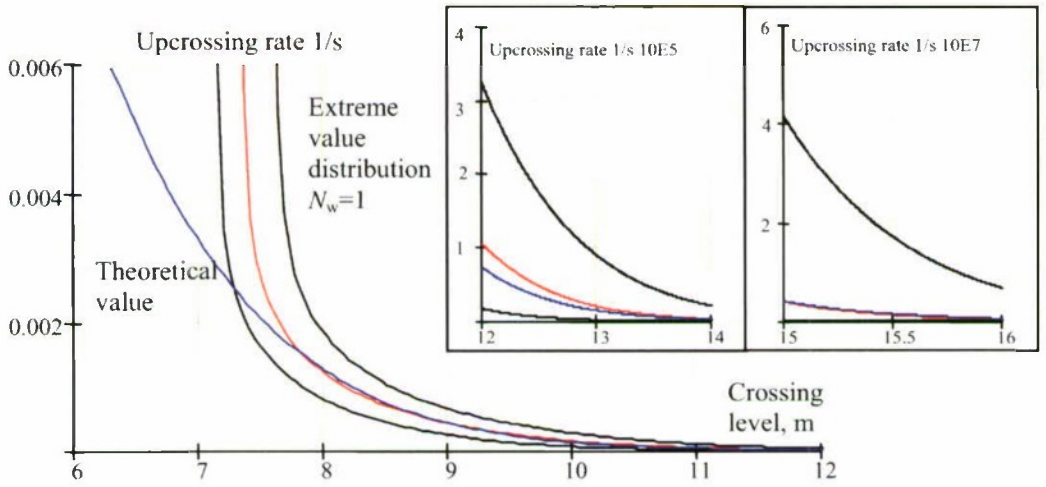

Figure 2.10 Estimate of upcrossing rate based on extreme value distribution with confidence intervals as a function of crossing level N_w=1

Making windows smaller, however, decreases performance of the method for higher levels. As it can be seen from the second insert in Figure 2.11, the theoretical solution leaves the confidence interval somewhere around 15.4 m.

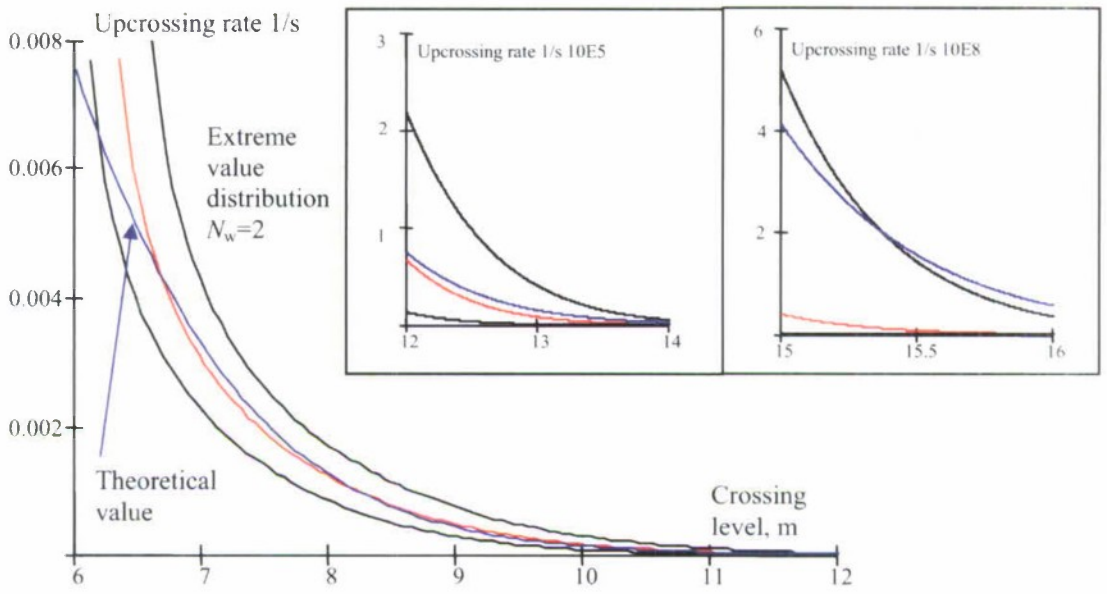

Figure 2.11 Estimate of upcrossing rate based on extreme value distribution with confidence intervals as a function of crossing level N_w=2

2.3.Summary

Order statisties deseribe the behavior of the k-th largest observation out of total number n. Indeed, it is a random variable and, as any other random variable, can be characterized by a distribution.

The behavior of the largest observation (case when $k = n$) is the subject of the study of Extreme Value Theory (EVT). The distribution of the extreme values is a limit distribution and does not depend on the distribution of the random variable of a stochastic proeess. If the extreme value distribution is applied to a stochastic process, all observations must be done over the same time interval.

The parameters of an extreme value distribution can be determined from the observations using the Method of Maximum Likelihood Estimation (MLE). The MLE method is based on the faet that the obsereved data points are, aetually, random numbers. As these particular values were observed, therefore they are "more likely", or their probability of oeeurring is maximum.

The extreme value distribution parameters are random numbers, as they are ealculated from random variables. Therefore the extreme value distribution fitted to the observed data is also a random figure and subjeet to statstistieal uncertainty. The confidenee interval is evaluated for the extreme valuc distribution as a measure of statistical uncertainity.

The extreme value distribution can be used for the evaluation of the upcrossing rate, based on the probability of no upcrossing events oeeurring during the observation time. The eonfidenee interval also ean be evaluated for for the upcrossing rate calculated with this method.

This page is intentionally left blank

3. Peaks over the Threshold

This section describes a method of statistical extrapolation using the probabilistic properties of the peaks of the envelope that exceed a given threshold.

3.1. The Problem of Rarity

3.1.1. Introduction

Large roll events are rare. The main objective of this work is to develop a method of that would be able to charaeterize the probability of events that are too rare to observe in a model test or numerical simulation. This problem is known in the Naval Arehiteeture eommunity as "The Problem of Rarity".

The problem of rarity arises when the average time before a stability failure may oceur is very long in comparison with the natural roll period, which serves as the main time-seale for the roll motion process (definition from SLF 51/WP.2 Annex 1 paragraph 6.3.2).

While the problem of rarity was the main obstacle for application of time domain methods during the last two decades, the term was introduced only relatively recently (SLF 50/4/4). Some review of available treatments of this problem is available from Belenky, *et al*, 2008.

3.1.2. Statistical Extrapolation as a Solution of Problem of Rarity

The main challenge of the problem of rarity comes from the nonlinear nature of large-amplitude roll motions. To illustrate this statement, one can imagine that roll motions can be deseribed by a linear differential equation; then the roll response could be completely eharaeterized by a response amplitude operator within the frequeney domain. As a linear operator does not change the normality of the distribution and the wave excitation can be eonsidered as a normal process, the distribution of the response would be known to be normal. In this case, the theory of uperossing would provide the necessary probabilistic eharaeterization of erossing any level and the problem would be fully solved.

Even if the nonlinearity would be mild, application of a linearization procedure could be justified. This means that it would be possible to find such a linear system that would describe the roll motions with suffieient aceuraey within a relatively wide range of variances of excitation.

The physical reality is different, however. It is well known that large-amplitude roll motions cannot, in general, be eharacterized by normal distribution (Belenky & Sevastianov 2007). The type of distribution depends strongly on the shape of the ship's righting arm curve, whieh may ehange significantly in waves. This leaves time domain numerical simulations and model testing as the only available options to characterize the large-amplitude roll behavior of a ship.

The principle of separation is what allows the problem of rarity to be solved. Instead of one problem with very rare events, two or more related problems are considered: "non-rare" and "rare". The "non-rare" problem, by its definition, should be solvable by a conventional numerical simulation or model test. For example the time-split method (Belenky, *et al* 2007) considered upcrossing of a level around the maximum of the GZ curve as the "non-rare" problem. The "rare" problem then considered the probability of capsizing once this threshold was crossed. The "rare" problem was solved by a series of short simulations trying to find the initial conditions at upcrossing that will lead to capsize. For a single DOF roll problem, this means finding the critical roll rate, such that exceeding this critical roll rate when the threshold is crossed leads to capsize, see Figure 3.1. The procedure for finding the critical roll rate is illustrated in the insert of Figure 3.1.

The solutions for the non-rare and rare problems can then be combined. The combined solution gives the probability of crossing the threshold with initial conditions that would lead to capsize (roll rate exceeding the critical roll rate).

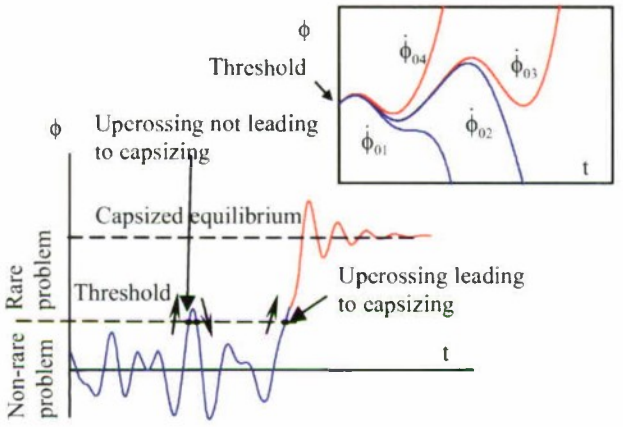

Figure 3.1. Summary of time-split method: separation principle and critical roll rate1

The same principle is used here. The "non-rare" problem is crossing a threshold that is low enough that a statistically significant number of crossings can be observed in a model test or numerical simulation. The "rare" problem is a statistical extrapolation of the data above this threshold, see Figure 3.2.

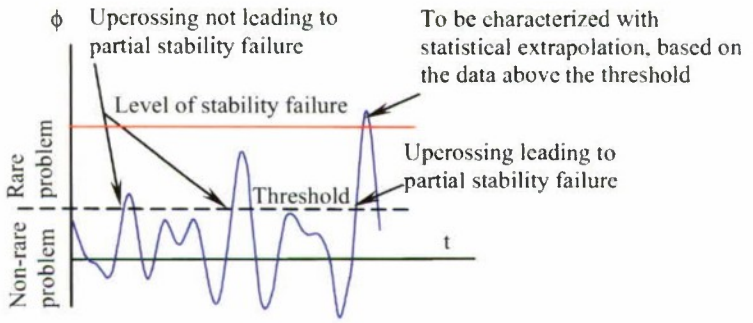

[1] Belenky *et al* 2008b

Figure 3.2 Summary of the current method: separation principle

Nonlinearity is aeeounted for by separating the small and large-amplitude motions with the threshold. If any sort of statistieal fit is used on roll motion data in its entirety, the resulting fit will be dominated by the small-amplitude motions where the roll motion is still relatively linear, and the influence of nonlinearity will generally not be represented properly. The threshold must therefore be high enough, so that the influenee of nonlinearity above that threshold can be considered substantial. It eannot be chosen based purely on statistics. Physical considerations based on the shape of the GZ eurve must be ineluded as well, see Figure 3.3. These eonsiderations, however, are outside of the scope of this report, so therefore the threshold is assumed given.

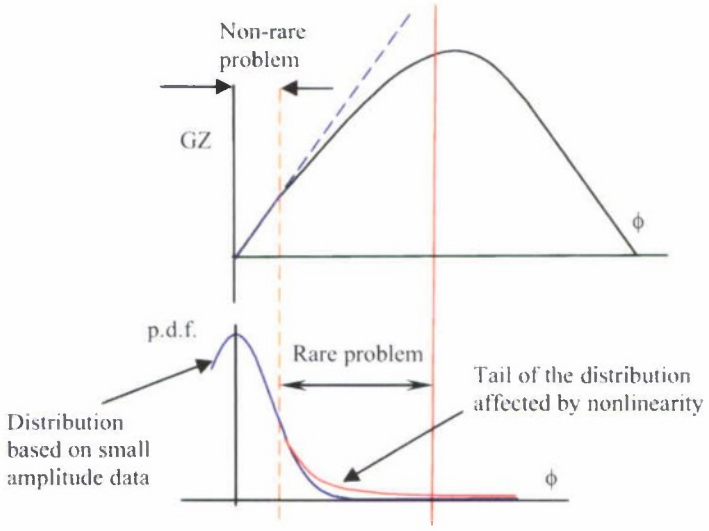

Figure 3.3 Nonlinearity and location of the threshold

3.1.3. Crossing of Two Levels

Prior to considering the statistical extrapolation, consider the relationship between the upcrossing rates of two levels. Consider a stationary differentiable process $x(t)$. The objective is to find different ways to express the uperossing rate of level a_2 through the upcrossing rate of level a_1, provided that $a_2 > a_1$.

Generie formulae for upcrossing rates are as follows:

$$\xi_1 = f(a_1)\int_0^\infty \dot{x} f(\dot{x})d\dot{x} \quad \xi_2 = f(a_2)\int_0^\infty \dot{x} f(\dot{x})d\dot{x} \tag{3.1}$$

The formulae (3.1) immediately yield one way:

$$\xi_2 = \xi_1 P \quad P = \frac{f(a_2)}{f(a_1)} \tag{3.2}$$

If the first level is crossed, the value P can be interpreted as a conditional probability to cross the second level.

Consider an envelope defined as:

$$A(t) = \sqrt{x(t)^2 + y(t)^2} \tag{3.3}$$

Here $y(t)$ is a complimentary process obtained as a the result of a Hilbert transform.

If an upcrossing of a level has occurred, a value of the envelope exceeding that level exists in the local vicinity. The local vicinity is defined as an interval of time while the process $x(t)$ remains above the level a_2. The local maximum (defined as a maximum of the envelope located in the local vicinity) of the envelope limits the local maxima of the process. Therefore whether the process will cross the level a_2 depends if the local maximum of the envelope exceeds this level or not.

The probability of the envelope exceeding the level a_2 can be expressed as:

$$P(A > a_2) = \int_{a_2}^{\infty} f_A(A)dA \tag{3.4}$$

The conditional probability that the envelope exceeds level a_2 under the condition that level a_1 was previously exceeded:

$$P(A > a_2 \mid A > a_1) = \frac{\int_{a_2}^{\infty} f_A(A)dA}{\int_{a_1}^{\infty} f_A(A)dA} \tag{3.5}$$

Therefore another way to express the second upcrossing rate is:

$$\xi_2 = \xi_1 \frac{\int_{a_2}^{\infty} f_A(A)dA}{\int_{a_1}^{\infty} f_A(A)dA} \tag{3.6}$$

Equivalency of formula (3.6) can be formally proven for a normal process, as the distribution of the envelope is known to follow Rayleigh

$$f(x)=\frac{1}{\sqrt{2\pi V_x}}\exp\left(-\frac{x^2}{2V_x}\right)\qquad f_A(A)=\frac{A}{V_x}\exp\left(-\frac{A^2}{2V_x}\right) \tag{3.7}$$

Substitution of (3.7) into (3.6) yields:

$$\xi_2=\xi_1\int_{a_2}^{\infty}\frac{A}{V_x}\exp\left(-\frac{A^2}{2V_x}\right)dA\left(\int_{a_1}^{\infty}\frac{A}{V_x}\exp\left(-\frac{A^2}{2V_x}\right)dA\right)^{-1}=$$

$$\xi_1\frac{\exp\left(-\frac{a_2^2}{2V_x}\right)}{\exp\left(-\frac{a_1^2}{2V_x}\right)}=\xi_1\frac{\frac{1}{\sqrt{2\pi V_x}}\exp\left(-\frac{a_2^2}{2V_x}\right)}{\frac{1}{\sqrt{2\pi V_x}}\exp\left(-\frac{a_1^2}{2V_x}\right)}=\xi_1\frac{f(a_2)}{f(a_1)}=\xi_1 P \tag{3.8}$$

For any type of distribution of process $x(t)$, comparison of formulae (3.2) and (3.6) yields:

$$P=\frac{f(a_2)}{f(a_1)}=\frac{\int_{a_2}^{\infty}f_A(A)dA}{\int_{a_1}^{\infty}f_A(A)dA} \tag{3.9}$$

Having in mind that the envelope contains all the peaks, the formula (3.9) also can be interpreted as the relationship between an uperossing and a peak. As it is shown in Figure 3.4, if a peak is above the threshold, upcrossing did occur as the stochastic process is continuous. There is, therefore, a one-to-one correspondenee of the occurrence of an up-crossing of a level and the oeeurrence of a peak value over that level. The eonsequenee of this is a praetieal one. The peaks may simply be used as a surrogate for the occurrence of upcrossings.

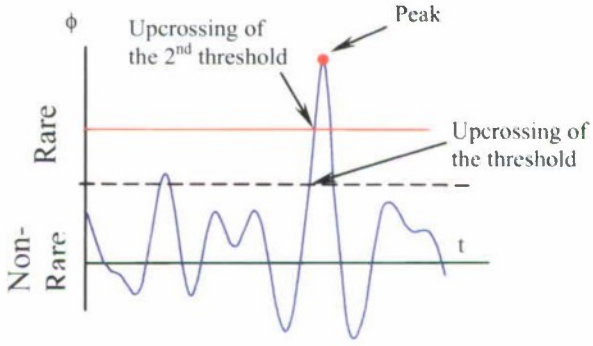

Figure 3.4 Relations between peak and upcrossing

3.2. Properties of Peaks

As the peaks over the threshold, in principle, can be used as surrogate for upcrossing, it makes sense to study the characteristics of peaks in detail.

3.2.1. Distribution of Peaks

The total number of positive peaks found in the wave elevation sample dataset was 31,065. Positive peaks were defined from the following conditions:

$$x_{\max} = x(t_{\max}) \quad | t_{\max} : \quad (\dot{x}(t_{\max}) = 0) \cap (\ddot{x}(t_{\max}) < 0) \tag{3.10}$$

Figure 3.5 shows a histogram of positive peaks superimposed with a Rayleigh distribution. A notable feature of the positive peak sample shown in the histogram is the presence of negative values. They correspond to secondary peaks, which could be expected as the spectrum is not narrow.

Obviously a Rayleigh distribution is not suitable here. It known that peaks of a normal process, characterized by a moderate bandwith spectrum, have a Rice distribution that tends to a Rayleigh distribution with a decrease of the bandwith and to the normal distribution with an increase of bandwith.

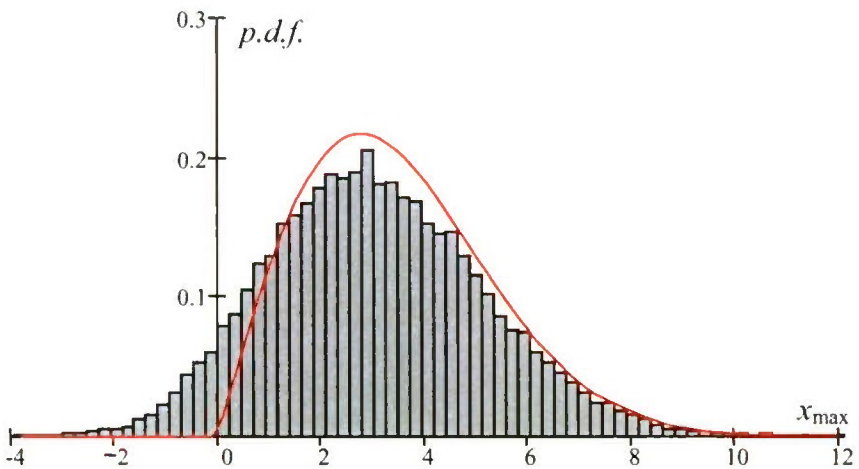

Figure 3.5 Histogram of positive peaks and Rayleigh distribution

Part of the distribution of the positive peaks, nevertheless, can be described by a truncated Rayleigh distribution, defined as follows:

$$f_{at}(a) = k_n(a_t)\frac{a}{V_x}\exp\left(-\frac{a^2}{2V_x}\right) \tag{3.11}$$

Here k_n is a normalization coefficient depending on the truncation value a_t, V_x is the variance of the process x. The normalization coefficient can be evaluated in closed form as:

$$k_n(a_t)=\left(\int_{a_t}^{\infty}\frac{a}{V_x}\exp\left(-\frac{a^2}{2V_x}\right)da\right)^{-1}=\exp\left(\frac{a_t^2}{2V_x}\right) \tag{3.12}$$

However it is better to evaluate it in diseretized form using the width of the bucket Δx:

$$k_n(a_t)=\left(\sum_{i=beg}^{Nb}f_a(a_t)\Delta x\right)^{-1};\quad a_t=a_{beg} \tag{3.13}$$

Where *beg* is the index corresponding to the value of truncation a_t. The histogram also needs to be re-normalized:

$$k_h(a_t)=\left(\sum_{i=beg}^{Nb}h_i\Delta x\right)^{-1};\quad a_t=a_{beg} \tag{3.14}$$

The truneated Rayleigh distribution and truncated histogram are shown in Figure 3.6. The value of truncation was chosen to pass the Pearson chi-square goodness-of-fit test; the results of which are also shown in this figure.

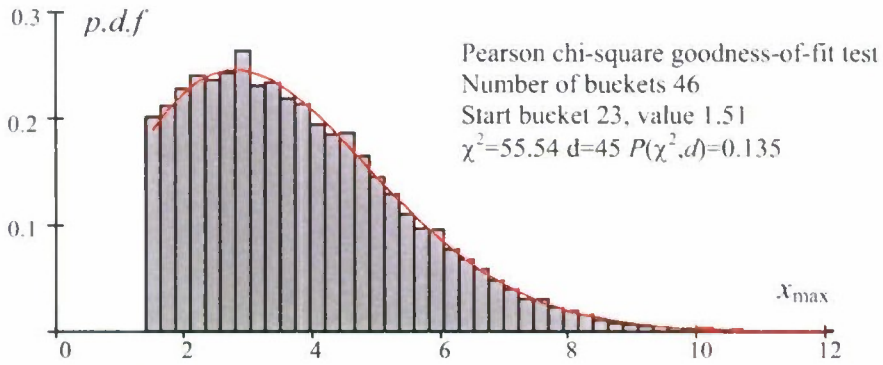

Figure 3.6 Histogram of positive peaks and truncated Rayleigh distribution

As it can be seen, the results of Pearson chi-square goodness-of-fit test shown in Figure 3.6 does not rejeet Rayleigh distribution for peaks starting from the bin 23, whieh corresponds to 1.51 m. This means that above the truncation value, secondary peaks are not statistically signifieant, so most of the sample population consists of primary peaks that belong to the envelope. The latter circumstance leads to applicability of Rayleigh distribution.

A similar picture can be observed for the sample of wave elevation reeorded by a wave probe moving with constant speed and direetion (see subseetion 4.2). For following seas, the eneounter spectrum becomes very narrow banded (see Figure 4.10 in

subsection 4.4.1). The entire histogram is shown in Figure 3.7. Visually, it looks much more like Rayleigh distribution with a very small negative area. However, it takes setting the truncation starting at bucket 5 with the value of 0.54 m to get the Pearson chi-square goodness of fit test to pass, see Figure 3.8.

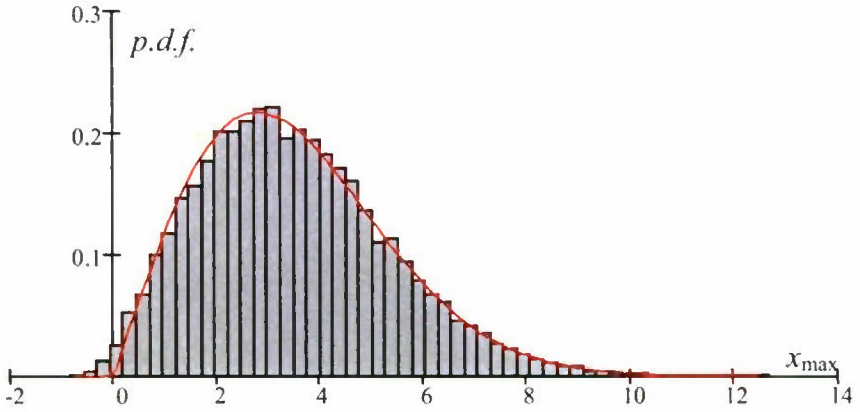

Figure 3.7 Histogram of positive peaks for the case with forward speed 15 knots and Rayleigh distribution

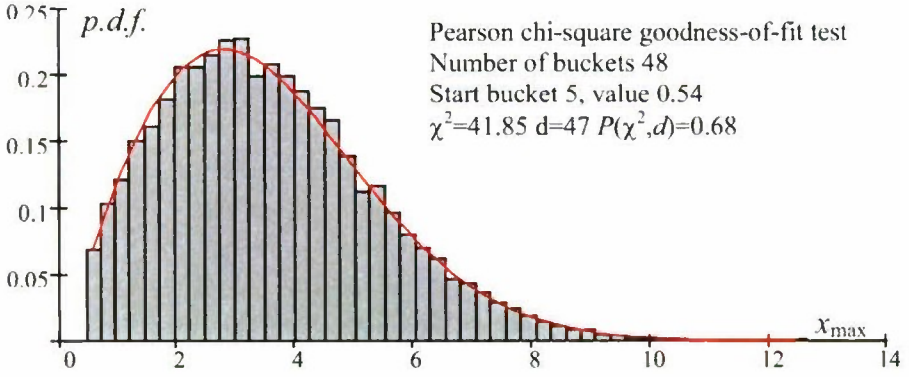

Figure 3.8 Histogram of positive peaks for the case with forward speed 15 knots and truncated Rayleigh distribution

3.2.2. Estimate of Rate of Events for Positive Peaks

Following the concept of the upcrossing rate, it is possible to come to similar formulations for positive peaks using statistical extrapolation.

Consider a sample of stochastic process x, presented in the form of an ensemble of N_R records. Each record is represented by a time history of N_{PT} points with the time step Δt, totaling $n = N_{PT}-1$ time steps. Then the event of occurrence of a peak exceeding a given threshold, or the level a, can be associated with an auxiliary random variable, W, defined for each time step as follows (see Figure 3.9):

$$W_{i,j} = \begin{cases} 1 & x_{i,j} > a \cap x_{i,j} > x_{i-1,j} \cap x_{i,j} > x_{i+1,j} \\ 0 & Otherwize \end{cases} \qquad (3.15)$$
$$i = 1,..,n; \quad j = 1,...,N_R$$

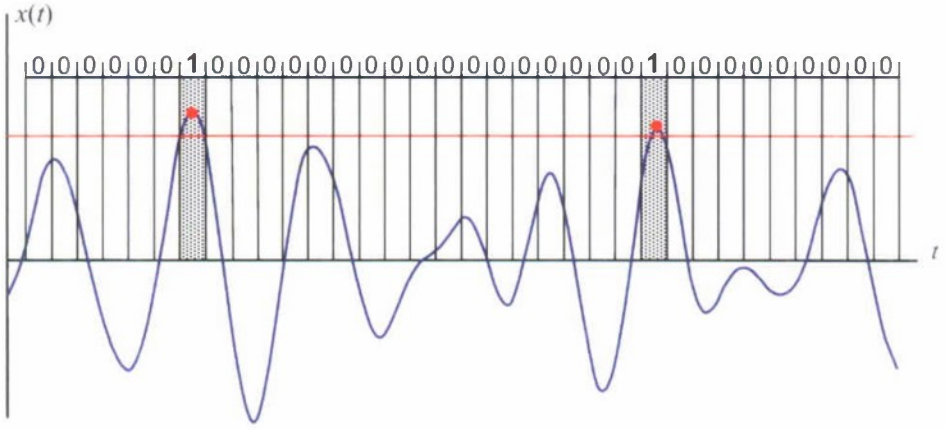

Figure 3.9 Auxiliary random variable for positive peaks over the threshold

This random variable W is defined analogously to auxiliary random variable U, see the subsection 1.2.1. Following the same logic, the total number of all crossings is just the sum of the values of the auxiliary variable for all time steps for all records:

$$N_W = \sum_{i=1}^{n} \sum_{j=1}^{N_R} W_{i,j} \qquad (3.16)$$

An estimate of the probability that a peak exceeding the threshold will occur at any given instance of time is given by:

$$p_{ZW}^{\cdot} = \frac{N_W}{nN_R} = \frac{1}{nN_R} \sum_{i=1}^{n} \sum_{j=1}^{N_R} W_{i,j} \qquad (3.17)$$

The mean number of peaks over the threshold per record:

$$m_W^{\cdot} = \frac{N_W}{N_R} = \frac{1}{N_R} \sum_{i=1}^{n} \sum_{j=1}^{N_R} W_{i,j} \qquad (3.18)$$

The rate of events for the positive peaks over the threshold can be introduced analogously to the rate of the upcrossing. Its estimate over a finite volume of data is defined as:

$$\lambda^*_{PPoT} = \frac{m^*_W}{n\Delta t} = \frac{1}{nN_R\Delta t}\sum_{i=1}^{n}\sum_{j=1}^{N_R} W_{i,j} \tag{3.19}$$

While the theoretical definition can be obtained as a result of a limit of transition for an infinite number of records and infinitely small time step:

$$\lambda_{PPoT} = \lim_{\substack{N_R\to\infty \\ n\to\infty \\ \Delta t\to 0}} \lambda^*_{PPoT} = \lim_{\substack{N_R\to\infty \\ n\to\infty \\ \Delta t\to 0}} \frac{1}{nN_R\Delta t}\sum_{i=1}^{n}\sum_{j=1}^{N_R} W_{i,j} = \frac{1}{dt}\lim_{\substack{N_R\to\infty \\ n\to\infty}} \frac{1}{nN_R}\sum_{i=1}^{n}\sum_{j=1}^{N_R} W_{i,j} =$$
$$= \frac{1}{dt}\lim_{\substack{N_R\to\infty \\ n\to\infty}} \frac{N_W}{nN_R} = \frac{1}{dt}\lim_{\substack{N_R\to\infty \\ n\to\infty}} p^*_W = \frac{dp_W}{dt} \tag{3.20}$$

The confidence interval for the estimate of the rate can be computed using a binomial distribution for the auxiliary variable W, exactly in the same way as it was done for upcrossings. The results for the 9 m crossing level shown in Figure 3.10 (for zero-speed case)

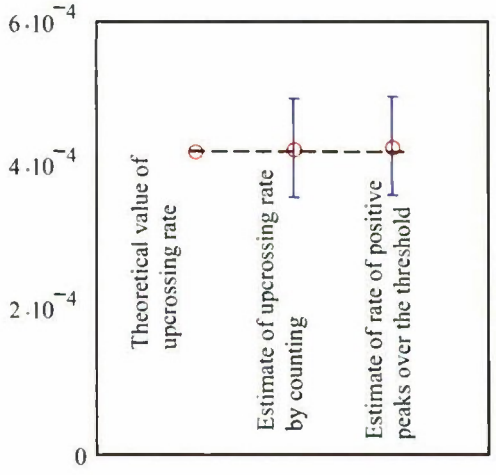

Figure 3.10 Upcrossing rate and rate of positive peaks over the threshold. Crossing level 9 m

Similar results for a range of levels are shown in Figure 3.11, while numerical values can be seen in Table 5. For all of the cases, with the exception of one (a=10 m), the confidence interval of the estimate of the rate of events for positive peaks over the threshold contains the theoretical upcrossing rate. The exception is likely to be caused by random reasons, as it is local. In fact it can be caused by a peak in the beginning of the record, so it was counted as part of sample of peaks, but there were no upcrossing corresponding to that peak, as the process probably crossed the level before time zero (for 10 m crossing level there were 60 peaks and only 58 upcrossings, so two peaks were in the beginning of the records).

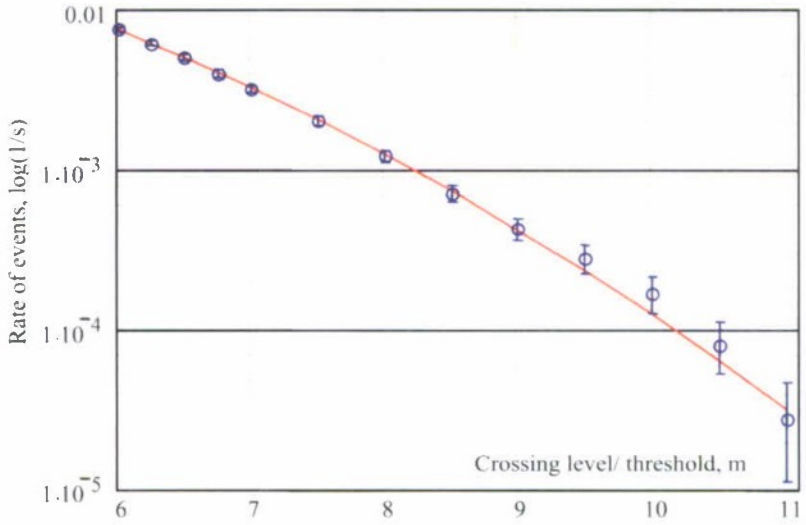

Figure 3.11 Theoretical upcrossing rate (red line) vs. rate of events of positive peaks over the threshold

3.2.3. Poisson Flow and Positive Peaks

The equivalence between an upcrossing and a positive peak over the threshold can be further illustrated by demonstrating that positive peaks over the threshold follow a Poisson flow. A direct test of a Poisson flow was applied as described in the subsection 1.3.5 on page on page 49.

Each record was divided by N_w windows of length T_w to keep the maximum number of event below 7. Then, the sample was created by counting the number of positive peaks over the given threshold in each window. A Pearson chi-square goodness-of-fit test was used to check the applicability of the Poisson distribution based on the statistically estimated rate of events for positive peaks over the threshold. The results are shown in Table 5. The mean value and variance were estimated, and their ratio is also included in Table 5 as an indicator of applicability of Poisson distribution. Figure 3.12 shows details for the crossing level/ threshold of 9 m.

The results from Table 5 show that the Poisson distribution is not rejected until the threshold is lowered to between 5.5 and 5.25 m, which is the same as was for upcrossings, see section 1. This is one more indication of statistical equivalence of these random events. Finally, Figure 3.13 shows the histogram for 1 m level of crossing. Of course,the Poisson distribution is rejected, as most of the data is clustered around 3 and 4 events per 46 second windows, which corresponds to a variation around a mean period of the process of 12.6 s. A visual indication of the inapplicability of the Poisson distribution is given by the more sharp form of the histogram, caused by the concentration of data in buckets near the mean period.

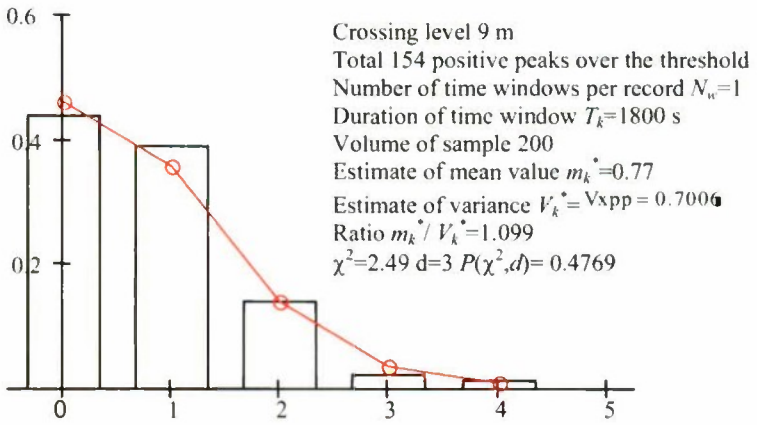

Figure 3.12 Probability mass function of number of positive peaks over the threshold during time window. Poisson distribution is not rejected

Table 5. Applicability of Poisson flow and rate of events of positive peaks over the threshold

Level	N_w	T_w	m_k/V_k	Direct Poisson Test				Theoretical rate of upcrossings	Rate of positive peaks over threshold		
				N_{max}	d	χ^2	$P_{RND}(\chi^2,d)$		low	estimate	upper
11	1	1800	1.047	2	0	0.02532	-	3.23E-05	1.11E-05	2.78E-05	4.72E-05
10.5	1	1800	1.077	3	1	0.5205	0.4706	6.44E-05	5.28E-05	8.06E-05	0.000111
10	1	1800	1.148	3	1	1.178	0.2778	0.000124	0.000125	0.000167	0.000211
9.5	1	1800	1.059	5	3	3.467	0.3251	0.000232	0.000225	0.000278	0.000333
9	1	1800	1.099	5	3	2.491	0.4769	0.00042	0.000361	0.000428	0.000497
8.5	1	1800	1.094	6	4	1.481	0.83	0.000737	0.000622	0.000708	0.000797
8	1	1800	1.384	7	5	7.443	0.1897	0.00125	0.001103	0.001217	0.001331
7.5	2	900	1.088	8	6	4.708	0.5818	0.002055	0.001903	0.00205	0.002197
7	4	450	1.047	7	5	1.746	0.8831	0.003272	0.003025	0.003208	0.003394
6.75	5	360	1.041	7	5	1.687	0.8905	0.004078	0.003814	0.004019	0.004228
6.5	9	200	1.024	6	4	4.585	0.3326	0.005044	0.004781	0.005011	0.005242
6.25	11	163.5	0.9925	6	4	1.585	0.8115	0.006187	0.005919	0.006175	0.006431
6	13	138.5	1.041	7	5	3.188	0.671	0.00753	0.007261	0.007544	0.007828
5.75	13	138.5	1.072	7	5	11.19	0.04774	0.009091	0.00885	0.009164	0.009475
5.5	15	120	1.073	7	5	9.331	0.09657	0.01089	0.01043	0.01077	0.01111
5.25	19	94.5	1.115	7	5	31.89	6.25E-06	0.01293	0.01251	0.01289	0.01325
5.25	19	94.5	1.115	7	5	31.89	6.25E-06	0.01293	0.01251	0.01289	0.01325
5	21	85.5	1.177	7	5	74.57	1.14E-14	0.01524	0.01476	0.01516	0.01556
4.75	22	82	1.218	7	5	87.16	0	0.01782	0.01746	0.01789	0.01833
3	32	56.5	2.271	6	4	1299	0	0.04253	0.04175	0.04242	0.04308
1	39	46	6.204	7	5	6305	0	0.07103	0.07286	0.07375	0.0746

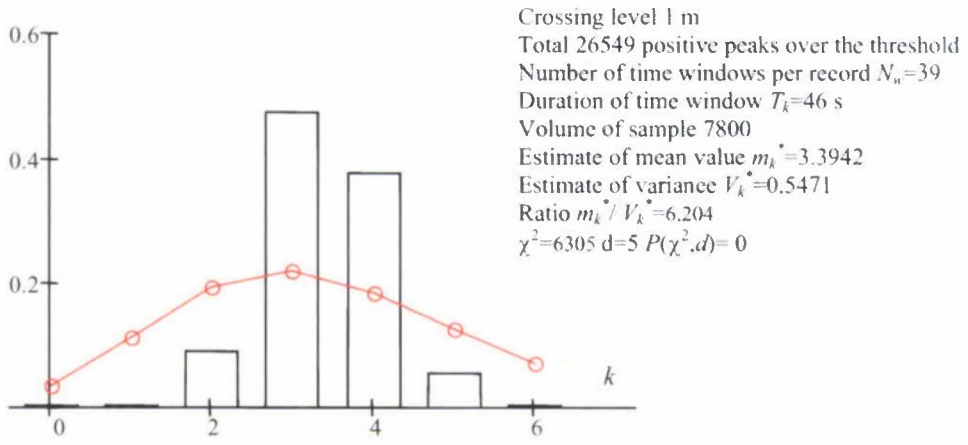

Figure 3.13 Probability mass function of number of positive peaks over the threshold during time window. Poisson distribution is rejected

3.3.The Rare Problem

Solving the rare problem means finding the probability that the process will exeeed a given level after an uperossing of the threshold has oeeurred. The only information available is the data of the proeess beyond the threshold; these data may not go as far as the level of interest, so it is a typieal extrapolation problem.

It was shown above that if the distribution of peaks is known, then the rate of uperossings through the given level ean be found using formula (3.6). In faet, if the data of peaks over the threshold is used to fit the distribution, this distribution already is eonditional, therefore:

$$\xi_2 = \xi_1 \int_{a_2}^{\infty} f_A(A \mid A > a_1) dA = \xi_1 \left(1 - F(A \mid A > a)\right) \qquad (3.21)$$

Therefore the objeetive of the rare problem is finding the conditional CDF of positive peaks above the threshold.

3.3.1. POT Distribution and the Confidence Interval

For a general stoehastie proeess, the distribution of amplitudes and conditional distribution of peaks above the threshold are not known. As the process of interest is a response of a highly nonlinear dynamieal system, there is a very small ehanee that such a distribution ean be obtained in elosed form. Therefore it needs to be fitted with some approximate formula using available data.

On the other hand, such distribution is known to be Rayleigh for a normal proeess. As the proeess of interest is a response of a nonlinear dynamieal system on normal exeitation, it may be meaningful to try a Weibull distribution as an

approximation, keeping in mind that the Rayleigh distribution is formally a particular case of the Weibull distribution.

Using a Weibull distribution in such a context, however, should not imply any limiting characteristics of the distribution. In principle, Weibull distribution is an extreme value distribution (see section 2). Extreme value distribution is a limit distribution to which the maximum value observed during a given time tends. However, using just peaks over the threshold, to fit the Weibull, means that it is used only as an approximation formula that possesses some convenient characteristics, like normalization.

Figure 3.14 shows a histogram of peaks over the threshold (for 9 m) fitted with a Weibull distribution along with the results of the goodness-of-fit for the Weibull distribution fitted with the moment method and the method of maximum likelihood. Both ways of fitting the Weibull distribution were not rejected as well as the truncated Rayleigh distribution. A similar picture can be seen from the Figure 3.15

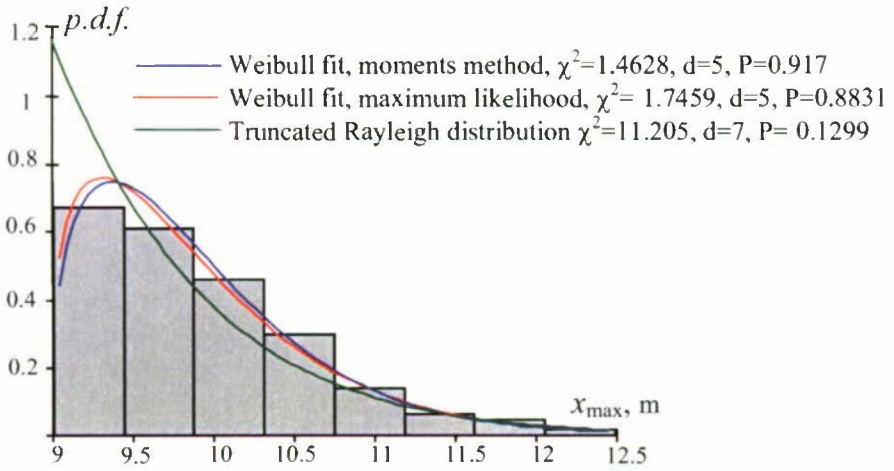

Figure 3.14 Fitting the distribution for positive peaks over the threshold 9 m, 154 peaks total

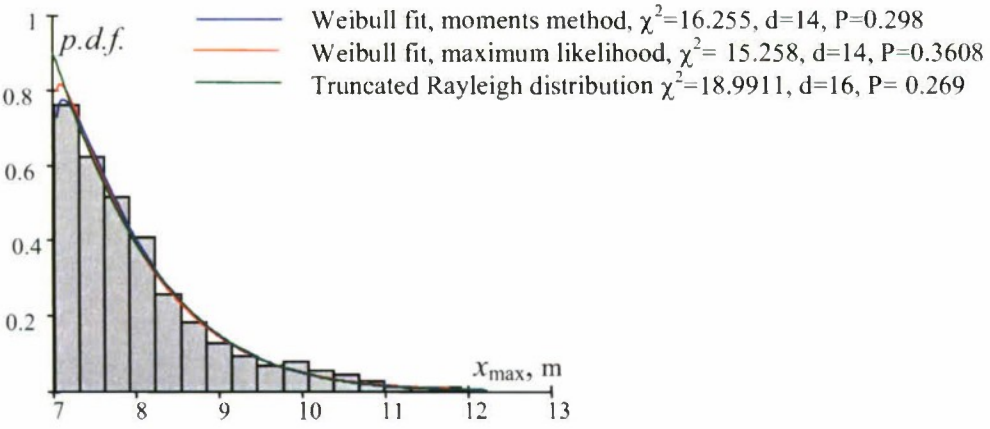

Figure 3.15 Fitting the distribution for positive peaks over the threshold 7 m, 1155 peaks total

The procedure for calculating the confidence interval for a fitted Weibull distribution has been described in Section 2. The only difference here is that the shift parameter is known and it is equal to the threshold. Figure 3.16 shows the confidence interval for the Weibull distribution fitted with the moment method for a 9 m threshold, with both PDF and CDF are shown. As it has been demonstrated earlier, the true distribution of this case is Rayleigh; and it is also shown in the CDF plot. It can be clearly seen that Rayleigh differs from thw fitted distribution enough, so that part of the curve is actually outside of the confidence band. The difference, however, is not very large and the theoretical curve returns back to the confidence band around a peak value of 10 m.

The results are better if the Weibull distribution is fitted with the method of maximum likelihood, see Figure 3.17. Here the theoretical Rayleigh distribution remains within the confidence band all the time. The evident outcome is that the method of maximum likelihood provides better results; this is consistent with existing statistical practice, where the moment method is only used to get initial values for the method of maximum likelihood.

Lowering the threshold naturally leads to increase the of number of peaks over the threshold and, as a result, a more accurate fit. As seen from the Figure 3.18, the confidence band has shrunken and it contains a theorctical Rayleigh distribution within.

This consideration shows that the choice of the threshold is not only dictated by the applicability of the Poisson distribution, but also by statistical accuracy of fitting the distribution. This question, however, needs to be addressed later when the entire result will be obtained and compared with the "true" theoretical answer.

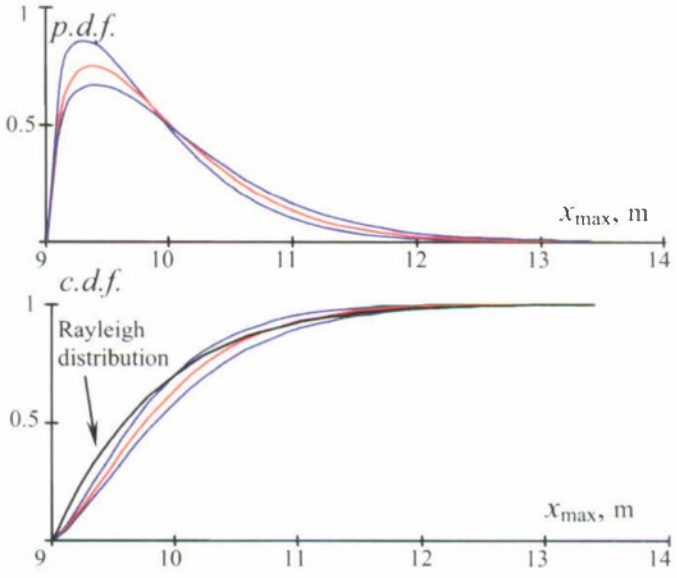

Figure 3.16 Confidence interval on Weibull distribution fitted with moments method. The threshold 9 m, 154 peaks total

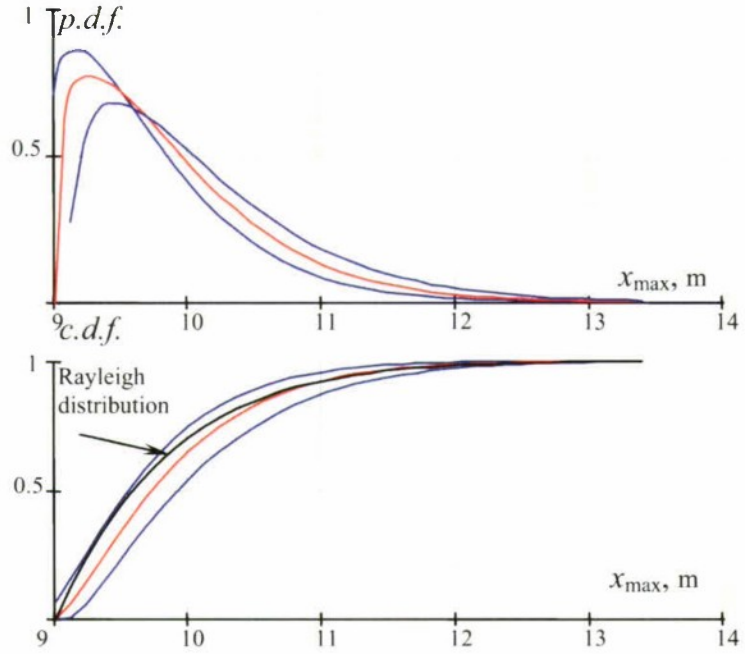

Figure 3.17 Confidence interval on Weibull distribution fitted with maximum likelihood method. The threshold 9 m, 154 peaks total

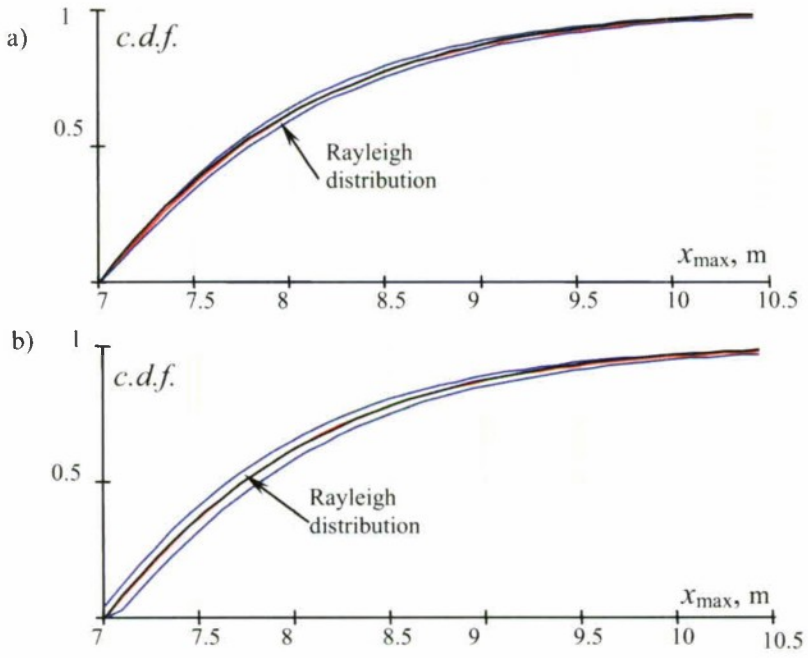

Figure 3.18 Confidence interval on Weibull distribution fitted with method of moments (a) maximum likelihood method (b). The threshold 7 m, 1155 peaks total

3.3.2. *Statistical Extrapolation of Peaks Over the Threshold*

Formula (3.21) gives the final expression for the extrapolated estimate of uperossing rate for the level interest (the second level a_2):

$$\lambda^*_X = \lambda^* \left(1 - F^*(a_2)\right) \tag{3.22}$$

Here λ^*_X is an estimate of the uperossing rate extrapolated to the level of interest a_2, λ^* is the statistieal estimate (by counting) of the uperossing rate of the given threshold a_1. $F^*(a_2)$ is the CDF fitted to peaks over the given threshold a_1.

As all the terms in the equation (3.22) have their boundaries of confidence interval defined, it is possible to express these boundaries for the final result:

$$\lambda^*_{Xlow} = \lambda^*_{low} \left(1 - F^*_{low}(a_2)\right) \tag{3.23}$$

$$\lambda^*_{Xup} = \lambda^*_{up} \left(1 - F^*_{up}(a_2)\right) \tag{3.24}$$

To evaluate the quality of the extrapolation, the extrapolated value can be compared with the theoretical solution, as it is available for consideration, see Figure 3.19.

$$\lambda(a_2) = \sqrt{\frac{V_{\dot{x}}}{V_x}} \exp\left(-\frac{a_2^2}{2V_x}\right) \tag{3.25}$$

Here V_x is the varianee of the proeess and $V_{\dot{x}}$ is the varianee of the derivative of the process $x(t)$.

Figure 3.19 shows exeellent quality of extrapolation, as the theoretical solution remains within the confidence interval before the numbers become too small to handle. Unfortunately, it is not always the case. Lowering the threshold may deerease the quality of extrapolation, see Figure 3.20. The theoretical solution leaves the confidence interval on the level 11.18 m. It may not look like a good quality of extrapolation; however it still was able to prediet amplitudes more than 4 m above the threshold of 7 m, which is above 50% of the threshold.

Therefore, the choiee of the threshold is important. Figure 3.21 shows a "breakpoint" of the method as a function of the threshold. The "breakpoint" is the level below whieh the extrapolation is still good. As it ean be seen from Figure 3.21, the dependenee is not monotonie. It remains almost horizontal until a threshold of 8 m, then starts to inerease and reaches its maximum of 26 m somewhere around 9 m. This is the situation shown in Figure 3.19, where the theoretieal value is eontained in the eonfidence interval of the extrapolated value. The level of 26 m is where the calculations were stopped as arithmetieal diffieulties, related with handling a very small number, were eneountered. Also, rarity of the uperossing level of 26 m is such that it makes consideration impraetieal as the mean value before/ between the events is around 10^{20} seeonds – is about 3.1 10^{12} years.

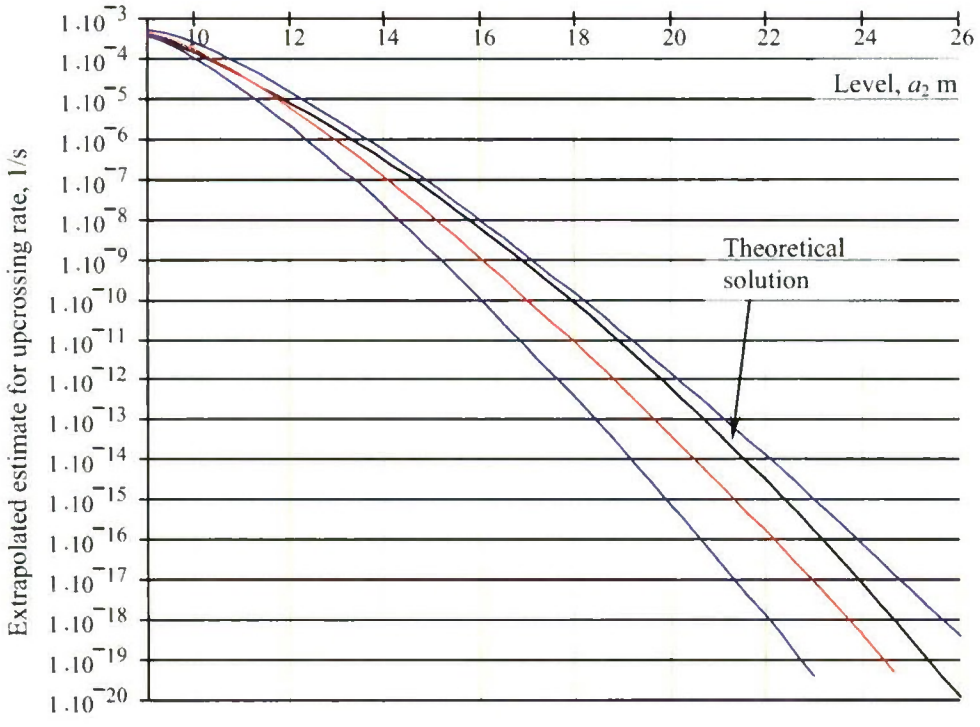

Figure 3.19 Extrapolated estimate of upcrossing rate with confidence interval as a function crossing level vs. theoretical upcrossing rate. The threshold 9 m, 154 peaks total.

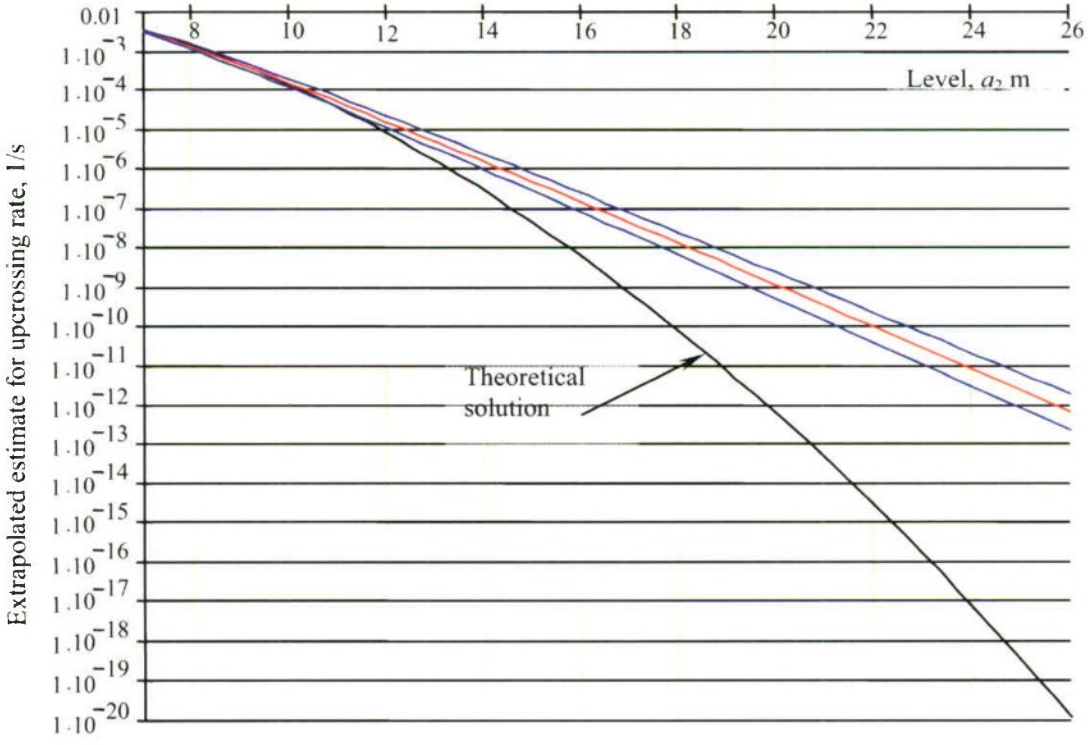

Figure 3.20 Extrapolated estimate of upcrossing rate with confidence interval as a function crossing level vs. theoretical upcrossing rate. The threshold 7 m, 1155 peaks total.

Around the threshold of 9.25 m, the breakpoint falls baek to the 13-14 m level (see Figure 3.23) and remains there until the 9.75 m threshhold. Then it goes back to "no breakpoint" (26 m) and remains there (Figure 3.24) until the data for fitting the distribution "runs out". The volume of data available for fitting the distribution is placed in Table 6.

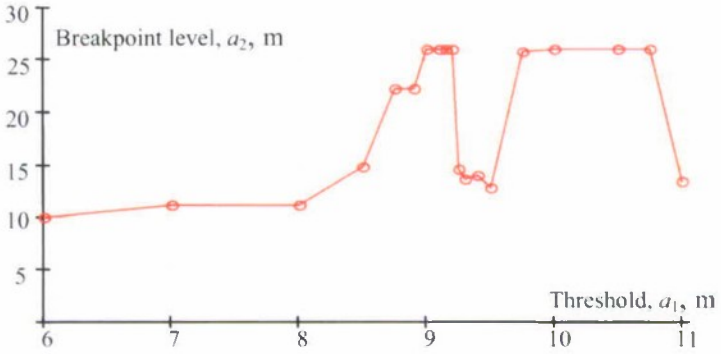

Figure 3.21 Breakpoint level (the level below which the extrapolation is still good) vs threshold

Figure 3.22 illustrates the performanee of the method for the 14 m level. This level is aetually quite high; the mean time before/between events for uperossing this level is about 44 days. Roughly, aeeeptable performanee (with very few dropouts) can be seen from the level exeeeding 8.5 m

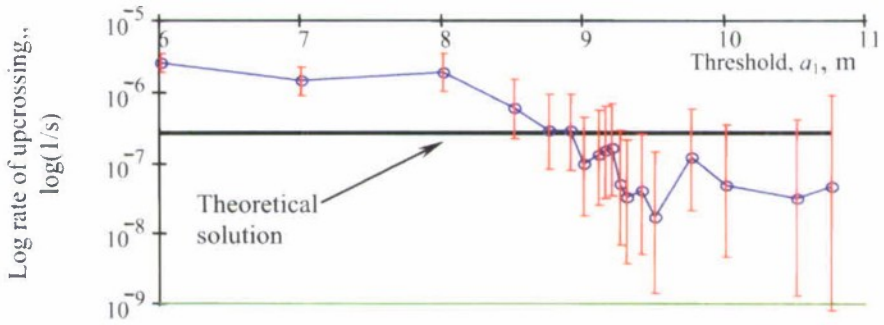

Figure 3.22 Comparison of performance of extrapolation method for 14 m using different values for the threshold

Table 6. Number of positive peaks over threshold

Threshold	Number of POT	Breakpoint level, m	Threshold	Number of POT	Breakpoint level, m
6	2716	10	9.25	124	14.61
7	1155	11.18	9.3	119	13.64
8	438	11.24	9.4	111	14.05
8.5	255	14.8	9.5	100	12.8
8.75	197	22.2	9.75	83	25.67
8.9	174	22.24	10	60	26
9	154	26	10.5	29	26
9.1	144	26	10.75	16	26
9.15	138	26	11	10	13.4
9.2	132	26			

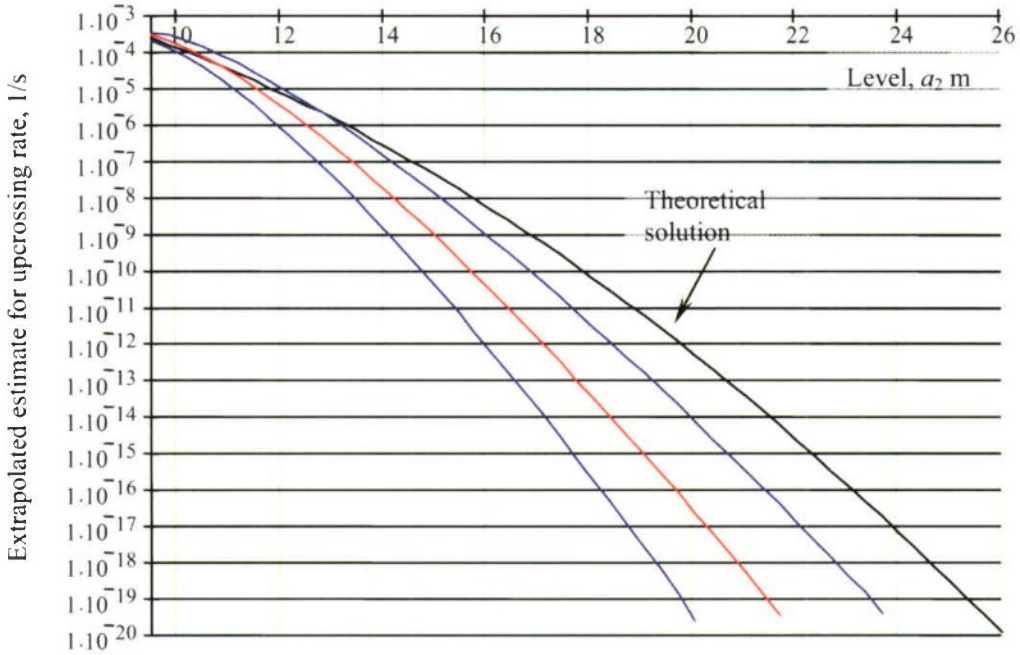

Figure 3.23 Extrapolated estimate of upcrossing rate with confidence interval as a function crossing level vs. theoretical upcrossing rate. The threshold 9.5 m, 100 peaks

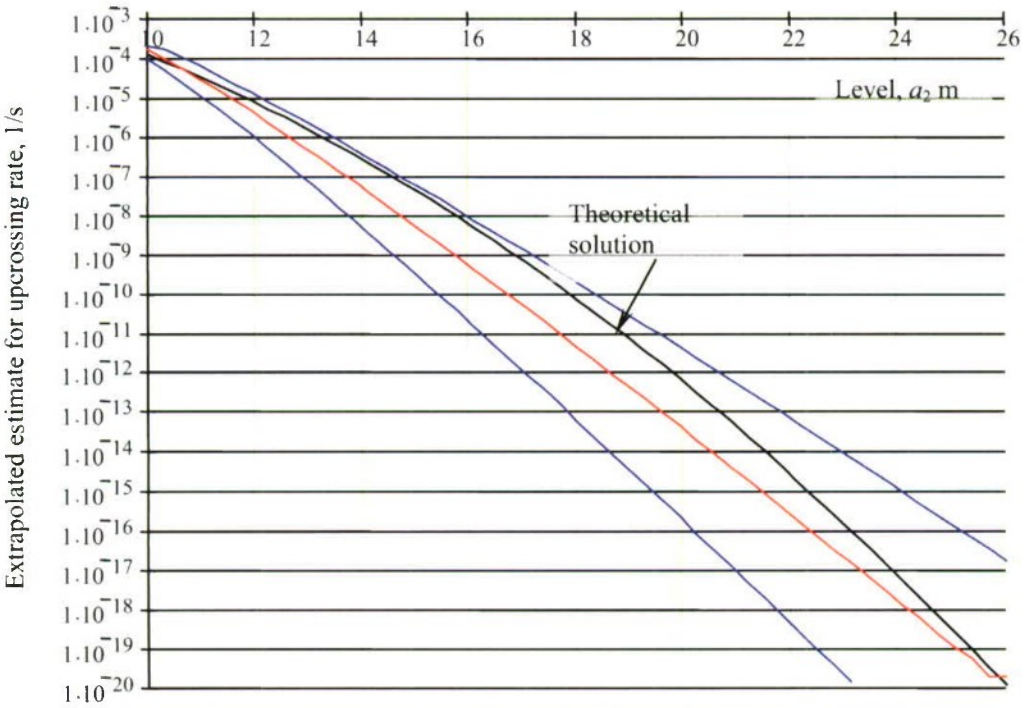

Figure 3.24 Extrapolated estimate of upcrossing rate with confidence interval as a function crossing level vs. theoretical upcrossing rate. The threshold 10 m, 29 peaks

Based on these observations, two questions need to be answered: 1) What is the main eontributor to the quality of extrapolation? 2) How random are these results, or can the same pieture be observed with other reeords of the same proeess?

To answer the first question, eonsider the eomponents of the extrapolated estimate: the rate of upcrossing through the threshold (see Figure 3.25) and the conditional probability of the given level (14 m) is exeeeded if the threshold was crossed (see Figure 3.26). As it can be seen from Figure 3.25, the estimate of threshold crossing behaves relatively smoothly, keeping the theoretieal solution within its confidence interval. The estimate of the eonditional probability in Figure 3.26 behaves in a more random manner. It "eatehes" the theoretical solution with its confidenee interval starting about 8.5 m, then "loses" it, than "catehes" it again. Obviously, the estimate of conditional probability is the one "responsible" of quality extrapolation, at least for the sample eonsidered.

To answer the seeond question, two more examples were considered. The process was constructed from exactly the same spectrum and discretization as deseribed in Seetion 1. The only difference was the set of random phases that makes these sets independent from the first one.

Figure 3.27 shows the "breakpoints" behavior vs. the threshold for two alternative datasets. Comparing these plots with the similar one in Figure 3.26 made from the original dataset one can see that despite their different shapes, still there are some common features. There is a relative monotonic part up to about 8 m, then the dependence becomes oscillatory, but keeping the similar tendeney to grow. Comparing performance of the extrapolation method for a level of 14 m (Figure 3.28) for the alternative datasets one can see that for the alternative dataset 1, the extrapolation starts working at 9.5 m and for the alternative dataset 2 at 8.75 m. The original dataset gave the value around 8.5 m (Figure 3.22), so, in general, the range is about 8.5-9.5 m.

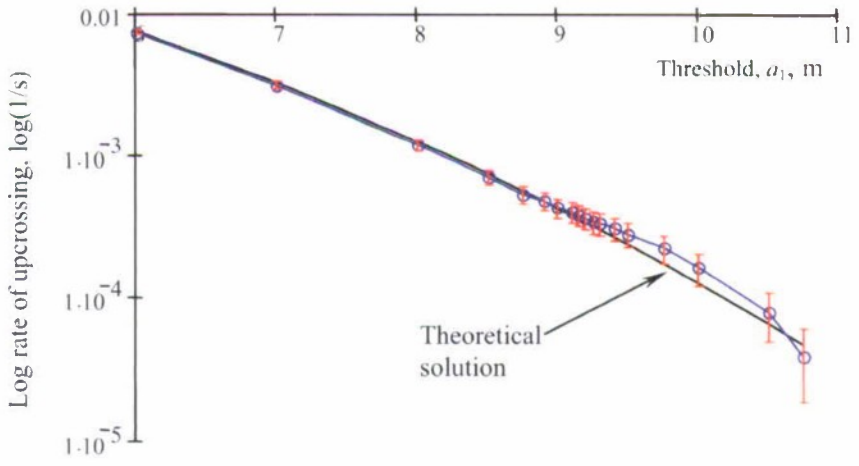

Figure 3.25 Statistical estimate of upcrossing rate through the threshold

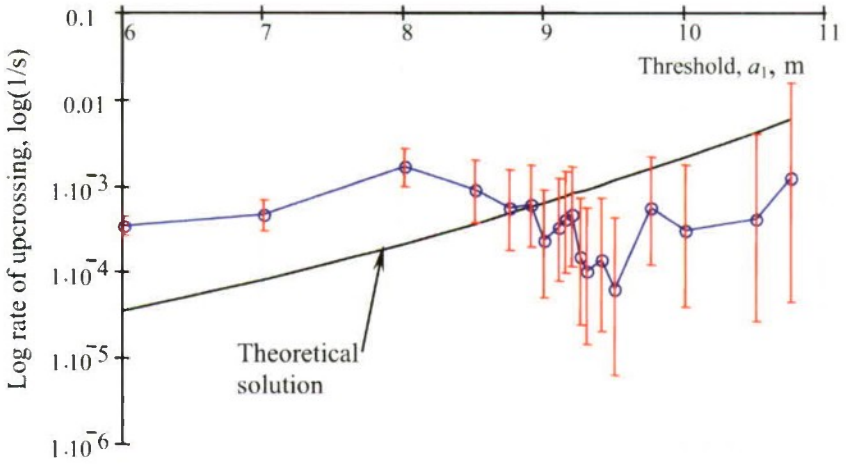

Figure 3.26 Extrapolated estimate of conditional probability that the process will exceed the level of 14 m if the threshold has been crossed

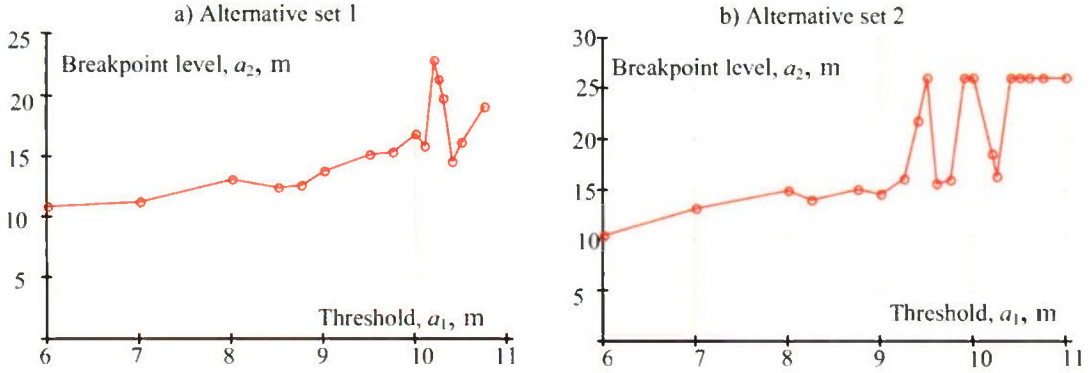

Figure 3.27 Breakpoint level (the level below which the extrapolation is still good) vs threshold

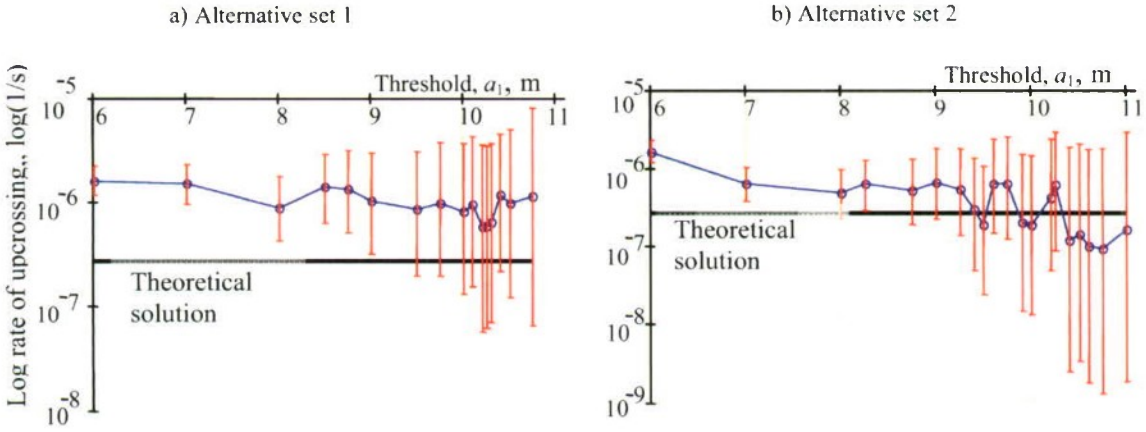

Figure 3.28 Comparison of performance of extrapolation method for 14 m using different values for the threshold

Figure 3.29 shows behavior of two components of the POT extrapolation method for two alternative datasets for 14 m level. The upper plots show the statistical estimate of rate of upcrossing of the threshold. The plots are very similar to each other and to the

plot based on the original dataset in Figure 3.25. The estimate is almost indistinguishable with the theoretical solution for the lower thresholds. With an increase of the threshold, the estimate slowly oscillates around the theoretical solution, while it remains within the confidence interval. The latter one increases monotonically with the rise of the threshold and decrease of the number of observed upcrossings.

The behavior of the estimate of the conditional probability (lower plots of Figure 3.29) is characterized by more oscillations. The estimates on both plots, as well as for the original dataset, in Figure 3.26, have a relatively monotonic range for the thresholds, but the theoretical solution is not "caught" by the confidence interval. With the increase of the threshold, the behavior becomes oscillatory, the confidence interval increases and theoretical solution is included now. At least, the tendency is roughly traced, which was not clear from Figure 3.26 alone.

Concluding the consideration of these two questions, it can be stated that the prediction capability of the method can be advanced, by improving the technique for estimating the conditional probability.

It is also clear that when the threshold is too low, the fitted conditional distribution is dominated by the data not very far from the threshold itself, which is not necessarily allowing the correct prediction of the tail of the distribution.

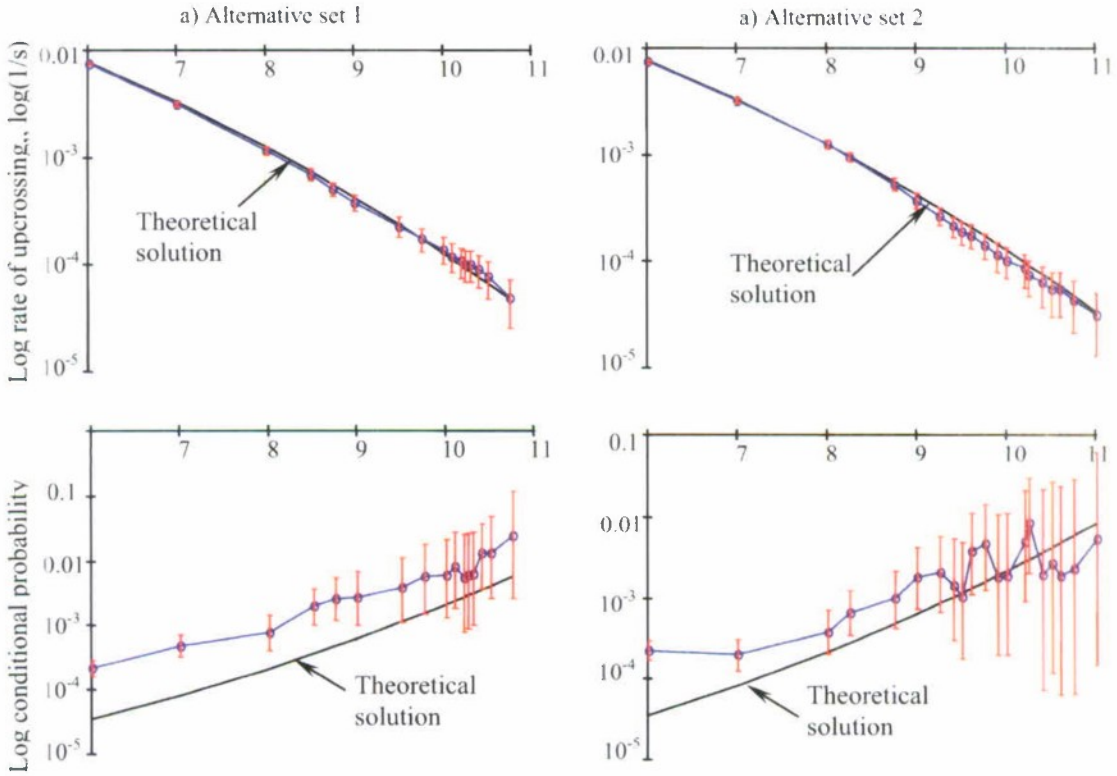

Figure 3.29 Statistical estimate of upcrossing rate through the threshold (upper plots) and extrapolated estimate of conditional probability that the process will exceed the level of 14 m if the threshold has been crossed (lower plots) for two alternative data sets

3.3.3. *Alterative Solution for Rare Problem*

Difficulties predicting the behavior of the tail of fitted distributions are not new. These difficulties were one of the motivations for the development of the extreme value theory; therefore it is quite logical to try to use extreme distributions for the rare problem.

Consider the probability that no upcrossing will occur through the level a_2 during time T; assuming applicability of Poisson flow:

$$P_2(n_2 = 0, T) = \exp(-\lambda_2 T) \tag{3.26}$$

Here, n_2 is number of upcrossing through the level a_2, $\lambda_2$is rate of upcrossing through the level a_2.

Now consider upcrossing through the level a_1, such as:

$$a_2 > a_1 \tag{3.27}$$

The probability that no upcrossing will occur through the level a_2 during time T; assuming applicability of Poisson flow can be expressed as:

$$P_1(n_1 = 0, T) = \exp(-\lambda_1 T) \tag{3.28}$$

Here n_1 is number of upcrossings through the level a_1, $\lambda_1$is rate of upcrossing through the level a_1.

Probability P_2 can expressed through the probability P_1. That is, if there are no upcrossings through the level a_1, there are no upcrossings through a_2; or there are some upcrossings through a_1, but the process never reached the level a_2. As the events of no upcrossing through the level a_1 and at least one upcrossing through the level a_1 are incompatible, the probability P_2 is expressed as:

$$P_2 = P_1 + P(n_2 = 0 \cap n_1 > 0) \tag{3.29}$$

Here $P(n_2=0 \cap n_1>0)$ is a probability that no upcrossing occurs through the level a_2 and there is at least one upcrossing through the level a_1. This probability can be expressed as:

$$P(n_2 = 0 \cap n_1 > 0) = P(n_2 = 0 \mid n_1 > 0) P(n_1 > 0) \tag{3.30}$$

Here $P(n_2=0 \mid n_1>0)$ is a probability that no upcrossing occurs through the level a_2 if there is at least one upcrossing through the level a_1, while $P(n_1>0)$ is a probability of at least one crossing through the level a_1. This is the probability of a complimentary event to equation (3.28):

$$P(n_1 > 0) = 1 - P(n_1 = 0, T) = 1 - \exp(-\lambda_1 T) \tag{3.31}$$

Consider an extreme value distribution obtained over time T (the distribution of the maximum value observed during time T). By definition, the cumulative distribution function is:

$$F_{EV}(x, T) = P(\max(x, T) < x) \tag{3.32}$$

Here $\max(x,T)$ stands for a maximum value of proeess $x(t)$ observed during time T.

Using the technique proposed by G. Hazen and described in detail in Seetion 2, a probability of a complimentary event (at least one upcrossing during time T) can be expressed using an assumed Poisson flow:

$$1 - \exp(-\lambda_2 T) = 1 - F_{EV}(a_2, T) \tag{3.33}$$

So, it elear from equations (3.32) and (3.33) that the probability of no upcrossing through the level a_2 is equal to the CDF of the extreme value observed during time T and calculated for the level a_2:

$$\exp(-\lambda_2 T) = F_{EV}(a_2, T) \tag{3.34}$$

Consider a eonditional distribution of an extreme value reaehing the level a_2 under condition that it has exceeded the level a_1, minding the eondition (3.27):

$$f_{EV}(x = a_2, T \mid x > a_1) = \frac{f_{EV}(a_2, T)}{F_{EV}(a_1, T)} \tag{3.35}$$

Here divisor $F_{EV}(a_1,T)$ plays the role of a normalization coefficient.

Conditional CDF can be exprcssed analogously to the equation (3.35):

$$F_{EV}(x = a_2, T \mid x > a_1) = \frac{F_{EV}(a_2, T)}{F_{EV}(a_1, T)} \tag{3.36}$$

By the definition of CDF:

$$F_{EV}(x = a_2, T \mid x > a_1) = P(\max(x, T) < a_2 \mid \max(x, T) > a_1) \tag{3.37}$$

If an extremc value observed during time T has exceeded the level a_1, then the number of upcrossings through this level observed during time T differs from zero:

$$\{\max(x, T) > a_1\} \Leftrightarrow \{n_1 > 0\} \tag{3.38}$$

If the extreme value observed during time T has not exeeeded the level a_2, then the number of upcrossings through this level, observed during time T, is zero.

$$\{\max(x,T) < a_2\} \Leftrightarrow \{n_2 = 0\} \tag{3.39}$$

Equations (3.36) and (3.37) lead to the following:

$$P(n_2 = 0 \mid n_1 > 0) = P(\max(x,T) < a_2 \mid \max(x,T) > a_1) \tag{3.40}$$

Formula (3.35) relates the conditional probability of no upcrossings of the level a_2 given there are upcrossings through the level a_1 conditional extreme value CDF:

$$P(n_2 = 0 \mid n_1 > 0) = F_{EV}(x = a_2, T \mid x > a_1) \tag{3.41}$$

Substitution of (3.41) and (3.36) into (3.29), taking into account (3.30) and (3.31), leads to:

$$P_2 = P_1 + (1 - P_1)\frac{F_{EV}(a_2,T)}{F_{EV}(a_1,T)} \tag{3.42}$$

Taking into account formulae (3.26) and (3.28) allows expressing the rate of upcrossings of the level a_2 through the rate of upcrossing of the level a_1 and extreme value distributions:

$$\lambda_2 = -\frac{1}{T}\ln\left(\exp(-\lambda_1 T) + (1 - \exp(-\lambda_1 T))\frac{F_{EV}(a_2,T)}{F_{EV}(a_1,T)}\right) \tag{3.43}$$

Formula (3.43) represents the complete solution of the problem with a different formula than (3.8) . A combination of a rare and non-rare problem. It is trivial, however to express the solution of rare problem from (3.43) explicitly:

$$P = -\frac{1}{\lambda_1 T}\ln\left(\exp(-\lambda_1 T) + (1 - \exp(-\lambda_1 T))\frac{F_{EV}(a_2,T)}{F_{EV}(a_1,T)}\right) \tag{3.44}$$

Formula (3.44) allows the use of an extreme value distribution for the rare problem.

3.3.4. Extreme Value Distribution for Peak over Threshold

To use the alternative solution for the rare problem described in the previous section, the conditional extreme value distribution of peaks over the threshold is needed. The procedure of fitting the extreme value distribution was described in detail in section 2 and briefly revisited below.

First the window size has to be set up. It should be large enough so that the maximum value observed in each window can be considered as an independent realization. For all further calculations, window size was taken equal to the record length unless otherwise stated.

The sample data has to be collected to fit a Weibull distribution. The data points are the maximum values observed in each window. To avoid dealing with uncertainty of the shift parameter, only points that have exceeded the threshold a_1 are collected. Next, the fitted distribution is actually the conditional extreme value distribution, needed for formulae (3.43) and (3.44). The conditional distribution in CDF form is expressed as:

$$F_{EV}(x_{\max} \mid x_{\max} > a_1) = \frac{F_{EV}(x_{\max}, T)}{F_{EV}(a_1, T)} = \begin{cases} 0 & x_{\max} < a_1 \\ 1 - \exp\left(-\left(\dfrac{x_{\max} - a_1}{\alpha} \right)^k \right) & x_{\max} \geq a_1 \end{cases} \qquad (3.45)$$

Parameters of the distribution k and α are determined using the method of maximum likelihood, with the initial values coming from the method of moments. Evaluation of the confidence interval is not different than in the previous case. An example for the threshold value of 9 m is shown in Figure 3.30.

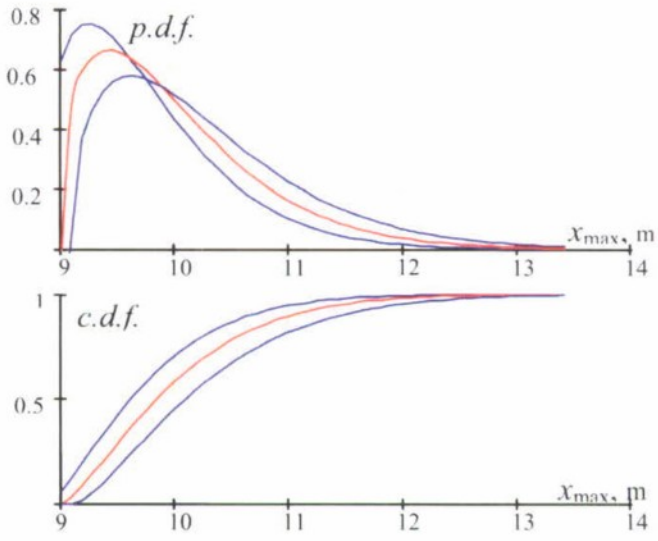

Figure 3.30 Fitting the Weibull distribution with confidence interval for peak over the threshold data, the threshold 9 m, and window time 1800 s (time duration of entire record)

3.3.5. Extrapolation with Extreme Value Distribution of POT

Once the distribution has been fitted, formula (3.43) can be used for extrapolation. Figure 3.31 shows sample results for the 9 m threshold, using the distribution shown in Figure 3.30.

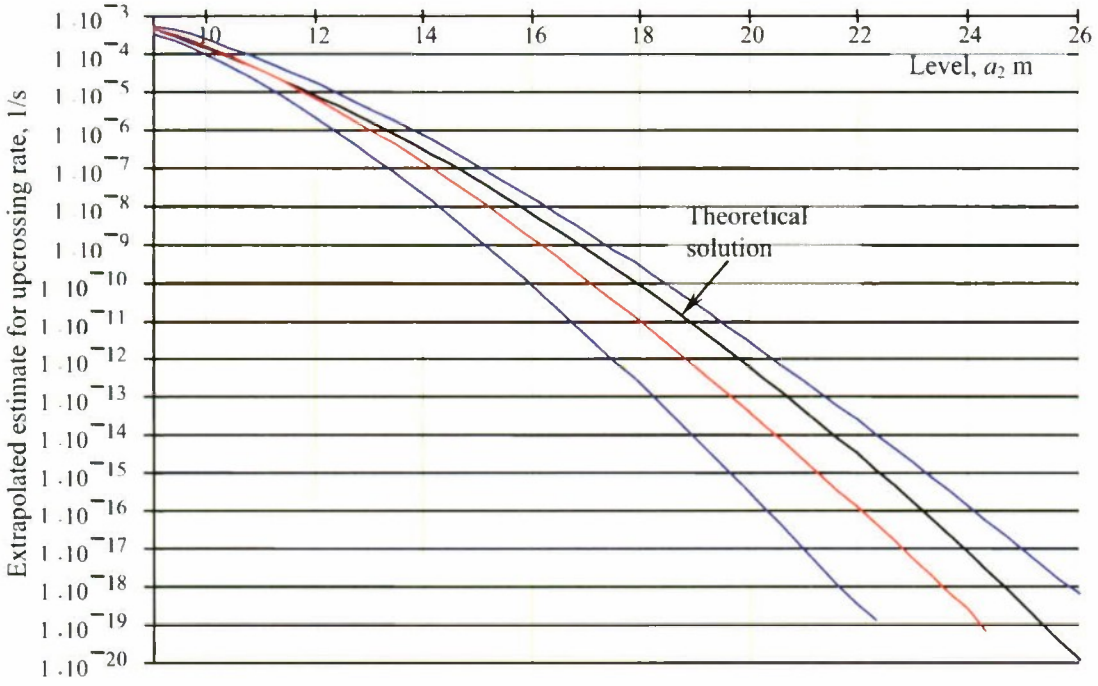

Figure 3.31 Extrapolated estimate of upcrossing rate with confidence interval as a function crossing level vs. theoretical upcrossing rate based on extreme value distribution of peaks over the threshold. The threshold 9 m, 111 peaks

Unfortunately, good extrapolation shown in Figure 3.31 does not mean that it remains the same for any threshold. Figure 3.32 shows "breakpoint" value for the extrapolation based on extreme value distribution. In principle, a general picture is similar to Figure 3.21; however the lower level of the breakpoint seems to be a bit higher.

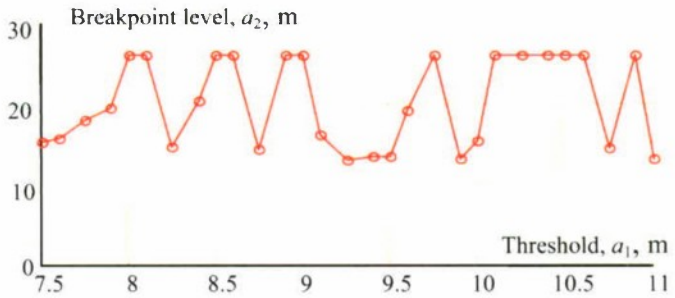

Figure 3.32 Breakpoint level (the level below which the extrapolation is still good) for the extrapolation based on extreme value distribution vs threshold

The difference between two techniques of extrapolations becomes clearer when comparing the rare solution calculated for a particular target level – 14 m (the level where the prediction is needed); see Figure 3.33 and compare with Figure 3.26. In general, a solution based on extreme value distribution is closer to the theoretical one. Most importantly, the prediction is correct for relatively low levels where more data exist and the confidence interval is narrower.

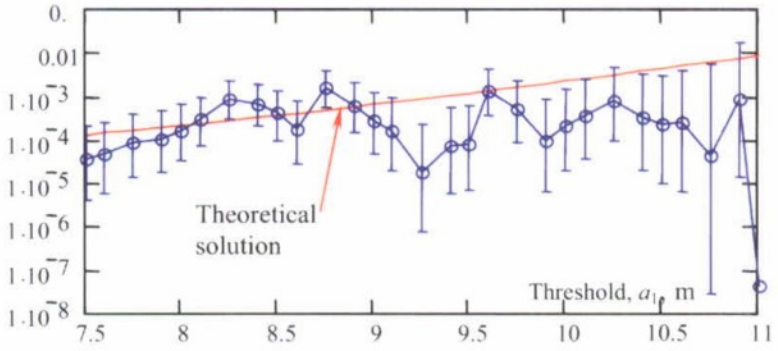

Figure 3.33 The extrapolated estimate of conditional probability that the process will exceed the level of 14 m if the threshold has been crossed (based on extreme value distribution)

Similar conclusions can be made comparing the complete results of extrapolations between the two methods, see Figure 3.34 and Figure 3.22. Acceptable performance can be observed for almost the entire range of the thresholds for the extreme-value based technique in Figure 3.34 vs. direct POT fitting shown in Figure 3.22. This difference can be explained by the extreme value distribution model's much better behavior of the tail of the distribution as it is its main "specialty".

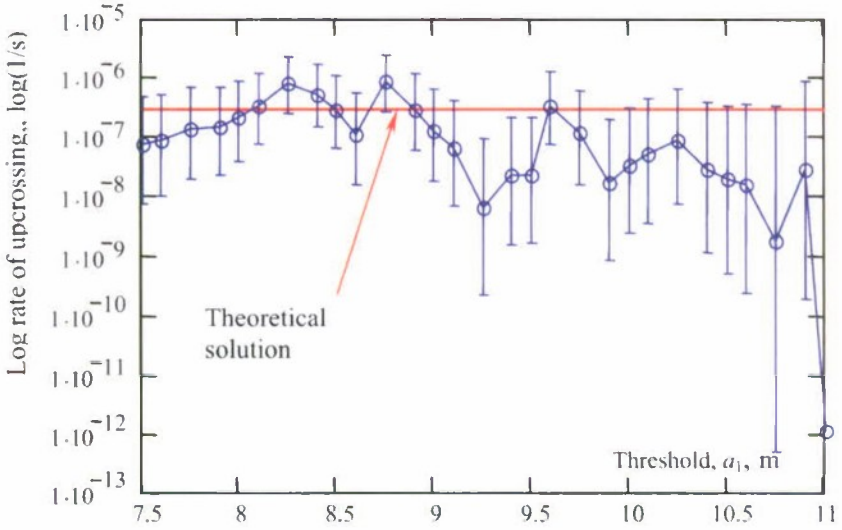

Figure 3.34 Comparison of performance of extrapolation method for 14 m using different values for the threshold (based on extreme value distribution)

Figure 3.34 shows some oscillation of the extrapolated estimate around the theoretical solution. As the threshold increases, the oscillations become larger and the confidence interval no longer contains the theoretical solution. The deterioration of the extrapolated estimated made with increasing threshold can be explained by a decrease in the amount of available data to fit the extreme value distribution, as fewer and fewer values exceed the threshold.

Averaging of the estimates over a portion of the threshold range seems to be the natural way to improve stability of these calculations. As it is known from experience,

100~150 data points is considered a minimum amount of data to fit the distribution. This number can be used as a criterion for the high-end threshold.

$$\lambda_{2a} = \frac{1}{N_{a1}} \sum_{i=1}^{N_{a1}} \lambda_2(a_{1i}) \tag{3.46}$$

Here λ_{2a} is the extrapolated estimate averaged over N_{a1} threshold values a_{1i}, and $\lambda_2(a_{1i})$ is a value of the extrapolated estimated based on the threshold a_{1i}.

Lower and upper boundaries of the confidence interval can be also be averaged in the first expansion:

$$\lambda_{a2}^{low} = \frac{1}{N_{a1}} \sum_{i=1}^{N_{a1}} \lambda_2^{low}(a_{1i}) \qquad \lambda_{a2}^{up} = \frac{1}{N_{a1}} \sum_{i=1}^{N_{a1}} \lambda_2^{up}(a_{1i}) \tag{3.47}$$

Here λ_{a2}^{low} and λ_{a2}^{up} are lower and upper boundaries of the confidence interval for the averaged extrapolated estimate. $\lambda_2^{low}(a_{1i})$ and $\lambda_2^{up}(a_{1i})$ are the boundaries for the extrapolated estimated based on the threshold a_{1i}.

Figure 3.35 shows the result for the target level a_2=14 m. The theoretical solution hits almost exactly in the middle of confidence interval.

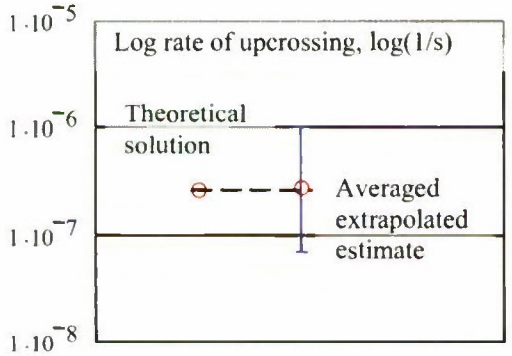

Figure 3.35 Level 14 m: theoretical solution and extrapolated estimate averaged for the thresholds 7.5-8.5 m. The distribution for the threshold 8.5 m was fitted with 149 points

Figure 3.36 shows the performance for all levels from a_2=9 to 22 m. The break point is 20 m, which gives an upcrossing rate of 5.5×10^{-13}; this is more than enough for practical calculations as the mean time to an event is about 57,000 years.

Successful application of the averaging over several thresholds for the current numerical example does not yet prove that it will work as well for all other cases. While it seems to be impossible to prove, it still makes sense to try it at least on two alternative data sets used earlier in this section. Figure 3.37 shows the dependence of the breakpoints of these datasets as a function of the threshold, similar to Figure 3.32. The lowest point is about 13 m in both cases.

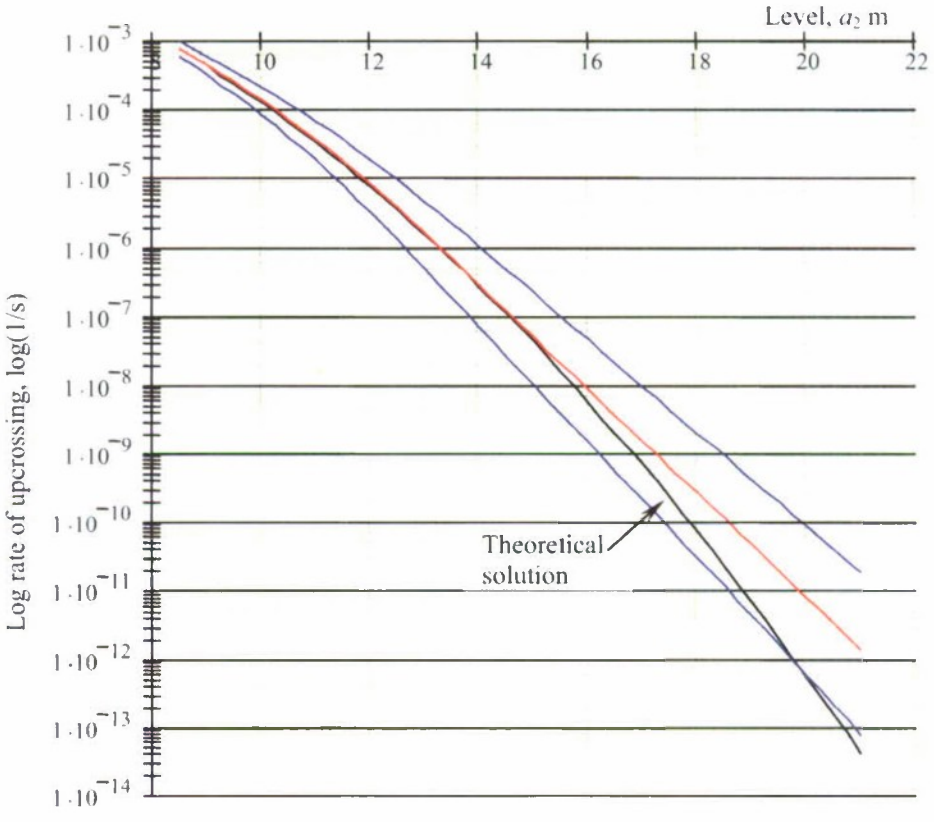

Figure 3.36 Theoretical solution and extrapolated estimate averaged for the thresholds 7.5-8.5 m. The distribution for the threshold 8.5 m was fitted with 149 points

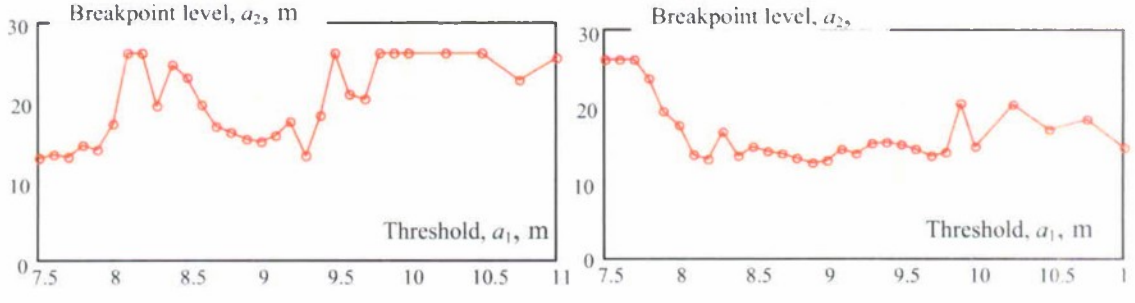

Figure 3.37 Breakpoint level (the level below which the extrapolation is still good) for the extrapolation based on extreme value distribution vs threshold for two alternative data sets

Figure 3.38 shows behaviors of the rare solution and the complete extrapolated estimate for a_2=14 m using two alternative datasets. These behaviors are principally similar to the original set seen in Figure 3.33 and Figure 3.34. Quite a number of threshold values enables the estimate "to eatch" theoretical solution in its confidence interval.

Figure 3.39 shows results of the averaging technique for the two alternative datasets. The performance is not as dramatic as the original one, but is still usable.

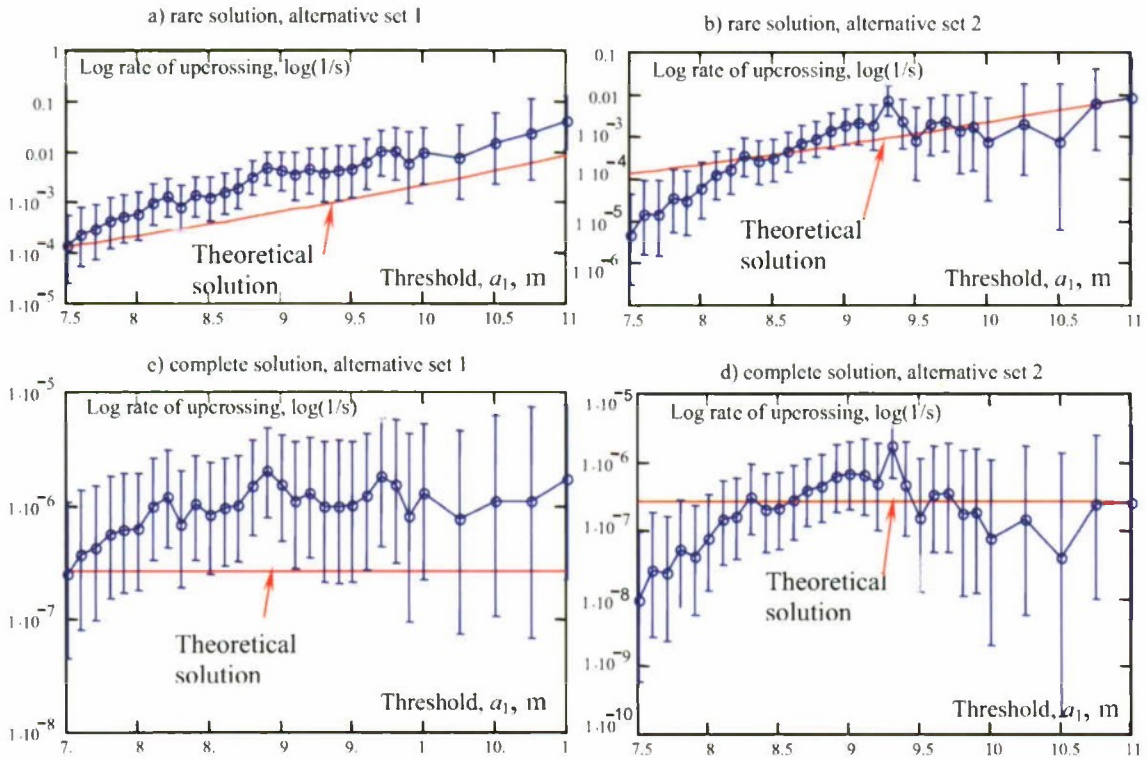

Figure 3.38 extrapolated estimate of eonditional probability that the proeess will exceed the level of 14 m if the threshold has been crossed – rare solutions (upper plots: a, b) and complete extrapolated estimate (lower plots: e, d) for two alternative data sets for a_2=14 m

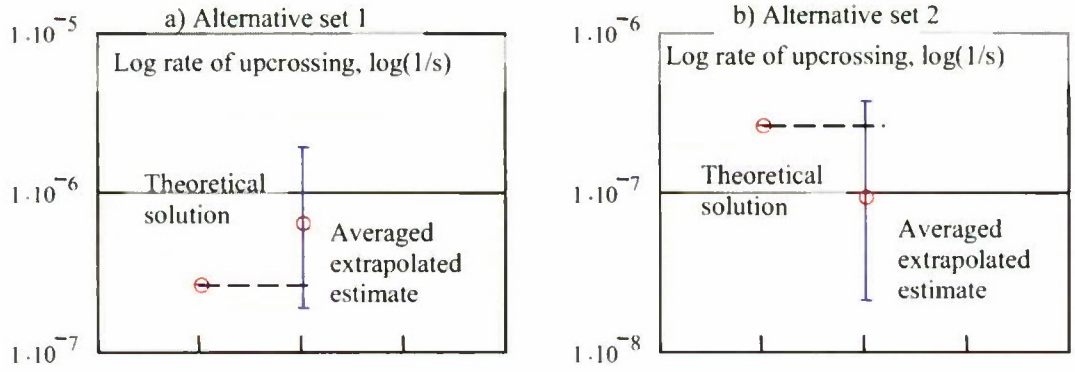

Figure 3.39 Level 14 m: theoretical solution and extrapolated estimate averaged for the set 1 thresholds 7.5-8.5 m. The distribution for the threshold 8.5 m was fitted with 145 points. For the set 2 range is 7.5-8.6 m with 146 points for the threshold 8.6 m.

Finally, Figure 3.40 compares the theoretical solution with the extrapolated estimate averaged through a range of the thresholds. Breakpoints for the alternative dataset lay on the levels of 15.25 m and 21.1 m respectively. Even the lowest breakpoint corresponds to the value of the rate $2.531 \cdot 10^{-8}$ s^{-1}; while the mean time before the event is 1.25 years. Of course, it is less than the original dataset has shown, but still good enough for 200 records 30 minutes each, as the method allowed extrapolating data from 100 hrs to 10,000 hrs.

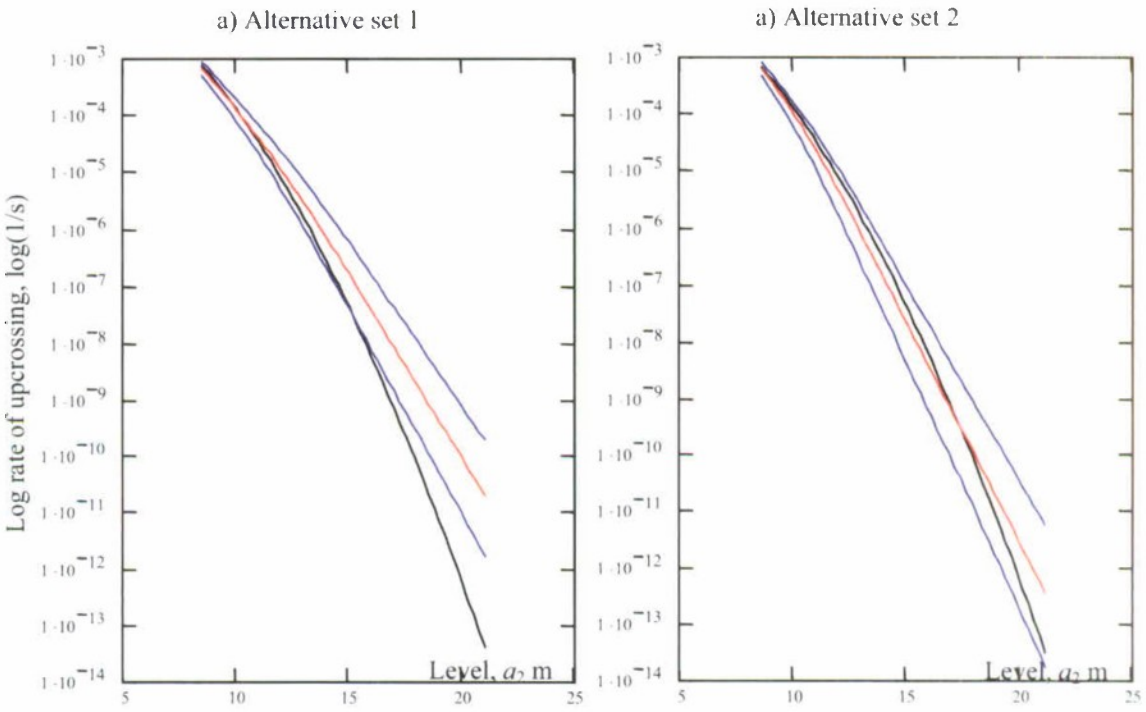

Figure 3.40 Theoretical solution and extrapolated estimate averaged for the alternative data set.
Set 1: Range 7.5-8.5 m; 145points for the threshold 8.5 m
Set 2: 7.5-8.6 m; 146 points for the threshold 8.6 m

3.4.Summary

The main difficulty associated with characterizing the likelihood of a large roll angle occurring is related to the problem of rarity. The nonlinearity of the dynamical system describing large roll motions of a ship creates additional difficulties. The natural frequency of roll of a ship changes as a function of roll amlitude. This frequency shift makes the response significantly different for small and large-amplitude motions. These difficulties are overcome by separating the problem into "non-rare" and "rare" sub-problems. The "non-rare" sub-problem is based on relatively small-amplitude motions. Its solution provides the rate of uperossing a threshold, a boundary that separates small, almost linear motions from moderate and large-amplitude motions, where nonlinearity is significant. This threshold is the boundary between the "non-rare" and "rare" sub-problems. The non-rare problem was considered in the seetion 1 of this report. Further work is focused on "rare" problem.

The solution of the "rare" problem is based on the statistical properties of the data points above the threshold. The idea is to use them to prediet large angles, as the influenee of nonlinearity is already significant above the threshold. Among the data points above the threshold, the peaks are of speeial interest and they can also be considered for Poisson flow. It ean also be shown that reaching a peak above the threshold is an event equivalent to upcrossing of this threshold.

A distribution that is fit to the peaks over the threshold is a conditional distribution. This conditional distribution describes the probability that, once the threshold is crossed, a higher level is crossed. This constitutes the solution of the "rare" problem. The distribution may also be considered as an extreme value distribution, in which case the maximum values from fixed length windows are used in place of the peaks. The extreme value distribution describes the behavior of the tail of a distribution and may therefore provide more accurate extrapolation. Averaging results obtained with several thresholds also seem to improve the accuracy of the method.

4. Envelope Theory

This section examines the properties of the envelope and then considers its application, along with upcrossing theory, as a method of evaluation of the probability of rare events.

4.1. Definition and Background

As it was demonstrated in the Section 1, a violation of Poisson flow is caused by too many crossings of neighboring periods. This is especially pronounced when the spectrum is narrow, which leads to significant grouping or clustering. Such a situation may be typical for following and stern quartering waves when the encounter spectrum can become very narrow. Envelope theory may be useful in these cases. Belenky and Breuer (2007) show an example of successful application of the envelope for the case of parametric roll, a process known for its narrow spectrum.

Most Naval Architecture applications dealing with irregular waves use a Fourier presentation of a stochastic process:

$$x(t) = \sum_{i=1}^{N_W} r_{Wi} \cos(\omega_i t + \varphi_i) \tag{4.1}$$

Here, ω_i is set of frequencies used for discretization of the given spectral density, r_{Wi} is amplitude of the i-th component and φ_i is a phase shift for the i^{th} component. If a process is normal, like in the case of elevations of irregular waves, amplitudes of components are taken from a spectrum, while phase shifts are considered as a set of independent random numbers with uniform distribution from 0 to 360 degrees.

The concept of the envelope came from envelope presentation, which is an alternative way to describe the time history of a stochastic process:

$$x(t) = a(t)\cos\big(\Phi(t)\big) \tag{4.2}$$

Here the process $x(t)$ is presented through two other stochastic processes: amplitude or envelope $a(t)$ and phase $\Phi(t)$. Originally the envelope presentation was developed for a stationary normal processes (Rice, 1944, 1945); the principles it is based upon may, however, be extendible to non-Gaussian processes as well. The role of phase $\Phi(t)$ is keeping the "memory" of the process; it makes sure that the presentation (4.2) does not alter the autocorrelation function of the process $x(t)$. The role of the envelope ($a(t)$) is to ensure the variance is maintained, see (Belenky, *et al* 2006) where an example application of the envelope presentation is shown.

Formally, the envelope is defined through a complementary stochastic process. It is $y(t)$ is defined as:

$$y(t) = \sum_{i=1}^{N_w} r_{Wi} \sin(\omega_i t + \varphi_i) \tag{4.3}$$

The stochastic processes $x(t)$ and $y(t)$ are not correlated if the time is fixed, as the correlation moment at the fixed time is zero, since the phases were shifted 90 degrees (if the process $x(t)$ and y(t) are normal they are also independent at the fixed time). However, the values of the processes may be correlated if they are taken at different instances of time. The operation of obtaining the complimentary process is known as Hilbert Transform.

The envelope $a(t)$ is defined as:

$$a(t) = \sqrt{x^2 + y^2} \tag{4.4}$$

The envelope is a stochastic process with its own autocorrelation function and distribution that differs from the distribution of $x(t)$ and $y(t)$.

Further considerations rely on the same numerical example of wave elevations. It is described in detail in section 1. Figure 4.1 shows the envelope along with the process, it was derived from. The negative reflection of the envelope has been added for better visualization. Figure 4.1 makes clear the origin of the term "envelope". The actual envelope and its negative reflection cover the entire process and serve as its outer boundary.

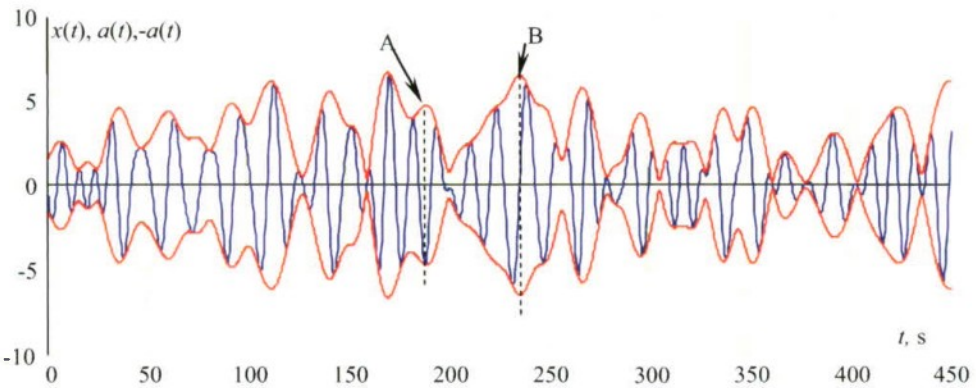

Figure 4.1 Stochastic process of wave elevations and its envelope. Negative reflection of the envelope is added for visualization only

A closer look reveals that the envelope is not just a smooth curve that connects the peaks of the process. It accounts for negative peaks (case A in Figure 4.1). Sometimes the envelope has a peak when the process itself has neither negative nor positive peak (case B in Figure 4.1). The origin of this "unclaimed" peak of the envelope can be clarified by plotting the complimentary process $y(t)$ along with the original process $x(t)$

and its envelope, see Figure 4.2. It becomes clear that the peak of the envelope can be also caused by the peak of the complimentary process.

Moreover, it is possible to show that all the points of the envelope are, in fact, peaks of the process $x(t)$ shifted by an angle. Consider a process $z(t)$:

$$z(t \mid \gamma) = \sum_{i=1}^{N_w} r_{Wi} \cos(\omega_i t + \varphi_i - \gamma) \tag{4.5}$$

Here γ is the shift angle. Figure 4.3 shows the shifted process $z(t)$ along with original process $x(t)$ and complimentary process $y(t)$. Each peak of the shifted process $z(t)$ belongs to the envelope. This provides a graphical interpretation of the envelope and explains the origins of its peaks.

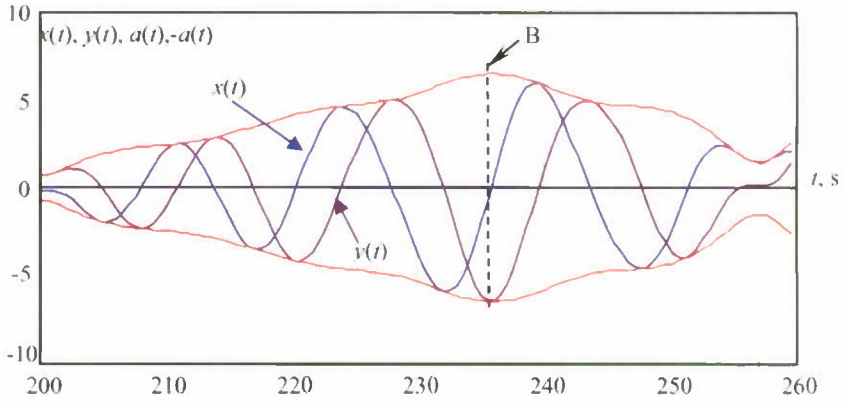

Figure 4.2 Origin of peaks of envelope: original stochastic process $x(t)$ and its complimentary process $y(t)$

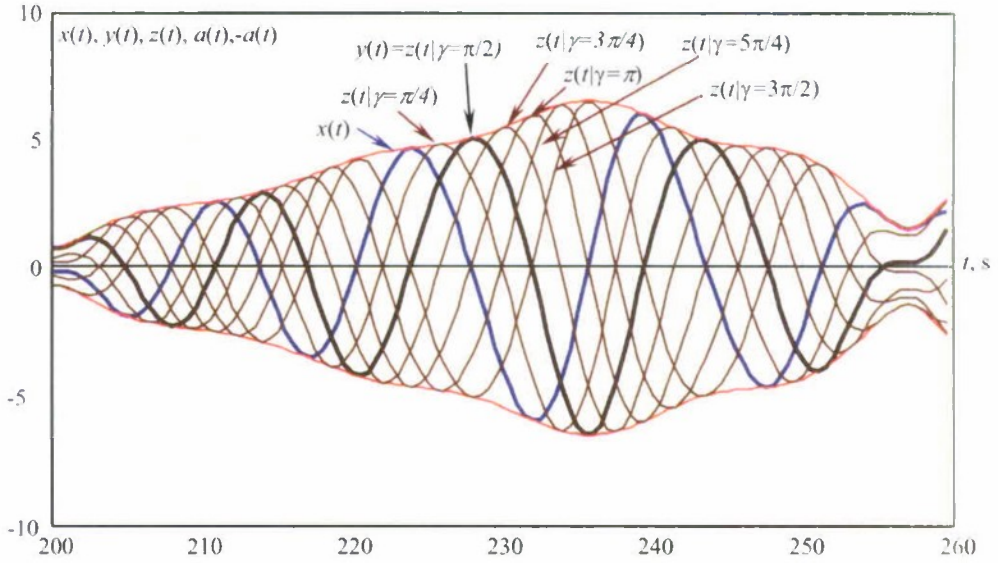

Figure 4.3 Envelope and peaks of the shifted process

4.2.Outline of the Theory of the Envelope

This subsection examines an outline of the basics of the theory of the envelope for a normal process. It is assumed the process $x(t)$ is normal and has zero mean value, but it does not limit generality, as it is always possible to introduce a shift. Consideration generally follows the classical text by Sveshnikov (1968).

4.2.1. Distribution of the Envelope and the Phase

The complimentary process $y(t)$, as the result of Hilbert transform, can also be expressed as:

$$y(t) = \sum_{i=1}^{N_\omega} r_{Wi} \sin(\omega_i t + \varphi_i) = a(t)\sin(\Phi(t)) \tag{4.6}$$

Assumption of normality is extended to the complimentary process $y(t)$. It is naturally followed if Fourier presentation (4.1) is used for the original process $x(t)$ and uniform distribution of phases of components is assumed.

Consider a probability that the envelope takes a particular value. Taking into account (4.4), it can be expressed in a form of the following inequality:

$$a \le \sqrt{x^2 + y^2} < a + da \tag{4.7}$$

The probability of satisfying the inequality (4.7) is directly related with the PDF of the envelope $f(a)$:

$$P\left(a \le \sqrt{x^2 + y^2} < a + da\right) = f(a)da \tag{4.8}$$

The probability (4.8) can be evaluated if the joint distribution of x and y is known:

$$f(a)da = P\left(a \le \sqrt{x^2 + y^2} < a + da\right) = \iint_{a \le \sqrt{x^2+y^2} < a+da} f(x,y)dxdy \tag{4.9}$$

Here $f(x,y)$ is joint distribution of the original process and its complimentary process. As a normal distribution was assumed for both of them the joint distribution is expressed as:

$$f(x,y) = \frac{1}{2\pi\sqrt{V_x V_y\left(1 - r_{xy}^2\right)}} \exp\left(-\frac{1}{2\left(1 - r_{xy}^2\right)} \left(\frac{x^2}{V_x} - \frac{2r_{xy}xy}{\sqrt{V_x V_y}} + \frac{y^2}{V_y} \right) \right) \tag{4.10}$$

Here V_x and V_y are variances of the original and complimentary process, respectively; r_{xy} is the correlation coefficient of the original and complimentary processes:

The variances of the original and complimentary processes are identical. Taking into account presentation (4.1) and (4.3):

$$V_x = V_y = \frac{1}{2}\sum_{i=1}^{N_\omega} r_{Wi}^2 \tag{4.11}$$

As noted in the previous subsection, the original and the complimentary processes are not correlated, as the shift between them is 90 degrees. It can be clearly seen for the known formula for the correlation coefficient between two processes expressed with Fourier series:

$$\begin{aligned} r_{xy} &= \frac{1}{\sqrt{V_x V_y}}\sum_{i=1}^{N_\omega} r_{Wi}\cos(\Delta\varphi_i) = \frac{1}{\sqrt{V_x V_y}}\sum_{i=1}^{N_\omega} r_{Wi}\cos(\varphi_i - (\varphi_i - 0.5\pi)) = \\ &= \frac{1}{\sqrt{V_x V_y}}\sum_{i=1}^{N_\omega} r_{Wi}\cos(0.5\pi) = 0 \end{aligned} \tag{4.12}$$

Here $\Delta\varphi_i$ is the difference between phase of components. For the details of derivation of this formula, see (Belenky & Sevastianov 2007) or (Belenky, *et al*, 2007).

Taking into account (4.11) and (4.12), the distribution (4.10) can be simplified.

$$f(x,y) = \frac{1}{2\pi V_x}\exp\left(-\frac{1}{2}\left(\frac{x^2+y^2}{V_x}\right)\right) \tag{4.13}$$

Substitution of the distribution (4.13) into (4.9) and transition to polar coordinates yields:

$$\begin{aligned} f(a)da &= \iint_{a\le\sqrt{x^2+y^2}<a+da} f(x,y)dxdy = \\ &= \frac{1}{2\pi V_x}\iint_{a\le\sqrt{x^2+y^2}<a+da}\exp\left(-\frac{1}{2}\left(\frac{x^2+y^2}{V_x}\right)\right)dxdy = \\ &= \left|\begin{array}{ll} a = \sqrt{x^2+y^2} & x = a\cos(\Phi) \\ \Phi = \arctan\left(\dfrac{y}{x}\right) & y = a\sin(\Phi) \end{array}\right| = \\ &= \frac{1}{2\pi V_x}\int_a^{a+da}\int_0^{2\pi} a\exp\left(-\frac{1}{2}\left(\frac{a^2}{V_x}\right)\right)d\Phi\, da \end{aligned} \tag{4.14}$$

At the same time, consider $f(a)$ as a marginal distribution of the joint distribution $f(a,\Phi)$:

$$f(a)da = \int_{a}^{a+da} \int_{0}^{2\pi} f(a,\Phi)\, d\Phi\, da \tag{4.15}$$

This joint distribution $f(a,\Phi)$, then is expressed as:

$$f(a,\Phi) = \frac{a}{2\pi V_x} \exp\left(-\frac{1}{2}\left(\frac{a^2}{V_x}\right)\right) \tag{4.16}$$

The right-hand side does not eontain the variable Φ. It means that the variables a and Φ are independent. The PDF of a ean be found by the integration of (4.16) by Φ from 0 to 2π.

$$f(a) = \int_{0}^{2\pi} f(a,\Phi)\, d\Phi = \frac{a}{V_x} \exp\left(-\frac{1}{2}\left(\frac{a^2}{V_x}\right)\right) \tag{4.17}$$

This distribution is known as a Rayleigh distribution.

The distribution of the phase ean be easily found from the formula (16) using the established faet of independenee of envelope and phase:

$$f(\Phi) = \frac{f(a,\Phi)}{f(a)} = \frac{1}{2\pi}; \quad 0 \le \Phi < 2\pi \tag{4.18}$$

The phase in the envelope presentation (4.2) follows unformed distribution from 0 to 2π. This eoncludes consideration of PDFs of the envelope and the phase.

4.2.2. Autocorrelation Function of the Envelope

To find autoeorrelation funetion of the envelope, the joint distribution of two values of the envelope $a(t)$ and $a(t+\tau)$ need to be obtained first. This can be done through four-dimensional distribution of values x and y at the time instanees t and $t+\tau$. Consider a system of four random variables:

$$U = \left(x(t)\,,\, x(t+\tau)\,,\, y(t)\,,\, y(t+\tau)\right) \tag{4.19}$$

These random variables are values of the original and eomplimentary stochastic process and in two time instanees, t and $t+\tau$. As proeesses x and y are normal, all four variables have normal distributions. The processes x and y are independent; that means that the variables $x(t)$ and $y(t)$ are independent as well as the variables $x(t+\tau)$ and $y(t+\tau)$. It does mean, however, that the variables $x(t)$ and $y(t+\tau)$ are independent. Viee versa, they are dependent and their correlation coefficient is expressed using formula (4.12) as:

$$m(x(t), y(x+\tau)) = \frac{1}{2V_x}\sum_{i=1}^{N_\omega} r_{Wi}^2 \cos(\omega_i \tau - 0.5\pi) = \frac{1}{2V_x}\sum_{i=1}^{N_\omega} r_{Wi}^2 \sin(\omega_i \tau) \tag{4.20}$$

A similar conclusion can be reached for another "cross-pair" of the random variables $x(t+\tau)$ and $y(t)$:

$$m(x(t+\tau), y(x)) = \frac{1}{2V_x}\sum_{i=1}^{N_\omega} r_{Wi}^2 \cos(\omega_i \tau + 0.5\pi) = -\frac{1}{2V_x}\sum_{i=1}^{N_\omega} r_{Wi}^2 \sin(\omega_i \tau) \tag{4.21}$$

It is convenient to express these figures as:

$$r(\tau) = -m(x(t+\tau), y(x)) = m(x(t), y(x+\tau)) = \frac{1}{2V_x}\sum_{i=1}^{N_\omega} r_{Wi}^2 \sin(\omega_i \tau) \tag{4.22}$$

Dependence between random variables $x(t)$ and $x(t+\tau)$ as well as between $y(t)$ and $y(t+\tau)$ can beexpressed through an autocorrelation function of the processes x and y, which in the considered case is identical to the application of formula (4.12):

$$m(x(t), x(x+\tau)) = \frac{1}{2V_x}\sum_{i=1}^{N_\omega} r_{Wi}^2 \cos(\omega_i \tau) \tag{4.23}$$

$$m(y(t), y(x+\tau)) = \frac{1}{2V_x}\sum_{i=1}^{N_\omega} r_{Wi}^2 \cos(\omega_i \tau) \tag{4.24}$$

It is convenient to express these figures as:

$$k(\tau) = m(x(x), x(t+\tau)) = m(y(t), y(x+\tau)) = \frac{1}{2V_x}\sum_{i=1}^{N_\omega} r_{Wi}^2 \cos(\omega_i \tau) \tag{4.25}$$

In fact $k(\tau)$ is the normalized autocorrelation function that is the same for the processes $x(t)$ and $y(t)$.

The relationship between these variables is summarized with the following covariance matrix:

$$C(\tau) = V_x \begin{pmatrix} 1 & k(\tau) & 0 & r(\tau) \\ k(\tau) & 1 & -r(\tau) & 0 \\ 0 & -r(\tau) & 1 & k(\tau) \\ r(\tau) & 0 & k(\tau) & 1 \end{pmatrix} \tag{4.26}$$

All these variables have a normal distribution; therefore dependence between them is completely characterized by the correlation expressed by the covariance matrix (4.26).

Next, their joint distribution is completely defined by the following 4-variate normal distribution:

$$f(U)=\frac{1}{(2\pi)^2\sqrt{\det(C)}}\exp\left(-\frac{1}{2}U^T C^{-1}U\right)= \\ =\frac{1}{(2\pi)^2\sqrt{\det(C)}}\exp\left(-\frac{1}{2}\sum_{i=1}^{4}\sum_{j=1}^{4}C_{ij}^{-1}U_i U_j\right) \tag{4.27}$$

Here the superscript T stands for the transpose operation. It converts a vector-column into vector-row. C^{-1} is an inverse covariance matrix. It is expressed as:

$$C^{-1}(\tau)=\frac{1}{V_x\cdot p(\tau)^2}\begin{pmatrix}1 & -k(\tau) & 0 & -r(\tau)\\ -k(\tau) & 1 & r(\tau) & 0\\ 0 & r(\tau) & 1 & -k(\tau)\\ -r(\tau) & 0 & -k(\tau) & 1\end{pmatrix} \tag{4.28}$$

Here:

$$p(\tau)^2=1-k(\tau)^2-r(\tau)^2 \tag{4.29}$$

The determinant of covariance matrix is:

$$\det(C(\tau))=V_x^4\left(1-k(\tau)^2-r(\tau)^2\right)^2=V_x^4 p(\tau)^4 \tag{4.30}$$

Substitution of the formulae (4.28) and (4.30) into (4.27) leads to the following expression for the joint distribution of considered random variable:

$$f(U)=\frac{1}{(2\pi V_x)^2 p^2}\exp\left(-\frac{1}{2V_x p^2}\left(x_1^2+y_1^2+x_2^2+y_2^2-2k(x_1x_2+y_1y_2)-2r(x_1y_2+y_1x_2)\right)\right) \tag{4.31}$$

To avoid a bulky formula, the following nomenclature was used in formula (4.31):

$$x_1=x(t)\ ;\quad x_2=x(t+\tau) \\ y_1=y(t)\ ;\quad y_2=y(t+\tau) \tag{4.32}$$

Formula (4.31) describes probability density in the four-dimensional space with coordinates x_1, x_2, y_1, y_2. The next step is to re-write in the polar coordinates defined as follows:

$$a = \sqrt{x^2 + y^2} \qquad x = a\cos(\Phi)$$
$$\Phi = \arctan\left(\frac{y}{x}\right) \qquad y = a\sin(\Phi) \tag{4.33}$$

The new coordinates are:

$$a_1 = a(t) \;;\quad a_2 = a(t+\tau)$$
$$\Phi_1 = \Phi(t) \;;\quad \Phi_2 = \Phi(t+\tau) \tag{4.34}$$

To complete the transition, two pairs of reetangular eoordinates (x_1, y_1) and (x_2, y_2) are substituted with (a_1, Φ_1) and (a_2, Φ_2). Then the expression needs to be multiplied by $a_1\, a_2$ as the element of the area in the polar coordinates $a\, d\Phi\, da$.

$$f(a_1,a_2,\Phi_1,\Phi_2) = \frac{a_1 a_2}{(2\pi V_x)^2 p^2}\exp\left(-\frac{1}{2V_x p^2}\left(a_1^2 + a_2^2 - \right.\right.$$
$$\left.\left. - 2ka_1a_2\cos(\Phi_2 - \Phi_1) - 2ra_1a_2\sin(\Phi_2 - \Phi_1)\right)\right) \tag{4.35}$$

The expression (4.35) ean be further simplified by the substitution:

$$\gamma = \arctan\left(\frac{r}{k}\right) \tag{4.36}$$

$$f(a_1,a_2,\Phi_1,\Phi_2) = \frac{a_1 a_2}{(2\pi V_x)^2 p^2}\exp\left(-\frac{1}{2V_x p^2}\left(a_1^2 + a_2^2 - \right.\right.$$
$$\left.\left. - 2a_1a_2\sqrt{1-p^2}\,\mathrm{eos}(\Phi_2 - \Phi_1 - \gamma)\right)\right) \tag{4.37}$$

The next step is to obtain the joint distribution of a_1, a_2. It can be done by integration of the distribution (4.37) twice by Φ_1 and Φ_2:

$$f(a_1,a_2) = \frac{a_1 a_2}{V_x^2 p^2}\int_0^{2\pi}\int_0^{2\pi}\exp\left(-\frac{1}{2V_x p^2}\left(a_1^2 + a_2^2 - \right.\right.$$
$$\left.\left. - 2a_1a_2\sqrt{1-p^2}\cos(\Phi_2 - \Phi_1 - \gamma)\right)\right) d\Phi_1 d\Phi_2 \tag{4.38}$$

The integration ean be eompleted:

$$f(a_1,a_2) = \frac{a_1 a_2}{V_x^2 p^2}\exp\left(-\frac{a_1^2 + a_2^2}{2V_x p^2}\right)\mathbf{I}_0\left(\frac{a_1 a_2\sqrt{1-p^2}}{V_x p^2}\right) \tag{4.39}$$

Here $\mathbf{I_0}$ is the zero-order modified Bessel function of the first kind (Abramowitz and Stegun 1972).

Finally, the autoeorrelation funetion ean be obtained from the PDF (4.39) using its definition:

$$R_a(\tau) = \int_0^\infty \int_0^\infty f(a_1, a_2)(a_1 - m_a)(a_2 - m_a) da_1 da_2 \tag{4.40}$$

Here m_a is a mean value of the envelope. As it was shown that the envelope follows the Rayleigh distribution, the mean value is known:

$$m_a = \int_0^\infty a f(a) da = \frac{1}{V_x} \int_0^\infty a^2 \exp\left(-\frac{1}{2}\left(\frac{a^2}{V_x}\right)\right) da = \sqrt{0.5\pi V_x} \tag{4.41}$$

The integration results in the following formula for the autoeorrelation function:

$$R_a(\tau) = V_x\left(2\mathbf{E}\left(1 - p^2\right) - p^2\mathbf{K}\left(1 - p^2\right) - 0.5\pi\right) \tag{4.42}$$

Here **E** and **K** are elliptie integrals of the first and the seeond kind:

$$\mathbf{E}(x) = \int_0^{\pi/2} \frac{dz}{\sqrt{1 - x \cdot \sin^2 z}}; \quad \mathbf{K}(x) = \int_0^{\pi/2} \sqrt{1 - x \cdot \sin^2 z}\, dz \tag{4.43}$$

An example of the calculation of the autocorrelation function of the envelope, as well as its comparison with a statistieal estimate, is given in the subsection below.

4.2.3. Distribution of the Derivative of the Envelope

The theory of the envelope also offers the PDF of the derivative of the envelope. This result may be important for an application of the uperossing theory to the envelope.

To find the distribution of the derivative of the envelope, the joint distribution of the envelope and its derivative need to be found first and then integrated from zero to infinity by the value of the envelope:

$$f(\dot{a}) = \int_0^\infty f(a, \dot{a}) da \tag{4.44}$$

The joint distribution of the envelope and its derivative ean be derived from the joint distribution of two values of the envelope (4.39). This problem can be elassified as multivariate probability transformation, when the distribution of one random veetor is derived from the distribution of the other random veetor. It also implies that these random vectors are related to the deterministie vector valued function.

$$\begin{pmatrix} a(t) \\ \dot{a}(t) \end{pmatrix} = \Xi \begin{pmatrix} a(t) \\ a(t+\tau) \end{pmatrix} \quad \text{or} \quad \begin{pmatrix} a_1 \\ \dot{a}_1 \end{pmatrix} = \Xi \begin{pmatrix} a_1 \\ a_2 \end{pmatrix} \tag{4.45}$$

Generally, a derivative is defined as a limit:

$$\dot{a}(t) = \lim_{\tau \to 0} \frac{a(t+\tau) - a(t)}{\tau} \quad \text{or} \quad \dot{a}_1 = \lim_{\tau \to 0} \frac{a_2 - a_1}{\tau} \tag{4.46}$$

Formula (4.46) represents a component of a veetor-valued deterministic function of a random vector; the other component is obvious:

$$\vec{\Xi} \begin{pmatrix} a_1 \\ a_2 \end{pmatrix} = \begin{pmatrix} a_1 \\ \lim_{\tau \to 0} \dfrac{a_2 - a_1}{\tau} \end{pmatrix} \tag{4.47}$$

Sinee the first eomponent of the funetion (4.47) maps a_1 into itself and does not depend on τ, the symbol of limit can be applied to the entire function:

$$\vec{\Xi} \begin{pmatrix} a_1 \\ a_2 \end{pmatrix} = \lim_{\tau \to 0} \begin{pmatrix} a_1 \\ \dfrac{a_2 - a_1}{\tau} \end{pmatrix} \tag{4.48}$$

Assume that τ is small. Then introduce approximation for the function (4.48):

$$\vec{\Xi} \begin{pmatrix} a_1 \\ a_2 \end{pmatrix} \approx \vec{\Xi}^* \begin{pmatrix} a_1 \\ a_2 \end{pmatrix} = \begin{pmatrix} a_1 \\ \dfrac{a_2 - a_1}{\tau} \end{pmatrix} \tag{4.49}$$

The formulation of the problem of multivariate probability transformation is eompleted. Its solution is well-known from the general theory of probability (see, for example, Goodman, 1985):

$$f^*(a_1, \dot{a}_1) = \left| J\left(\bar{\Psi}^*\right) \right| f\left(\Psi_1^*(a_1, a_2), \Psi_2^*(a_1, a_2)\right) \tag{4.50}$$

Here the veetor valued funetion Ψ^* is an inverse to the vector valued function Ξ^* and J stands for the determinant of Jacobean matrix.

$$\begin{pmatrix} a_1 \\ a_2 \end{pmatrix} = \vec{\Psi}^* \begin{pmatrix} a_1 \\ \dot{a}_1 \end{pmatrix} = \begin{pmatrix} a_1 \\ a_1 + \dot{a}_1 \tau \end{pmatrix} \tag{4.51}$$

The second component of the inverse function (4.51) was formally derived from the second component of (4.49):

$$\dot{a}_1 = \Xi_2^*(a_1, a_2) = \frac{a_2 - a_1}{\tau} \quad \Leftrightarrow \quad a_2 = a_1 + \dot{a}_1 \tau = \Psi_2^*(a_1, \dot{a}_1) \tag{4.52}$$

However, it is also follows from the assumption that τ is small:

$$a(t + \tau) = a(t) + \tau \dot{a}(t) \quad \text{or} \quad a_2 = a_1 + \tau \dot{a}_1 \tag{4.53}$$

The determinant of the Jacobean matrix of the inverse function is expressed as:

$$J(\Psi^*) = \det \begin{pmatrix} \dfrac{\partial \Psi_1^*(a_1, \dot{a}_1)}{\partial a_1} & \dfrac{\partial \Psi_1^*(a_1, \dot{a}_1)}{\partial \dot{a}_1} \\ \dfrac{\partial \Psi_2^*(a_1, \dot{a}_1)}{\partial a_1} & \dfrac{\partial \Psi_2^*(a_1, \dot{a}_1)}{\partial \dot{a}_1} \end{pmatrix} = \det \begin{pmatrix} 1 & 0 \\ 1 & \tau \end{pmatrix} = \tau \tag{4.54}$$

Substitution of (4.54) and (4.51) into (4.50) lead to the following expression for the approximate joint distribution:

$$f^*(a_1, \dot{a}_1) = \tau f(a_1, a_1 + \dot{a}_1 \tau) \tag{4.55}$$

The exact distribution of the envelope and its derivative is actually a limit of (4.55) when τ tends to zero:

$$f(a_1, \dot{a}_1) = \lim_{\tau \to 0} f^*(a_1, \dot{a}_1) = \lim_{\tau \to 0} \tau f(a_1, a_1 + \dot{a}_1 \tau) \tag{4.56}$$

Substitution of (4.39) into (4.56) yields (index 1 may be dropped now):

$$f(a, \dot{a}) = \lim_{\tau \to 0} \frac{\tau a (a + \tau \dot{a})}{V_x^2 p^2} \exp\left(-\frac{2a^2 + 2a\dot{a}\tau + \dot{a}^2 \tau^2}{2 V_x p^2} \right) \mathbf{I}_0 \left(\frac{a(a + \tau \dot{a}) \sqrt{1 - p^2}}{V_x p^2} \right) \tag{4.57}$$

To carry out the limit transition in the formula (4.57), p needs to be considered in more detail as it is a function of τ, see formula (4.29), repeated here for convenience:

$$p(\tau)^2 = 1 - k(\tau)^2 - r(\tau)^2$$

The function $k(\tau)$ is a normalized autocorrelation function. It was defined by the formula (4.25), which is based on discretization of spectrum with frequency set ω_i, $i=1,..,N_\omega$. Formally, it is the cosine Fourier transform of the spectral density $s(\omega)$:

$$k(\tau) = \frac{1}{V_x}\int_0^\infty s(\omega)\cos(\omega\tau)d\omega \qquad (4.58)$$

The function $r(\tau)$ is a normalized cross-correlation function. It was defined by formula (4.22) based on the same discretization. It is a result of sine Fourier transform of the spectral density:

$$r(\tau) = \frac{1}{V_x}\int_0^\infty s(\omega)\sin(\omega\tau)d\omega \qquad (4.59)$$

Figure 4.4 shows the function $p(\tau)$ along with normalized autocorrelation function $k(\tau)$ and normalized cross-correlation function $r(\tau)$ calculated for the numerical example.

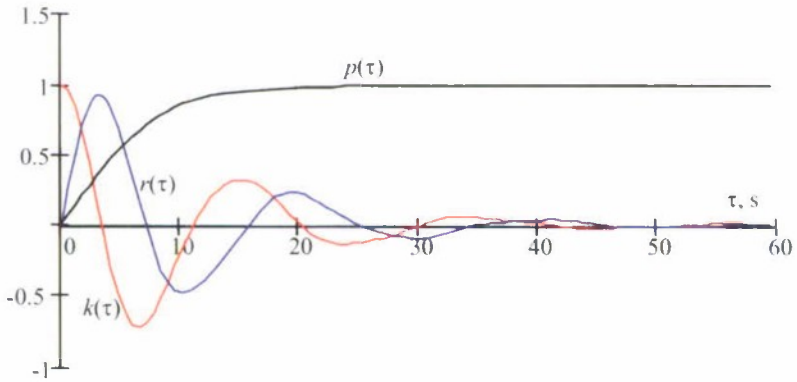

Figure 4.4 Function p, normalized auto- and cross-correlation functions

As it ean be seen from Figure 4.4 the function $p(\tau)$ tends to zero with the deerease of time duration τ. To describe behavior of this function near zero, it is convenient to expand it into the Taylor series about the zero point (actually, then it is Maclaurin series):

$$p(\tau)^2 = p(0)^2 + \frac{1}{1!}\dot{p}(0)^2\tau + \frac{1}{2!}\ddot{p}(0)^2\tau^2 + \ldots \qquad (4.60)$$

Consider each term of (4.60):

$$p(0)^2 = 1 - k(0)^2 - r(0)^2 = 1 - 1 - 0 = 0 \tag{4.61}$$

$$\dot{p}(0)^2 = \frac{d}{d\tau}\left(1 - k(\tau)^2 - r(\tau)^2\right)\Big|_{\tau=0} = -2\left(k(\tau)\dot{k}(\tau) + r(\tau)\dot{r}(\tau)\right)\Big|_{\tau=0} \tag{4.62}$$

$$\begin{aligned}\ddot{p}(0)^2 &= \frac{d}{d\tau}\left(-2k(\tau)\dot{k}(\tau) - 2r(\tau)\dot{r}(\tau)\right)\Big|_{\tau=0} = \\ &= -2\left(k(\tau)\ddot{k}(\tau) + \dot{k}(\tau)^2 + r(\tau)\ddot{r}(\tau) + \dot{r}(\tau)^2\right)\Big|_{\tau=0}\end{aligned} \tag{4.63}$$

Values of the auto- and cross correlation at $\tau = 0$ are expressed as:

$$k(0) = 1 \;;\; r(0) = 0 \tag{4.64}$$

Derivatives of the auto- and cross-correlation functions are:

$$\dot{k}(\tau) = \frac{1}{V_x}\int_0^\infty s(\omega)\omega\sin(\omega\tau)d\omega \;;\; \ddot{k}(\tau) = -\frac{1}{V_x}\int_0^\infty s(\omega)\omega^2\cos(\omega\tau)d\omega \tag{4.65}$$

$$\dot{r}(\tau) = -\frac{1}{V_x}\int_0^\infty s(\omega)\omega\cos(\omega\tau)d\omega \;;\; \ddot{r}(\tau) = -\frac{1}{V_x}\int_0^\infty s(\omega)\omega^2\sin(\omega\tau)d\omega \tag{4.66}$$

The values of these derivatives at $\tau = 0$ are expressed as:

$$\dot{k}(0) = \frac{1}{V_x}\int_0^\infty s(\omega)\omega\sin(\omega\tau = 0)d\omega = 0 \tag{4.67}$$

$$\dot{r}(0) = -\frac{1}{V_x}\int_0^\infty s(\omega)\omega\cos(\omega\tau = 0)d\omega = -\frac{1}{V_x}\int_0^\infty s(\omega)\omega d\omega = \omega_1 \tag{4.68}$$

The value $-\dot{r}(0)$ is the mean frequency ω_1 as determined from the spectral density.

$$\ddot{k}(0) = -\frac{1}{V_x}\int_0^\infty s(\omega)\omega^2\cos(\omega\tau = 0)d\omega = -\frac{1}{V_x}\int_0^\infty s(\omega)\omega^2 d\omega = -\omega_2^2 \tag{4.69}$$

The quantity $-\ddot{k}(0)$ has a meaning of the second moment of the spectral area, normalized by the variance. Its usual nomenclature is ω_2^2.

$$\ddot{r}(0) = -\frac{1}{V_x}\int_0^{\infty} s(\omega)\omega^2 \sin(\omega\tau = 0)d\omega = 0 \tag{4.70}$$

Formulae (4.61) through (4.70) allow us to express the expansion (4.61) near $\tau = 0$ as:

$$\begin{aligned} p(\tau)^2 &= 0 - \tau\left(k(0)\dot{k}(0) + r(0)\dot{r}(0)\right) - \\ &- \tau^2\left(k(0)\ddot{k}(0) + \dot{k}(0)^2 + r(0)\ddot{r}(0) + \dot{r}(0)^2\right) + \ldots \approx \\ &\approx -\tau(1\cdot 0 - 0\cdot\omega_1) - \tau^2\left(-1\cdot\omega_2^2 - 0 - 0 + \omega_1^2\right) \approx \tau^2\left(\omega_2^2 - \omega_1^2\right) \end{aligned} \tag{4.71}$$

The above derivation completed with formula (4.71) allows making an important conclusion of the behavior of the function $p(\tau)$ near $\tau = 0$.

$$\lim_{\tau\to 0} p(\tau)^2 = \lim_{\tau\to 0} \tau^2\left(\omega_2^2 - \omega_1^2\right) \tag{4.72}$$

Consider behavior of the argument of the Bessel function in (4.57) near $\tau = 0$:

$$\begin{aligned} &\lim_{\tau\to 0}\left(\frac{a(a+\tau\dot{a})\sqrt{1-p(\tau)^2}}{V_x p(\tau)^2}\right) = \lim_{\tau\to 0}\left(\frac{a(a+\tau\dot{a})\sqrt{1-\tau^2\left(\omega_2^2-\omega_1^2\right)}}{V_x\tau^2\left(\omega_2^2-\omega_1^2\right)}\right) = \\ &= \lim_{\tau\to 0}\left(\frac{a^2}{V_x\tau^2\left(\omega_2^2-\omega_1^2\right)} + \frac{\dot{a}a}{V_x\tau\left(\omega_2^2-\omega_1^2\right)}\right) = \infty \end{aligned} \tag{4.73}$$

Using the known quality of the modified Bessel function of the first kind:

$$\lim_{x\to\infty} \mathbf{I}_0(x) = \frac{1}{\sqrt{2\pi x}}\exp(x) \tag{4.74}$$

This allows substituting the Bessel function with its approximation in the formula (4.57):

$$\begin{aligned} f(a,\dot{a}) = \lim_{\tau\to 0}\Bigg(&\frac{\tau a(a+\tau\dot{a})}{V_x^2 p(\tau)^2}\frac{p(\tau)\sqrt{V_x}}{\sqrt{2\pi a(a+\tau\dot{a})\sqrt{1-p(\tau)^2}}} \\ &\exp\left(-\frac{\dot{a}^2\tau^2}{2V_x p(\tau)^2}\right)\exp\left(-\frac{a(a+\dot{a}\tau)}{V_x p(\tau)^2}\right)\exp\left(\frac{a(a+\tau\dot{a})\sqrt{1-p(\tau)^2}}{V_x p(\tau)^2}\right)\Bigg) \end{aligned} \tag{4.75}$$

Substitution of the approximation (4.71) for the function $p(\tau)$ into the equation (4.75) allows completing the evaluation of the limit:

$$f(a,\dot{a}) = \frac{a}{V_x}\exp\left(-\frac{a^2}{2V_x}\right)\frac{1}{\sqrt{2\pi V_x\left(\omega_2^2-\omega_1^2\right)}}\exp\left(-\frac{\dot{a}^2}{2V_x\left(\omega_2^2-\omega_1^2\right)}\right) \tag{4.76}$$

The structure of formula (4.76) reveals independence of the envelope and its derivative (see formula (4.17)). This is, actually, an expected result. Since the process x is stationary, its envelope also can be expected to be stationary; and the stationary process is independent of its derivative.

$$f(a,\dot{a}) = f(a)f(\dot{a}) \tag{4.77}$$

Finally the distribution of the derivative is expressed as:

$$f(\dot{a}) = \frac{1}{\sqrt{2\pi V_x\left(\omega_2^2-\omega_1^2\right)}}\exp\left(-\frac{\dot{a}^2}{2V_x\left(\omega_2^2-\omega_1^2\right)}\right) \tag{4.78}$$

It is a normal distribution with zero mean and the following variance:

$$V_a = V_x\left(\omega_2^2-\omega_1^2\right) \tag{4.79}$$

4.2.4. Numerical Example

The envelope is a stochastic process; therefore it makes sense to start its numerical exploration by comparing its statistical estimate of the autocorrelation function with its theoretical counterpart (4.42).

The values of the envelope were computed for each time step with formula (4.4). The estimate of its mean value is expressed as:

$$m_a^* = \frac{1}{N_R N}\sum_{j=1}^{N_R}\sum_{i=1}^{N} a_{ij} \tag{4.80}$$

Calculation of the estimate of the autocorrelation function may encounter significant difficulties for larger values of time due to insufficient data. Averaging of the estimate over the records alleviates this problem (Belenky *et al* 2007):

$$R_k^* = \frac{1}{N_R}\sum_{j=1}^{N_R}\frac{1}{N-j}\sum_{i=1}^{N-k}(a_i - m_a^*)(a_{k+i} - m_a^*) \tag{4.81}$$
$$i = 1,..N\ ;\quad j = 1,..N_R\ ;\quad k = 1,..N-1$$

Figure 4.5 shows theoretical autocorrelation function of the envelope (4.42) and its statistical estimate (4.81). Although in-depth statistical analysis was not performed, it is clear from this figure that both the shape of the autocorrelation function and its time of decay are fairly close.

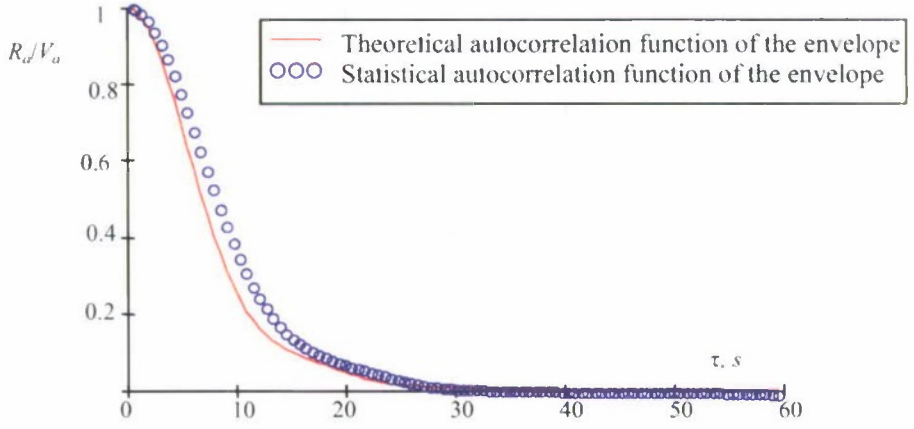

Figure 4.5 Normalized autocorrelation functions of the envelope

As an ultimate purpose of using the envelope is upcrossing, it makes sense to check the distribution of the envelope and its derivative. This can be done using Pearson chi-square goodness-of-fit test. However, in order to use this test, all the points included in the sample must represent independent data. The points a_i are dependent, as the process of the envelope has a certain memory represented by the autocorrelation function shown in Figure 4.5. To provide the goodness-of-fit test with independent data, Belenky *et al* (2007) used a skipping procedure, with the time interval sufficient for the autocorrelation function to decay. In this case it may be about 30 seconds, which corresponds to 60 steps. So only one point over 60 steps is included in the sample.

Figure 4.6 and Figure 4.7 show the distributions of the envelope and its derivative, respectively. The results of Pearson chi-square goodness-of-fit test were included in these figures. As it can be seen the test was passed in both cases.

The goodness-of-fit test does not reject the theoretical distributions. It means that the theory of envelope was correctly interpreted and applied in this case.

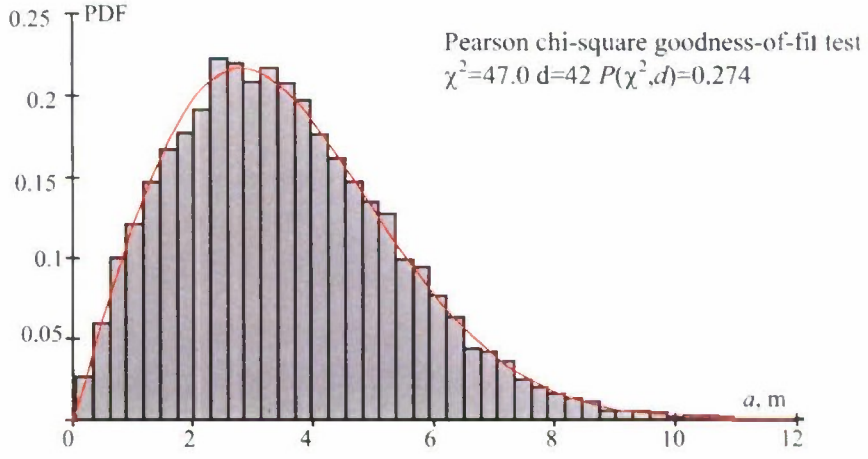

Figure 4.6 Distribution of the envelope

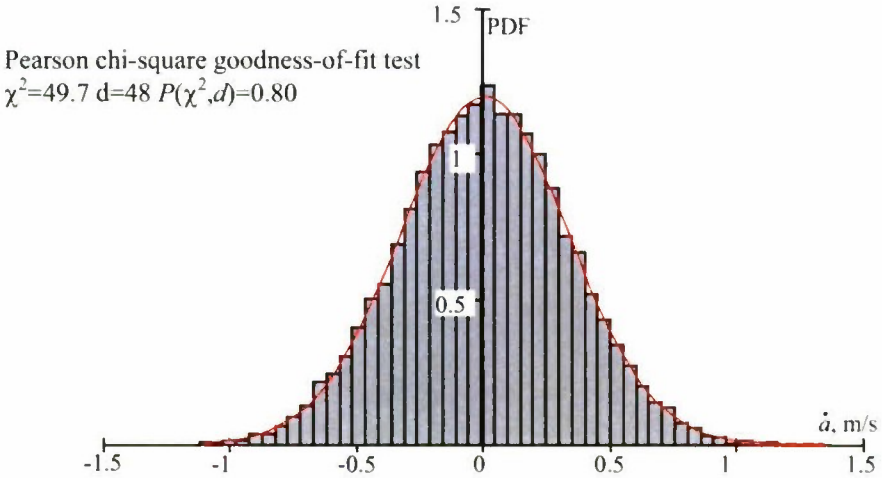

Figure 4.7 Distribution of the derivative of the envelope

4.3. Application of the Theory of Upcrossing to the Envelope

To obtain the theoretical upcrossing rate, distributions of the envelope and its derivative need to be substituted into the general formula for the upcrossing rate of a stationary process:

$$\begin{aligned}
&\lambda_e = f(a=b)\int_0^\infty \dot{a} f(\dot{a})d\dot{a} = \\
&= \frac{b}{V_x}\exp\left(-\frac{b^2}{2V_x}\right)\int_0^\infty \frac{\dot{a}}{\sqrt{2\pi V_x\left(\omega_2^2-\omega_1^2\right)}}\exp\left(-\frac{\dot{a}^2}{2V_x\left(\omega_2^2-\omega_1^2\right)}\right)d\dot{a} = \\
&= \frac{b}{V_x}\exp\left(-\frac{b^2}{2V_x}\right)\left(-\sqrt{\frac{V_x\left(\omega_2^2-\omega_1^2\right)}{2\pi}}\exp\left(-\frac{\dot{a}^2}{2V_x\left(\omega_2^2-\omega_1^2\right)}\right)\Bigg|_0^\infty\right) = \\
&= b\sqrt{\frac{\left(\omega_2^2-\omega_1^2\right)}{2\pi V_x}}\exp\left(-\frac{b^2}{2V_x}\right)
\end{aligned} \tag{4.82}$$

Here, b is the level of crossing.

Evaluation of the statistical estimate of the upcrossing rate does not differ from the procedure described in Section 1. Numerical results are shown in Figure 4.8, the theoretical value and statistical estimates agree as the theoretical value is inside of the confidence interval.

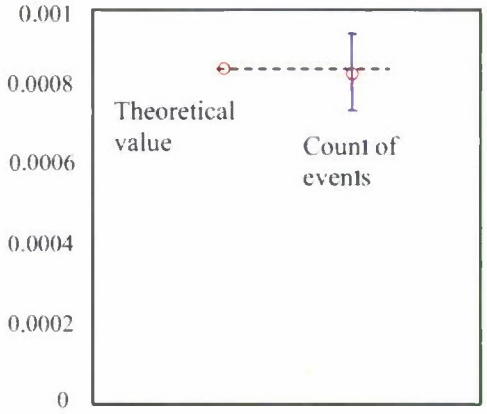

Figure 4.8 Theoretical and statistical rate of upcrossing of the envelope. Level of crossing b=9 m, total number of upcrossing is 302

Following the method developed in section 1, applieability of Poisson flow has been tested for 9 m erossing level, see Figure 4.9. As seen from this figure, the observation of uperossing of the envelope does not reject Poisson distribution. Caleulations for different levels are summarized in Table 7. As seen from this table, the uperossing of the envelope stops following the Poisson flow somewhere between the levels of 7 and 7.5 m. This is aetually higher than the process itself. As it was shown in the seetion 1, the Poisson flow lost applieability between the levels 5.25 and 5 m.

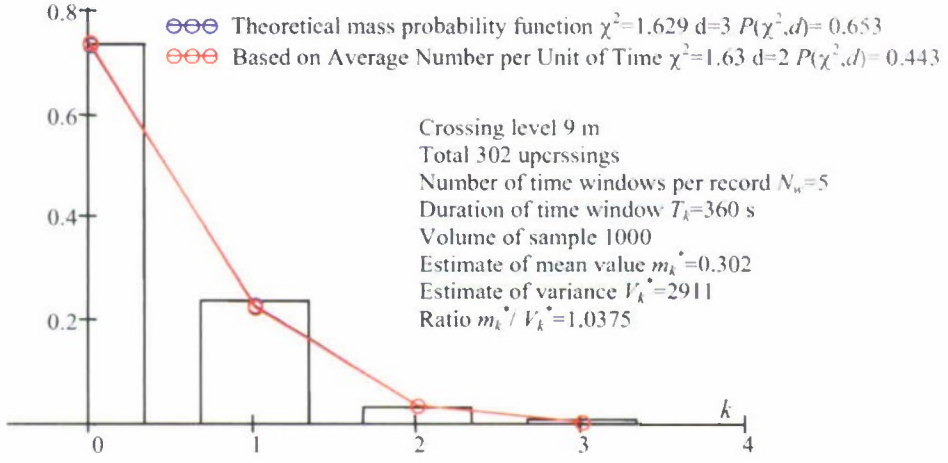

Figure 4.9. Probability mass function of number of upcrossing of the envelope during time window

Obviously using the envelope in this ease does not help with applieation of Poisson flow for the lower levels. However, the numerieal example used so far eonsidered waves derived from a Bretshneider speetrum. It is a model for fully developed waves in unrestrieted waters and the speetrum is not exaetly narrow. This situation ehanges completely when the eneounter speetrum in following or stern-quartering waves is considered. This is the eontent of the next subseetion.

Table 7. Evaluation of applicability of Poisson flow for the upcrossing by the envelope

Level, m	Number of crossings	N_w	m_k/V_k	N_{max}	Pearson chi-square test for Poisson distribution based on					
					Formula (83)			Averaged number of crossing		
					χ^2	d	$P(\chi^2,d)$	χ^2	d	$P(\chi^2,d)$
11	31	1	0.958	3	0.8147	2	0.665	0.5251	1	0.469
10	108	1	1.1	4	4.210	3	0.2396	3.239	2	0.198
9	302	5	1.0375	4	1.629	3	0.653	1.63	2	0.443
8	787	10	1.047	4	1.6636	3	0.645	1.382	2	0.501
7.5	1224	25	1.0111	4	0.6589	3	0.8828	0.301	2	0.8605
7	1799	25	1.0683	4	9.4395	3	0.024	9.0013	2	0.0111
6.75	2210	25	1.1008	4	15.4754	3	0.0015	15.8483	2	0.0004
6.5	2632	25	1.135	4	25.1708	3	1.42E-5	25.9098	2	2.36E-5
5	6121	40	1.5325	4	554.98	3	0	561.14	2	0

4.4. Effect of Speed and Wave Direction

4.4.1. Encounter Spectrum of Waves

The wave excitation acting on a ship depends on speed and wave direction, even if the consideration is limited by Fourde-Krylov forces and moments. The effect is caused by the relative motion of the wave and the ship. It is a particular case of the Doppler effect, when the frequency is increasing when the source of a signal and a recipient of a signal move towards each other and decreasing of frequency when they move away from each other. This effect is known in Naval Architecture under the term of encounter spectrum that becomes wider in the head and oblique waves and narrower in the following and stern quartering seas.

The calculation of the encounter spectrum and its effect on ship motions are described in details by Kobylinski and Kastner (2003). Calculation of the encounter spectral density s_e can be carried out using the series of formulae below:

$$\omega_e = \omega - \frac{\omega^2}{g} V_S \cos\beta \tag{4.83}$$

Here ω_e is the frequency of encounter, ω is the true wave frequency β is the wave heading angle and V_S the speed of the ship (in m/s, if S.I. is used).

$$s_e(\omega_e)=\begin{cases}\left.\begin{cases} s_{e1}(\omega_e)+s_{e2}(\omega_e)+s_{e3}(\omega_e) & if \quad \omega_e < \dfrac{g}{4V_S\cos\beta} \\ 0 \quad if \quad \omega_e \geq \dfrac{g}{4V_S\cos\beta} \end{cases}\right\} if\ \cos(\beta) > 0 \\ s_e(\omega_e)=\dfrac{s(f_1)}{1-2\dfrac{f_1}{g}V_S\cos\beta} \quad if\ \cos(\beta)\leq 0 \end{cases} \tag{4.84}$$

With the following expression for the parameters:

$$\begin{aligned} s_{e1}(\omega_e)&=\frac{s(f_1)}{1-2\dfrac{f_1}{g}V_S\cos\beta} \quad ; \quad f_1=g\frac{1-\sqrt{D(\omega_e)}}{2V_S\cos\beta} \\ s_{e2}(\omega_e)&=\frac{s(f_2)}{1-2\dfrac{f_2}{g}V_S\cos\beta} \quad ; \quad f_3=g\frac{1+\sqrt{D(\omega_e)}}{2V_S\cos\beta} \\ s_{e3}(\omega_e)&=\frac{s(f_3)}{1-2\dfrac{f_3}{g}V_S\cos\beta} \quad ; \quad f_3=g\frac{1+\sqrt{D_1(\omega_e)}}{2V_S\cos\beta} \end{aligned} \tag{4.85}$$

$$D(\omega_e)=1-4\frac{\omega_e}{g}V_S\cos\beta\,; \quad D_1(\omega_e)=1+4\frac{\omega_e}{g}V_S\cos\beta \tag{4.86}$$

Figure 4.10 shows the encounter spectrum calculation for the numerical example (see subsection 1.2.3) calculated with formulae ((4.83)-(4.86)) for pure following waves (β=0) and speed of 15 knots. The dramatic effect of speed and wave direction is very vivid.

These calculations are much simpler for the case when a spectrum is already presented in amplitude and the frequency of components; the new set of frequencies consists of absolute values of the encounter frequencies (4.83):

$$x(t)=\sum_{i=1}^{N_w} r_{Wi}\cos\left(|\omega_{ei}|t+\varphi_i\right) \tag{4.87}$$

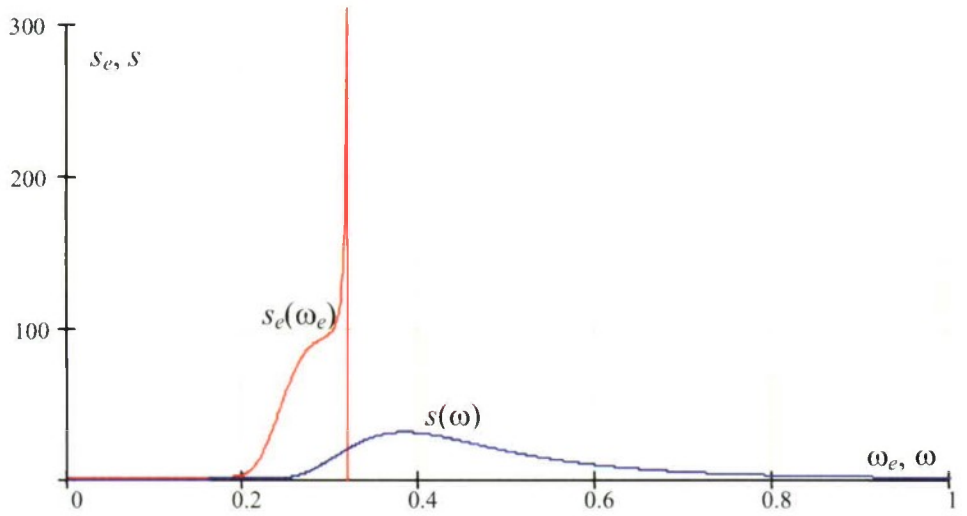

Figure 4.10 Encounter (red) and true (blue) spectra of wave for pure following waves (β=0) and speed of 15 knots

4.4.2. Time History and the Envelope

The time history of the 19th record is shown in Figure 4.11. The upper part (a) of the figure shows the original process "recorded" by a fixed "gauge". The lower part (b) is "recorded" by a "gauge" moving in pure following waves (β=0°) with a speed of 15 knots. There is a significant visual difference between these two time histories. The effect of speed and direction leads to appearance of groups or clusters. These clusters may create problems with Poisson flow. If there is one upcrossing, the next period is very likely to have one too. This breaks the requirement of the independence of these events as the autocorrelation function still has significant numbers after one period.

At the same time the autocorrelation function decays at a significantly slower pace: compare Figure 4.12 with a similar figure from section 1. The autocorrelation function in Figure 4.12 keeps some values even at the end of the record. It is a result of the "moving" gauge; there may be a component that moves with celerity very close to the "gauge",. Itmay take a very long time (up to eternity) for such a component to pass the "gauge", and therefore its influence can be felt for such long time. As a result, it is not obvious, how long it takes for the autocorrelation to die out; if such a parameter is still required, it can be set based on practical consideration such as "when the autocorrelation function peaks become less than 10%". For this example it takes 400 seconds.

Figure 4.13 shows the same record 19 along with its envelope and makes visual yet another effect of speed and direction: the envelope becomes a slowly changing process in comparison with the wave elevations even "recorded" by the moving "gauge". This effect is actually expected, as the spectrum becomes narrow- banded.

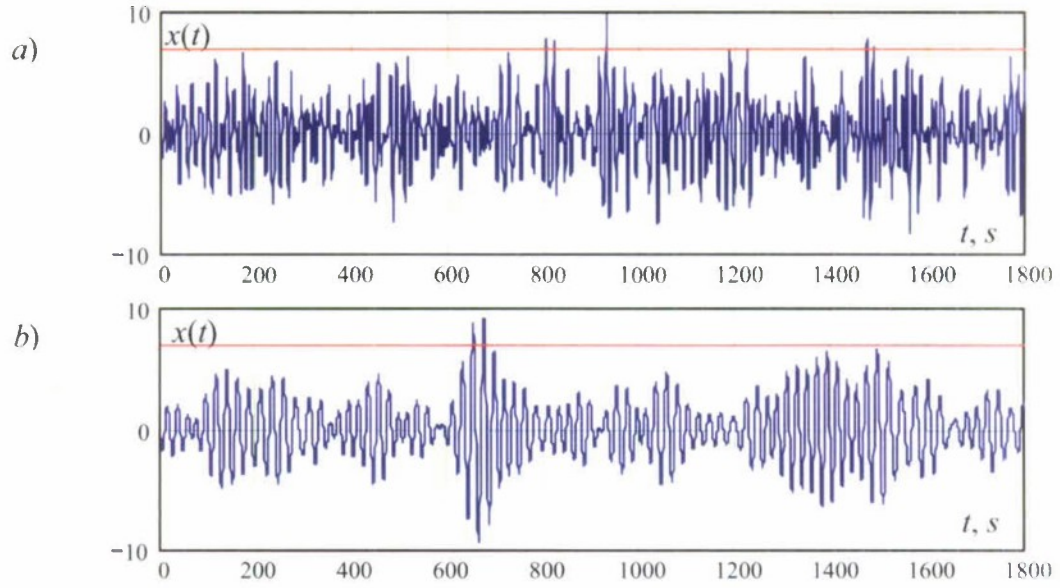

Figure 4.11 Time history of the record 19 of the numerical example wave for zero speed (a) and for pure following waves (β=0) and speed of 15 knots (b)

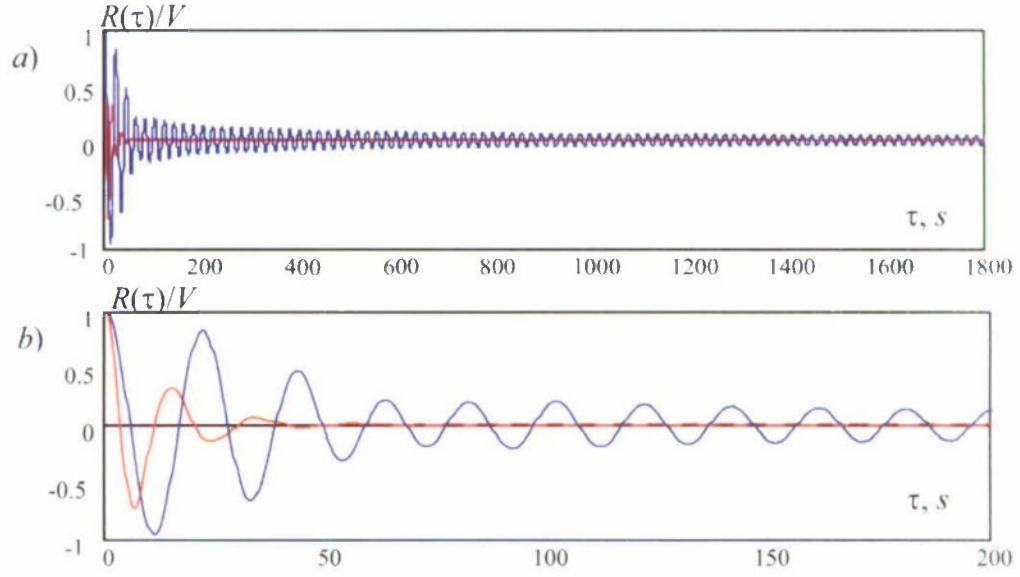

Figure 4.12 Ensemble-averaged normalized autocorrelation function, evaluated for the entire length of a record (a) and zoomed out in the first 200 seconds (b) for the process of wave elevations recorded from a "gauge" moving in following seas with the speed of 15 knots

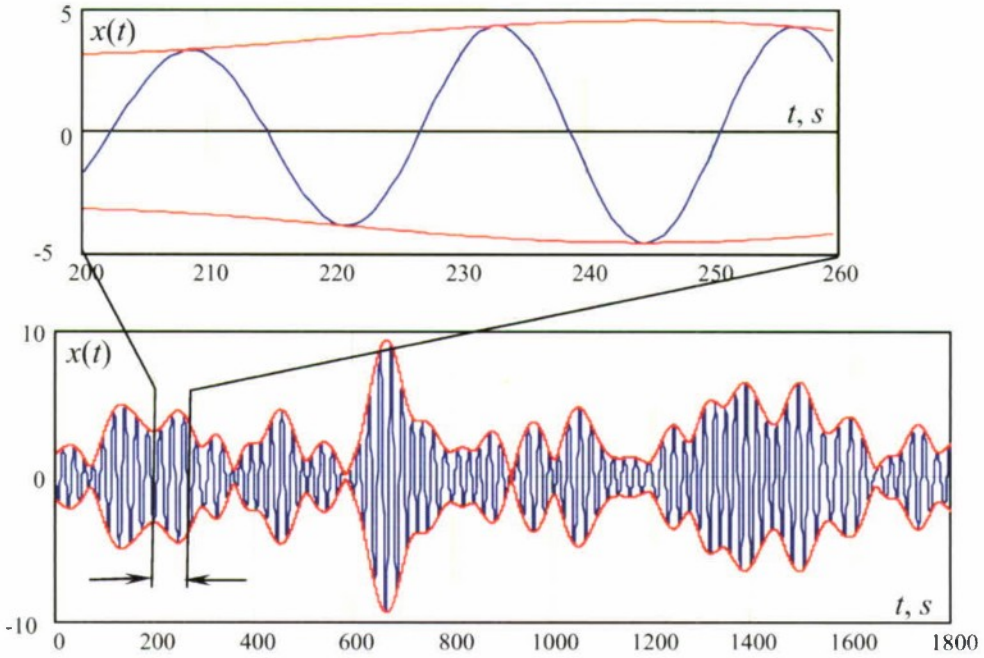

Figure 4.13 Time history of the record 19 of the numerical example wave for pure following waves (β=0) and speed of 15 knots with the envelope. The zoomed in fragment shows how the envelope becomes slowly changing process.

4.4.3. Applicability of Poisson Flow

The most dramatic effect the speed and heading is on the applicability of Poisson flow. As it was noted above, string clustering of periods leads to similar clustering of upcrossings that violates the independence requirement and renders Poisson flow inapplicable. Figure 4.14 shows distribution of the time interval between the upcrossings. As expected none of the hypotheses is supported by the data. The histogram does not resemble exponential distribution at all. The first bin is much taller than the other bins, showing that the distribution is dominated by the time interval close to the mean encounter period (22 s). These calculations were done for the crossing level of 7.5 m where without the influence of speed and heading, the applicability of the Poisson flow did not raise any doubts, see Figure 1.21.

The direct test of the applicability of Poisson flow (Figure 4.15) also rejects the hypothesis. This distribution is also dominated by the first bin, corresponding to zero number of upcrossing during the time window. The height of the second bin is almost equal to the third and the fourth. It means that the number of cases when one, two, or three crossings are almost equal. In the case of Poisson distribution they are expected to decrease with the number of crossings.

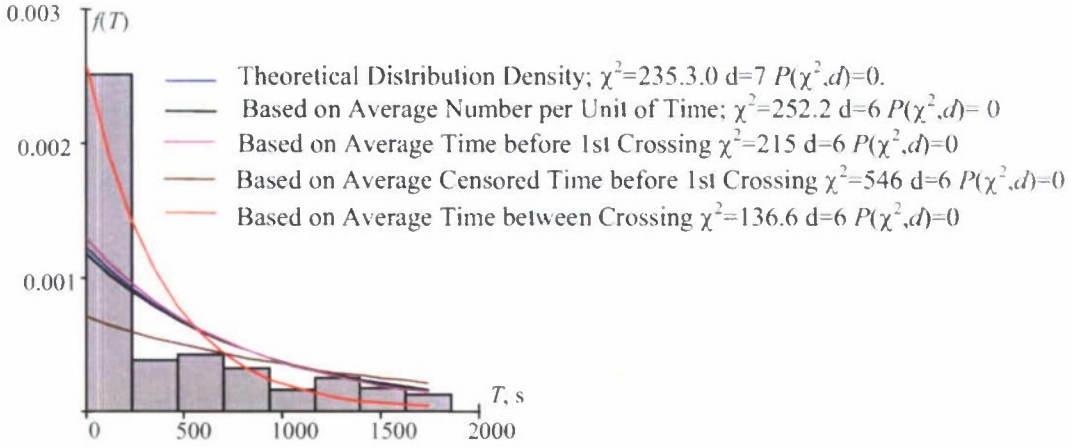

Figure 4.14 Distribution of time intervals between upcrossing for pure following waves speed 15 knots, level of crossing 7.5 m

These calculations were carried out systematically for the crossing level ranging from 11 m down to 5.5 m and compared with the similar calculation for the envelope. The results are summarized in Table 8. There was no level where the Poisson flow could be applied to the process of wave elevations recorded from a "gauge" moving in the following seas with the speed of 15 knots.

At the same time, applicability of the Poisson flow to the envelope is easily achievable and it is good all the way until the level between 6.25 and 6.5 m. This is very close to the result obtained in section 1 for the wave elevation "recorded" by a fixed "gauge". Therefore the envelope can be used for detecting upcrossing events when the spectrum is narrow and Poisson flow cannot be applied directly to the process.

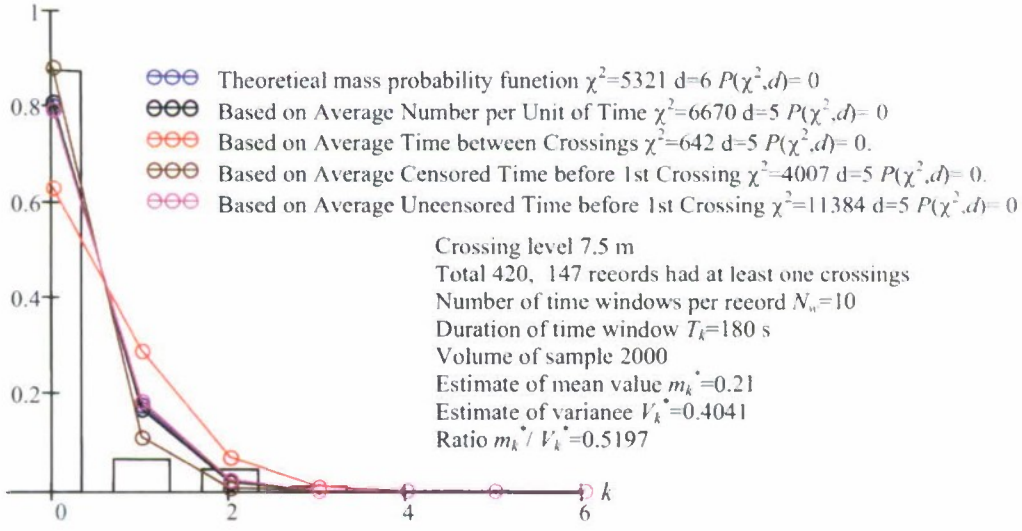

Figure 4.15 Probability mass function of number of upcrossing during time window for pure following waves speed 15 knots

Table 8. Applicability of Poisson flow for the case of following waves with 15 knots: the process vs. its envelope

level	Wave elevations						The envelope					
	Number of crossings	N_w	m_k/V_k	N_{max}	Pearson chi-square test		Number of crossings	N_w	m_k/V_k	N_{max}	Pearson chi-square test	
					χ^2	$P(\chi^2,d)$					χ^2	$P(\chi^2,d)$
11	6	1	0.6	3	34.23	3.6879E-8	5	1	1.02	2	0.256	0.8798
10	24	1	0.61	3	49.49	1.795E-11	16	1	1.82	2	1.721	0.4231
9	75	1	0.56	5	56.76	1.386E-11	55	1	1.097	3	2.218	0.6958
8	247	3	0.469	7	611.89	0	168	1	1.1538	5	1.997	0.92
7.5	420	3	0.45	7	695.41	0	262	2	1.0522	5	1.418	0.9647
7	683	10	0.488	7	4155.1	0	373	3	1.079	5	3.794	0.7045
6.75	854	10	0.4902	7	3879.0	0	459	4	1.119	5	5.540	0.4766
6.5	1044	10	0.4874	7	2447.3	0	542	4	1.131	5	6.214	0.3997
6.25	1296	15	0.539	7	1227.4	0	647	4	1.1463	5	7.445	0.2817
6	1571	15	0.5305	7	1220.0	0	740	4	1.19	5	13.32	0.0383
5.75	1894	15	0.5312	7	1221.7	0	862	4	1.368	5	36.978	1.7781E-6
5.5	2284	15	0.5407	7	1121.9	0	992	4	1.432	5	43.539	9.1214E-8

4.5. The Envelope Based on Peaks

4.5.1. Appearance and Distribution for Zero-Speed Case

As it was shown earlier in this section, the peaks of the envelope do not necessarily correspond to the peak of the real process. It can be seen in Figure 4.2 and Figure 4.3. Thus the effect is much less pronounced when the spectrum is narrow like in the case of waves "recorded" by a "gauge" moving in the same direction (pure following waves) with the speed of 15 knots, see Figure 4.13.

Consider an approximation for the envelope that does not produce artificial peaks; each upcrossing of the level then must correspond to at least on upcrossing by the process itself. Such an approximation can be achieved by a piecewise linear function using absolute values of peaks of the process as nodes. Figure 4.16 shows this approximation along with the true envelope, with a zoomed in picture shown in Figure 4.17. As it can be seen from Figure 4.17, the true envelope oscillates about piecewise linear approximation.

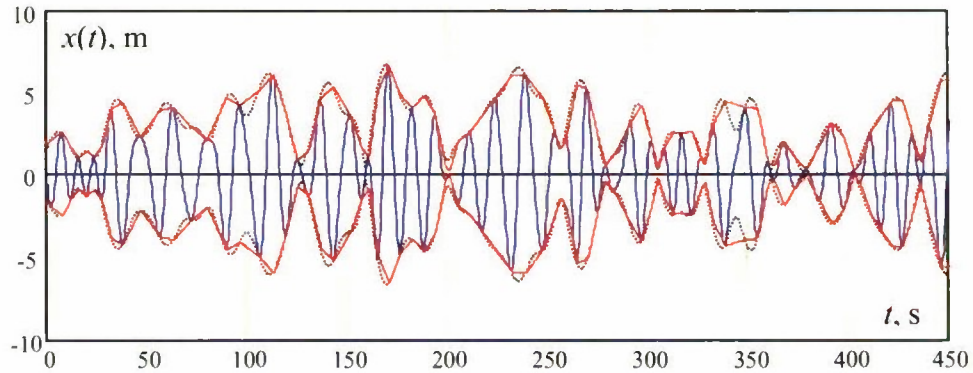

Figure 4.16 Peak-based or piece linear approximation of the envelope; shown for the record # 19; true envelope is shown with the dotted line. The wave is "recorder" from a fixed point.

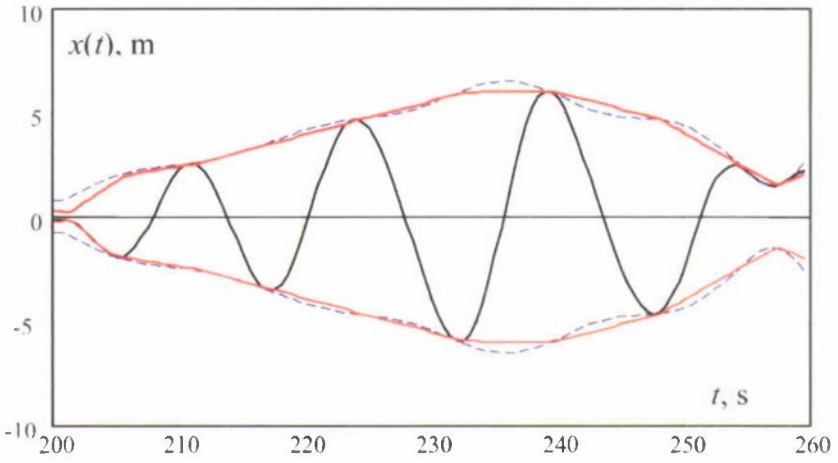

Figure 4.17. Zoomed in peak-based or piece linear approximation of the envelope; shown for the record # 19; true envelope is shown with the dashed line. The wave is "recorder" from a fixed point

Distribution of the peak-based envelope is shown in Figure 4.18. The current value of the peak-based envelope is calculated linearly between the nodes. Comparing the histogram with the theoretical Rayleigh distribution, one can find visual similarity. However, the Pearson chi-square goodness of fit test does not support this hypothesis. Numerical disruptions caused by linear interpolation seem to be statistically significant in this case.

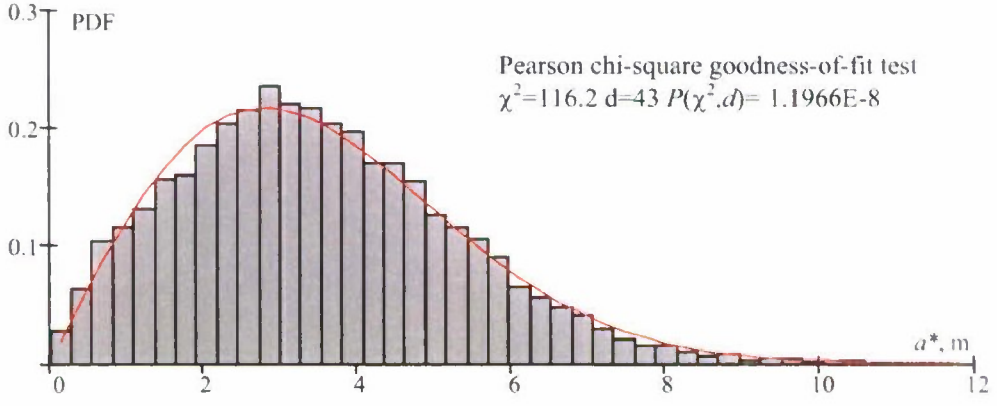

Figure 4.18 Distribution of the peak-based envelope for the zero-speed case. Skip 30 seconds

Calculation of the distribution of the derivatives was carried out as follows. The cubic spline with free ends was fit to run through the peaks of the process (Forsythe, *et al* 1977):

$$y = y_i + b_i(x - x_i) + c_i(x - x_i)^2 + d_i(x - x_i)^3 \tag{4.88}$$

Here $(x_i\, y_i)$ are coordinates of the nodes, b_i, c_i, d_i are spline coefficients. Once the spline was fitted, the derivative can be expressed as:

$$y' = b_i + 2c_i(x - x_i) + 3d_i(x - x_i)^2 \tag{4.89}$$

The values of the derivative in each node simply are:

$$y_i' = b_i \tag{4.90}$$

The values of the derivative outside of the nodes were calculated with linear interpolation at each time step. The distribution of the derivatives of the peak-based envelope is shown in Figure 4.19. Theoretical distribution (4.78) is not supported by the Pearson chi-square goodness of fit test. Visually, however, the distribution seems to be normal but would be characterized by significantly less variance.

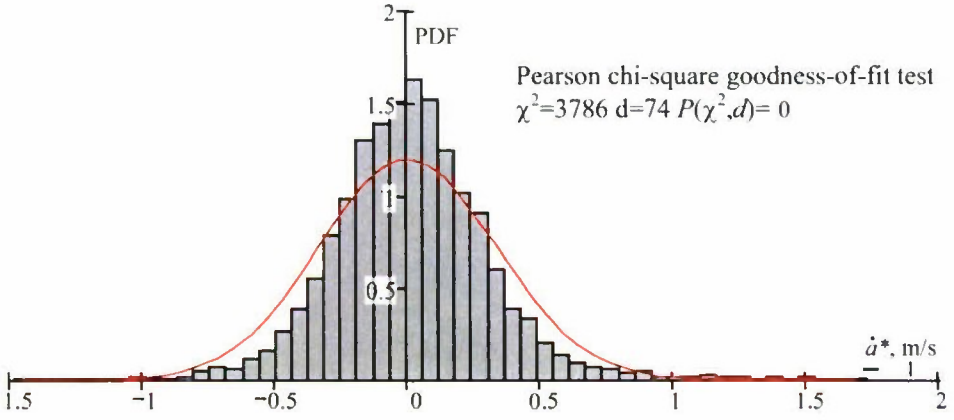

Figure 4.19 Distribution of the derivatives peak-based envelope for the zero-speed case. Skip 30 seconds

Piecewise linear approximation of the envelope further refereed as a peak-based envelope allows us to avoid artificial peaks that could be found in the true envelope. Every peak of this approximated envelope corresponds to the uperossing of the level by the original process. However, in the case of zero-speed, the numerical disruptions introduced by the approximation lead to a deviation of the distribution of the peak-based envelope and its derivative from the theoretical PDFs.

4.5.2. Appearance and Distribution the Peak-Based Envelope for Narrow Spectrum

For the process of encounter waves described by the spectrum in Figure 4.10, the appearance of the peak-based envelope is shown in Figure 4.20. The peak-base envelope

becomes visually indistinguishable from the true envelope. The zoomed-in image in Figure 4.21 still shows a very small difference between the two envelopes. Actually this is an expected result. Once the spectrum is narrow, the envelope becomes a slowly changing curve in comparison with the original process. Curvature of the true envelope decreases, therefore accuracy of its approximation with the broken line increases. Figure 4.22 and Figure 4.23 show the distribution of the values of the peak-based envelope and its derivative. Both figures were calculated in the same way as in the previous case with zero-speed. Skip time was 140 seconds as the autocorrelation in following waves dies out slower (see Figure 4.12). As it could be expected both histogram support theoretical distributions.

As it has been seen from the above considerations the peak-based envelope represents a much better approximation for the case of the narrow spectrum in comparison with the case of zero-speed.

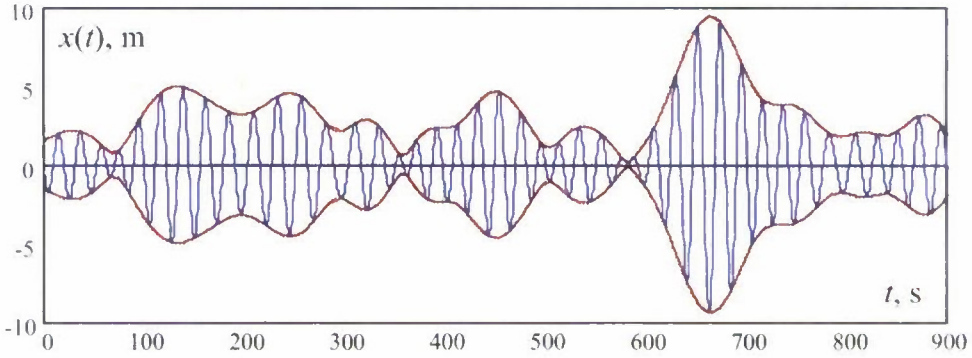

Figure 4.20 Peak-based or piece linear approximation of the envelope; shown for the record # 19; true envelope is shown with the dotted line. The wave is "recorded" by the "gauge" moving with the waves (pure following seas) with the speed 15 knots

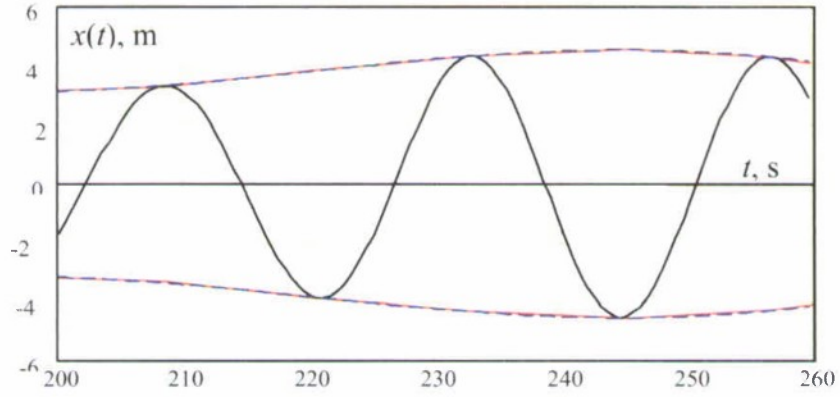

Figure 4.21 Zoomed in peak-based or piece linear approximation of the envelope; shown for the record # 19; true envelope is shown with the dashed line. The wave is "recorded" by the "gauge" moving with the waves (pure following seas) with the speed 15 knots

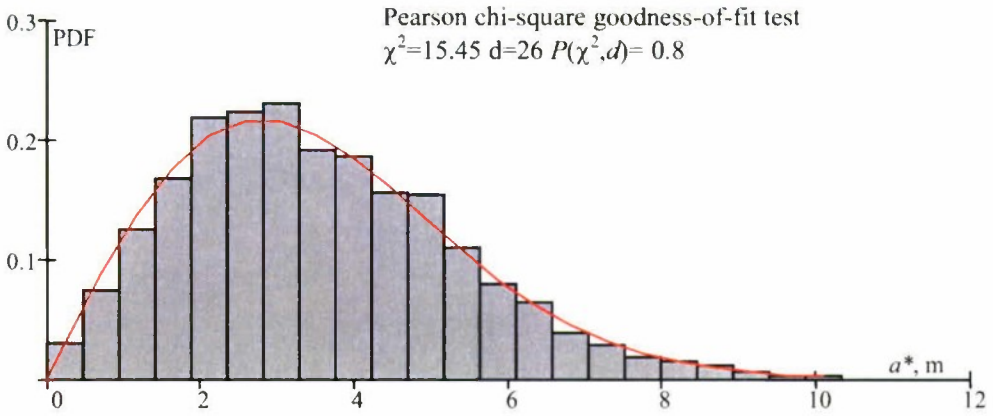

Figure 4.22 Distribution of the peak-based envelope for the following wave case and speed of 15 knots; skip 140 seconds

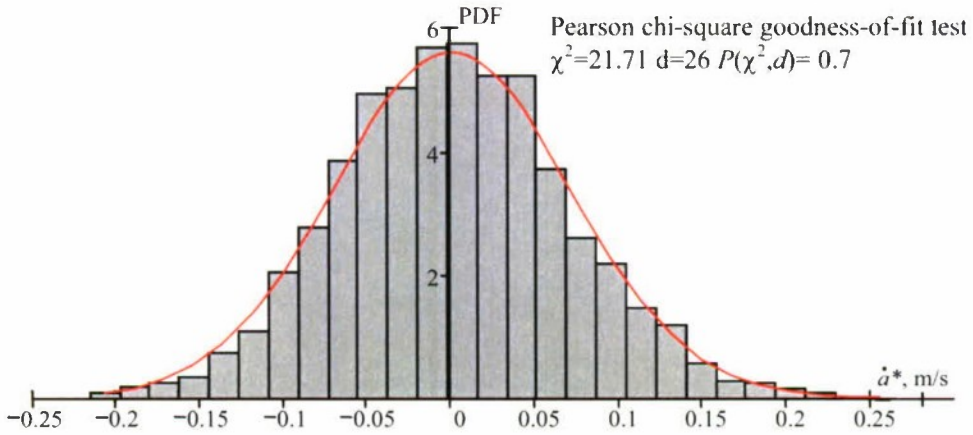

Figure 4.23 Distribution of the derivative of the peak-based envelope for the following wave case and speed of 15 knots; skip 140 seconds

4.5.3. Upcrossings of Peak-Based Envelope

Statistical estimates for the rate of upcrossings of the peak-based envelope are shown in Figure 4.24 for both zero-speed (a) and the following wave cases (b). The confidence interval for the estimates was evaluated assuming binomial distribution (see subsection 1.2.2). For the zero-speed case, the estimate of the upcrossing rate does not contain theoretical values inside the confidence interval. Similar to the results with distributions (see Figure 4.18 and Figure 4.19), numerical disturbances introduced by the linear interpolation caused the observed difference. Following the same tendency, upcrossing rates of the true envelope and peak-based envelope for the following wave, 15-knots case are statistically identical.

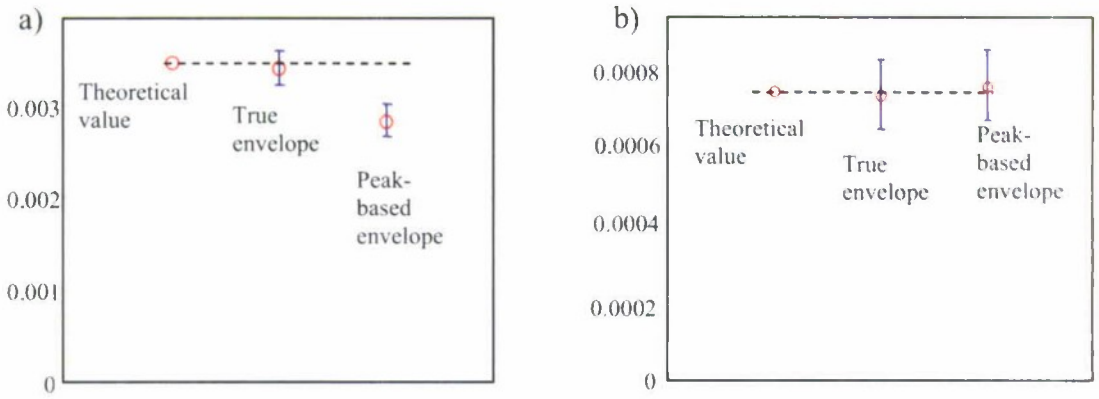

Figure 4.24 Theoretical and statistical rate of upcrossings of the true and peak-based envelopes. Level of crossing b=7.5 m, zero speed case (a); following waves with speed 15 knots (b)

Significant statistical difference between the theoretical upcrossing rate of the true envelope and statistical estimate of the upcrossing rate of the peak-based envelope also reflect the statistical significance of the artificial peaks of a true envelope.

Nevertheless, these numerical disturbances did not much affect the Poisson character of upcrossings. The distribution of the number of upcrossings during a given time window remains Poisson for both considered cases of upcrossing of the peak-based envelope, see Figure 4.25.

Table 9 contains results of calculations for systematically changing the crossing level to see where applicability of Poisson flow breaks down for the peak-based envelope. These calculations were carried out for both cases: zero-speed and following waves / 15 knots (narrow spectrum). Histograms were compared with the probability mass function calculated with the statistical rate of upcrossing, as the theoretical distribution is no longer applicable for the zero-speed case. Using the level of significance of 0.05, one can see that the boundary of applicability of Poisson flow lays somewhere between 7 and 7.5 m for the zero-speed case and between 6 and 6.25 m for the following wave case. These number are essentially are the same for the true envelope, see Table 7 for the zero-speed case and Table 8 for following wave case. Thick lines are used in these tables to show the boundary applicability.

Comparing the number of upcrossings for the true and peak-based envelope, the significant difference existing for the zero-speed case could be expected, as numerical discrepancies were significant enough to change the distribution. The difference in the number of upcrossings for the following sea case is much less, but the numbers are not identical, despite that there were no visual differences in the appearance of peak-based and true envelope for the following sea case.

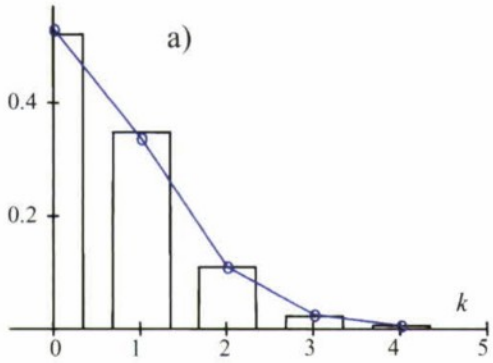

Total 1019 crossings
Number of time windows per record N_w=8
Duration of time window T_k=225 s
Volume of sample 1600
Estimate of mean value m_k^*=0.6369
Estimate of variance V_k^*=0.6029
Ratio m_k^*/V_k^*=1.0564
χ^2=1.87 d=3 $P(\chi^2,d)$= 0.6

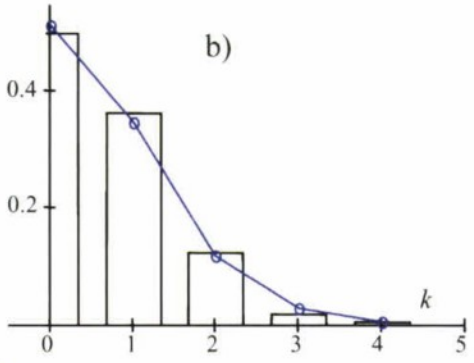

Total 271 crossings
Number of time windows per record N_w=2
Duration of time window T_k=900 s
Volume of sample 400
Estimate of mean value m_k^*=0.6775
Estimate of variance V_k^*=0.6775
Ratio m_k^*/V_k^*=1.0753
χ^2=1.76 d=3 $P(\chi^2,d)$= 0.625

Figure 4.25 Probability mass function of number of upcrossing during time window of the peak-based envelope for zero speed case (a) and pure following waves speed 15 knots (b); crossing level 7.5 m

Table 9. Applicability of Poisson flow for upcrossing of peak-based envelope

level	Zero-speed case						Following waves 15 knots					
	Number of crossings	N_w	m_k/V_k	N_{max}	Pearson chi-square test		Number of crossings	N_w	m_k/V_k	N_{max}	Pearson chi-square test	
					χ^2	$P(\chi^2,d)$					χ^2	$P(\chi^2,d)$
11	20	1	1.05	2	0.21	-	5	1	1.021	2	3.1E-3	-
10	83	1	1.079	4	1.89	0.39	16	1	1.082	2	0.1	-
9	243	4	1.059	4	2.41	0.30	53	1	1.077	3	0.18	0.6749
8	620	8	1.073	4	2.85	0.245	170	2	1.036	4	1.0356	0.7209
7.5	1019	8	1.056	5	1.87	0.60	271	2	1.075	5	1.76	0.6247
7	1520	8	1.2	5	19.93	0.0002	387	4	1.11	5	5.89	0.1172
6.75	1841	20	1.11	5	19.13	0.0003	463	4	1.125	5	6.78	0.0791
6.5	2217	20	1.15	5	32.98	3.2547E-7	550	4	1.126	5	4.71	0.1946
6.25	2695	20	1.196	5	54.82	7.504E-12	659	4	1.159	5	6.54	0.0882
6	3131	20	1.2621	5	92.78	0	750	4	1.199	5	10.3	0.0162
5.75	3655	25	1.348	5	189.78	0	873	4	1.401	5	38.37	2.3558E-8
5.5	4183	25	1.4093	5	243.0	0	1014	5	1.403	5	44.03	1.4892E-9

4.6.Summary

Envelope theory describes the presentation of a stationary stochastic process via two other stationary stochastic processes: the amplitude and phase of the envelope. Most of the theoretical results of envelope theory are applicable only for a normal process; however some principles of envelope theory can be used for the stationary process with any type of distribution.

The envelope contains the absolute values of all of the peaks of the original process. The peaks of the envelope, however, do not necessarily belong to the original process (artificial peaks).

A portion of envelope theory was reviewed here, including the marginal distributions of amplitude (Rayleigh) and phase (uniform distribution), the autocorrelation function of the envelope, and the distribution of the derivative of the envelope (normal). Numerical examples demonstrated successful reproduction of the theoretical results.

Treating the envelope as a stationary process allows the application of the upcrossing theory. It is possible to obtain the closed-form solution for the upcrossing rate of the envelope if the original process is normal. This result was verified numerically.

Upcrossings of the envelope follow Poisson flow, if the crossing level is high enough and upcrossings can be treated as independent random events.

The spectral bandwidth of the process has a significant influence on the envelope. If the spectrum is narrow, the envelope becomes a slowly changing function in comparison with the original process. It was demonstrated with another numerical example of encountered waves; the wave elevations were virtually "recorded" by a "wave probe" moving in the same direction as the waves (pure following seas) with a speed of 15 knots.

It was shown that for the encountered waves Poisson flow is no longer applicable. Due to significant clustering or grouping, all of the upcrossings become dependent on each other.

A piecewise linear approximation of the envelope was considered (the peak-based envelope). The approximation contains only actual peaks of the process and all other points are calculated by linear interpolation between peaks.

Numerical discrepancies introduced by such approximations lead to the inapplicability of the theoretical solution for the distribution and upcrossing rates for the envelope in the original wave example (zero-speed case). However, all theoretical results were applicable for the following wave, 15-knots case.

The applicability of Poison flow was not affected by the approximation.

This is page intentially left balnk

5. Envelope Peaks over the Threshold

This section describes a method of statistical extrapolation using probabilistic properties of the peaks of the envelope exceeding a given threshold.

5.1. Both-Sides Crossings

5.1.1. Large Roll Event as Both-Sides Crossing

Partial stability failure in the form of large roll event is equally dangerous on either side of a ship. Therefore, a random event of upcrossing is not yet a complete model of partial stability failure. A complete model of the partial stability failure should include both upcrossing of a specified level on the positive side and downcrossing of the specified level on the negative side. This random event can be written as:

$$X = ((\phi(t) < a) \cap (\phi(t+dt) \geq a)) \cup ((\phi(t) > b) \cap (\phi(t+dt) \leq b)) \tag{5.1}$$

Here, X is a random event associated with partial stability failure; a is a positive level of exceedance and b is negative level of exceedance. Obviously, if the mean value of roll is zero then requirements are the same for the both sides:

$$if\,(m(\phi) = 0) \Rightarrow a = -b \tag{5.2}$$

Consider a probability of both-sides crossing in a particular instant of time t. As it is known from upcrossing theory (and has been demonstrated earlier in this report) this probability is infinitely small:

$$dP(X) = P(((\phi(t) < a) \cap (\phi(t+dt) \geq a)) \cup ((\phi(t) > b) \cap (\phi(t+dt) \leq b))) \tag{5.3}$$

The roll process is single-valued (has only one value at the same instant of time), therefore it cannot cross two distinct levels simultaneously and the events of upcrossing of the level a and downcrossing the level b at the time instant t are incompatible:

$$P(((\phi(t) < a) \cap (\phi(t+dt) \geq a)) \cap ((\phi(t) > b) \cap (\phi(t+dt) \leq b))) = 0 \tag{5.4}$$

Therefore:

$$dP(X) = P((\phi(t) < a) \cap (\phi(t+dt) \geq a)) + P((\phi(t) > b) \cap (\phi(t+dt) \leq b)) \tag{5.5}$$

Since dt is an infinitely small increment, equation (5.5) can be presented as (value at the instant t is assumed and the symbol (t) is dropped):

$$dP(X) = P\left(\left(\phi < a\right) \cap \left(\phi + \dot{\phi}dt \geq a\right)\right) + P\left(\left(\phi > b\right) \cap \left(\phi + \dot{\phi}dt \leq b\right)\right) = \\ = P\left(\left(\phi < a\right) \cap \left(\phi \geq a - \dot{\phi}dt\right)\right) + P\left(\left(\phi > b\right) \cap \left(\phi \leq b - \dot{\phi}dt\right)\right) \tag{5.6}$$

It is obvious that upcrossing occurs with positive roll rate and the downcrossing with the negative roll rate:

$$dP(X) = P\left(\left(\phi < a\right) \cap \left(\phi \geq a - \dot{\phi}dt\right) \cap \left(\dot{\phi} > 0\right)\right) + \\ + P\left(\left(\phi > b\right) \cap \left(\phi \leq b - \dot{\phi}dt\right) \cap \left(\dot{\phi} < 0\right)\right) \tag{5.7}$$

If the joint distribution of roll and roll rate $f(\phi, \dot{\phi})$ is known, the probability can be expressed as:

$$dP(X) = \int_{a-\dot{\phi}dt}^{a} \int_{0}^{\infty} f(\phi, \dot{\phi}) d\dot{\phi} d\phi + \int_{b}^{b-\dot{\phi}dt} \int_{-\infty}^{0} f(\phi, \dot{\phi}) d\dot{\phi} d\phi \tag{5.8}$$

Both external integrals in the equation (5.8) have limits that are infinitely close to each other. Then application of the mean value theorem (for integration) yields the following:

$$dP(X) = dt \int_{0}^{\infty} f(a, \dot{\phi}) \dot{\phi} d\dot{\phi} - dt \int_{-\infty}^{0} f(b, \dot{\phi}) \dot{\phi} d\dot{\phi} \tag{5.9}$$

Assuming that the roll motion is a stationary process leads to independence of the process value and its first derivatives:

$$f(\phi, \dot{\phi}) = f(\phi) f(\dot{\phi}) \tag{5.10}$$

This circumstance allows rewriting the equation (5.9) as:

$$dP(X) = dt \left(f(a) \int_{0}^{\infty} f(\dot{\phi}) \dot{\phi} d\dot{\phi} - f(b) \int_{-\infty}^{0} f(\dot{\phi}) \dot{\phi} d\dot{\phi} \right) \tag{5.11}$$

The expression in parenthesis is finite and represents a rate of the random event of both-sides crossing:

$$dP(X) = \lambda_{ab} dt \\ \lambda_{ab} = f(a) \int_{0}^{\infty} f(\dot{\phi}) \dot{\phi} d\dot{\phi} - f(b) \int_{-\infty}^{0} f(\dot{\phi}) \dot{\phi} d\dot{\phi} \tag{5.12}$$

Compared with formula (1.19), it is easy to see that the first component is actually a rate of upcrossing through the level a. It can be shown the second component represents the rate of downcrossings:

$$\lambda_a = f(a)\int_0^{\infty} f(\dot{\phi})\dot{\phi}d\dot{\phi}$$
$$\lambda_b = -f(b)\int_{-\infty}^{0} f(\dot{\phi})\dot{\phi}d\dot{\phi} \tag{5.13}$$

The rate of downcrossing is actually always positive as the value of the integral is negative.

If the distribution of the roll rate is symmetric, the integrals in (5.13) have the same absolute value, but different signs:

$$\lambda_a = f(a)\int_0^{\infty} f(\dot{\phi})\dot{\phi}d\dot{\phi};\quad \lambda_b = f(b)\int_0^{\infty} f(\dot{\phi})\dot{\phi}d\dot{\phi} \quad if \quad f(\dot{\phi}) = f(-\dot{\phi}) \tag{5.14}$$

Finally if the roll process has zero mean, its distribution is symmetric and for $b = -a$:

$$\lambda_{ab} = 2\lambda_a = 2\lambda_b = 2f(a)\int_0^{\infty} f(\dot{\phi})\dot{\phi}d\dot{\phi} \quad if \quad b = -a \quad \cap \quad f(\dot{\phi}) = f(-\dot{\phi}) \tag{5.15}$$

In partieular, for the generie normal process $x(t)$:

$$\lambda_{ab} = \frac{1}{\pi}\sqrt{\frac{V_{\dot{x}}}{V_x}}\exp\left(-\frac{a^2}{2V_x}\right) \tag{5.16}$$

Statistieal estimates of the both-sides crossing can be obtained as averaged number of erossing of both sides per unit of time:

$$\lambda^*_{ab} = \frac{m^*_U + m^*_D}{T_R} \tag{5.17}$$

Here m^*_U is an estimate of the mean value of the number of upcrossings through the level a and m^*_D is an estimate of the mean value of the number of downcrossings through the level b, T_R is the duration of the record.

5.1.2. Confidence Interval for Both-Sides Crossings

Following the same steps as in the case of upcrossings, consider a sample of stoehastie process x, presented in a form of an ensemble of N_R records. Each reeord is represented by a time history of N_{PT} points with the time step Δt, totalling $n = N_{PT}$-1 time steps. Then the event of both-sides upcrossing of the level a can be assoeiated with a random variable D defined for eaeh time step as follows (see Figure 5.1):

$$D_{i,j} = \begin{cases} 1 & |x_{i,j}| \le a \cap |x_{i+1,j}| > a \\ 0 & Otherwize \end{cases} \qquad i = 1,..,n; \quad j = 1,...,N_R \tag{5.18}$$

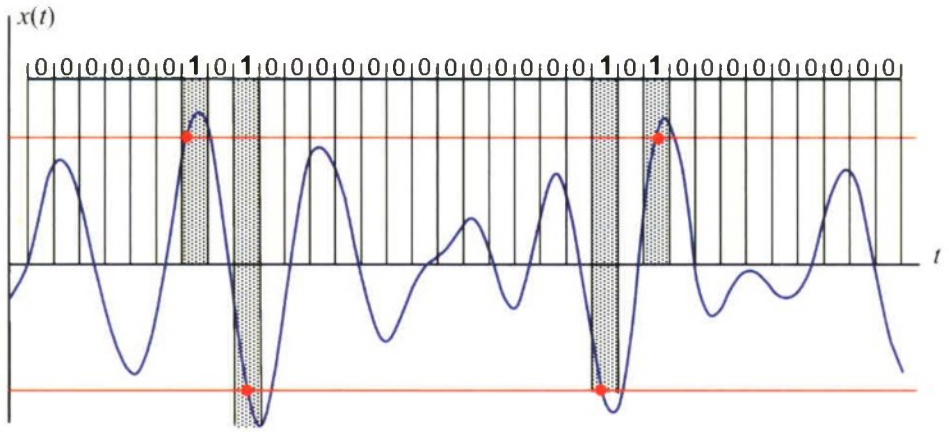

Figure 5.1 Auxiliary random variable for both-side crossing

Total number of both-sides crossings:

$$N_D = \sum_{i=1}^{n} \sum_{j=1}^{N_R} D_{i,j} \tag{5.19}$$

Estimate of probability that a both-sides crossing will occur at any given instance of time:

$$p_D^* = \frac{N_D}{nN_R} = \frac{1}{nN_R} \sum_{i=1}^{n} \sum_{j=1}^{N_R} D_{i,j} \tag{5.20}$$

Mean number of both-sides crossing per record:

$$m_D^* = \frac{N_D}{N_R} = \frac{1}{N_R} \sum_{i=1}^{n} \sum_{j=1}^{N_R} D_{i,j} \tag{5.21}$$

Estimate of rate of both-sides crossing also can be expressed through the characteristics of an auxiliary variable:

$$\lambda_{ab}^* = \frac{m_D^*}{n\Delta t} = \frac{1}{nN_R\Delta t} \sum_{i=1}^{n} \sum_{j=1}^{N_R} D_{i,j} \tag{5.22}$$

Evaluation of the confidence interval for the estimate of the rate of both-sides crossing encounters certain methodological difficulties. The method of evaluation of the confidence interval, described in the Section 1, was based on the binomial distribution of

the auxiliary variable. The binomial distribution assumes Bernoulli trials, which implies the independenee of the conseeutive events. If the level is high enough, the uperossings are independent events; as a result of that, the time between them has an exponential distribution and the number of these uperossings during a finite duration of time has Poisson distribution. Conseeutive both-sides erossings ean be as elose to each other as a half a period. This is not enough time for the autoeorrelation funetion to die out, therefore the neighbor both-sides erossings may be dependent.

On the other hand, if time is fixed, all of the events are independent as the records are independent. In this ease, eonditions of Bernoulli trials are satisfied and the distribution of the auxiliary variable is binomial. The independenee of the event in the time seetion, however does not neeessarily lead to the exponential distribution of time between events or Poisson distribution of a number of events during fixed time, as these figures require temporal eonsideration and do not exist in the time seetion.

Binomial distribution depends on the probability of the event oeeurring at a partieular instant of time estimated by formula (5.20). Averaging over the time seetion (averaging over all the reeords at the given instant of time) and temporal averaging both are present here. This allows for mitigating possible errors in the evaluation of the eonfidenee interval. Further evaluation was done in a similar way as deseribes in the seetion 1.

Figure 5.2 shows this estimate ealeulated for the numerical example. The erossing level is ±9 m; as the proeess used in the example has zero mean and normal distribution (wave elevations), formula (5.16) was used for the theoretieal value. As it is elearly seen from this figure the theoretieal value is ineluded in the eonfidenee interval of the estimate. Therefore, the derivations above, and the formula (5.16) in partieular, are not rejeeted by the numerieal example.

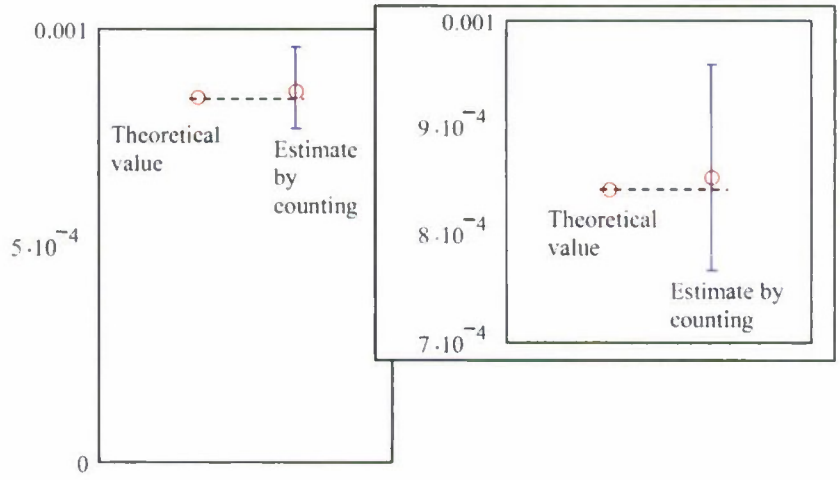

Figure 5.2 Both-sides crossing rate: theoretical value and statistical estimate by counting. Crossing level ±9 m

5.1.3. Applicability of Poisson Flow to Both-Sides Crossing

Theoretical derivation and statistical estimation of rate of both-sides crossing was very similar to upcrossing. However the random event of both-sides crossing hardly can be expected to follow the Poisson flow because crossing of one side may be too close in time to the crossing of the other side for the independence condition to appy.

This can be very clearly seen from the numerical example considered through and this report. As it was shown in the Section 1, the Poisson flow becomes applicable to the upcrossing event when the level of crossing exceeded a value between 5.25 and 5.5 m while the autocorrelation function could be considered to have died out after about 40-45 seconds. The mean time between crossings was somewhere between 75 and 89 seconds; this provided enough separation between events to consider them independent.

For the both-sides crossing, time between crossing one side or another can be as small as a half of zero-crossing period. For the considered example it is only about 5.8 seconds, which is obviously not enough to ensure independence. However, it is possible that applicability of Poisson flow may be preserved for the very high levels, where a statistically significant number of cases with only one-side crossing can exist.

To check the hypothesis above, a series of calculations for systematically changed levels was performed for the considered numerical example. Using the method described in the subsection 1.3.5 and keeping the maximum number of crossings per windows around 7-9 (if possible), the boundary of applicability was determined to be between 10 and 10.5 m, see Table 10.

Table 10. Test on applicability of Poisson flow for both-sides crossings

Level ±, m	Number of crossings	N_w	m_k/V_k	N_{max}	Pearson chi-square test for Poisson distribution based on					
					Formula (5.16)			Averaged number of crossings		
					χ^2	d	$P(\chi^2,d)$	χ^2	d	$P(\chi^2,d)$
12	3	1	1.01	2	0.9491	1	0.33	0.0007	0	-
11.5	9	1	1.04	3	0.5928	2	0.74	0.212	1	0.6452
11.0	22	1	0.93	3	0.9024	2	0.64	0.92	1	0.3359
10.5	54	1	0.85	4	7.0184	3	0.07	4.38	2	0.1119
10.0	101	1	0.76	5	38.895	4	7.3E-8	25.062	3	1.50E-5
9.5	179	2	0.77	6	51.8343	5	5.8E-10	40.66	4	3.16E-8
9.0	307	2	0.73	6	30.142	5	1.38E-5	28.99	4	7.85E-6
8.5	517	2	0.87	7	13.4984	6	0.0358	13.6851	5	0.0177
8.0	860	4	0.75	7	65.106	6	4.10E-12	67.867	5	2.85E-13
7.5	1441	12	0.65	7	370.7	6	0	391.1	5	0
7	2266	18	0.66	8	505.2	7	0	542.1	6	0
6.5	3514	36	0.65	7	1011	6	0	1068	5	0
6.0	5354	36	0.66	7	1015	6	0	1031	5	0
5.5	7676	36	0.6969	8	900.0	7	0	904.39	6	0
5.0	10852	36	0.734	8	875.86	7	0	870.56	6	0
4.5	14860	36	0.8186	9	666.76	8	0	665.69	7	0
4.0	19482	36	0.9532	9	496.39	8	0	494.97	7	0

The outcome of the direct Poisson applicability test of the both-sides crossings can be sensitive to the windows size. Results of calculations shown in Table 11 were obtained with the specific purpose to take the method beyond its breaking point. A similar procedure was carried over for upcrossing in Section 1; there it was found that the results of direct applicability test were not sensitive to the size of window. Behavior of the both-sides crossings was found to be different and the results are sensitive to windows size.

At all the levels (with exception of 9.5 m), the applicability of Poisson flow was not rejected if the larger windows were used. Fractions in the column of number of windows (marked N_w) mean that the window was of a larger duration than a record. For example N_w=1/4 means that four records makes one window, while N_w=1.2 means that each window uses one record on its full length and 20% of length of the next record.

Results in Table 11 cannot be explained other than as a numerical artifact. Properties of Poisson flow cannot be supported if the events are not independent. It was quite clearly seen from a number of calculations discussed in Section 1; once events are too close to each other, while the autocorrelation functions have not died out yet, the hypothesis of Poisson flow was clearly rejected. To verify that results in Table 11 are, in fact, a numerical artifact, another method of testing was applied.

Table 12 shows the results of a Kolmogorov-Smirnov goodness-of-fit test (K-S test) applied as described in Section 1. Its application is completely justified if a theoretical distribution is used; however it may be too "optimistic" on the statistical fit, as it does not have a mechanism to apply a penalty for statistically estimated parameters (see Section 1). Results in Table 12, however, do not show large differences in judgment on the applicability of Poisson flow to both-sides crossings.

Table 11. Test on applicability of Poisson flow for both-sides crossings (Increased window size)

Level ±, m	Number of crossings	N_w	m_k/V_k	N_{max}	Pearson chi-square test for Poisson distribution based on					
					Formula (5.16)			Averaged number of crossings		
					χ^2	d	$P(\chi^2,d)$	χ^2	d	$P(\chi^2,d)$
12	3	1/4	1.0426	2	0.7626	1	0.38	0.11	-	-
11.5	9	1/4	0.94	4	0.6459	3	0.8859	0.2322	2	0.8904
11.0	22	1/4	0.88	4	0.7307	3	0.866	0.7651	2	0.6821
10.5	54	1/4	1.0652	4	4.7329	3	0.1924	1.7518	2	0.4165
10.0	101	1/4	1.0206	8	10.4581	7	0.1641	5.137	6	0.5264
9.5	179	1	0.82	7	24.615	6	0.0004	16.963	5	0.0046
9.0	307	1	0.88	8	7.4806	7	0.38	6.9313	6	0.3272
8.5	517	1	1.1	8	2.3842	7	0.9356	2.3616	6	0.8836
8.0	860	1	1.2	10	12.4697	9	0.2549	11.5471	8	0.2401
7.5	1441	1	1.21	16	11.0447	15	0.7494	10.9491	14	0.69
7	2266	1.2	0.8675	21	26.3937	20	0.1532	21.2171	19	0.3249
6.5	3514	1.2	0.9172	27	21.9401	26	0.692	17.6174	25	0.9172
6.0	5354	1.2	1.0115	37	29.276	36	0.7788	26.1945	35	0.8588
5.5	7676	2	0.9526	33	40.97	32	0.1329	34.0338	31	0.3236
5.0	10852	2	1.0136	41	28.7651	40	0.9068	26.5423	39	0.9356
4.5	14860	2	1.1773	54	34.3761	53	0.9779	34.4415	52	0.9712
4.0	19482	3	1.1015	47	18.68	46	0.999	19.0462	45	0.998

Table 12. Kolmogorov-Smirnov test on applicability of Poisson flow for both-sides crossings

Level ±, m	Number of crossings	Formula (5.16)			Averaged number of crossings		
		Max difference	Value of Criterion	Probability that fit is good	Max difference	Value of Criterion	Probability that fit is good
12	3	0.0139	0.0241	1	0.0057	0.0099	1
11.5	9	0.0147	0.0442	1	0.0067	0.0202	1
11.0	22	0.0151	0.0706	1	0.0108	0.0507	1
10.5	54	0.0229	0.1682	1	0.0216	0.1589	1
10.0	101	0.0201	0.2024	1	0.0503	0.5053	0.9604
9.5	179	0.0558	0.747	0.6323	0.0785	1.0496	0.2205
9.0	307	0.0709	1.2419	0.0915	0.0754	1.3212	0.0609
8.5	517	0.0904	2.0553	0.0004	0.0812	1.8461	0.0022
8.0	860	0.1046	3.0662	1.3648E-8	0.0878	2.5759	3.4488E-6
7.5	1441	0.1187	4.5071	0	0.109	4.1374	2.66E-15
7	2266	0.1235	5.8811	0	0.1094	5.2094	0
6.5	3514	0.1314	7.7869	0	0.1193	7.0746	0
6.0	5354	0.1302	9.5234	0	0.1258	9.2021	0
5.5	7676	0.1249	10.9419	0	0.1174	10.2896	0
5.0	10852	0.107	11.1445	0	0.1036	10.7952	0
4.5	14860	0.081	9.8696	0	0.0804	9.7988	0
4.0	19482	0.0579	8.0867	0	0.0569	7.9386	0

The theoretical distribution (5.16) and statistical fit both provide applicability of Poisson flow above a level located between 8.5 and 9 m. This is somewhat lower than the boundary found by the direct test of applicability of Poisson flow in Table 10, where it was between 10 and 10.5 m. Such a discrepancy, however, has been observed when applying both tests to just one-side upcrossing in Section 1.

The direct test of the applicability of Poisson flow seems to be more conservative than the K-S test. However, in the case of both-sides crossing, it may give the wrong answer if the size of the window is too large. To ensure reliable judgment of applicability of Poisson flow, the direct test needs to be complemented by the K-S test.

5.1.4. Relation between Both-sides Crossing and Absolute Value of Peaks

Consider a sample of stochastic process x, presented in a form of an ensemble of N_R records. Each record is represented by a time history of N_{PT} points with the time step Δt, totaling $n = N_{PT}-1$ time steps. Then the event of occurrence of a peak, exceeding a given threshold or the level a, is associated with an auxiliary random variable Z defined for each time step as follows (see Figure 5.3):

$$Z_{i,j} = \begin{cases} 1 & |x_{i,j}| > a \cap |x_{i,j}| > |x_{i-1,j}| \cap |x_{i,j}| > |x_{i+1,j}| \\ 0 & Otherwize \end{cases} \qquad (5.23)$$

$$i = 1,..,n; \quad j = 1,...,N_R$$

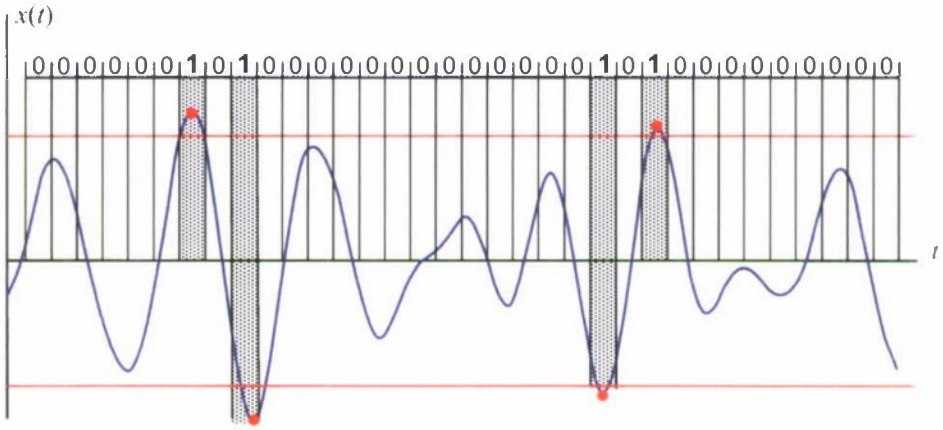

Figure 5.3 Auxiliary random variable for peak over the threshold

This random variable Z is defined analogously to the auxiliary random variable D, see the previous subsection. Following the same logic, the total number of all crossings is just a sum of the values of the auxiliary variable for all time steps for all records:

$$N_Z = \sum_{i=1}^{n} \sum_{j=1}^{N_R} Z_{i,j} \qquad (5.24)$$

An estimate of the probability that a peak exceeding the threshold will occur at any given instance of time:

$$p_Z^* = \frac{N_Z}{nN_R} = \frac{1}{nN_R} \sum_{i=1}^{n} \sum_{j=1}^{N_R} Z_{i,j} \qquad (5.25)$$

The mean number of peaks over the threshold per record:

$$m_Z^* = \frac{N_Z}{N_R} = \frac{1}{N_R} \sum_{i=1}^{n} \sum_{j=1}^{N_R} Z_{i,j} \qquad (5.26)$$

The rate of events for the peak over the threshold can be introduced analogously to the rate of upcrossing. Its estimate over a finite volume of data is defined as:

$$\lambda_{PoT}^* = \frac{m_Z^*}{n\Delta t} = \frac{1}{nN_R \Delta t} \sum_{i=1}^{n} \sum_{j=1}^{N_R} Z_{i,j} \qquad (5.27)$$

While the theoretical definition can be obtained as a result of a limit transition for the infinite number of records and infinitely small time step:

$$\lambda_{PoT} = \lim_{\substack{N_R\to\infty \\ n\to\infty \\ \Delta t\to 0}} \lambda^*_{PoT} = \lim_{\substack{N_R\to\infty \\ n\to\infty \\ \Delta t\to 0}} \frac{1}{nN_R\Delta t}\sum_{i=1}^{n}\sum_{j=1}^{N_R} Z_{i,j} = \frac{1}{dt}\lim_{\substack{N_R\to\infty \\ n\to\infty}} \frac{1}{nN_R}\sum_{i=1}^{n}\sum_{j=1}^{N_R} Z_{i,j} =$$
$$= \frac{1}{dt}\lim_{\substack{N_R\to\infty \\ n\to\infty}} \frac{NZ}{nN_R} = \frac{1}{dt}\lim_{\substack{N_R\to\infty \\ n\to\infty}} p_Z^* = \frac{dp_Z}{dt} \qquad (5.28)$$

The discussion of applicability of binomial distribution for the auxiliary variable Z follows the same thread as for the auxiliary variable D in the case of both-sides crossings. Figure 5.4 shows an example calculation at the level/threshold ±9 m. As it can be seen from that figure, the estimate of the rate of peaks over the threshold is statistically identical to the estimate of the rate of the both-sides crossing. The theoretical result for the rate of the both-sides crossing is not rejected by either of the estimates.

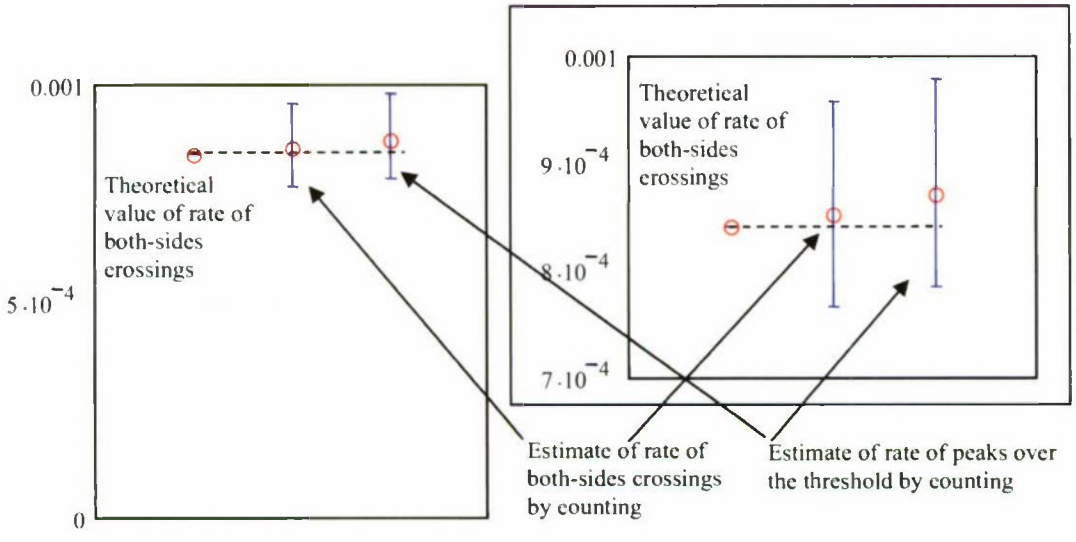

Figure 5.4 Both-sides crossing rate: theoretical value and statistical estimate by counting vs. rate of peaks over the threshold. Crossing level ±9 m

Figure 5.5 shows a comparison between the theoretical values of the both-sides crossing rate, its estimate by-counting, and the estimate of rate of the absolute value of the peaks. The points and the curve practically coincide. The confidence interval was too tight to plot on the figure.

To show the confidence interval, a log scale was used, see Figure 5.6. Even in the log scale the confidence interval remains too tight to be drawn, with the exception of the level 10 m and higher. To avoid any further cluttering, the smallest of the two upper boundaries was shown for the upper limit, while the largest of the lower boundaries was shown for lower limit. All the numbers are also shown in Table 13.

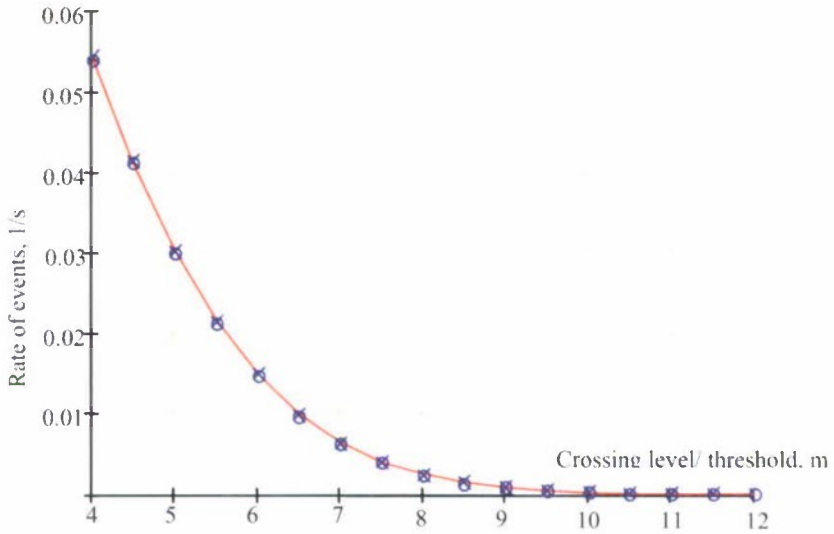

Figure 5.5 Theoretical value both-sides crossing rate (red curve), statistical estimate of both-sides crossing rate by counting (circles) and statistical estimate of rate of absolute value of peaks over the threshold (crosses).

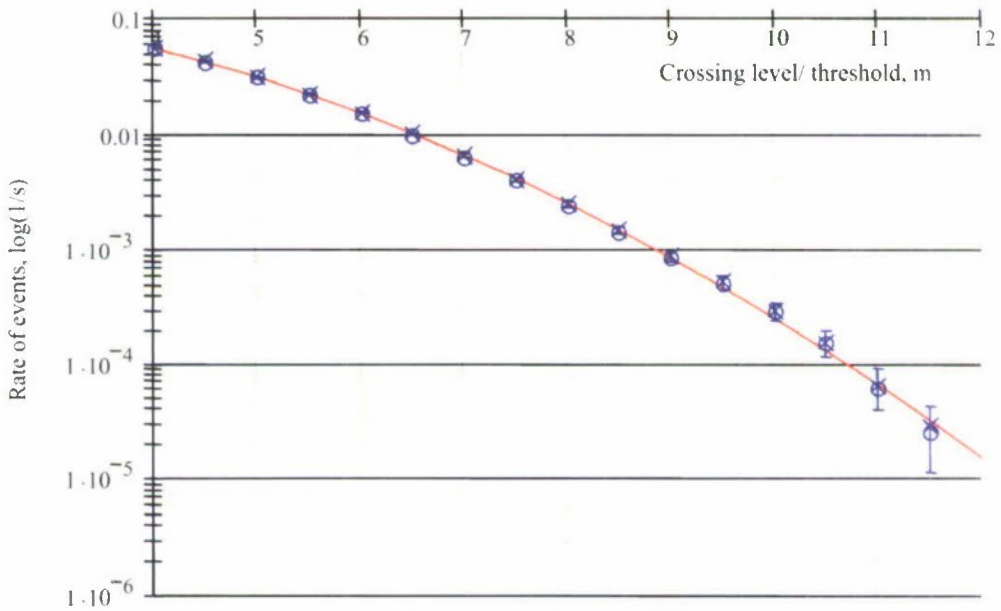

Figure 5.6 Theoretical value both-sides crossing rate (red curve), statistical estimate of both-sides crossing rate by counting (circles) and statistical estimate of rate of absolute value of peaks over the threshold (crosses).

Table 13. Both-sides crossing rates and rates of peaks

Crossing level / threshold, m	Theoretical both-sides crossing rate	Estimate of both-sides crossing rate			Estimate of rate of absolute value of peaks		
		low	mid	upper	low	mid	upper
4	0.0543	0.0539	0.05412	0.0554	0.05417	0.05439	0.05568
4.5	0.04134	0.04102	0.04128	0.04234	0.04131	0.04156	0.04264
5	0.03049	0.02988	0.03014	0.03101	0.03013	0.0304	0.03127
5.5	0.02177	0.02106	0.02132	0.02201	0.02126	0.02152	0.02221
6	0.01506	0.01462	0.01487	0.01542	0.01479	0.01504	0.01559
6.5	0.01009	9.54E-03	9.76E-03	0.01018	9.66E-03	9.88E-03	0.01031
7	6.54E-03	6.10E-03	6.29E-03	6.62E-03	6.19E-03	6.39E-03	6.71E-03
7.5	4.11E-03	3.84E-03	4.00E-03	4.25E-03	3.90E-03	4.07E-03	4.32E-03
8	2.50E-03	2.25E-03	2.39E-03	2.58E-03	2.31E-03	2.45E-03	2.64E-03
8.5	1.47E-03	1.33E-03	1.44E-03	1.58E-03	1.36E-03	1.47E-03	1.61E-03
9	8.41E-04	7.67E-04	8.53E-04	9.58E-04	7.86E-04	8.72E-04	9.78E-04
9.5	4.65E-04	4.31E-04	4.97E-04	5.78E-04	4.44E-04	5.11E-04	5.92E-04
10	2.49E-04	2.31E-04	2.81E-04	3.39E-04	2.36E-04	2.86E-04	3.44E-04
10.5	1.29E-04	1.14E-04	1.50E-04	1.92E-04	1.14E-04	1.53E-04	1.97E-04
11	6.47E-05	3.61E-05	6.11E-05	8.89E-05	3.89E-05	6.39E-05	9.17E-05
11.5	3.14E-05	1.11E-05	2.50E-05	4.17E-05	1.11E-05	2.78E-05	4.72E-05
12	1.48E-05	0	8.33E-06	1.94E-05	0	8.33E-06	1.94E-05

Looking at the numbers in Table 13, one can confirm that estimates of the rates of the absolute value of peaks over the thresholds are statistically identical to estimates of the both-sides crossing rate. Both estimates include the theoretical value for the both-sides crossing rate into their confidence intervals. Therefore, statistics of the absolute value of peaks over the threshold can be used to characterize events of both-sides crossing.

5.2. Theoretical Solution for Both-sides Crossings

The theoretical solution for the upcrossing problem was readily available. It is not the case for the peak-based envelope. At the same time, the approximate theoretical solution is needed to verify the extrapolation method being developed.

5.2.1. Distribution of Absolute Value of Peaks

The total number of peaks (both positive and negative) found in the wave elevation sample data set was 62,135. The absolute value of a peak is defined as:

$$x_{peak} = \left| x\left(t_{peak}\right) \right| \quad \Big| \quad t_{peak} : \quad \left(\dot{x}\left(t_{peak}\right) = 0 \right) \tag{5.29}$$

Figure 5.7 is a histogram of absolute values of peaks superimposed with Rayleigh distribution. The histogram is somewhat similar to the distribution of positive peaks (see section 3); however, it cannot have any negative values by the definition (5.29). It shows larger values in the vicinity of zero in comparison with the histogram of positive peaks; the value of the first bucket is well above 0.1, while the first bucket of the positive peaks is below 0.1.

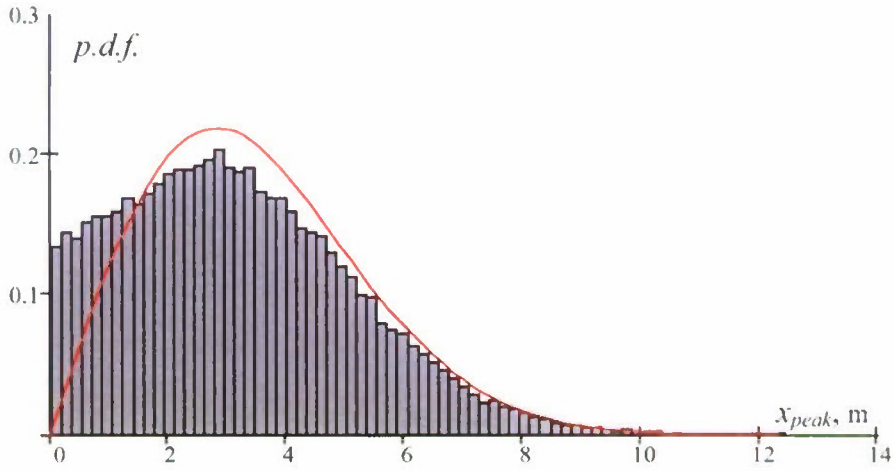

Figure 5.7 Histogram of absolute values of peaks of wave elevations with superimposed Rayleigh distribution

Obviously, the absolute values of peaks do not follow a Rayleigh distribution. This result can be explained in a wave, similar to the case of positive peaks. The reason why a Rayleigh distribution is inapplicable as a whole, is existence and statistical influence of secondary peaks. It is known that number (and statistical influence) of secondary peaks depends on the spectrum bandwidth. As it was already mentioned in the section 3, peaks of a normal process with "moderate" bandwidth follow a Rice distribution. Once the bandwidth becomes very large, the autocorrelation function dies out very quickly and the process becomes effectively white noise. If there is no autocorrelation, peaks are encountered totally randomly; they become distributed just like any other value of the process. Therefore, for the limit case of the spectrum bandwidth, the peaks take a normal distribution. The other limit case is a very narrow spectrum. As it was mentioned in Section 3, the distribution of peaks of narrow-banded process follows Rayleigh. It also can be explained by the fact that the narrow spectrum makes the envelope a slowly changing function, and the variance of the zero-crossing period becomes very small. It also means that there are very few secondary peaks; they become statistically insignificant. The envelope contains all of the peaks; sampling the envelope with almost constant step makes the peaks keep the distribution of the envelope, e.g. Rayleigh distribution. This was demonstrated in Section 3 for the positive peaks of wave elevations recorded from the moving gauges (encounter wave sample).

Similar to the distribution of positive peaks, the distribution of absolute values of peaks follows a truncated Rayleigh distribution (see Section 3) starting from a certain bucket.

$$f_{at}(a) = k_n(a_t)\frac{a}{V_x}\exp\left(-\frac{a^2}{2V_x}\right) \quad ; \quad a > a_t \tag{5.30}$$

Here $k_n(a_t)$ is normalization coefficient calculated at the truncation value a_t. The following formula was derived in Section 3 for the truncation coefficient:

$$k_n(a_t) = \exp\left(\frac{a_t^2}{2V_x}\right) \tag{5.31}$$

Substitution of formula (5.31) into formula (5.30) gives the following expression for the truncated Rayleigh distribution:

$$f_{at}(a) = \frac{a}{V_x}\exp\left(-\frac{(a^2 - a_t^2)}{2V_x}\right) \quad ; \quad a > a_t \tag{5.32}$$

The cumulative distribution is expressed as:

$$F_{at}(a) = 1 - \exp\left(-\frac{(a^2 - a_t^2)}{2V_x}\right) \quad ; \quad a > a_t \tag{5.33}$$

The truncated Rayleigh distribution and truncated histogram are shown in Figure 5.8; the value of truncation has been chosen to pass Pearson chi-square goodness-of-fit test. The results of the Pearson chi-square goodness of-fit test are also shown in Figure 5.8.

The explanation is similar to the one given in Section 3. Secondary peaks are relatively small. Large peaks are primary peaks; therefore they belong to the envelope. It is also known from the theory of the envelope that conditional variance of the period decreases when the amplitude increases. This means that large-amplitude oscillations have periods very close to the mean period; the illustration of this effect can be seen in the appendix to (Belenky and Bassler 2010). Again, if the peaks belong to the envelope and are sampled with almost a constant step, they keep the distribution of the envelope, e.g. Rayleigh distribution.

Consider the sample with a narrow spectrum (see Section 4), created by the wave elevations "recorded" with a "gauge" moving in the same direction with the waves (following encounter waves). It was shown in Section 3 that the distribution of its positive peaks is closer to Rayleigh; the positive peaks start following truncated a Rayleigh distribution from the amplitudes of 0.54 m, while for the "zero-speed" case for this value was 1.51 m.

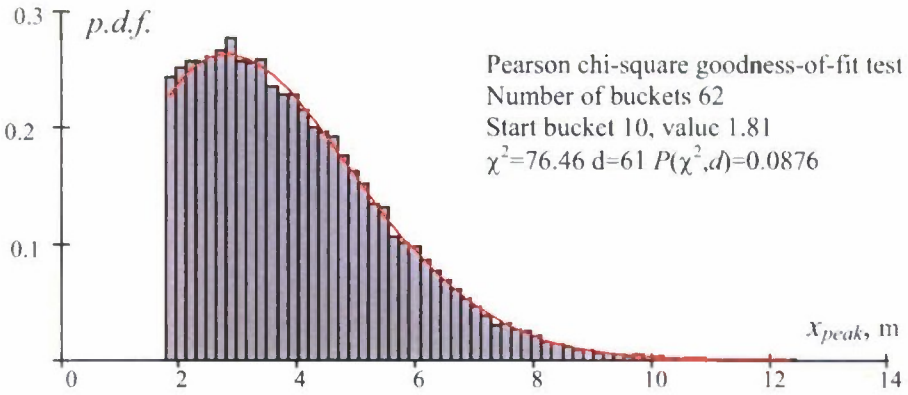

Figure 5.8 Histogram of absolute values of peaks and truncated Rayleigh distribution

A similar picture can be observed for the absolute value of the peaks. There were 32,717 peaks in total. Figure 5.9 shows a histogram of absolute values of peaks for 15-knot case of the encounter waves. Visually, the hypothesis of Rayleigh distribution looks very plausible. However, the Pearson chi-square goodness-of-fit test rejects the hypothesis, because of the first two buckets.

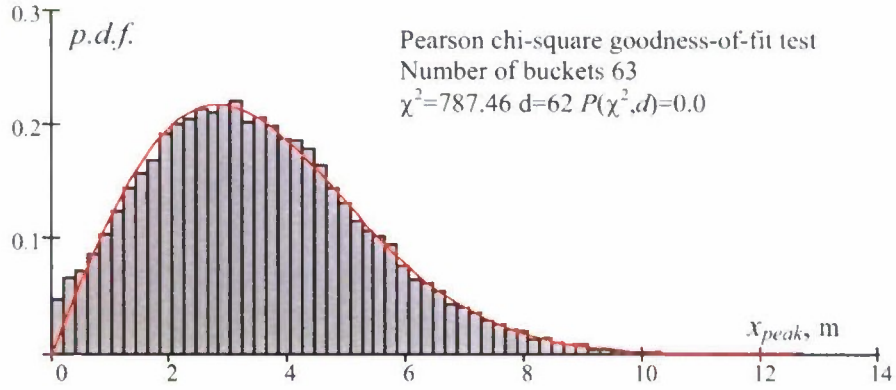

Figure 5.9 Histogram of absolute value of peaks for the case with forward speed 15 knots and Rayleigh distribution

As it could be expected, the truncated Rayleigh distribution becomes applicable to the absolute peaks of the following encounter waves with smaller values (Figure 5.10) in comparison with the zero-speed case (Figure 5.8). The reasoning is similar: the narrow band spectrum makes the secondary peaks less likely and large-amplitude data are likely to have a period close to the mean period.

Based on the considerations above, it seems reasonable to assume that large peaks follow the truncated Rayleigh distribution.

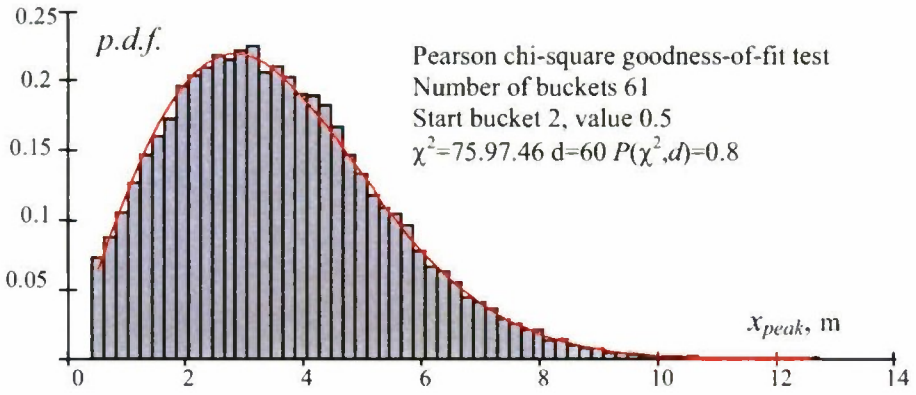

Figure 5.10 Histogram of absolute value of peaks for the case with forward speed 15 knots and truncated Rayleigh distribution

5.2.2. Rare Problem for Both-sides Crossing

Consider the rare problem for a peak-based envelope. The objective is to find a conditional probability such that if the peak-based envelope crosses a given threshold a_1, it will exceed a given level a_2.

Then, the conditional probability that the process will cross the level a_2 if the level a_1 is crossed (formula 3.9), provided $a_2 > a_1$, and taking into account Rayleigh distribution of the envelope:

$$P = \frac{f(a_2)}{f(a_1)} = \frac{\int_{a_2}^{\infty} f_A(A)dA}{\int_{a_1}^{\infty} f_A(A)dA} = \frac{1-F_A(a_2)}{1-F_A(a_1)} = \exp\left(-\frac{(a_2^2 - a_1^2)}{2V_x}\right) \qquad (5.34)$$

The value P expressed with formula (5.34) is the probability that if the process x up-crosses the threshold a_1, it will also up-cross the level a_2. It also can be considered as a fraction (actually a limit value of it) of the upcrossings through the threshold a_1, which also cross the level a_2.

As the sample-process x is normal (the normal distribution is symmetric) and centered (the mean value is zero), the same value P describes the conditional probability that the process x will down-cross the level $-a_2$ if it has previously down-crossed the threshold $-a_1$.

Then, this probability also describes a fraction of both-sides crossing of the threshold $\pm a_1$ that will also cross the level $\pm a_2$.

The above consideration concludes that the problems of upcrossing, downcrossing, and both-sides crossing have the same rare solution if the process is normal and centered. In principle, this statement can be generalized for any symmetric

distribution, but it is outside of the scope of the current consideration as the sample process is normal.

Finally, the solution of the rare problem for the both-sides crossing is identical to the solution of the rare problem for upcrossing:

$$P_B = \exp\left(-\frac{(a_2^2 - a_1^2)}{2V_x}\right) = P \quad a_2 > a_1 \tag{5.35}$$

Similar to the upcrossing, case formula (5.35) can be interpreted in terms of absolute values of peaks: formula (5.35) expresses a conditional probability, that an absolute value of a peak exceeding the threshold a_1 will also exeeed the level a_2. As the absolute values of peaks have a truncated Rayleigh distribution, such an interpretation of (5.35) is only valid for $a_t < a_1$.

The complete theoretical solution for the both-sides crossing rate of the level a_2 can be expressed as:

$$\lambda_{ab}(a_2) = \lambda_{ab}(a_1) P_B \tag{5.36}$$

Taking into aceount formula (5.25) for the both-sides erossing of the threshold a_1 and simultaneously substitute (5.35):

$$\lambda_{ab}(a_2) = \frac{1}{\pi}\sqrt{\frac{V_x}{V_x}}\exp\left(-\frac{a_1^2}{2V_x}\right)\exp\left(-\frac{(a_2^2 - a_1^2)}{2V_x}\right) \tag{5.37}$$

After simplification, the formula (5.37) yields:

$$\lambda_{ab}(a_2) = \frac{1}{\pi}\sqrt{\frac{V_x}{V_x}}\exp\left(-\frac{a_2^2}{2V_x}\right) \tag{5.38}$$

Formula (5.38) is identical to Formula (5.16). It is the direct expression for the rate of the both-sides crossing of a normal process with zero mean. This confirms the applicability of the rare solution (5.35) for the both-sidess crossings.

Direet applieation of the formula (5.36) for extrapolation may encounter difficulties related to applicability of Poisson flow.

Strietly speaking, the applicability of the Poisson flow is required only for the level where the probability of failure will be evaluated. In this case, this would be the level a_2. Therefore, theoretieally, Poisson flow may be not applieable at the threshold a_1, but the method is still valid. However, by the very meaning of extrapolation, the crossing events of the level a_2 are not expected to be seen. Therefore, it is impossible to verify applicability of the Poisson flow for the level a_2.

A practical way to insure applicability of the Poisson flow on the level a_2 is to verify that it is applicable on the lower level, for which there is enough data to make a judgment. If applicability of the Poisson flow has been confirmed for the threshold a_1, then it is applicable for the level a_2.

As it was shown previously (see Table 10) the applicability of the Poisson flow for the both-sides crossing can only be seen above the threshold of 10.5 m. There were only 54 events on that level. As it was explained, due to strong autocorrelation, these events have a tendency to appear in pairs, so the threshold has to be very high, so one side is crossed and another one does not. This situation is expected to become even worse for the encounter waves as it takes longer for the autocorrelation function to die out. These difficulties justify application of the envelope instead of the process itself (see Section 4).

5.2.3. Rare Problem for Upcrossing of Envelope

Consider the rare problem for the theoretical envelope upcrossing. The theoretical envelope is a stationary stochastic process; its values have a Rayleigh distribution and its first derivative is distributed normally. Based on these considerations, it was shown in section 4 that the upcrossing rate of the envelope can be presented as, see formula ((4.82):

$$\lambda_e = a\sqrt{\frac{\left(\omega_2^2 - \omega_1^2\right)}{2\pi V_x}}\exp\left(-\frac{a^2}{2V_x}\right) \tag{5.39}$$

Application of the general formula for the rare solution (equation 3.9), for the case of the envelope, yields the following expression:

$$P_e = \frac{f_a(a_2)}{f_a(a_1)} = \frac{a_2}{V_x}\exp\left(-\frac{a_2^2}{2V_x}\right)\cdot\left(\frac{a_1}{V_x}\exp\left(-\frac{a_1^2}{2V_x}\right)\right)^{-1} = \frac{a_2}{a_1}\exp\left(-\frac{a_2^2 - a_1^2}{2V_x}\right) \tag{5.40}$$

Taking into account (5.35) the relation between the solutions for rare problem for the upcrossing of the normal process itself and its envelope:

$$P_e = \frac{a_2}{a_1}P \tag{5.41}$$

To verify the solution of the rare problem, consider the complete one, expressing the rate of the upcrossing of the envelope through the level a_2:

$$\lambda_e(a_2) = \lambda_e(a_1)P_e \tag{5.42}$$

Consider substitution of (5.39) and (5.40) into (5.42)

$$\lambda_c(a_2) = a_1\sqrt{\frac{\left(\omega_2^2-\omega_1^2\right)}{2\pi V_x}}\exp\left(-\frac{a_1^2}{2V_x}\right)\cdot\frac{a_2}{a_1}\exp\left(-\frac{a_2^2-a_1^2}{2V_x}\right) \tag{5.43}$$

After simplifieation, expression (5.43) yields the following:

$$\lambda_c(a_2) = a_2\sqrt{\frac{\left(\omega_2^2-\omega_1^2\right)}{2\pi V_x}}\exp\left(-\frac{a_2^2}{2V_x}\right) \tag{5.44}$$

Formula (5.43) is identieal in strueture to formula (5.39) and explieitly expresses the rate of upcrossing through the level a_2. This is the eonfirmation of eorrectness of the solution of the rare problem (5.40).

5.2.4. Upcrossing of Peak-based Envelope vs. Theoretical Solution

As it was shown in the subseetion 4.5, the rate of uperossing of a peak-based envelope may be quite different form the theoretieal solution. It depends on width of the speetrum, if the theoretieal solution can be used to describe the rate of uperossing. If the speetrum is narrow, the envelope is a slowly ehanging funetion (in eomparison with the proeess itself), then the peak-based envelope is quite elose to the theoretical envelope, see Figure 5.11 (a). If the spectrum is relatively wide the rate of change of the envelope is eomparable with the first derivative of the proeess and the differences between the peak-based and theoretieal envelope may not be insignificant, see Figure 5.11 (b).

This explains the effect described in the Seetion 4. The theoretical upcrossing rate of the theoretieal envelope (formula 4.83) has shown good agreement with the statistieal estimate of the uperossing rate of the peak-based envelope for the following wavc case (see Figure 5.12 a), while the theoretieal solution and statistical estimates do not agree for the zero-speed case (see Figure 5.12 b). This creates a problem: a theoretieal solution is needed to eompare with the results of EPOT method.

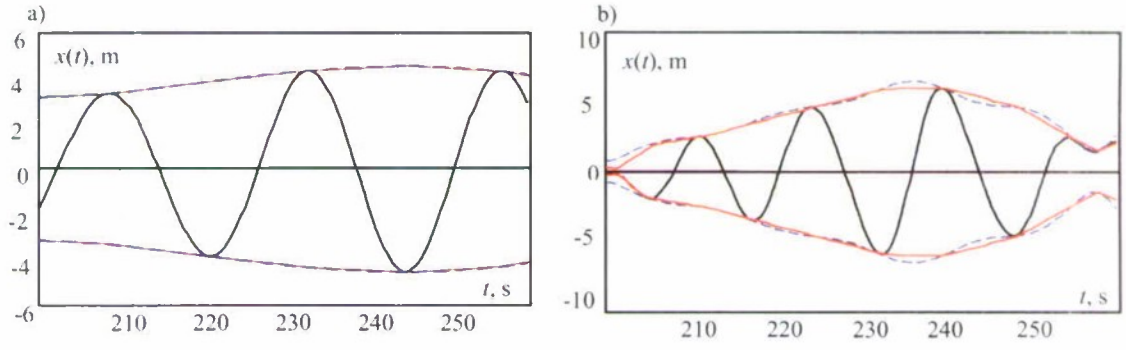

Figure 5.11 Zoomed in fragments of peak-based envelope superimposed on the theoretical envelope: a) recorded" by the "gauge" moving with the waves (pure following seas) with the speed 15 knots b) recorded by fixed "gauge" –zero speed case

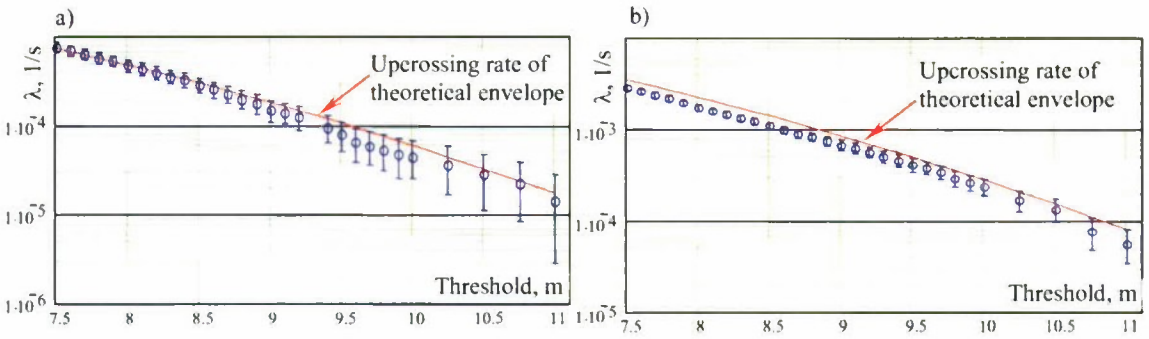

Figure 5.12 Statistical estimate of upcrossing rate (1/s) of the peak based envelope : a) recorded" by the "gauge" moving with the waves (pure following seas) with the speed 15 knots b) recorded by fixed "gauge" –zero speed case

5.2.5. Both-Sides Crossing Rate as the Theoretical Solution

As it was demonstrated above, there is a strong relationship between absolute value of peaks and both-sides crossings. It also was shown that the rate of the both-sides crossing has a theoretical solution. For the case of symmetric centered process, it equal to double upcrossing rate, see formula (5.15).

The event of the both-sides crossing through the prescribed level obviously is the partial stability failure. It was shown also that the Poisson distribution is not applicable to this event, and therefore its use in these calculations may be limited. However, it still makes sense to see the relationship between the rate of the both-sides crossing and rate of upcrossing of the peak-based envelope.

Comparison of the statistical estimates of upcrossings of the peak-based envelope with the theoretical rate of both-sides crossing is shown in Figure 5.13 for the following waves case. Obviously, these are two different values; the theoretical rate of both-sides crossings does not belong to the confidence interval of any of the statistical estimates. However, the tendency of the estimates shows some signs of conversion with the theoretical rate of both-sides crossing. This tendency can be confirmed by comparison of two theoretical curves, not limited by gathered statistics. They are shown in Figure 5.14; the convergence tendency is obvious.

The convergence of the rate of the both-sides crossing and the envelope upcrossing is not universal; it is not true for the zero speed case shown in Figure 5.15. After the crossing the curve shows the tendency to diverge. In principle, same effect can be seen for the following waves, but it occurs for higher levels (~25 m vs. 10 m) and much smaller number for the rates (1.E-18 vs. 1.E-3).

Figure 5.16 shows the theoretical rate of the both-sides crossing plotted along with statistical estimates of upcrossing of the peak-base envelope for the zero speed case. One can notice that the theoretical value starts belonging to the confidence interval from the level of 9.5 m and never leaves it after that level.

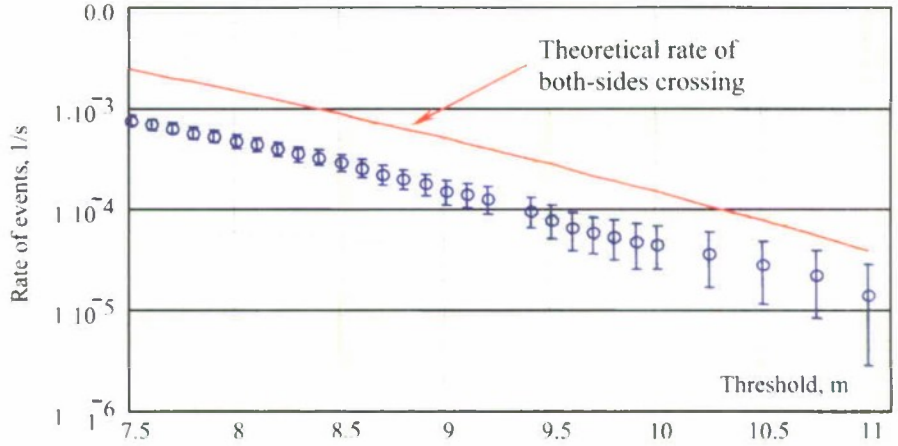

Figure 5.13 Theoretical rate of both-side crossing and statistical estimate of upcrossing of the peak-based envelope. Following Waves Case

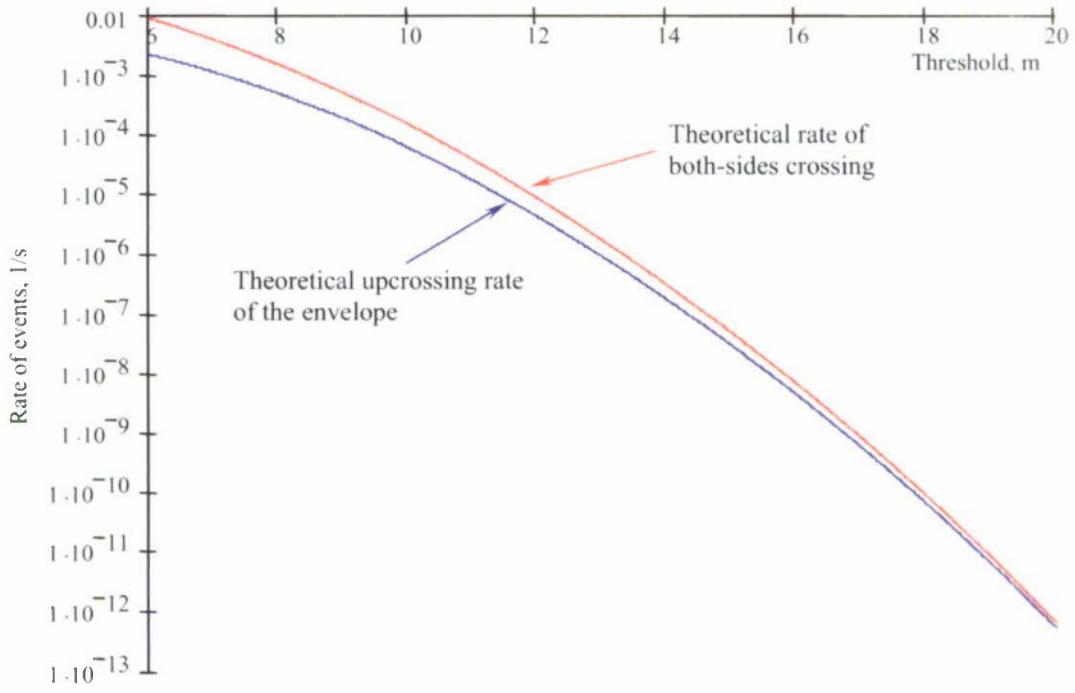

Figure 5.14 Theoretical rate of both-sides and upcrossing of the envelope. Following Waves Case

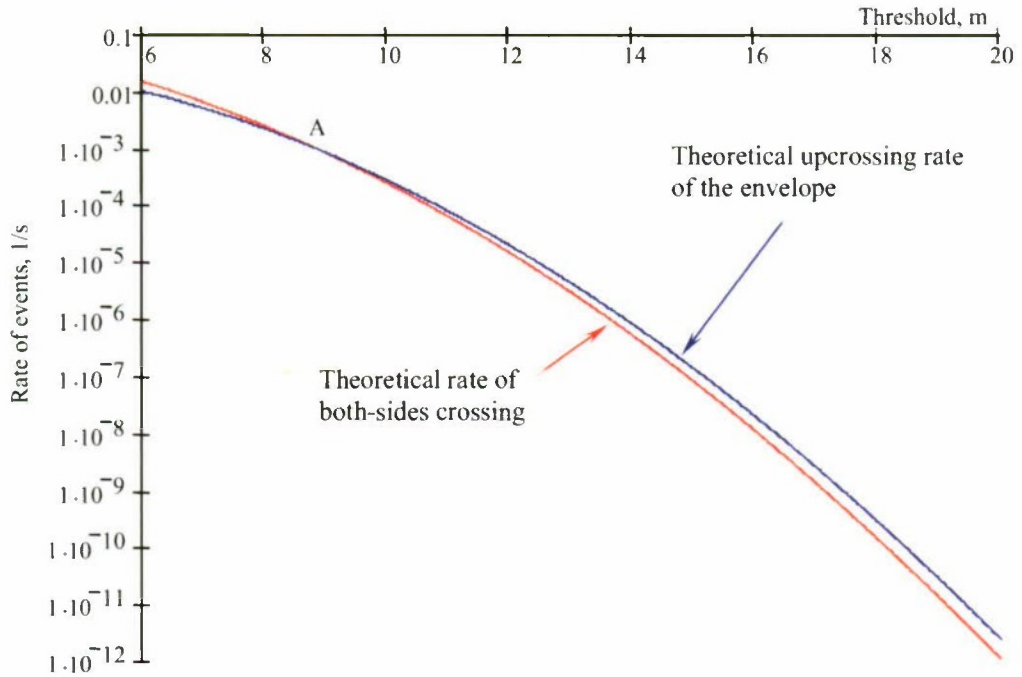

Figure 5.15 Theoretical rate of both-sides and upcrossing of the envelope. Zero-speed Case

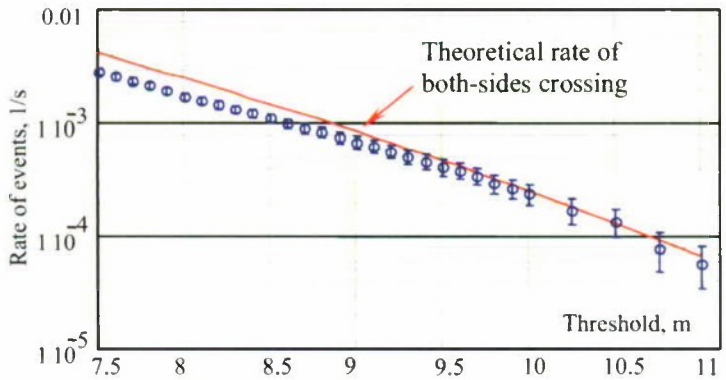

Figure 5.16 Theoretical rate of both-sides crossing and statistical estimate of upcrossing of the peak-based envelope. Zero-Speed Case

These comparisons show that both-sides crossing rate, in principle, can be used as a theoretical solution for the problem of upcrossing of peak-based envelope.

For the following waves case, asymptotic convergence of the both-sides crossing rate and envelope upcrossing rate confirms the above statement; since the peak-based envelope is a good approximation for the theoretical envelope, the theoretical envelope upcrossing rate can be used for a close approximation as well.

The reason why the convergence is asymptotic seems to be as follows. The rate of envelope upcrossing for lower levels is smaller then the rate of both-sides upcrossing,

then one crossing of the envelope corresponds to several both-sides crossings. The reason for that is significant clustering due to the narrow spectrum. Once the level increases, there are more chances that the process crosses the level only twice (both sides) corresponding to the highest peak in vicinity, as the chances that the two neighboring peaks are exactly the same is small.

For the zero-speed case, there is no convergence between the theoretical envelope upcrossing rate and both-sides crossing rate. The both-sides upcrossing rate goes higher than the envelope upcrossing rate until a certain point and then becomes slower (point A in Figure 5.15. This can be explained as follows. Before point A, the level is relatively low, so there are significant chances that several periods will be crossed once the peak-based envelope is crossing. This mechanism is similar to what was described for the following wave case. After point A, the crossing rate on the envelope upcrossing is higher than the both-sides crossing. That means the envelope has more crossings than the process itself (both sides). This occurs because the envelope oscillates between peaks (see Figure 5.12b) of the process and can cross the level while the peak remains below the level. This is exactly the reason why the peak-based envelope was introduced in section 4. Therefore, the both-sides crossing rate is the value to trust here.

Figure 5.16 shows a convergence of the statistical rate of the upcrossing of the peak based envelope with the theoretical rate of the both-sides crossing. The reason why the difference is large for smaller value of the threshold is likely to be the same as above, one crossing of the peak-based envelope corresponds to several crossings of the both-sides of the process. Once the level is high enough that only the highest peak in a cluster can reach it, the theoretical rate becomes included in the confidence interval.

5.2.6. Approximate Solution for Peak-Based Envelope Upcrossing

Considerations in the previous subsection established that the correct theoretical solution – the rate of the both-sides crossing – is achieved asymptotically. This may render inconclusive the comparison of the extrapolation results with the both-sides rate alone, as the failure always can be explained that the level is not "high enough".

Therefore it makes sense to use the upcrossing rate of the theoretical envelope for another comparison base for the following wave case. This makes the following wave case the only "clean" comparison, where the theoretical solution is available everywhere.

An approximate non-rare solution may be useful for the zero speed case. It can be developed by the least square approximation through the statistical estimate of upcrossing. At least such a solution can be used to test the solution for the rare problem. The upcrossing rate is searched in the following form:

$$\lambda_+(z) = \exp\left(c_0 + c_1 z + c_2 z^2\right) \quad ; \qquad z = a_1 \tag{5.45}$$

Taking the natural logarithm for both sides of (5.45) and introducing a new variable y yields:

$$y = c_0 + c_1 z + c_2 z^2 \quad ; \qquad y = \ln(\lambda_x) \tag{5.46}$$

Coefficients c_0, c_1, and c_2 are evaluated with the least square method using statistical estimates for the upcrossing rates. The values of these coefficients are characterized by significant variability from one dataset to another, see Table 14. The result is shown in Figure 5.17.

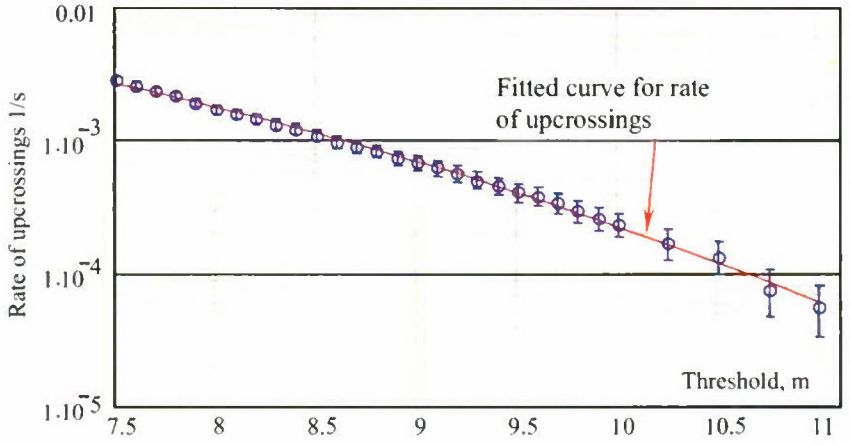

Figure 5.17 Rate of upcrossing of the peak-based envelope: zero-speed case

Table 14. Coefficients for curve fit for upcrossing rates

Coefficient for the curve fit	c_0	c_1	c_2
Original Data Set	-5.427	0.628	-0.093
Alternative Data Set 1	-1.054	-0.362	-0.038
Alternative Data Set 2	-5.209	0.715	-0.106

5.3. Extrapolation with EPOT: Following Wave Case

As it was demonstrated above, only the following wave case allows comparison with the robust theoretical solution. The reason is that as the encounter spectrum is narrow in the following waves, the theoretical envelope becomes a slowly changing function of time in comparison with the process itself. Therefore, the peak-based envelope becomes a reasonable approximation of the theoretical envelope. Then the rate of upcrossings of the peak-based envelope can be described by the theoretical formula, which is available for the theoretical envelope.

That said, the following wave case truly represents a test bed for the method since the true answer is known from theory.

5.3.1. *Distribution of Maxima of the Peak-Based Envelope*

Applieation of the EPOT method is only slightly different for the POT method that was deseribed in detail in Seetion 3. Therefore the foeus must be on these differenees.

The first step is the seareh for maxima of the peak-based envelope, see Figure 5.18. Distribution of the maxima of the peak-based envelope is shown in Figure 5.19(a) along with Rayleigh distribution (however, the eharaeter of the distribution looks lognormal rather than Rayleigh). At the same time, the truncated Rayleigh distribution (see formula 5.30) is not rejeeted by the ehi-square goodness-of-fit test for the tail of the distribution starting at the 7 m level, see Figure 5.19(b).

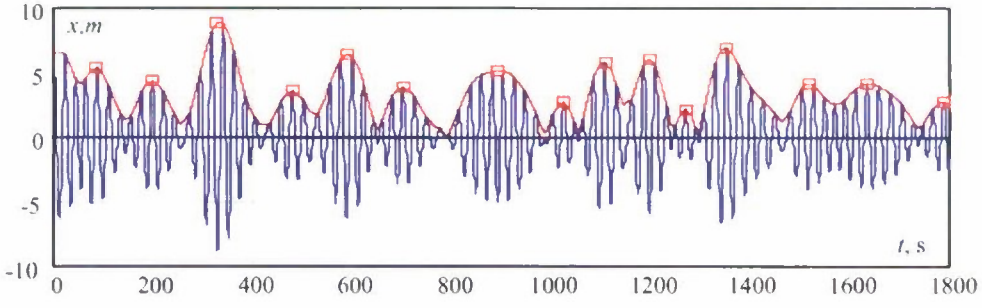

Figure 5.18 Peak based envelope (red) and its maxima

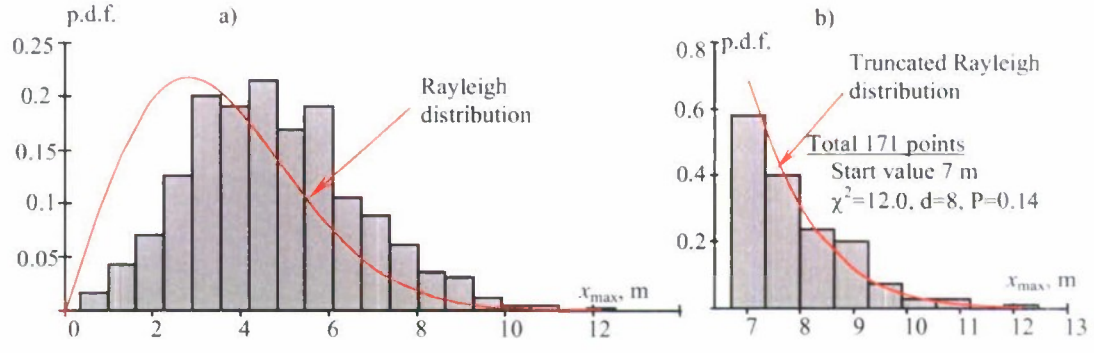

Figure 5.19 Distribution of maxima of the peak based envelope superimposed with Rayleigh distribution (a), truncated Rayleigh dustiribution

5.3.2. *Fitting Weibull for Maxima of the Peak-Based Envelope*

Similar to the POT method, the seeond step is fitting a histogram of maxima of the peak-based envelope and fitting the Weibull distribution to these data. In this context, the Weibull distribution is used just as a smoothing eurve for the empirieal distribution.

Only the data exeeeding a given threshold are used to fit the Weibull distribution. Exaetly like in the ease of the POT method described in Seetion 4 , the first guess for the parameters of the Weibull distribution is performed using the moments method described in Seetion 2 and then the method of maximum likelihood is applied. The samples are

shown in Figure 5.20 along with the results of testing of the goodness-of-fit. The fitted distribution was not rejected in both cases for the threshold equal to 8 m and 9 m.

The third step is evaluation of the confidence interval for the fitted distribution. The technique for evaluation of the confidence interval is described in the section 3. The idea is to find the confidence interval for the mean value and variance estimates and then shift and scale the data accordingly. Once done, two more Weibull fits are performed on the altered data, corresponding to upper and lower boundary. The sample result for 9 m threshold is shown in Figure 5.21.

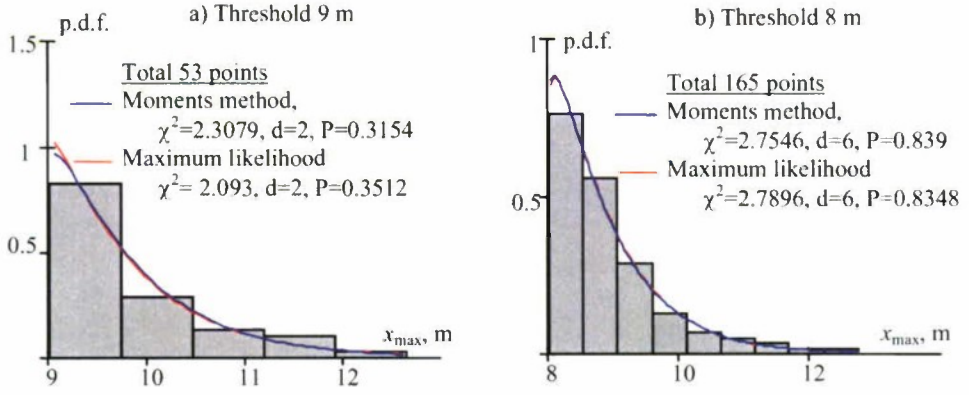

Figure 5.20 Weibull fit for the maxima of the peak-based envelope exceeding the threshold of a) 9 m and b) 8 m

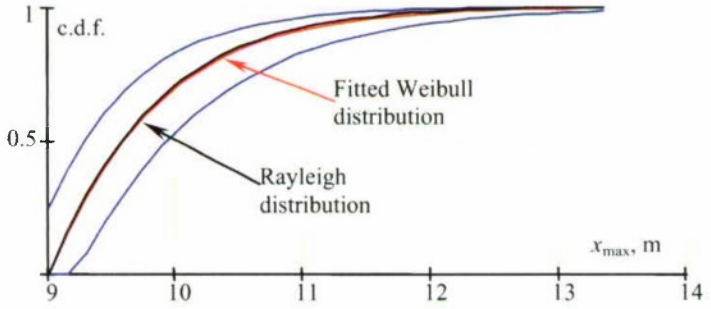

Figure 5.21 Weibull CDF with confidence interval fitted for the maxima of the peak-based envelope exceeding the threshold of 9 m

Figure 5.21 also shows the Rayleigh distribution completely contained (at least visually) within the confidence interval and almost coinciding with the Weibull fit. This is consistent with previously made conclusions that the Rayleigh distribution is not rejected for the tail of the maxima of the peak-based envelope.

The Weibull fit actually represents the conditional distribution for a peak of the envelope to exceed a level if the given threshold was already exceeded.

5.3.3. *Extrapolation with the Distribution of the Peak-Based Envelope*

Once both non-rare and rare solutions are obtained, the procedure of extrapolation is trivial: it is the application of formulae (3.22-3.24). The sample result is shown in Figure 5.22 for the threshold of 9 m. The extrapolated solution is shown with its confidence interval and superimposed with the rate of upcrossing of theoretical envelope as well the theoretical rate for both-sides crossings. As the peak-based envelope is considered as a reasonable approximation of the theoretical envelope, the upcrossing rate of the latter is expected to stay within the confidence interval of the extrapolated solution. As it can be seen from the Figure 5.22, the theoretical solution stays within the confidence interval until a certain level (it equals 18.5 m for the 9 m of the threshold), the breaking point as it was defined in Section 3.

Similar to the upcrossing problem, discussed in Section 3, the position of the breaking points depends on the threshold, see Figure 5.23.

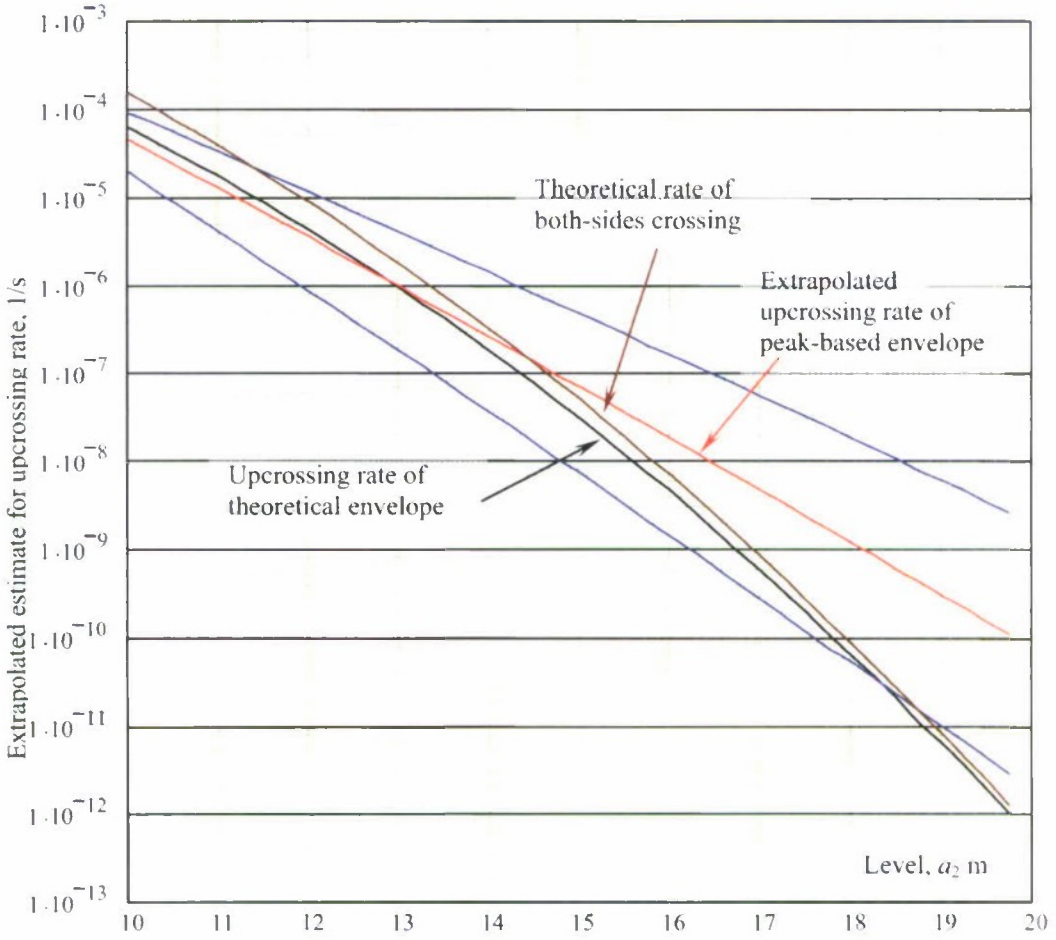

Figure 5.22 Extrapolated estimate of upcrossing rate of the peak-based envelope with confidence interval as a function crossing level. The threshold is 9 m, 53 peaks

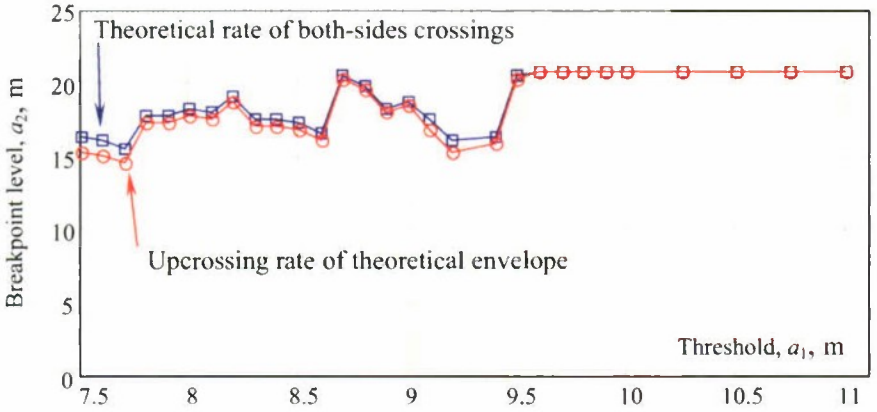

Figure 5.23 Breakpoint level (the level below which the extrapolation is still good) vs. threshold

Figure 5.22 also shows the theoretical rate of the both-sides crossing. As it was shown above, this solution gives "the correct" answer only for the very high level and only for the case of narrow spectrum. This is the reason why the confidence interval does not include the rate of the both-sides crossing for smaller levels; however, starting at the level of ~11.4 m, the theoretical rate of the both-sides crossings enters the confidence interval of the extrapolated solution and stays there until the level of 18.75 m because of the convergence discussed above.

The breaking point evaluated for the both-sides crossing rate behaves similarly to the "envelope breaking point" as it can be seen from Figure 5.23.

Further analysis of the performance of the EPOT method is done for the level of 15 m. As it can be seen from Figure 5.23, this is the level where the method starts breaking up for some of the thresholds. Also the event of upcrossing the level of 15 m is very rare. The mean time for the event (based on theoretical envelope upcrossing rate) is about 7 years and 4 months. So, if 10 events are needed to estimate the rate, it will take about 73 years of data, while the EPOT method only used 100 hours of data.

Figure 5.24 shows the influence of the choice of the threshold on the rare solution (probability that the peak-based envelope exceeds the level of 15 m, if the threshold is exceeded), while Figure 5.25 shows the complete solution. Similar to Figure 5.22, Figure 5.25 shows both theoretical solutions: the rate of upcrossings of the theoretical envelope and the both-sides crossing rates. It is clearly seen from Figure 5.25 that for the level of 15 m, the difference between the two theoretical solutions is small in comparison with the width of confidence interval of statistical extrapolation.

The estimates oscillate around the theoretical solution (compare to Figure 3.22 and Figure 3.26 plotted for the upcrossing problem in section 3), so averaging through several levels will make the estimate more stable. Formulae (3.46-3.47) express this averaging procedure. Averaging is performed for all the thresholds while the number of points remains above 30 (30 points is considered enough to evaluate a histogram and fit the distribution). The results of averaging are shown in Figure 5.26.

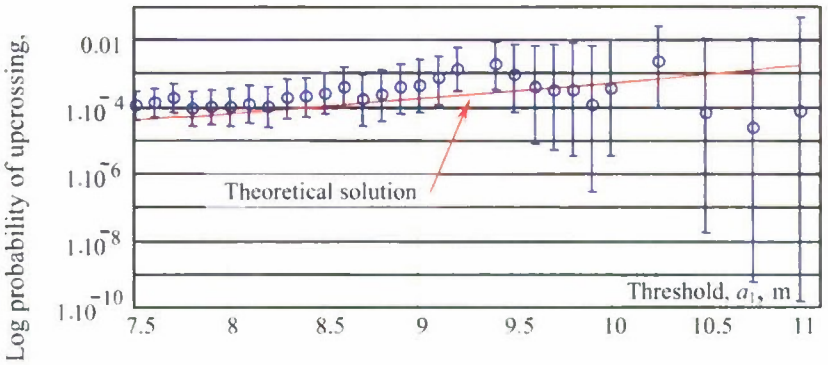

Figure 5.24 Rare solution for the level of 15 m

As it can be seen from the insert in Figure 5.26, both theoretical solutions are included in the confidence interval for the test level of 15 m. Breaking points are 16.5 m and 17 m for the theoretical envelope upcrossing rate and rate of both-sides crossings, respectively.

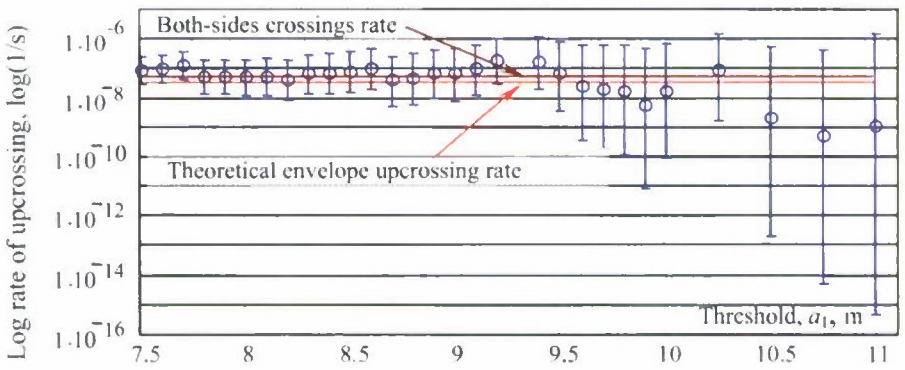

Figure 5.25 Statistical extrapolation of the upcrossing rate of peak-based envelope - complete solution for the level of 15 m

Successful application of the averaging over several thresholds for the current numerical example does not prove yet that it will work as well for all other cases. While it seems to be impossible to prove, it still makes sense to try it at least on two alternative data sets used earlier in the Section 3. Figure 5.27 shows dependence of the breakpoints of these datasets as a function of the threshold. The lowest point is about 12 m.

Figure 5.28 shows behaviors of a rare solution and the complete extrapolated estimate for a_2=15 m using two alternative datasets. These behaviors are principally similar to the original set seen in Figure 5.24 and Figure 5.25. Most of the threshold values enable the estimate "to catch" the theoretical solution in its confidence interval.

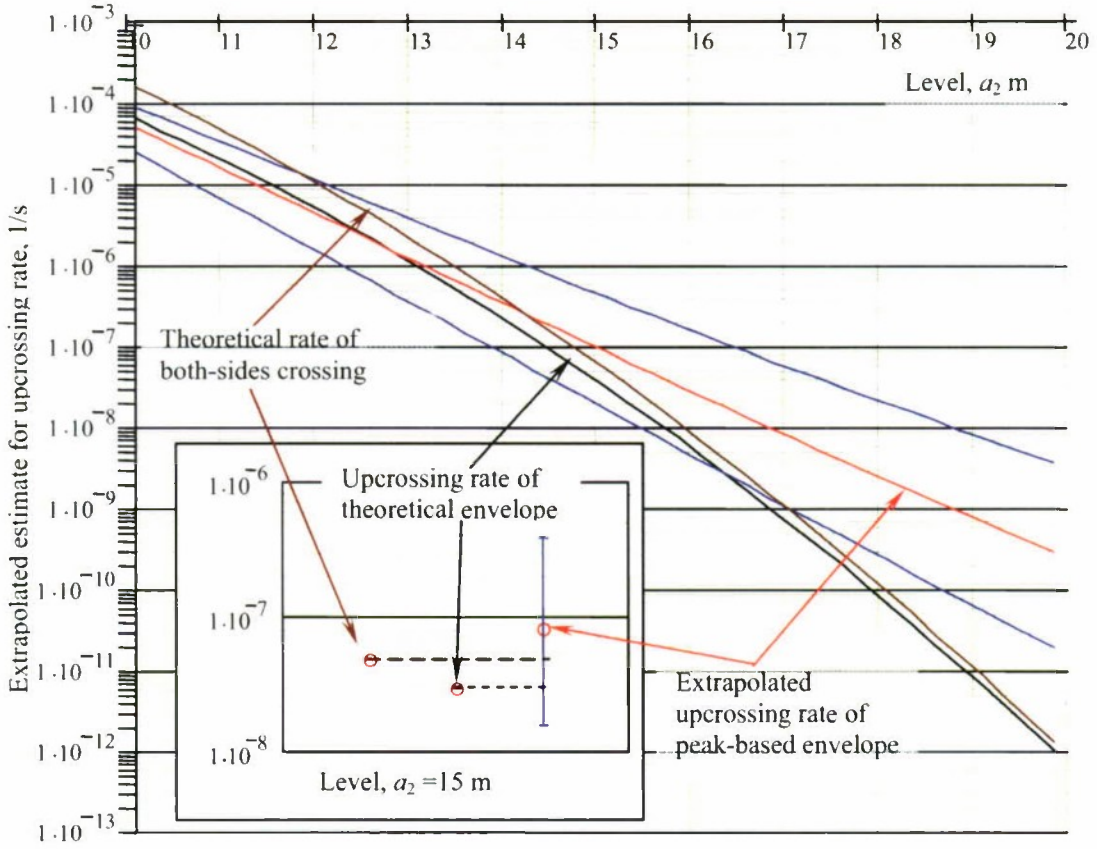

Figure 5.26 Averaged extrapolated estimate of rate of upcrossing of the peak-based envelope Insert shows the level of 15 m

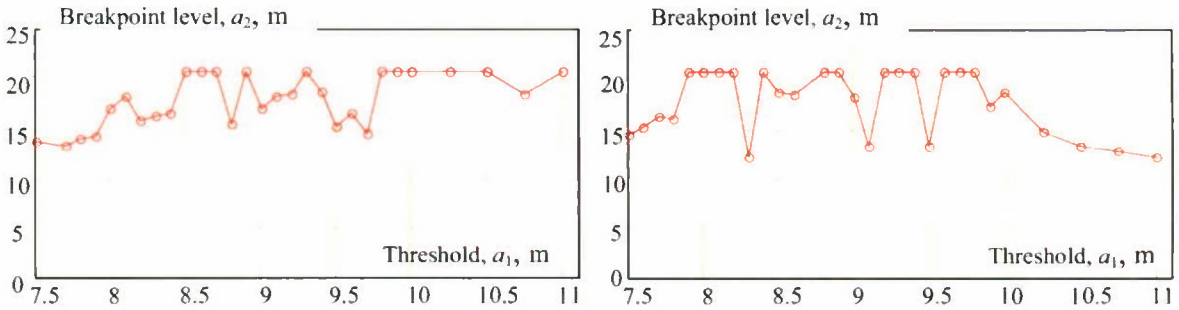

Figure 5.27 Breakpoint level (the level below which the extrapolation is still good) for the extrapolated estimate of upcrossing of peak-based envelope vs. threshold for two alternative data sets

Figure 5.29 shows results of the averaging technique for two alternative datasets. Both theoretical solutions, the rate of upcrossing of the theoretical envelope and the rate of both-sides crossing, are within the confidence interval of the extrapolated estimate. Data for breaking points are shown in Figure 5.29 as well.

In general, the performance of the method can be characterized as satisfactory taking into account the rarity of the event of crossing the level of 15 m.

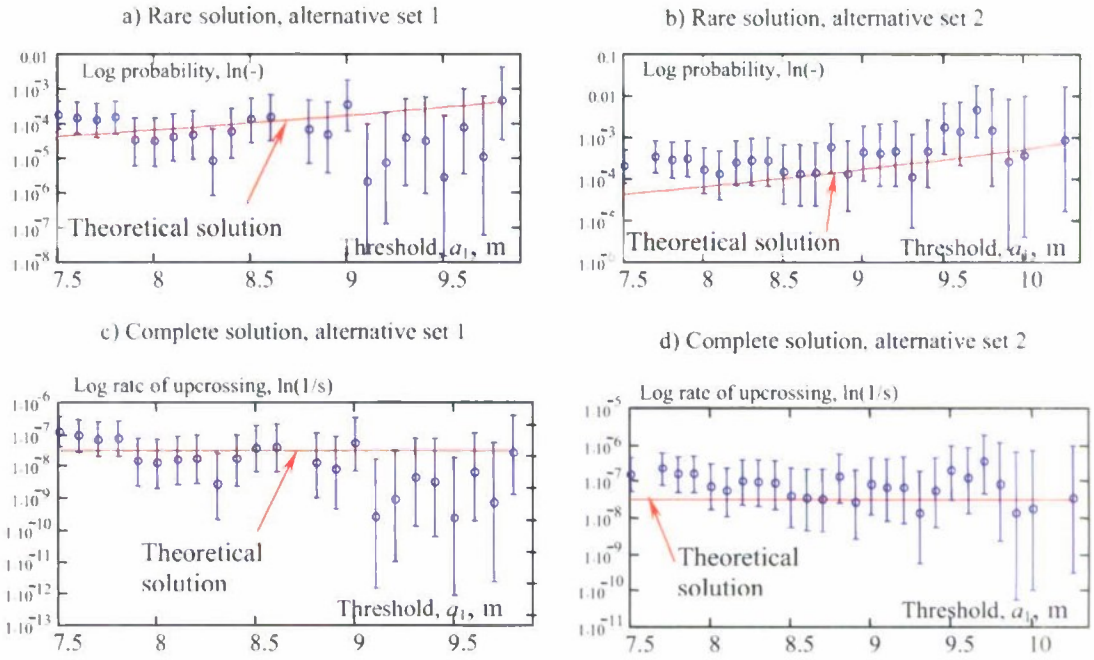

Figure 5.28 extrapolated estimate of conditional probability that the process will exceed the level of 15 m if the threshold has been crossed – rare solutions (upper plots: a, b) and complete extrapolated estimate (lower plots: c, d) for two alternative data sets for a_2=15 m

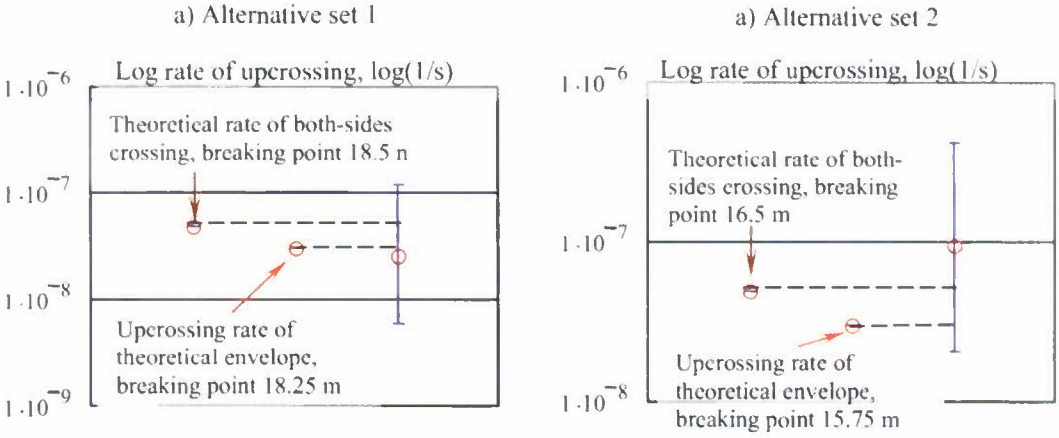

Figure 5.29 Level 15 m: theoretical solution and extrapolated estimate averaged for (a) the set 1 thresholds 7.5-9.6 m; the distribution for the threshold 9.6 m was fitted with 33 points. (b) For the set 2 range is 7.5-9.6 m with 30 points for the threshold 9.6 m.

5.3.4. Extreme Value Distribution of the Peak-Based Envelope

The extreme value distribution is an alternative way of solving the rare problem, as it was shown in Section 3. While the Weibull distribution is used in both cases, the way the dataset is sampled makes the difference. Classic extreme value theory uses the maxima of a process sampled within a constant time window. The size of this window

becomes a parameter that needs to be set in order to use the method. In principle, this size must produce independent data points in the neighboring windows. While the influence of the window size still needs to be studied, it was chosen to be 900 seconds for the sample in this section. Figure 5.30 illustrates that procedure: only a point in the window 1 was collected as the maximum value in the window 2 did not exceed the sample threshold of 9 m.

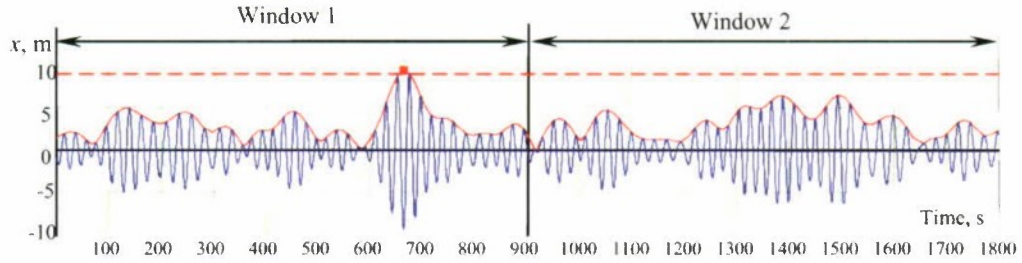

Figure 5.30 Collecting data for extreme value distribution, threshold 9 m

Further procedure and general character of the results are not very different from the previous case where the Weibull distribution was fitted using all maxima of peak-based distribution exceeding the threshold. Figure 5.31 shows dependence of the breakpoint level (the level until which the extrapolated estimate still contains a theoretical solution in its confidence interval) based on two theoretical solutions: the upcrossing rate of the theoretical envelope and theoretical rate of the both-sides crossings. Both breakpoints are quite close to each other, due to observed convergence of both of the theoretical solutions for higher levels.

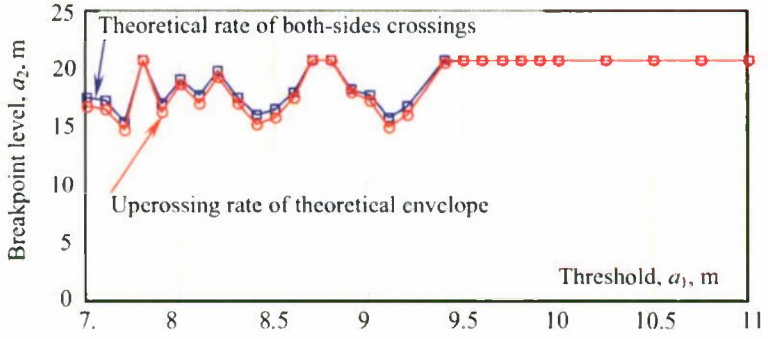

Figure 5.31 Breakpoint level (the level below which the extrapolation is still good) vs. threshold for the extrapolation based on extreme value distribution

Figure 5.32 shows the influence of the choice of the threshold on the rare solution for the level of 15 m (the probability that the peak-based envelope exceeds the level of 15 m, if the threshold is exceeded), see formula (3.44), while Figure 5.33 shows the complete extrapolated estimated along with both theoretical solutions. Due to convergence, the difference between the two theoretical solutions is small in comparison with the width of the confidence interval.

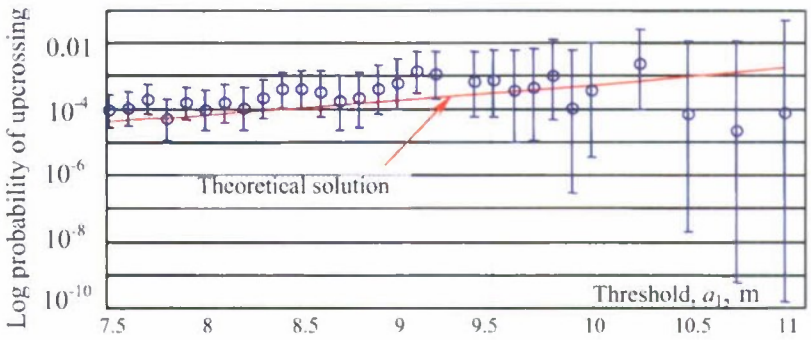

Figure 5.32 Rare solution for the level of 15 m using extreme value distribution

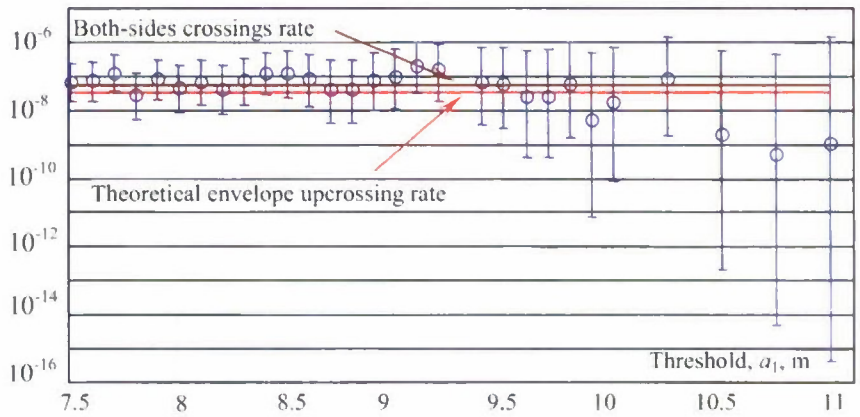

Figure 5.33 Statistical extrapolation of the upcrossing rate of peak-based envelope - complete solution for the level of 15 m based on extreme value distribution

Similar to Figure 5.24 and Figure 5.25 (as well as analogous to Figure 3.22 and Figure 3.26) plotted for the uperossing problem in Seetion 3, the estimates oscillates around the theoretical solution, so averaging through several levels will make the estimate more stable. Formulae 3.46-3.47 express this averaging proeedure. Similar to the first method (fitting Weibull to maxima, see previous subsections) averaging is performed for all the thresholds while the number of points remains above 30 (30 points is eonsidered enough to evaluate a histogram and fit the distribution). The results of averaging are shown in Figure 5.34. Both theoretical solutions are ineluded in the eonfidenee interval for the test level of 15 m. Breaking points are 17.75 m and 18 m for theoretical envelope uperossing rate and the rate of the both-sides crossings, respectively.

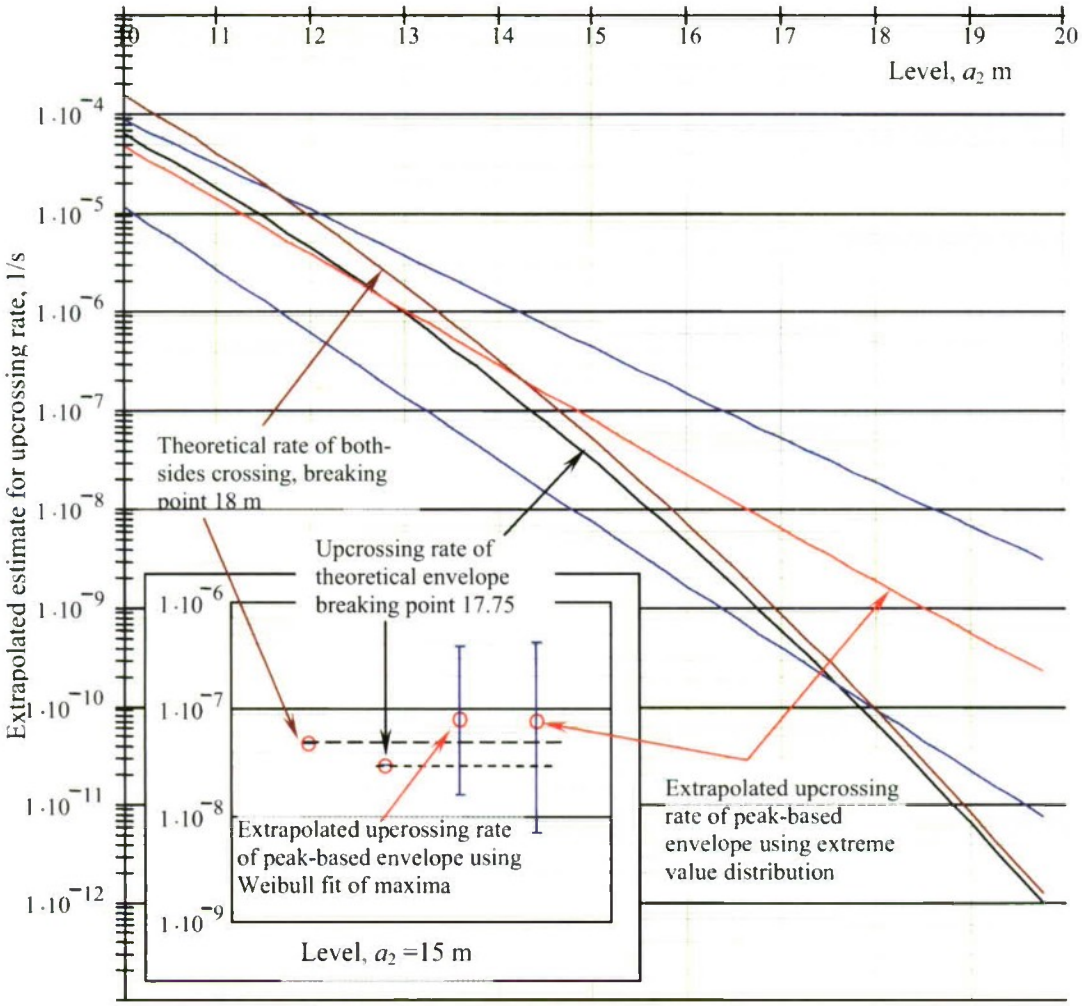

Figure 5.34 Averaged estimate of rate of upcrossing of the peak-based envelope extrapolated using extreme value distribution. Insert shows the level of 15 m

Successful application of the averaging over several thresholds for the current numerical example does not prove yet that it will work as well for all other cases. While it seems to be impossible to prove, it still makes sense to try it at least on two alternative data sets used earlier in Section 3. Figure 5.35 shows dependence of the breakpoints of these datasets as a function of the threshold. The lowest point is about 12 m.

Figure 5.36 shows behaviors of the rare solution and the complete extrapolated estimate for a_2=15 m using two alternative datasets. These behaviors are principally similar to the original set seen in Figure 5.32 and Figure 5.33 as well as Figure 5.24, Figure 5.25 and Figure 5.28. Most threshold values enable the estimate "to catch" the theoretical solution in its confidence interval.

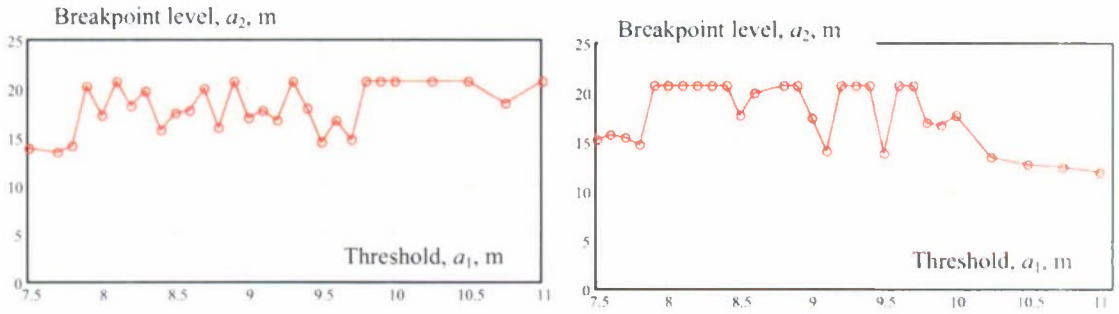

Figure 5.35 Breakpoint level (the level below which the extrapolation is still good) for the estimate of uperossing of peak-based envelope extrapolated using extreme value distribution vs. threshold for two alternative data sets

Figure 5.37 shows results of the averaging technique for two alternative datasets. Both theoretical solutions (the rate of upcrossing of the theoretical envelope and rate of the both-sides crossing) are within the confidence interval of the extrapolated estimate. Data for breaking points are shown in Figure 5.37.

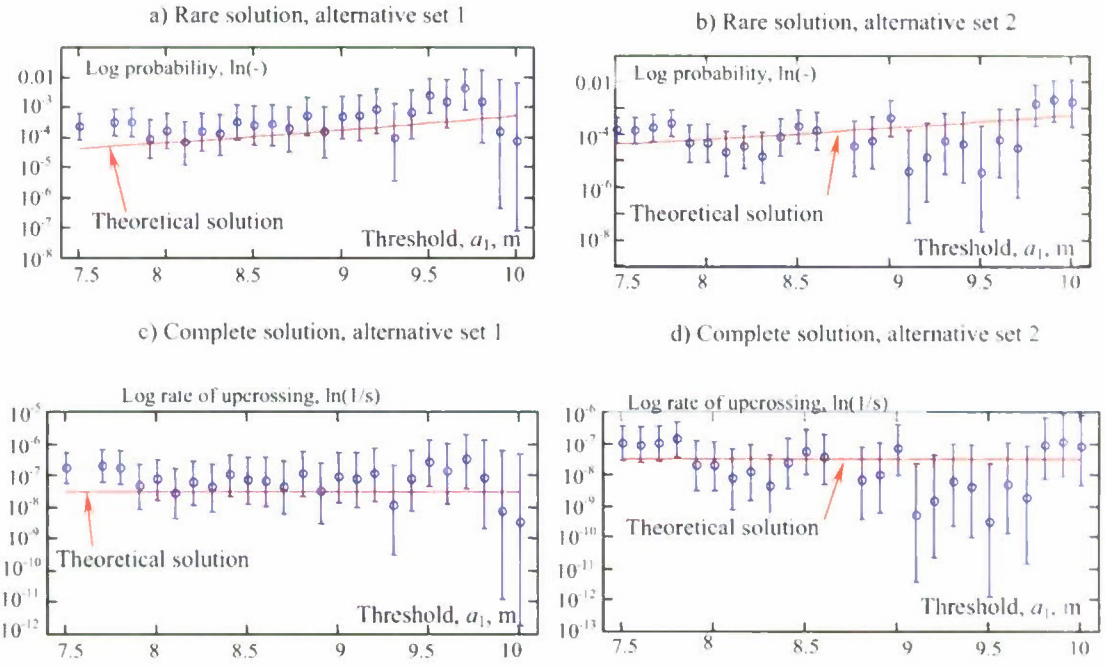

Figure 5.36 Extrapolated estimate of conditional probability that the process will exceed the level of 15 m if the threshold has been crossed – rare solutions (upper plots: a, b) and complete extrapolated estimate (lower plots: c, d) for two alternative data sets for a_2=15 m. Both cases use extreme value distribution for extrapolation

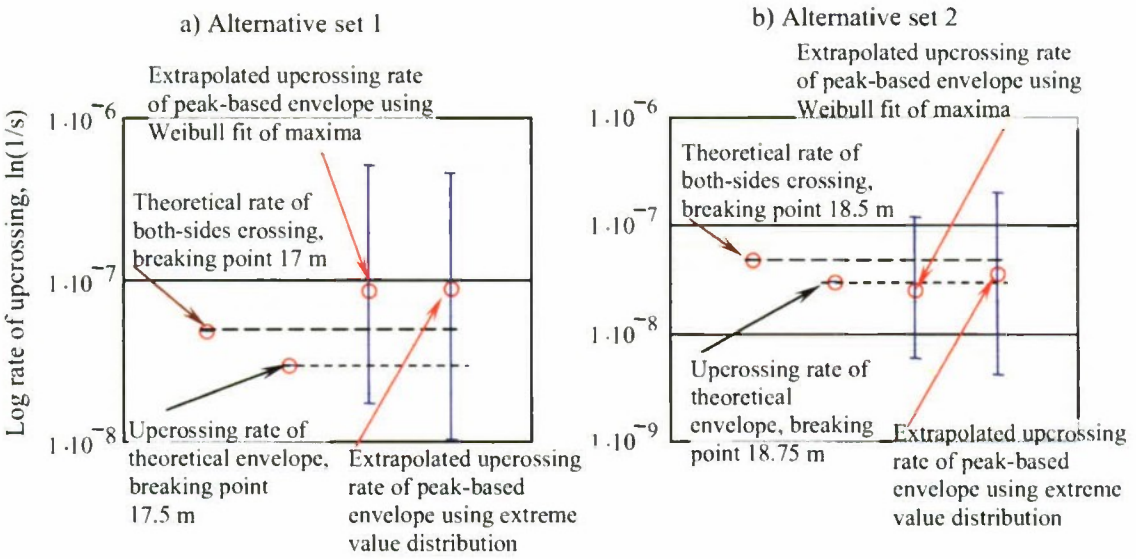

Figure 5.37 Level 15 m: theoretical solution and extrapolated estimate averaged for (a) the set 1 thresholds 7.5-9.6 m; the distribution for the threshold 9.6 m was fitted with 33 points. (b) For the set 2 range is 7.5-9.6 m with 30 points for the threshold 9.6 m.

Figure 5.34 as well as Figure 5.37 also shows comparison between two estimates based on the Weibull fit (described in the previous subsection) and extreme value distribution. Both confidence intervals have quite substantial common area, which means statistical equality of the two estimates.

The two estimates used the rare solution based on different ways of using Weibull distribution: as a distribution of maxima and an extreme value distribution. The fact that both of these ways have produced the same solution is notable; it can be used to check the estimates against each other when theoretical solutions are not available.

The average break point between all three datasets was 17.8 m (based on the rate of upcrossing of the theoretical envelope). The mean time before such an event is about 330 years. Assuming that at least 10 events are needed to get a statistical estimate, it will take about 3,300 years worth of data to get the result. The EPOT method produced this result with only 100 hours of data; this makes the data reduction factor equal to 290,500.

5.4. Extrapolation with EPOT: Zero-Speed Case

5.4.1. Approximate Theoretical Solution for Zero-Speed Case

As it was discussed above, there is no exact theoretical solution available for the upcrossing of the peak-based envelope in the general case. Such a solution is only available for the case of the relatively narrow-band spectrum, when the envelope becomes a slowly changing function of time (in comparison with the process itself) and the peak-based envelope becomes a relatively close approximation of the theoretical envelope.

To overcome this difficulty, the approximate solution was proposed in one of the previous subsections. The non-rare solution used regression to express dependence of the upcrossing rate on the threshold, see formula (5.45).

It is also assumed that the large-values of the peak-based envelope are likely to follow a Rayleigh distribution. This assumption can be partially justified as the absolute value of the peaks do follow a truncated Rayleigh distribution (5.32). However, the distribution of absolute value peaks is not identical to the distribution of peak-based envelope, as points of the latter are calculated with linear interpolation between the peaks (see Section 4). This assumption needs to be checked by the goodness of fit-test of maxima of the peak based envelope. Once this assumption has been checked and found to be acceptable, Formula (5.40) is to be used for the rare solution. Therefore the complete solution can be formulated. However, it is only an approximation. This means that an agreement between this solution and the extrapolation does not validate the method, neither the disagreement between the approximate solution and the extrapolation would invalidate it.

It still makes sense to see how two other theoretical solutions (the rate of upcrossing of theoretical envelope and theoretical rate of the both-side crossings) will compare with the extrapolation result.

5.4.2. Distribution of Maxima of the Peak-Based Envelope

A sample record with the maxima of the peak-based envelope is shown in Figure 5.38. Comparing to the similar picture for the following wave case in Figure 5.18, one can see that the envelope is no longer a slowly changing process; as a result, the population of maxima of the envelope should not be much different from the population of absolute values of peaks of the process itself.

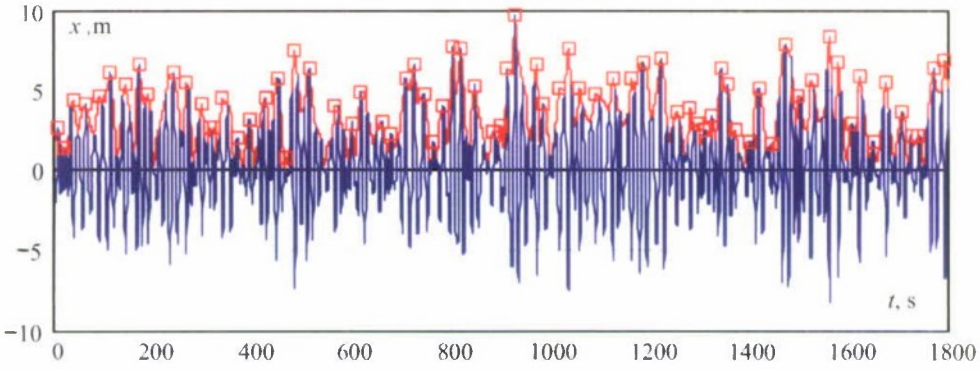

Figure 5.38 Peak based envelope (red) and its maxima: zero-speed case

This explains applicability of the truncated Rayleigh distribution, as shown in Figure 5.39 (b), while the Rayleigh distribution as whole remains inapplicable (see Figure 5.39 (a)). Also, this applicability can be used to justify the assumption made earlier for using formula (5.40) for the rare solution.

However, the applicability of the truncated Rayleigh distribution was judged based on the Pearson chi-square goodness-of-fit test, which did not reject this hypothesis for a particular dataset. So, at least, this applicability needs to be checked for all three datasets considered. The results of this check are summarized in Table 15. Note that without removal of a single outlier in the last bucket of the histogram for the Alternative Dataset 1, the goodness-of-fit test would reject the hypothesis for all starting values with an exception of 10.25 m.

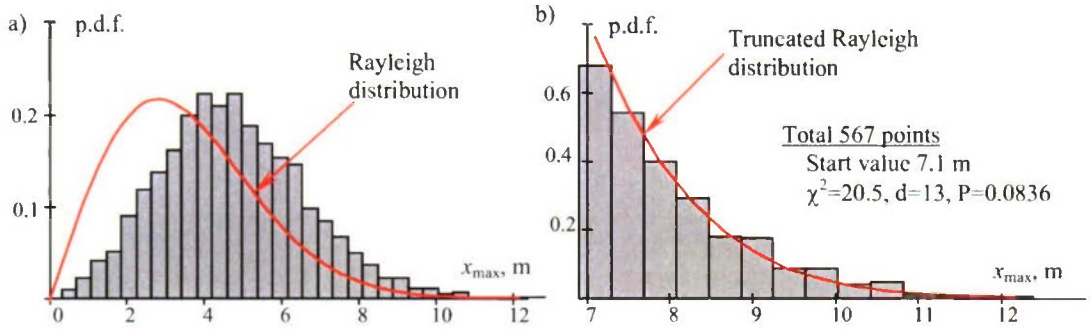

Figure 5.39 Distribution of maxima of the peak based envelope superimposed with Rayleigh distribution (a), truncated Rayleigh distribution. Zero-speed case

Table 15. Applicability of Truncated Rayleigh Distribution for Maxima of Peak-Based Envelope for the Zero-Speed Case

Dataset	Start value	Number of points	Value of χ^2	d	P	Comment
Original	7.10	567	20.5	13	0.0836	
Alternative 1	6.40	876	27.1	17	0.0566	Remove an outlier in the last bin
Alternative 2	6.44	931	24.6	14	0.0776	

5.4.3. Extrapolation with the Distribution of the Peak-Based Envelope

As it was noted above, there is no exact theoretical solution to perform a correct comparison with extrapolated estimate of peak-based envelope upcrossing of the zero speed case. There is one approximate solution based on the regression formula for the non-rare problem and two theoretical solutions known not to be completely applicable in this case. These solutions are the theoretical rate of the both-sides crossing and upcrossing rate of the theoretical envelope. The comparison may yield interesting information, however, strictly speaking, this comparison cannot be used to validate or invalidate the method.

Figure 5.40 shows the breakpoints based on an approximate solution, the theoretical rate of the both-sides crossings, and the rate of upcrossing of theoretical envelope. Surprisingly, they are not much different, with the lowest point at about 13 m. A similar picture can be seen in Figure 5.41 and Figure 5.42, except from 7.8-8.6 m in Figure 5.42.

There is one important detail of how the breaking point was calculated. The rate of upcrossing of the theoretical envelope may be significantly different from an

approximate solution as the latter is based on the regression formula for the upcrossing of the peak-based envelope. As it was shown in Section 4, the rate of upcrossing for theoretical and peak-based envelope is quite different for the zero-speed case. Therefore, it may be expected that the rate of the theoretical envelope may be outside of the confidence interval of the extrapolated estimate, especially for the lower threshold, where confidence interval is relatively narrow.

This is exactly what is observed in Figure 5.43. The alternative data set 2 clearly illustrates this effect. The inset of Figure 5.43 zooms in the initial range of curves.

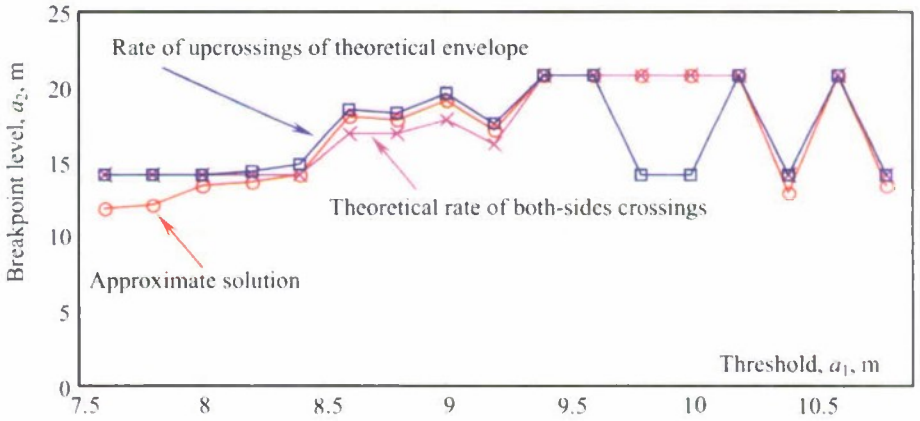

Figure 5.40 Breakpoint level (the level below which the extrapolation is still good) vs. threshold for the extrapolation based on fitted distribution of maxima for zero-speed case.

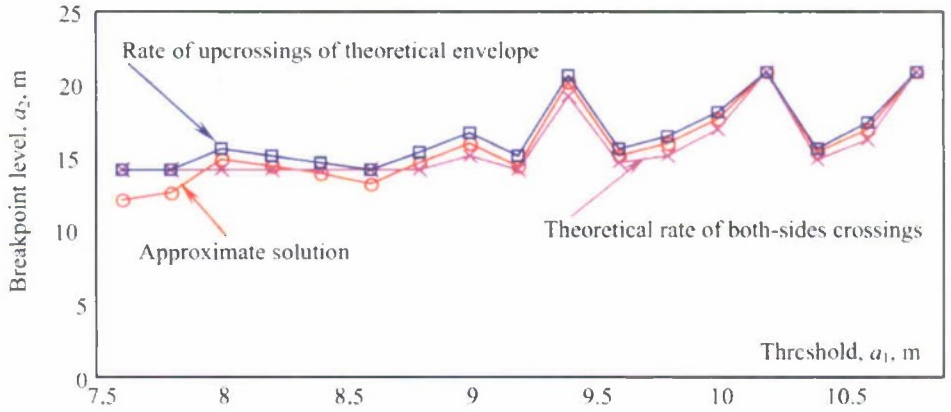

Figure 5.41 Breakpoint level (the level below which the extrapolation is still good) vs. threshold for the extrapolation based on fitted distribution of maxima for zero-speed case. Alternative data set 1

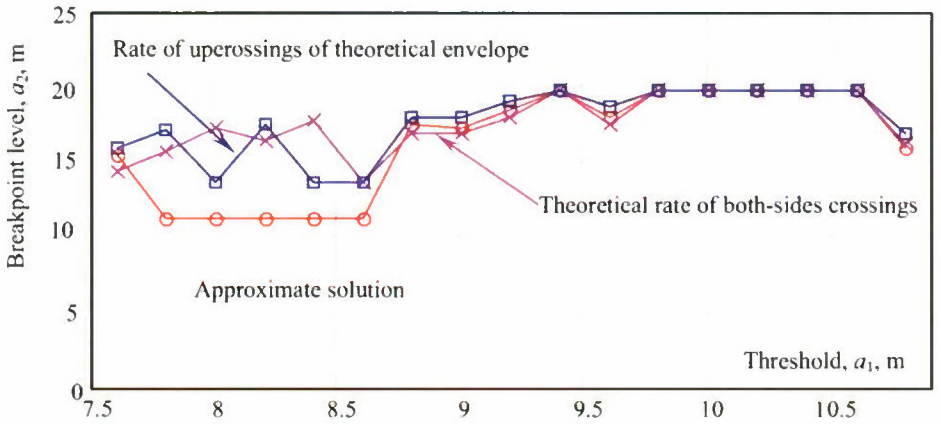

Figure 5.42 Breakpoint level (the level below which the extrapolation is still good) vs. threshold for the extrapolation based on fitted distribution of maxima for zero-speed case. Alternative data set 2

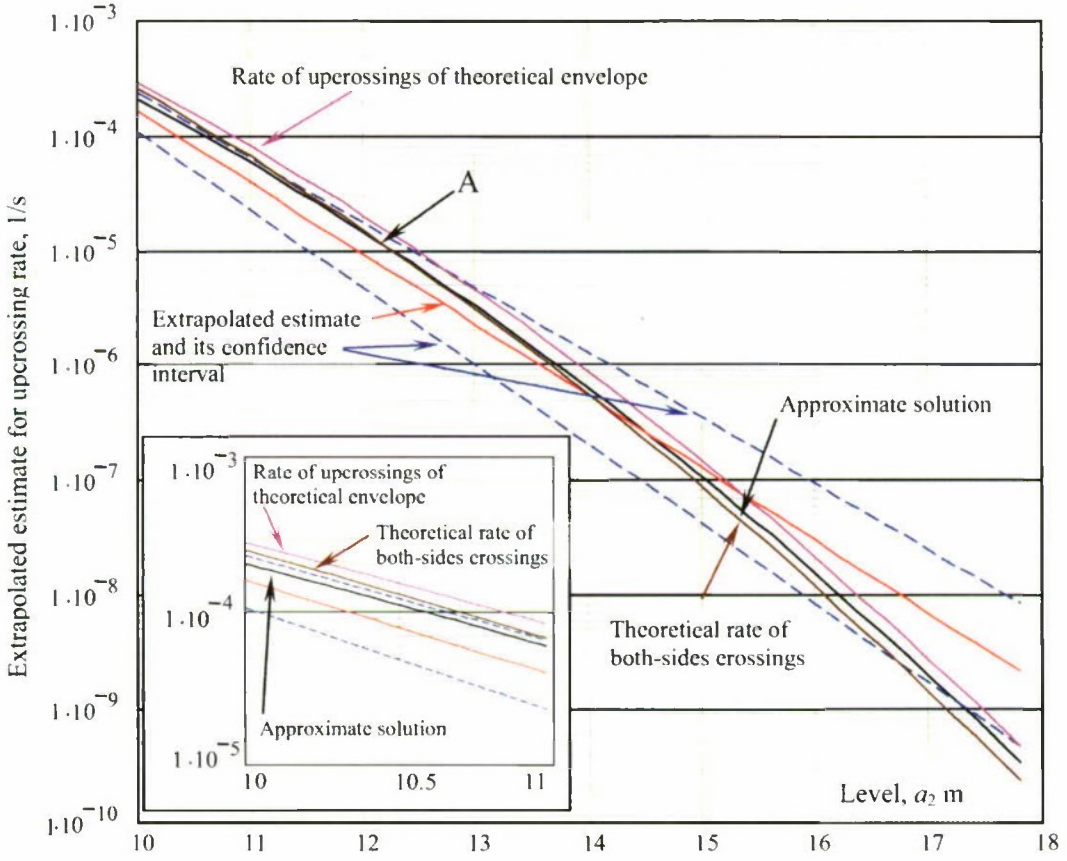

Figure 5.43 Extrapolated estimate of upcrossing rate of the peak-based envelope with confidence interval as a function crossing level. The threshold is 9 m, 227 peaks, alternative set 2

As it ean be clearly seen from Figure 5.43, the curve of the rate of the upcrossing of the theoretical envelope starts outside of the confidence interval of the extrapolated estimate. Then, somewhere around 13 m, it enters the eonfidenee interval. Then, it leaves the confidence interval just short of the level of 18 m.

Behavior of the theoretical rate of the both-sides crossing is somewhat similar. It also may start outside of the eonfidence interval. The reason is that sevcral both-sides crossing evcnts may be covered by one peak-based envelope upcrossing, say, for example, if two neighboring positive peaks happen to be above the threshold (see Figure 5.44). That is why the theoretical rate of the both-sides crossing is larger than the extrapolated estimate and the approximate solution for relatively lower levels. However, once the level increases thc situation, similar to the one shown in Figure 5.44, becomes very rare. Only one peak at a time has a chance to be above thc level. This makes the both-sides crossing rates eonverge and even eross the approximate solution in point A from Figure 5.43. As there is no reason why the theoretical rate of the both-sides crossing should be lower than the uperossing rate of the peak-based envelope, further behavior of thc curve can be explained by an approximate naturc of the solution that used the regression formula.

Behavior of theoretical rate of the both-sides crossing and rate of the theoretical envelope was compared and discussed earlier, see Figure 5.15.

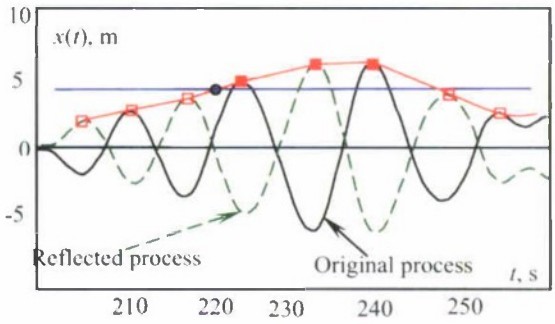

Figure 5.44 On difference between envelope-base peak crossing and both side crossing

Concluding the discussion, both the theoretical rate of the both-sides crossing and the upcrossing rate of thc theoretical envelope may take values outside of the confidence interval of the extrapolated estimate for lower thresholds. However, both curves may enter the confidence interval for larger values of the threshold. Therefore, it makes sense not to start the search for the breaking point from the very beginning. The level 13.25 m was used as an initial for the Figure 5.40 through Figure 5.42.

The breaking point for the approximate solution, however, was searched for starting from the very beginning. This made a differenee only in Figure 5.42 in the range of 7.8-8.6 m. If the breakpoint for the approximate solution is searched for starting at the level 13.35 m, like for other solutions, the flat segment disappears, see Figure 5.45.

Figure 5.46 shows how the approximatc solution has left thc confidence interval around 9.5 m and has re-entered it around 11.5 m. Possibly, the reason of such behavior is usage of the regression formula in the approximate solution that generally increases the

level of uncertainty. Figure 5.46 shows the approximate solution that stays very close to the upper boundary of the confidence interval. Also this problem does not exist for higher thresholds. This needs to be taken in to account when choosing the range of averaging.

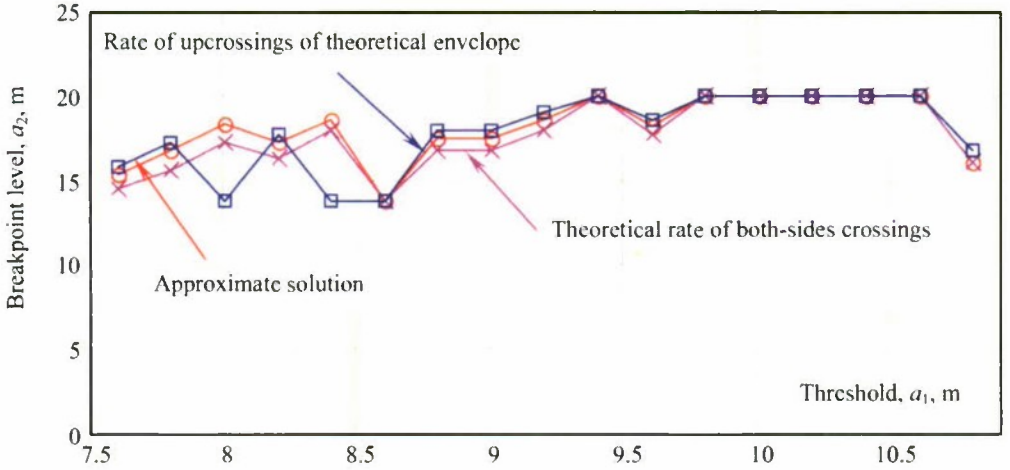

Figure 5.45 Breakpoint level (the level below which the extrapolation is still good) vs. threshold for the extrapolation based on fitted distribution of maxima for zero-speed case. Alternative data set 2

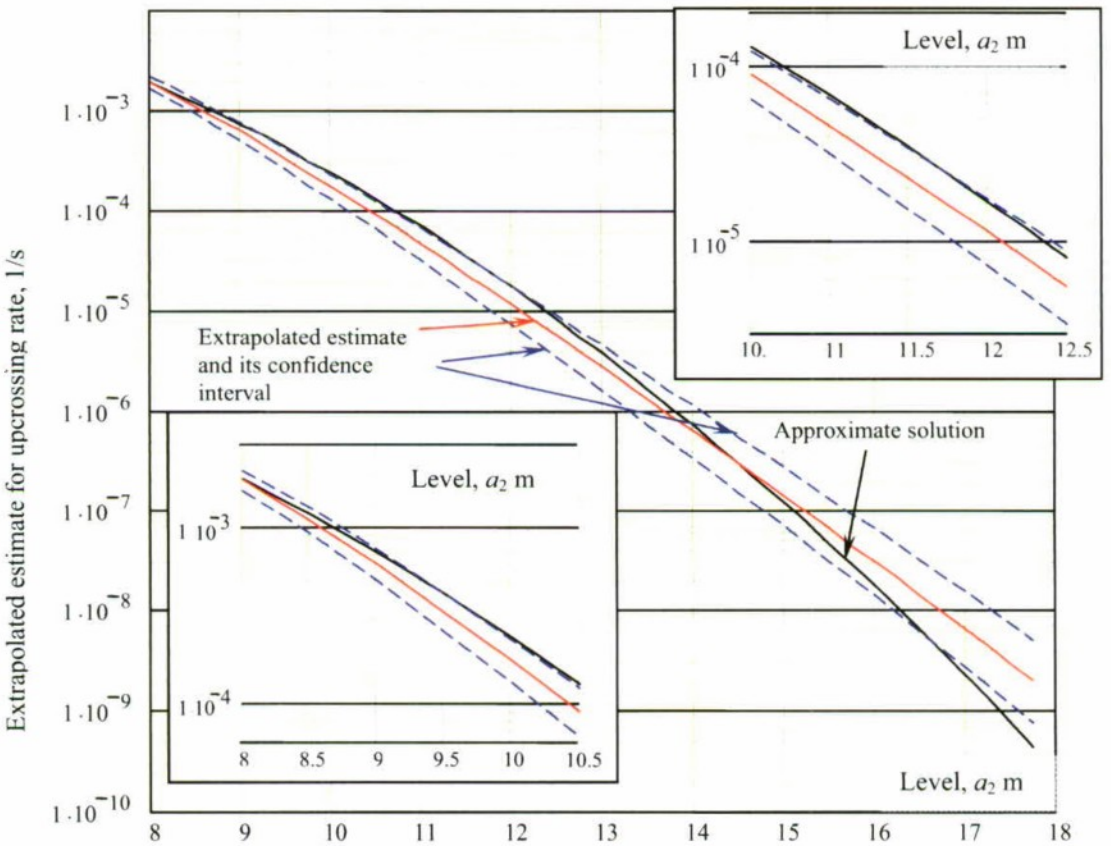

Figure 5.46 Extrapolated estimate vs. approximate solution for the threshold 7.8 m 791 peaks, alternative data set 2

5.4.4. *Averaged Extrapolation Based on Weibull Fit of Maxima*

The complete extrapolated solution plotted for different threshold levels (see Figure 5.47) shows some spreading of the extrapolated estimate around the theoretical solutions, therefore the averaging with formulae (3.46) and (3.47) can improve accuracy of the estimate. Figure 5.48 shows the averaged estimates for the different levels of the original dataset.

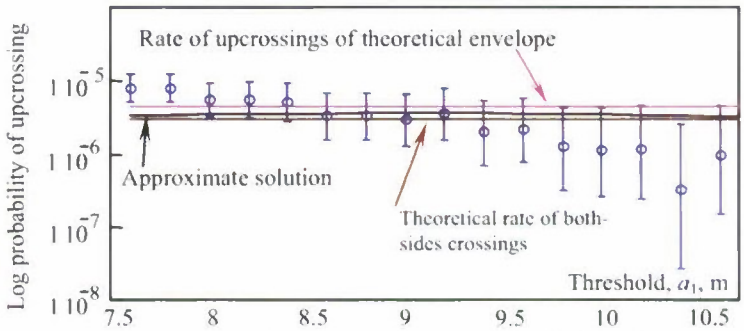

Figure 5.47 Statistical extrapolation of the upcrossing rate of peak-based envelope - complete solution for the level of 13 m based on distribution of peak-based envelope

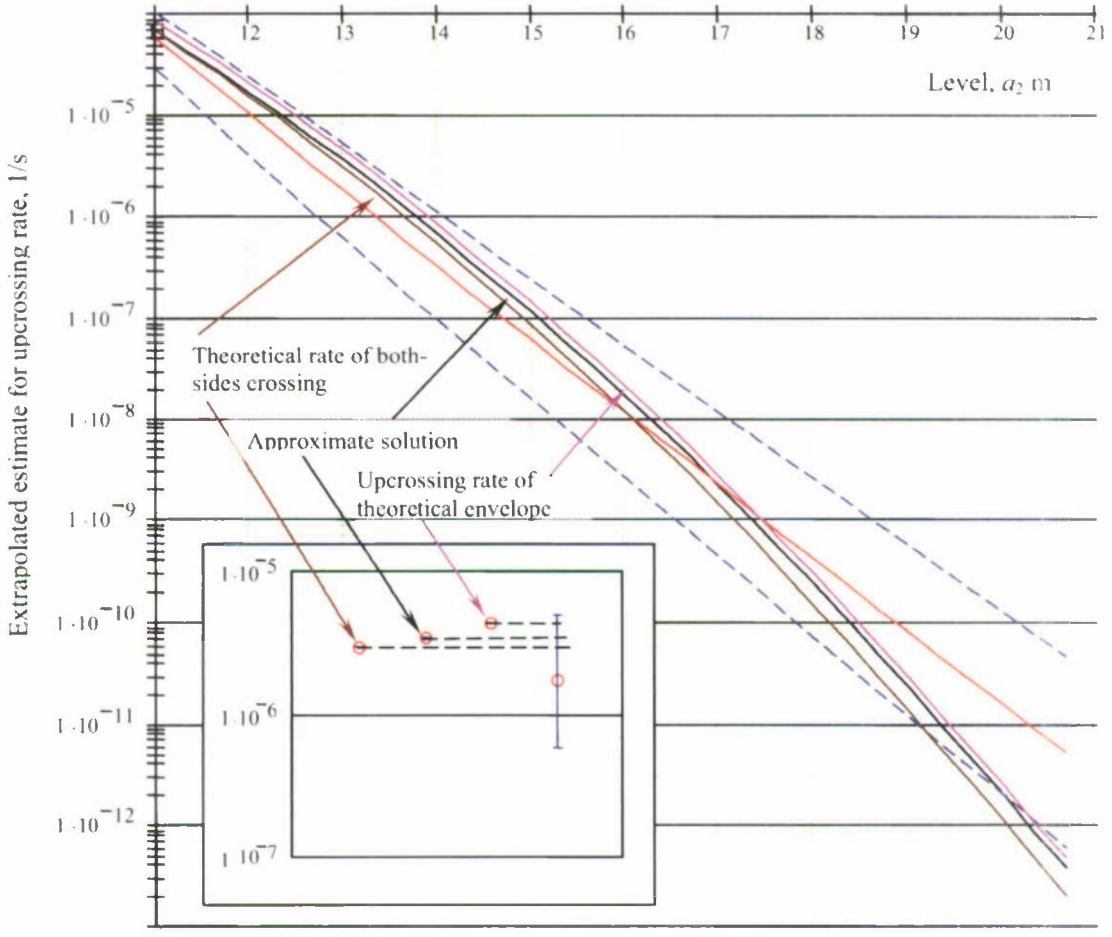

Figure 5.48 Averaged estimate of rate of upcrossing of the peak-based envelope extrapolated using Weibull fit of maxima. Insert shows the level of 13 m

Values of breakpoints of averaged estimates for all datasets are shown in Table 16. The averaging was done with the following rule: the highest threshold should have at least 30 points. The lowest threshold is half-way back from the highest threshold to the level where the Poisson flow is still applicable. This is an empirical rule based on the observation that the higher thresholds tend to perform better for the extrapolation based on the Weibull fit of maxima.

Table 16. Breakpoints for Averaged Estimates based on Weibull Fit of Maxima

Dataset	Breaking point m		
	Approximate solution	Theoretical rate of both-sides crossing	Upcrossing rate of theoretical envelope
Original	20.3	19.3	20.3
Alternative Set 1	15.75	15.25	16.25
Alternative Set 2	19.3	18.8	19.8

5.4.5. Extrapolation Based on Extreme Value

The procedure applied for extrapolation based on the extreme value distribution for the zero-speed case is exactly the same as it was for the following wave case. Figure 5.49 illustrates that while collecting data, only one point in Window 1 was collected as the maximum value, despite that there was one more peak exceeding the sample threshold of 9 m; there is only one point in Window 2 that is above the threshold.

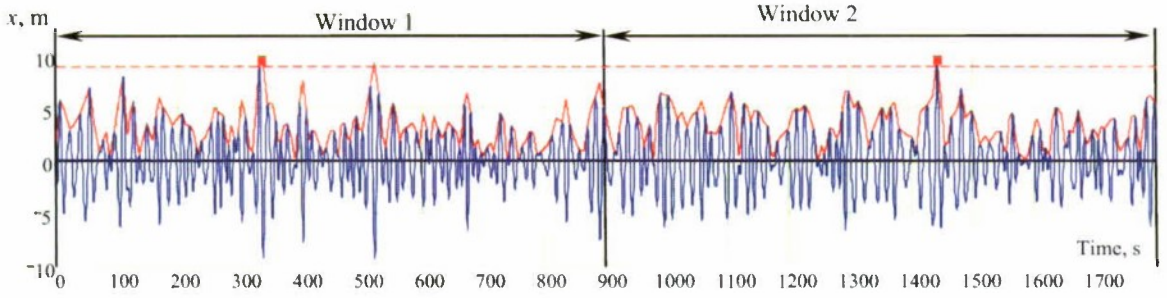

Figure 5.49 Collecting data for extreme value distribution, threshold 9 m, zero speed case

Since there is no exact theoretical solution the results may be compared with the same three solutions used for the extrapolation based on the Weibull fit of the maxima. Besides the approximate solution based on regression formula for the non-rare problem, these solutions include the theoretical rate of the both-sides crossing and upcrossing rate of theoretical envelope.

As it can be seen from the discussion in the previous subsection, the difference between these solutions is not that large, especially in comparison with the width of the confidence interval for the extrapolated estimate. Some difference was found for relatively low values of the threshold where two theoretical solutions could go outside of the confidence interval and this has to be accounted for while calculating the values of breakpoints.

The breakpoint values of the extrapolation based on the extreme value distribution are shown in Figure 5.50 through Figure 5.52 for all three data sets.

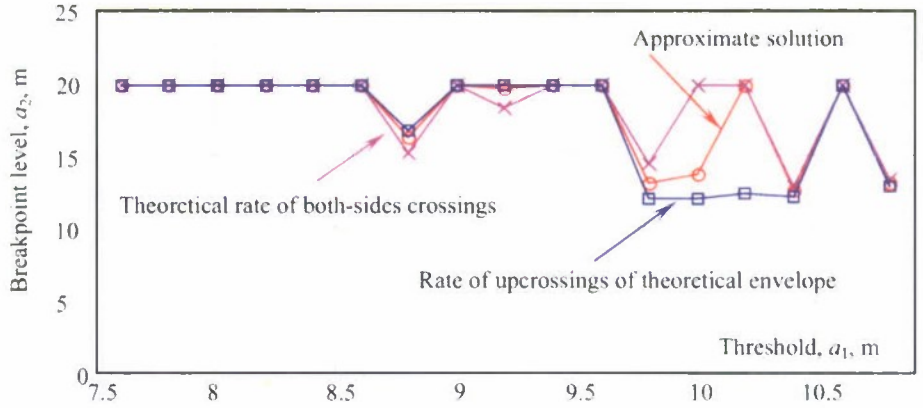

Figure 5.50 Breakpoint level (the level below which the extrapolation is still good) vs. threshold for the extrapolation based on extreme value distribution for zero-speed case. Original data set

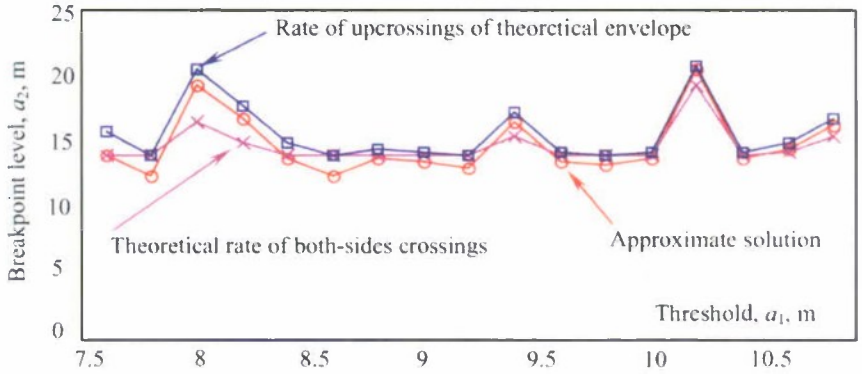

Figure 5.51 Breakpoint level (the level below which the extrapolation is still good) vs. threshold for the extrapolation based on extreme value distribution for zero-speed case. Alternative data set 1

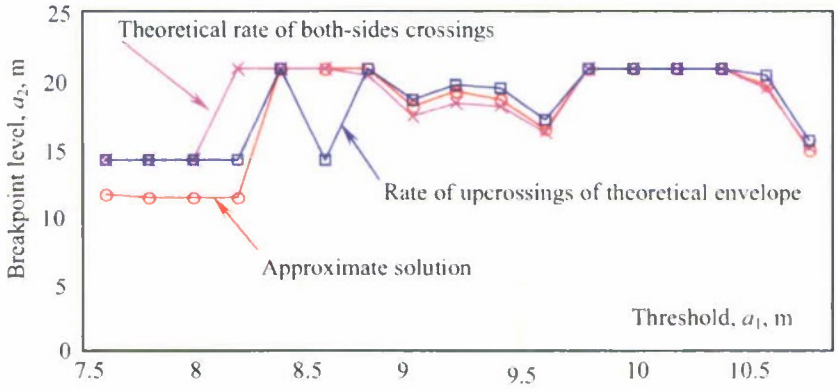

Figure 5.52 Breakpoint level (the level below which the extrapolation is still good) vs. threshold for the extrapolation based on extreme value distribution for zero-speed case. Alternative data set 2

Behavior of all three solutions in terms of the breakpoints are pretty similar and do not require any additional comments with the exception of Figure 5.52 where results for Alternative data set 2 are shown. All of the curves have a flat segment in the range of thresholds 7.5-8.2 m. This is an area where relatively poor performance was observed. The approximate solution left the confidence interval around the 11 m level and the two other solutions never entered the confidence interval at all. The rest of the threshold values have shown normal performance.

The averaging procedure was applied for all of the thresholds while the number of data points was above 30. The result for the original data set is shown in Figure 5.53. As one can see from this figure, all three solutions stay within the confidence interval until the level of 19.5 m was reached. The inset in Figure 5.53 shows the comparison between theoretical solutions and both extrapolated estimates for the level of 13 m.

The results on the breakpoints of the averaged extrapolated estimates based on the extreme value distribution are shown in Table 17.

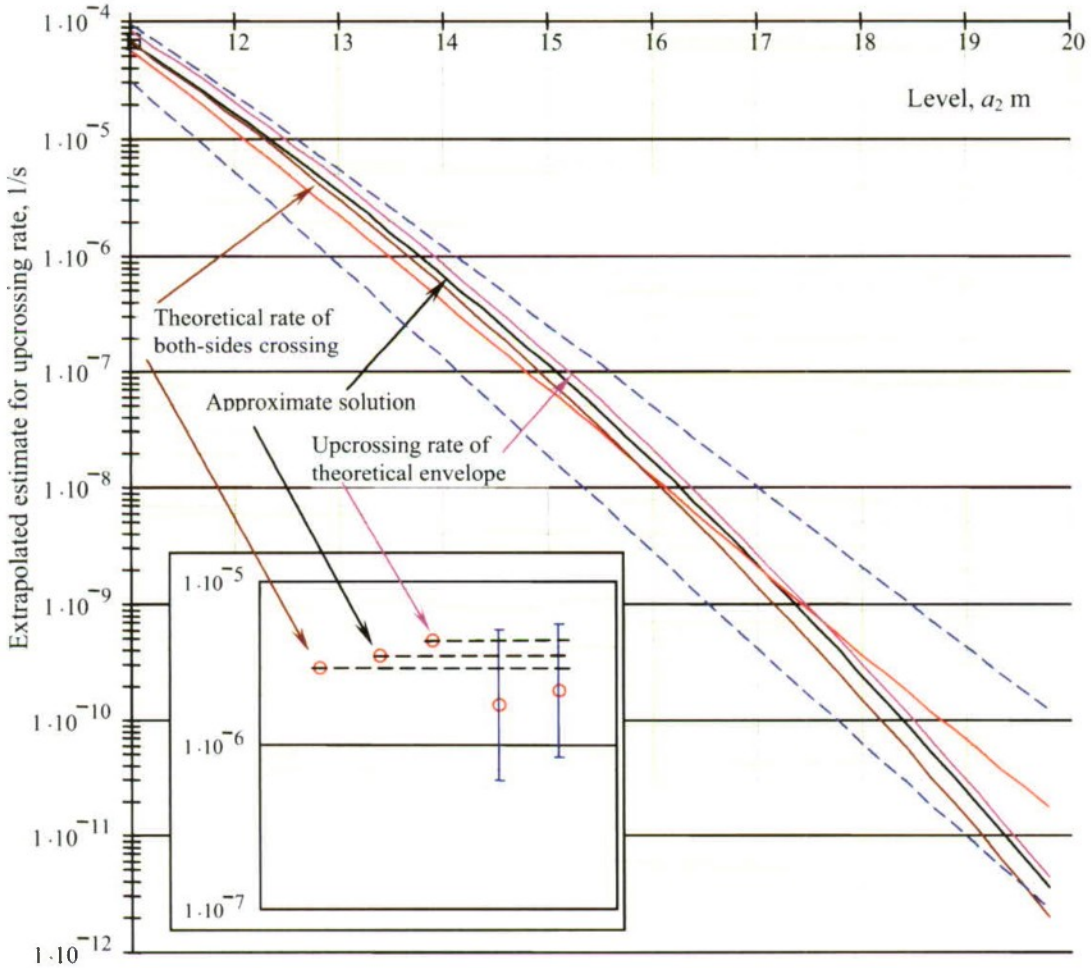

Figure 5.53 Averaged estimate of rate of upcrossing of the peak-based envelope extrapolated using extreme value distribution. Insert shows the level of 13 m

Table 17. Breakpoints for Averaged Estimates based on Extreme Value Distribution

Dataset	Breaking point m		
	Approximate solution	Theoretical rate of both-sides crossing	Upcrossing rate of theoretical envelope
Original	20.3	19.3	20.3
Alternative Set 1	13.75	15.25	14.5
Alternative Set 2	19.25	18.75	19.75

The lowest breakpoint in Table 17 is 13.75 m. It corresponds to the mean time to event of 11.89 days. So in order to get a statistically credible estimate, say, 10 events are needed. These 10 events may require almost 120 days worth of data. At the same time the method allowed us to get the estimate with only about 4 days of data (100 hours). So 120 days, or 2880 hours, was reduced to 100 hours by the use of the method. That said, the efficiency of the method in the worst case resulted in a data reduction factor of 28. Averaging the breakpoint between all three cases brings it to 17.77 m and the data reduction factor up to 71,260. These data, however has to be considered preliminary, as more performance checks are expected.

5.5. Summary

The principal objective of this work is to find a practical solution for the probability of a partial stability failure during a given time. The goal of this section is to find out how to use the Peak-Over-the-Threshold (POT) method for partial stability in the form of a large roll event.

The large roll event is equally dangerous on either side of a ship. Therefore it should be described as a random event of "both-sides crossing", a combining an upcrossing of a level on the positive side or downcrossing of a level on the negative side. If the boundary is the same for both sides and the process has symmetric distribution, the rate of the both-sides crossing is equal to twice of the rate of the upcrossing. The Poisson flow assumption is only applicable for a relatively high level of both-sides crossings, as upcrossing and downcrossing events occurring during one period are not independent.

An upcrossing of the envelope of the process is a random event, theoretically equivalent to the both-sides crossing. Poisson flow is applicable to the envelope upcrossing. Also, the envelope upcrossing is equivalent to a random event that an absolute value of a peak has exceeded that level. Since the peaks of the envelope are used, the new version of the method is call "Envelope Peaks-Over-the-Threshold" (EPOT).

The problem of the upcrossing of the peak-based envelope is that it does not have a closed-form solution for a generic spectrum even for a normal process. Nevertheless such a solution is needed to compare results of sample calculations. If a spectrum is narrow, then the peak-based envelope is a close approximation for the theoretical envelope. As a result, the formula for the upcrossing of the theoretical envelope of a normal process can be used. Therefore, only the example with a narrow-band spectrum can be used to complete the theoretical checking of the EPOT method.

To check the method using the example of a generic spectrum, an approximate solution is needed. Following the principle of separation, such a solution can be presented in the form of non-rare and rare sub-problems. The non-rare sub-problem is just an upcrossing of the peak-based envelope. It can be approximated by fitting a regression formula to the statistics of upcrossings. The solution of rare sub-problems is the probability that a process will exceed a given level if it has crossed a threshold below that level. This solution can be developed using the fact that absolute values of peaks of a normal process follow truncated Rayleigh distributions starting at a certain value. This value depends on a bandwith of the spectrum.

Finally, the EPOT method was checked against both examples and shows quite satisfactory performance with average data reduction factors of 290,500 and 71,260 respectively.

6. Algorithm Implementation

This section describes the reference implementation of the EPOT algorithm. The reference implementation is coded in Matlab (requires Matlab R2008a or later).

6.1. Envelope Construction

6.1.1. Peak Definition for the Process

Two definitions of a peak are implemented and may be used to define the envelope, then to define the peaks of the envelope. The first definition, referred to as a "zero-crossing peak" (ZC), defines a peak as the maximum value between a zero up crossing and a zero down crossing. Negative peaks (troughs) are computed as the minimum value between a zero down crossing and a zero upcrossing and then reflected about zero.

Alternatively, peaks may be defined as local maxima. In this formulation, a particular point is considered to be a peak if it is greater than the three previous and three following points.

The zero-crossing peak method is used for two reasons. First, the zero-crossing method is much more reliable on signals that have noise. Several assumptions (related to noise frequency, the motion frequency, sampling rate, etc.) need to be made (or filtering employed) to find the peaks on a noisy signal. Second, the zero-crossing method removes secondary peaks, which are not of interest to us.

6.1.2. Envelope Definition

To construct the composite peak-based envelope, the negative peaks are reflected about the reference level. For a process such as the rolling of a ship, this reference level is zero, since deviations from upright are what are important, not deviations from the mean value. For cases where deviations from the mean value are important, the signal should be de-meaned (and the levels of interest should be given relative to the mean of the process). The time history of the envelope is constructed through linear interpolation between the peaks at the sampling frequency of the input signal.

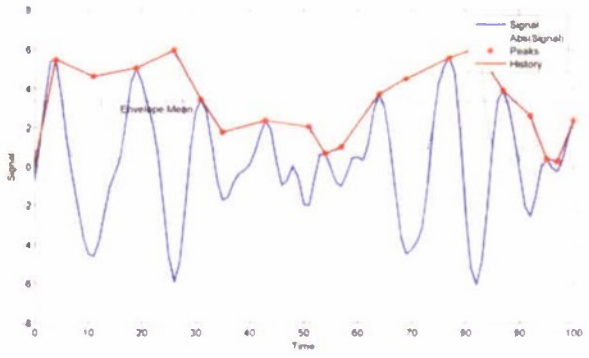

Figure 6.1. Sample Envelope With Linear Interpolation

6.1.3. Peak Definition for the Envelope

The peaks of the envelope are defined in a similar manner to the peaks of the signal. Instead of utilizing zero crossings, mean crossings of the envelope are used. The mean of the envelope is computed using the interpolated time history and the envelope peaks are the maxima and minima between mean crossings. Only the peaks above the envelope mean are used further in the algorithm.

6.2.Candidate Threshold Selection

Initially sixteen thresholds are defined. These thresholds are linearly spaced between the mean value of the envelope time history and an upper threshold. The upper threshold is defined by the requirement that we have at least 30 points to fit a distribution. The peaks of the envelope are sorted in descending order and the 31st entry in the sorted list is the upper threshold.

The candidate thresholds are analyzed for the applicability of Poisson Flow to exceedanees of the thresholds (using the envelope peak data). The tests for Poisson Flow applicability are discussed in Section 6.3. The lowest threshold that passes both tests for Poisson Flow applicability is taken as the lowest threshold for use in the statistical extrapolation. A new set of eight thresholds is linearly distributed between this lower threshold and the upper threshold deseribed in the above paragraph.

6.3.Analysis of Poisson Flow Applicability

Sections 1.3.5 and 5.1.3 describes two methods for assessing the applicability of Poisson Flow for a given threshold, chi-squared Pearson Test and a Kolmogorov-Smirnov Test (KS Test).

6.3.1. Pearson χ^2 Test

In a Pearson chi-squared test, the hypothesis is posited that the number of events in a certain time span is distributed via a Poisson distribution. To carry out this test, the envelopes derived from the time histories are first eoncatenated together. The peaks of the envelopes have already been found, so there are no peaks at the concatenation point. A window size (time span) is then defined to count events (peaks over the threshold). This time span is computed as:

$$WindowSize = \frac{T_{Sample}}{N_{POT}} \tag{6.1}$$

Where T_{Sample} is the total duration of the coneatenated envelopes and N_{POT} is the total number of peaks above the threshold in question. Defining the window size in this way generally limits the maximum number of events in a given window to about 4. This essentially sets the intensity (the single parameter) of the Poisson distribution to 1.0. The

concatenated envelope is then divided into sections each with a length of the window size. The number of POT in each window is counted. A Poisson distribution is fit to this data set using the maximum likelihood method. A good starting point for the intensity of the distribution in the fitting process is the mean number of events per window. This process is repeated for window lengths of 0.8 and 1.2 times the original length. The goodness of fit metric is then averaged between the three window spans. This is done since there is some variability of the results with window size due to the random process and the finite record length.

See Figure 6.2 for a sample PDF used for the chi-squared test. If the averaged goodness of fit metric is above the accepted significance level (0.05), then the distribution fit is accepted and one of the two criteria for Poisson Flow at this threshold is satisfied.

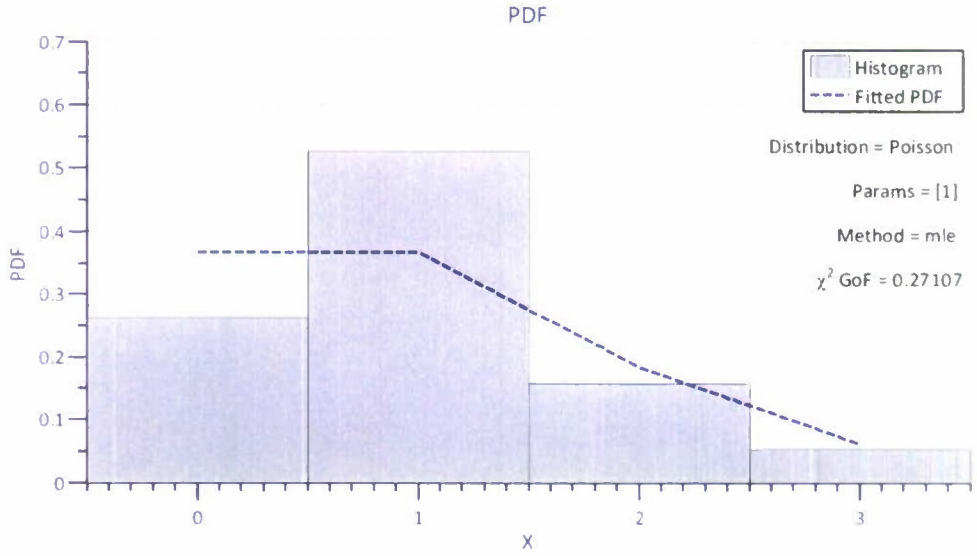

Figure 6.2. Sample Distribution Fit to Number of Events in Time Window

6.3.2. Kolmogorov Smirnov (K-S) Test

For the K-S Test, the empirical cumulative density function (CDF) of time with no event derived from the time history, is compared to the CDF that is computed using the exponential distribution and a statistically calculated mean crossing rate (see Section 6.4). The empirical CDF is derived from the time history as described in Section 1.3.4.

The smallest time window analyzed is based on the decay of the autocorrelation function of the process. The peaks of the autocorrelation function are found (using the zero crossing method) and the first peak with a value below 0.05 is found. The smallest time window is set to the time of this peak. If multiple records are available for a given condition, then the autocorrelation functions of the records are averaged before the peak search is performed. For short duration records, the computed autocorrelation functions can behave poorly (even after averaging); they do not decay as expected. The lack of decay is due almost entirely to a deficiency in the amount of data. If no peaks of the

averaged autocorrelation function are found to be below 0.05, then an alternative approach is taken. In this case, the peak based envelope of the autocorrelation function is computed and the time of first local minimum of the envelope is taken as the decay time.

Each window is examined to see if there is at least one event in it. An auxiliary variable p_1 is constructed that is equal to 1 if there is at least one event in the window and zero if there is no event in the window. The mean of p_1 is computed for each record. This value is the probability that at least one event will occur within the window. The windows are then grouped in sets of two and the process is reapeated for a window size twice as big. The original windows are then grouped in sets of three, etc. This combining of windows happens until one window is produced. For the case of multiple records, the probabilities are averaged across the records. This process creates the empirical cumulative density function (EDF) for the probability of at least one event occurring.

The theoretical CDF is then computed using the exponential distribution, as in equation (1.38). The K-S Test is carried out between these two density functions using equations (1.126), (1.127), and (1.129). Because of the limited data set, the EDF can become unrealiable for high values of probability. For this reason an upper limit is set, above which the comparison, using equation(1.126), neglects the data. The upper limit on the EDF is typically set at 0.65 (in terms of probability). The goodness of fit is only checked for values below this.

6.4.Calculation of Threshold Exceedance Rates

6.4.1. Esimate of Threshold Exceedance (Upcorssing) Rate

The threshold exceedance (upcrossing) rates are computed statistically. For the EPOT method the threshold crossing rate is given by:

$$\lambda = \frac{N_{POT}}{T} \tag{6.2}$$

Where N_{POT} is the number of peaks above the threshold and T is the total duration of the sample. Equation (6.2) is derived from equation (3.19).

The threshold crossing rate is not strictly needed when the extreme value distribution is used for the rare problem (EVPOT method). It may, however, be computed as follows:

$$\lambda = -\frac{1}{T} \cdot \ln\left(1 - \frac{N_{MOT}}{N_{Maxima}}\right) \tag{6.3}$$

Where N_{MOT} is the number of maxima over the threshold, N_{Maxima} is the total number of maxima, and T is again the total sample time. Equation (6.3) is equivalent to equation (2.60). Here, the quantity (N_{MOT}/N_{Maxima}) is the probability that a given maximum value will be above the threshold and the quantity ($1 - N_{MOT}/N_{Maxima}$) is the empirical CDF for the sample maxima.

6.4.2. *Esimate of Confidence Interval for Threshold Exceedance Rate*

The confidence interval on λ is computed by first computing the confidence interval for N_{POT} or N_{MOT}. Since each of these quantities may be considered the result of a set of Bernoulli trials, we may use the binomial distribution to compute the confidence interval.

The binomial distribution has two parameters, commonly taken as n and p. n is the number of trials (in our case the number of time steps) and p is the probability that any particular time step is a peak (or extremum) over the threshold. p is given simply by:

$$p = \frac{N_{POT}}{n} \tag{6.4}$$

The upper and lower bound of the confidence interval of the estimate of λ are then given by:

$$\lambda_{UB} = \frac{Q_{Binomial}\left(1-\beta/2 \mid n, p\right)}{T};\ \lambda_{LB} = \frac{Q_{Binomial}\left(\beta/2 \mid n, p\right)}{T} \tag{6.5}$$

Where β is the complimentary to confidenceprobability, Q is a function invere to CDF.

If n is sufficiently large (above 200), then a normal distribution may be substituted for the binomial distribution, since the factorials for the binomial distribution can be difficult to compute for large n. In this case one would use the mean and variance of the binomial distribution ($n \cdot p$ and $n \cdot p \cdot (1-p)$, respectively) as the parameters of the normal distribution. Details of theoretical background is given in Section 1.2.

6.5. Distribution Fits to Peaks/Maxima Over the Threshold

A two-parameter Weibull distribution is fit to the peaks and maxima over the threshold. Application of the method of maximum likelihood estimation (MLE) was discussed in Section 2.1.4. However, independent review of this work suggested that, when fitting a Weibull distribution with a shape parameter close to 1.0, the MLE method is known to have convergance issues. In general, the peak and maxima data being fit have this character. It was suggested that a least squares fitting approach may be more appropriate. For this reason the distribution is fit using a least squares fit to the empirically derived cumulative distribution function (EDF). The EDF is derived by ordering the data from smallest to largest. The EDF of a given value located at position i in the ordered set is computed as:

$$EDF_i = \frac{i}{n_{samples} + 1} \tag{6.6}$$

Where i is the index (starting at 1) of the value in the ordered set and n is the number of peaks or maxima over the threshold in the data set. A minimization of the squared error between the EDF and computed CDF is then performed by adjusting the Weibull distribution parameters.

6.6.Calculation of Exceedance Rates for Levels of Interest

6.6.1. Esimate of Level Exceedance Rates

Finally, the exeeedance rates for the levels of interest are eomputed. The ealeulation is comprised of the threshold erossing rate and the distribution fit to the peaks/maxima over the threshold. For the rare problem usng distribution fit (details are given in 3.3.1), λ_2, for an arbitrary level, a_2, is given by:

$$\lambda_2 = \lambda_1 \cdot \left(1 - F_{POT}(x < a_2)\right) \tag{6.7}$$

Where λ_1 is the threshold erossing rate and F_{POT} is the CDF for the distribution of envelope peaks over the threshold.

When the extreme value distribution is used for the rare problem (see subsection 3.3.3), we first compute the probability that a given maximum value is over the threshold:

$$p_{MOT} = \frac{N_{MOT}}{N_{Maxima}} \tag{6.8}$$

Where N_{Maxima} is the total number of maxima and N_{MOT} is the number of maxima over the threshold. Defining p_{MOT} allows easier definition of the eonfidenee interval on λ_2 in the subsequent section. The exceedanee rate, λ_2, is then given by:

$$\lambda_2 = -\frac{1}{T}\ln\left(1 - p_{MOT} \cdot (1 - F_{MOT}(x < a_2))\right) \tag{6.9}$$

Where F_{MOT} is the CDF of the distribution of maxima and T is the total duration of all sample data.

6.6.2. Esimate of Confidence Interval for Level Exceedance Rates

For the rare problem using the simple distribution fit for peaks, the eonfidence interval on the level exeeedanee rates is a eomposite value of the confidence intervals for the threshold erossing rate and the distribution fit.

$$\begin{aligned} \lambda_2^{UB} &= \lambda_1^{UB} \cdot \left(1 - F_{POT}^{UB}(x < a_2)\right) \\ \lambda_2^{LB} &= \lambda_1^{LB} \cdot \left(1 - F_{POT}^{LB}(x < a_2)\right) \end{aligned} \tag{6.10}$$

For the rare problem using extreme value distribution, we first define the eonfidenee interval on p_{MOT}. This is done using equation (6.5), where n is the total number of maxima and p is p_{MOT}. The confidenee interval on the exeeedanee rate is then given by:

$$\begin{aligned} \lambda_2^{UB} &= -\frac{1}{T}\ln\left(1 - p_{MOT}^{UB} \cdot (1 - F_{MOT}^{UB}(x < a_2))\right) \\ \lambda_2^{LB} &= -\frac{1}{T}\ln\left(1 - p_{MOT}^{LB} \cdot (1 - F_{MOT}^{LB}(x < a_2))\right) \end{aligned} \tag{6.11}$$

6.6.3. Averaging of Results for All Thresholds

As discussed in section 6.2, the level exceedance rates are computed using eight different thresholds. After computing the level exeeedanee rates using each threshold, the results for all thresholds are averaged together. This is actually done by averaging the logarithm of the erossing rate estimates as follows:

$$\lambda_{avg} = 10^{\left(\frac{1}{n_{Thresholds}} \cdot \sum_{i=1}^{n_{Thresholds}} \log(\lambda_i) \right)} \tag{6.12}$$

Where $n_{Thresholds}$ is the number of thresholds and λ_i is the estimate of the level crossing rate for threshold i.

This log averaging method is used beeause we are generally interested in the order of magnitude of the level exeedanee rate estimates. It is possible that one of the estimates is several orders of magnitudes larger than the others. In this case the order of magnitude of the result of straight averaging is the order of magnitude of the outlier divided by the number of estimates (eight in our case). That is, the presence of the outlier ean greatly skew the order of magnitude of the result if straight averaging is used.

6.7. Summary

The algorithm of EPOT (as implcmented) eonsists of the following steps:

1. Seareh for zero-erossing peaks.
2. Evaluate peak-based envelope by refleeting negative peaks and using linear interpolation.
3. Caleulation of the mean level of thc envelope and searching for the mean-crossing peaks of the envelope.
4. Define 16 thresholds; the upper threshold must have at least 30 peaks of the cnvelope above it; the rest of the thresholds arc linearly spaced between the upper threshold and the mean of the envelope.
5. Check Poisson flow applicability for each threshold with both Pearson chi-squared test and Kholmogorov-Smirnov test. The thresholds where both tests that passed are retained.
6. Estimate the threshold exceedance (upcrossing) rate and its confidence interval for eaeh threshold.
7. Evaluate empirical cumulative distribution funetion for peaks of the envelope, exceeding each threshold; fit two-parameter Weibull distribution with the least squares method. Calculate boundaries of eonfidenee interval for the fit.
8. Fit the two-parameter Weilbull distribution as an extreme value distribution using speeified time-window for peaks of the envelopc exceeding each threshold. Calculate boundaries of confidence interval for the fit.
9. Calculate exceedanee (upcrossing) rate for the level of interest using results

for each threshold; calculate boundaries of confidence interval for each value of the exceedance rate.

10. Find the average exceedance rate over all the threshold and boundaries of its confidence interval. This is the final result.

7. Concluding Comments

7.1.The Problem

Given a time history of the response of a nonlinear dynamieal system; the probability of exeeeding a given level during a given time is to be found. It is understood that there are no (or statistieally insignifieant number) of observations that exceed this level. Therefore the formulated problem implies statistieal extrapolation.

7.2.The Approach

By the very essenee of any extrapolation method, it is a judgment on data outside of observed range, but based on the data within the observed range. Ship motions data are statistieally dominated by relatively small values laying in the linear range; therefore, an attempt to use all the data for statistieal extrapolation, in faet, leads to predietion based on a linear assumption. To avoid "unintentional lineanerization" of the problem, only large-value data that eontain information of nonlinearity of the dynamical system should be used for extrapolation. The methods that use only the data above a eertain threshold are known as "Peak-over-Threshold" (POT) methods.

The POT method ean be eonsidered as an implementaion of the principle of separation, when the problem of the estimate of a probability of rare event is divided in two: non-rare and rare. The non-rare problem is meant to be solvable with conventional statistical method. In the ease of the problem being considered, the non-rare is an estimate of exceedanee (uperossing) for a threshold that separates small-valued data in the linear range from the data where influenee of nonlinearity may be considered as "signifieant". The rare problem is aetual statistieal extrapolation using only the data above the threshold.

7.3.The Study

As the probability of exeeedanee is dependent on time of exposure, the relation between the probabity and the time was the first subject of this study. It was concluded that Poisson flow should be used to relate probability and the time of exposure. Applieation of the Poisson flow allows use of the exponential distribution for time before/between the events of exeeedanee/upcrossing and requires that events must be independent. Pearson-ehi-square and Kholmogorov-Smirnov goodness-of-fit test ean be used to eheek applicability of Poisson flow.

The extreme value theory was and is eonsidered as the main tool to address the problem of evaluation of the probability of exeeedanee with statistieal extrapolation. In order to relate this study with other work in the field, the relation between extreme value distribution and time was examined. It was found that the eorrect interpretation of extreme value distribution is inherenrly related with a eertain time duration. Extreme value distribution deseribes the behavior of the largest value observed during a given time.

Further consideration was focused on the properties of peaks. Obviously, if peak of the process exceeds the level, the process had exceeded the level. At the same time, the peak data are easier to work with as they do not depend on sampling rate; although consecutive peaks are not independent, the correlation between them is less in comparison with two consecutive values of the time history.

The rare problem can be formulated in two ways, that involve fitting the two-parameter Weibull distribution. However, if the Weibull distribution is fit to all the peaks above the threshold, it is used to smooth the histogram. The second way is based on the properties of the Weibull formula as one of three extreme value distributions when only the largest peak observed during a time window is used for the fit.

Assumption of independence of consecutive exceedances (upcrossings) may turn out to be over-restrictive for certain types of practical applications. One of them is analysis of motions in stern quartering seas while the ship has significant forward speed. The encounter spectrum becomes quite narrow due to Doppler effect. As a result, motion response becomes highly clustered; satisfying the independence clause may become non-trivial. Another important practical consideration is when exceedance of the level on both sides is an objective. In the latter case the assumption of independence generally is not applicable, with the exception of a few very specific cases. If a ship had a large roll angle on one side, then it is very likely to have a large excursion on the other side as the autocorrelation function stays fairly substantial after just half a period of the motions. For such applications, it makes sense to work with the envelope of the process rather than with the time history of the process itself.

It is very efficient to use an envelope with a narrow band process as the envelope changes significantly slower than the process itself. For a more general case, piecewise linear or peak-based envelope (linear interpolation between the absolute values of local or zero-crossing peaks) is found to be more robust. It was shown that statsistical extrapolation is based on the envelope peak over the threshold. Also, it was shown that the procedure for the envelope peaks does not differ much from the procedure with the peaks of the time history of the process.

A numerical example was used throughout the study. The data set for the numerical example consisted from 200 time histories of wave elevations. Each time history was 30 minutes long and was reconstructed from Bretschneider spectra with a Fourier series. Distribution of these wave elevations is normal, so the probability of exceedance during a given time is known from upcrossing theory in closed form. Application of the EPOT method to this data set shows quite satisfactory performance with average data reduction factors from 71,260 to 290,500 (the factor of how much more data would be needed to get the same result directly from statistics).

7.4.The Outcome

As a result of the work described in this report, the EPOT procedure was developed , justified and implemented. The procedure requires input of time histories that can be both numerical or experimemnatal origin. The output is an estimate of exceedance

(uperossing) rate that allows ealculation of probability of exeeedanee during a given time. As the EPOT proeedure is related with statistieal estimates, eonfidenee intervals are evaluated and earried out through the entire proeedure until the final result. The procedure was partially validated using wave elevation data.

7.5.Future Work

The present report describes statistieal aspeets of the method. However, both the threshold and the level of interest may be subject to additional limitation eoming from the dynamieal aspect of the problem.

The eore approaeh assumes that there is available data that earries information on thenonlinear properties of dynamical system, and this data is located above a eertain threshold. Setting minimum levels for the threshold eannot be performed based solely on statistical data as it requires knowledge of when the system becomes nonlinear. As the first expansion, for roll motion of conventional ship, this minimum threshold can be taken from the ealm water GZ curve that is the stiffness of dynamieal system in roll. For the most eonventional ships, the boundary between linear and nonlincar is around 10-12 degrees.

Another limitation is related to the maximum level of interest for which the EPOT results ean still be eonsidered legitimate. While there are no statistieal limitations on the level of interest, physical characteristics of the dynamical system do change with the level. The instantaneous GZ curve that plays a role of stiffness for roll motions must have a maximum. For most ships, there are three equilibria for roll: upright position, angle of vanishing stability and capsized position. Maximum of the GZ eurve can be considered a boundary between the attraetor at the upright position and repeller at the angle of vanishing stability. Therefore, the eharaeter of nonlinearity is quite different before and after the maximum angle of the GZ eurve. As the roll angles exeeeding the maximum of the GZ eurve are quite rare, the ehanees are that the rare problem will not have enough information on the behavior of the system beyond the angle of the maximum. Therefore the upper limitation of EPOT may be expeeted somewhere around the maximum angle of the GZ eurve.

Setting up limits for the lowest threshold and the highest level of interest requires a formal proeedure that still needs to be developed. This proeedure is likely to be based on dynamieal eharaeteristie of the ship rather than statistieal data.

Thus far, the only validation whieh has been performed was done on a wave elevation dataset. This dataset essentially represents the simplest linear system. Therefore the next step in validation of the proeedure would be a validation of a response of a nonlinear dynamieal system. This system should be simple enough, so direct Monte-Carlo simulation should be available to generate enough data for "brute-force" statistical proeessing that will provide the "correet answer". The subset of the generated data should be used with EPOT to provided an extrapolated result, whieh is expeeted to match the "eorrect answer".

This page is intentionally left blank

References

Abramowitz, M. & I. A. Stegun (Eds.) (1972) Modified Bessel Functions *I* and *K*. §9.6 in *Handbook of Mathematical Functions with Formulas, Graphs, and Mathematical Tables*, 9th printing. New York: Dover, pp. 374–377.

Ananiev, D. M. and Savchuck, S. V. (1982). Experimental prove of applicability of exponential distribution to capsizing probability. *Trans. Russian Register Shipping*, Leningrad, **12**:115–119. (in Russian)

Ayyub, B. M., M. Kaminsky, P. R. Alman, A. Engle, B. L. Campbell & W. L. Thomas (2006) Assessing the Probability of the dynamic Capsizing of Naval Vessel. *J. Ship Research*, **50**(4):289–310.

Belenky, V. L. & C. Bassler (2010) Procedures for Early-Stage Naval Ship Design Evaluation of Dynamic Stability: Influence of the Wave Crest. *Naval Engineering J.* (accepted).

Belenky, V. & A. Breuer (2007) Intact and Damage Stability of Ships and Offshore Structures—Bridging the Gap. *Proc. PRADS 2007*, Houston, Texas.

Belenky, V., J. O. de Kat & N. Umeda, (2008) Toward Performance-Based Criteria for Intact Stability. *Marine Technology*, **45**(2):101–123.

Belenky, V. L. & N. B. Sevastianov (2007) *Stability and Safety of Ships: Risk of Capsizing*. SNAME, Jersey City, ISBN 0-939773-61-9.

Belenky, V. L., K. M. Weems & W. M. Lin (2007) A Probabilistic Procedure for Evaluating the Dynamic Stability and Capsizing of Naval Vessels, Phase 1: Technology Demonstration. SAIC Report #ASTD 08-017 (ONR Contract #N00016-06-C-037).

Belenky, V. L., K. M. Weems & W. M. Lin (2008) Numerical Procedure for Evaluation of Capsizing Probability with Split Time Method. *Proc. 27th Symp. Naval Hydrodynamics*. Seoul, 25 p.

Belenky, V., H.-Ch. Yu & K. M. Weems (2006) Numerical Procedures and Practical Experience of Assessment of Parametric Roll of Container Carriers. *Proc. 9th Int'l Conf. on Stability of Ships and Ocean Vehicles*, M. A. S. Neves, (ed), Rio de Janeiro, Vol. 1, pp. 119–130.

Cohen, C. A. (1965) Maximum Likelihood Estimation in the Weibull Distribution Based on Complete and On Censored Samples. *Technometrics*, 7(4):579–588.

Davison, A. C. (2003) Statistical Models, Cambrige, ISBN 0-521-77339-3

Forsythe, G. E., M. A. Malcolm & C. E. Moler (1977) *Computer Methods for Mathematical Computations*. Prentice-Hall.

Goodman, J. W. (1985) *Statistical Optics*. 1st edition, Wiley-Interscience, New York ISBN 0 471-01502-4 188

Gumbel, E. J. (1958) *Statistics of Extremes*. Colombia University Press, New York.

Kobylinski, L. K. & S. Kastner (2003) *Stability and Safety of Ships Volume I Regulation and Operation*. Elsevier Ocean Engineering Series, Vol. 9, R. Bhattacharyya, M. E.

McCormic, (eds), ISBN 0 08 043001 5, Amsterdam, 412 p.

McTaggart, K. A. (2000a) Improved Modelling of Capsize Risk in Random Seas. Defense Research Establishment Atlantic, DREA TM 2000-137.

McTaggart, K. A. (2000b) Ship Capsize Risk in a Seaway Using Fitted Distributions to Roll Maxima. *J. Offshore Mechanics and Arctic Engineering,* 122(2):141-146.

McTaggart, K. A. (2000c) Ongoing work examining capsize risk of intact frigates using time domain simulation. In *Contemporary Ideas of Ship Stability,* D. Vassalos, M. Hamamoto, A. Papanikolaou & D. Moulyneux (eds), Elsevier Science, pp. 587–595.

McTaggart, K. A. & J. O. de Kat (2000) Capsize risk of intact frigates in irregular seas. *Trans. SNAME*, **108**:147–177.

Meeker, W. O. & L. A. Escobar (1998) *Statistical Methods for Reliability Data.* Wiley, New York, 680 p.

Rice, S.O. (1944) Mathematical Analysis of Random Noise. *Bell System Techn J.* **23**(3):282–332.

Rice, S.O. (1945) Mathematical Analysis of Random Noise. *Bell System Techn J.* **24**(1):46–156.

Scott, D. W (1979) On Optimal and Data-based Histograms. *Biometrica*, **66**(3):605–610.

Sevastianov, N. B. (1963) On Probabilistic Approach to Stability Standards. *Trans. Kaliningrad Institute of Technology*, **18**:3–12. (in Russian)

Sevastianov, N. B. (1994) An Algorithm of Probabilistic Stability Assessment and Standards. *Proc. 5th International Conference on Stability of Ships and Ocean Vehicles*, Vol. 5, Melbourne, Florida.

SLF 50/4/4 (2007) Review of the Intact Stability Code. Framework for the development of new generation criteria for intact stability. Submitted by Japan, the Netherlands and the United States, IMO, London.

SLF 51/WP.2 (2008) Revision of the Intact Stability Code. Report of the working group (Part 1), IMO, London.

Sveshnikov, A. A. (1968) *Applied methods of stochastic function theory.* Nauka publishing, Moscow. (in Russian)

Hard Copies	PDF Copies	Agncy	Individual
		Initial Report Distribution	
1	2	NAVSEA PMS 500	CAPT J. Downey
0	1	NAVSEA 05D	J. Webster
1	1	NAVSEA 05D	B. Koehr
1	1	NAVSEA 05D	C. Higgins
0	1	NAVSEA 05D	M. Garner
1	1	NAVSEA 05P	R. Waters
0	1	NAVSEA 05P	D. Cimino
1	1	NAVSEA 05P	P. Alman
1	1	ONR 331	L. P. Purtell
1	1	DTIC	
		NSWWCD Internal Distribution	
1	1	0120	J. Barkyoumb
0	1	3452	TIC
1	1	50	J. Etxegoien
0	0	501 (w/o enclosure)	D. Intolubbe
1	1	504	A. Reed
0	1	505	T. Fu
1	1	506	D. Walden
1	1	508	J. Brown
1	1	55	T.Applebee
0	1	55	M. Dipper
1	1	551	T. Smith
1	1	551	C. Bassler
3	3	551	V. Belenky
1	1	551	W. Belknap
3	3	551	B. Campbell
0	1	552	D. Hayden
1	1	553	T. Carrico
0	1	58	R. Hurwitz
1	1	6501	R. Lewis
1	1	6540	A. Engle